The Tunneling Percolation Staircase

Isaac Balberg

Racah Institute of Physics,

The Hebrew University, Jerusalem, Israel

Stat. Mech. Day IV. 230611

GRANULAR METAL COMPOSITES

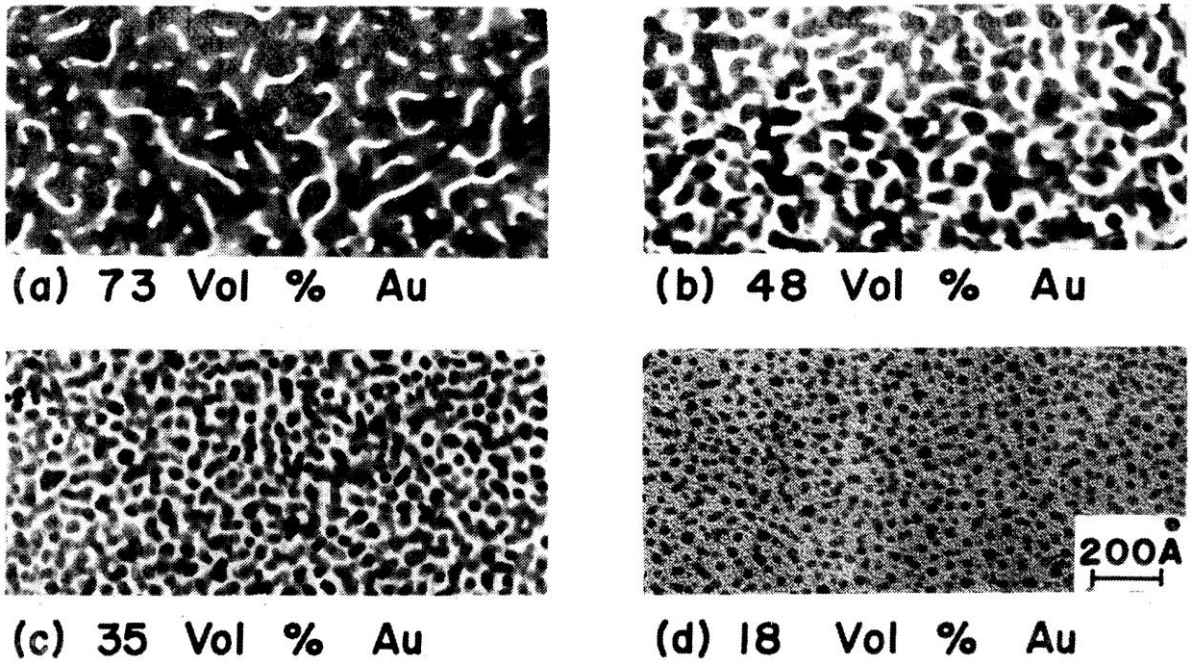

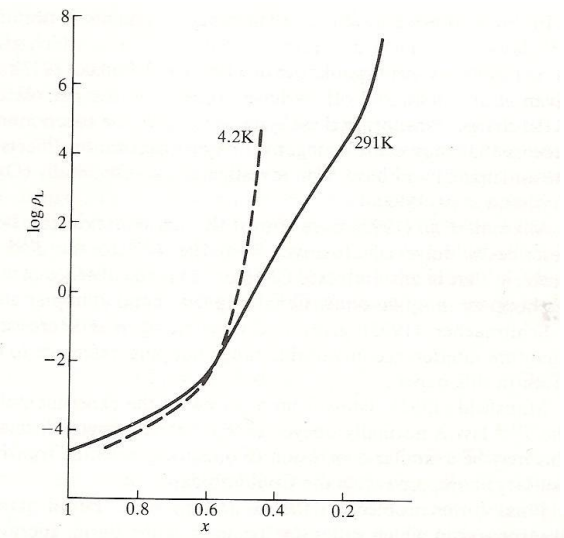

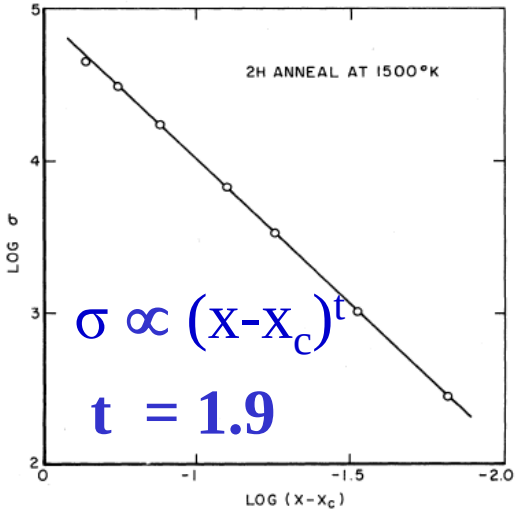

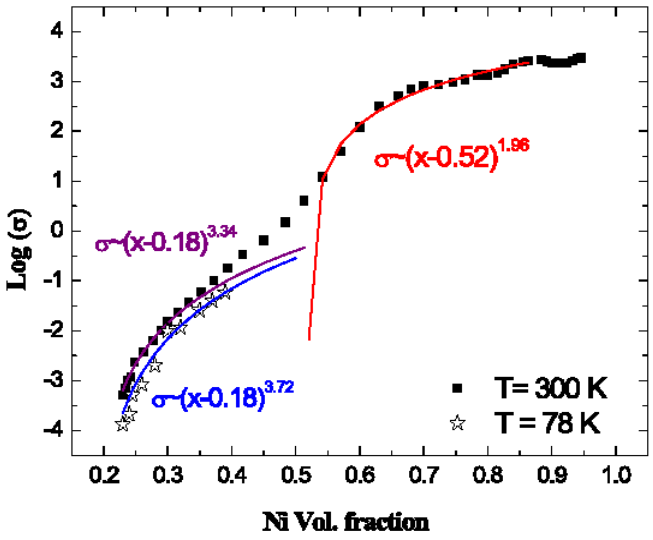

CB polymer composites and applications

CB

Thermal switches

Self regulated heaters

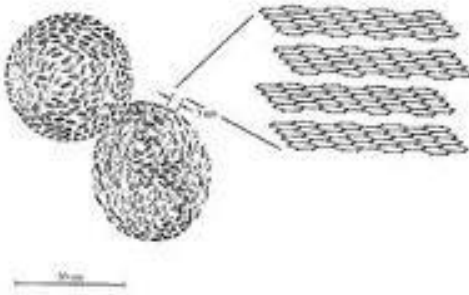

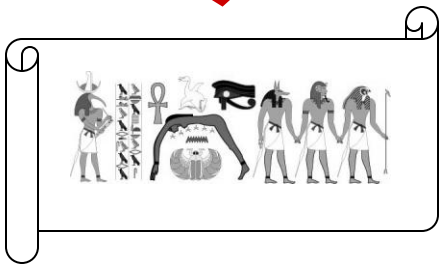

Papyrus glyphs

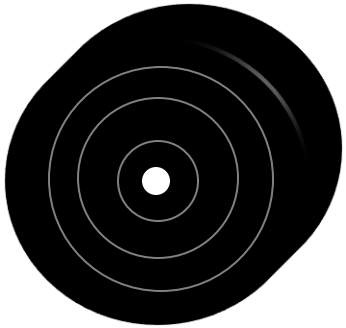

Airplane wheels

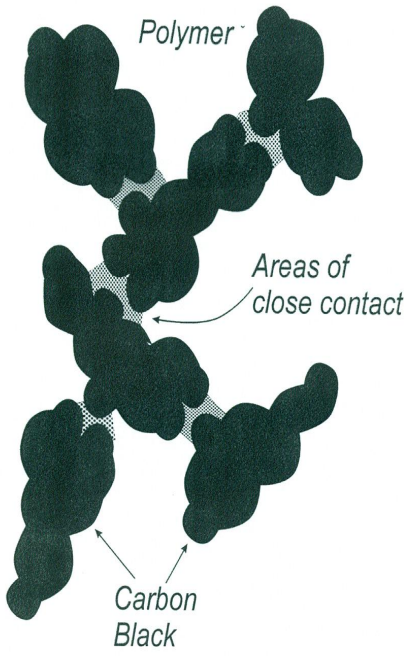

Two fundamental questions

1) What determines the conductivity threshold?

2) What determines the shape of the σ(Φ) dependence?

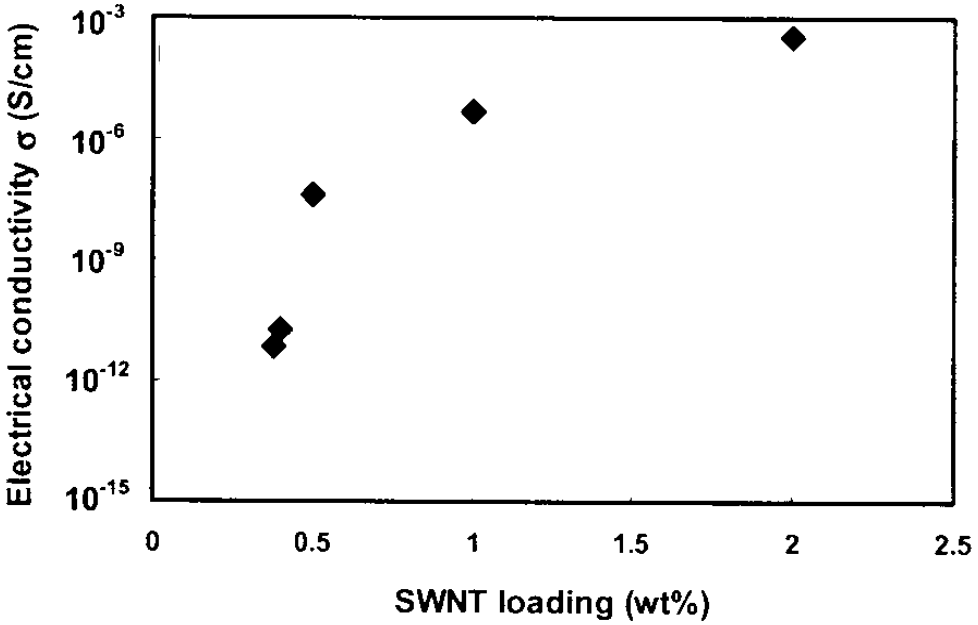

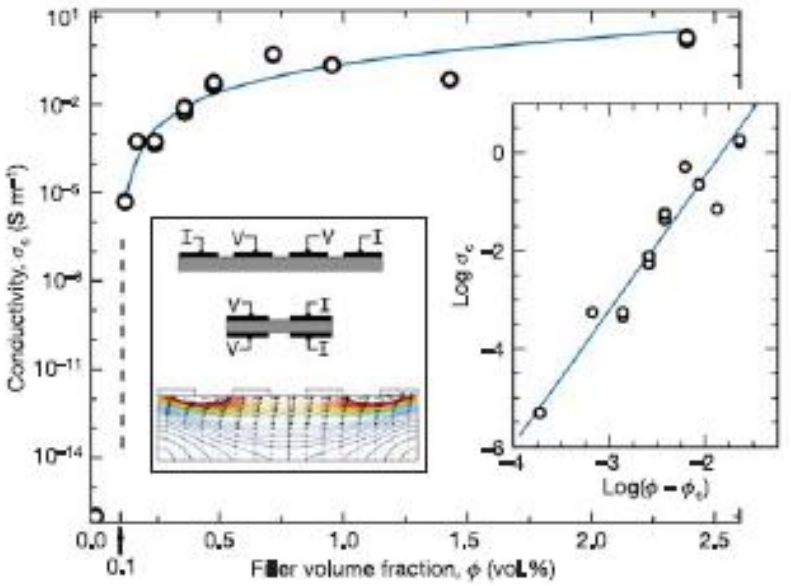

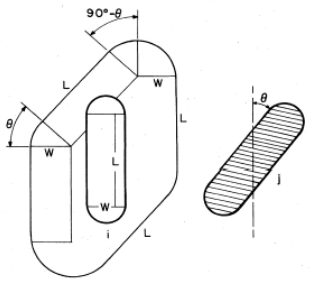

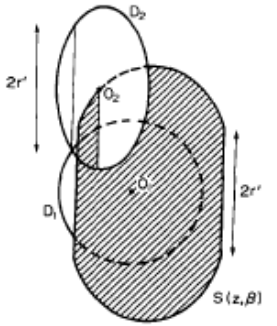

Phys. Rev. B, 30, 3933 (1984): 304 Q

Confirmation of universality

$$\sigma \propto (p - p_c)^t$$

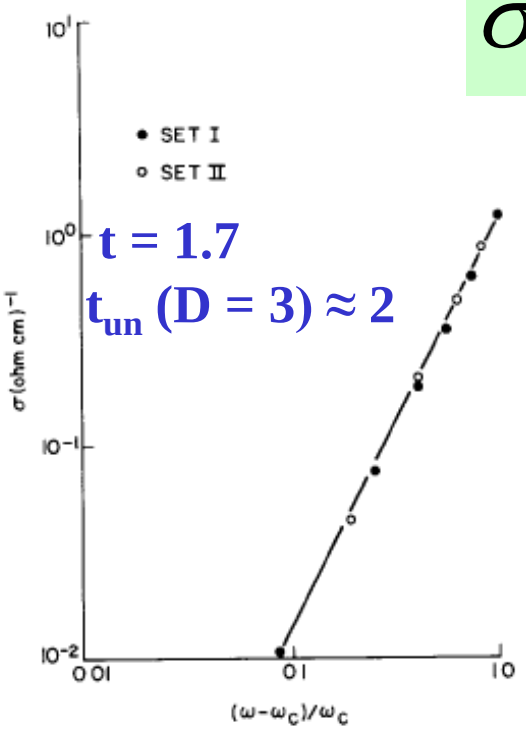

Fig 3 The dependence of the measured values of the conductivity on the normalized carbon loading of the carbon–PVC composites used in this study

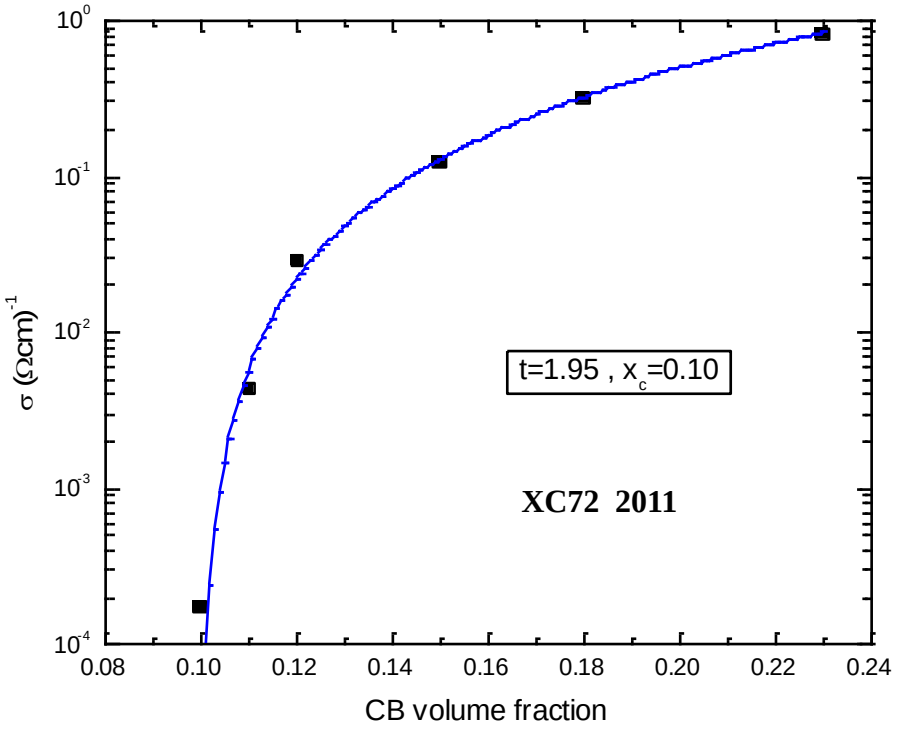

Experimentally observed non universal exponents

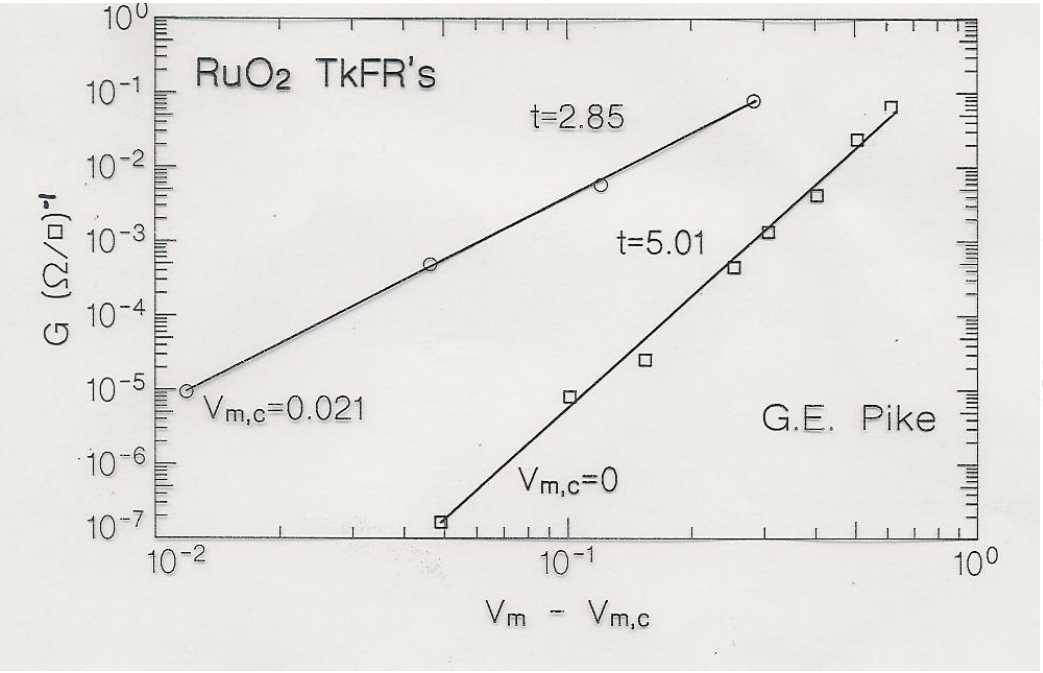

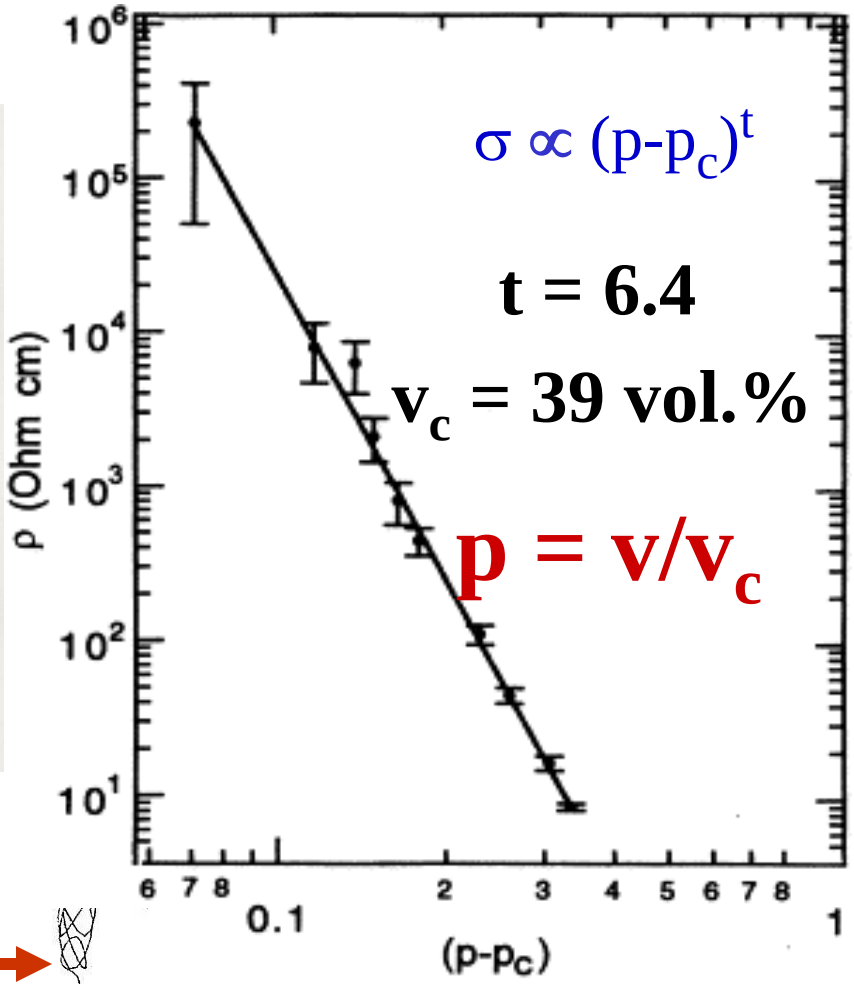

$\sigma \propto (p-p_c)^t$

t = 6.4

v_c = 39 vol.%

$p = v/v_c$

$R_L = R_\lambda (L/\lambda)/(L/\lambda)^{D-1}$

$\lambda \propto (p-p_c)^{-\nu}$

$R_\lambda \ (\geq R_0 L_1)$

$\langle R \rangle \propto (p-p_c)^{-(t-tun)}$

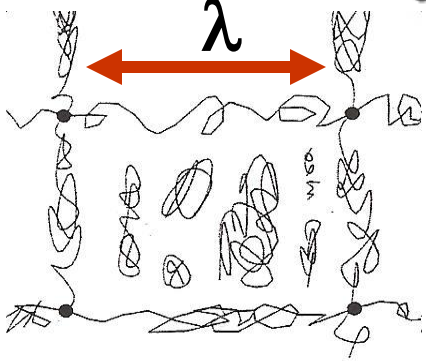

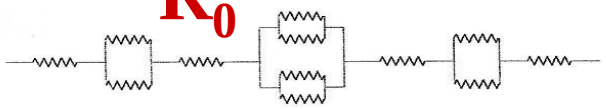

The diverging normalized distribution in the tunneling percolation problem

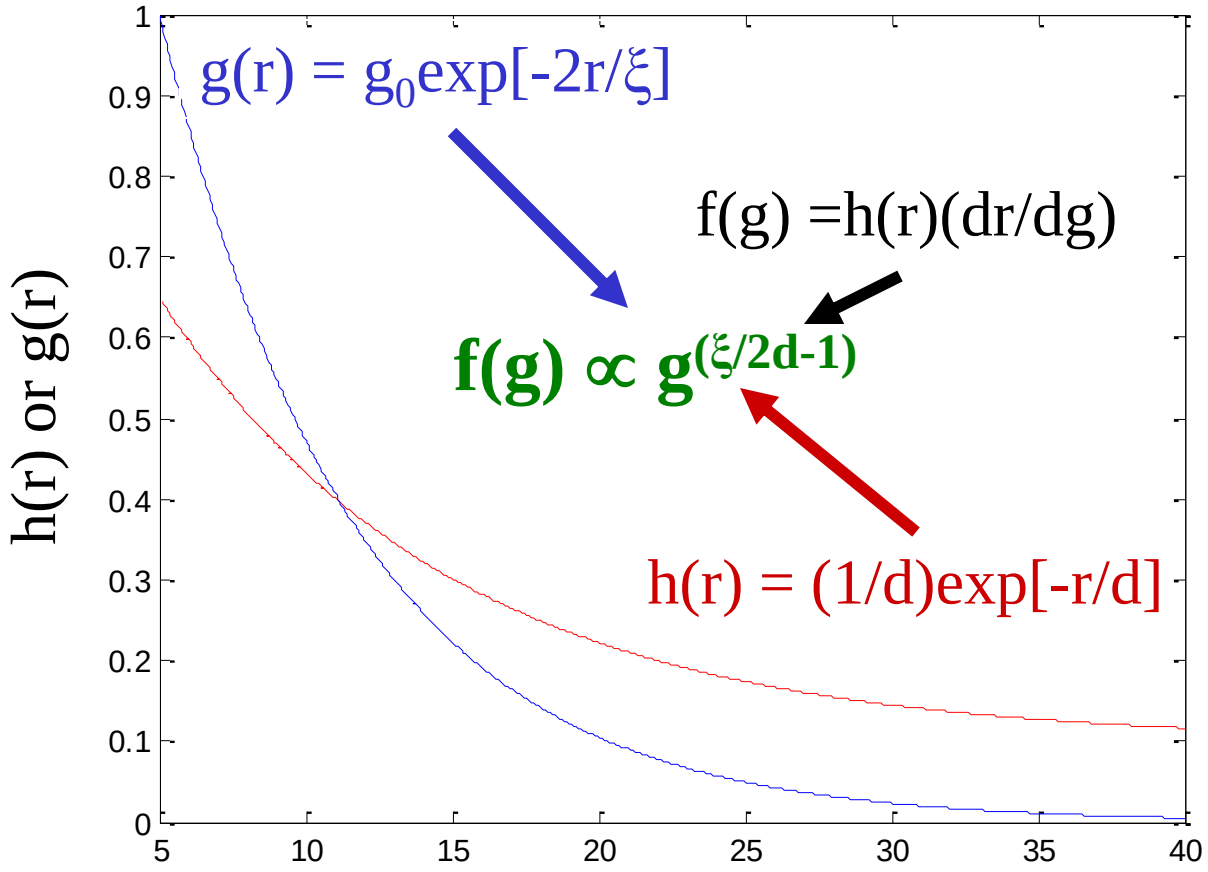

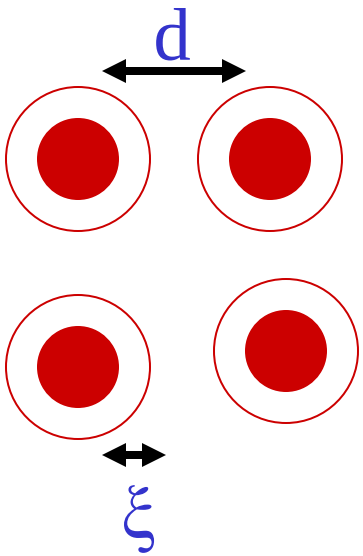

$p_c \leftarrow p$ $\qquad$ $0 \leftarrow g$

$\sigma \propto (p-p_c)^t$

$t = t_{un}+(2d/\xi)-1$

Phys. Rev. Lett, 59, 1305 (1987): 215 Q

Various carbon blacks

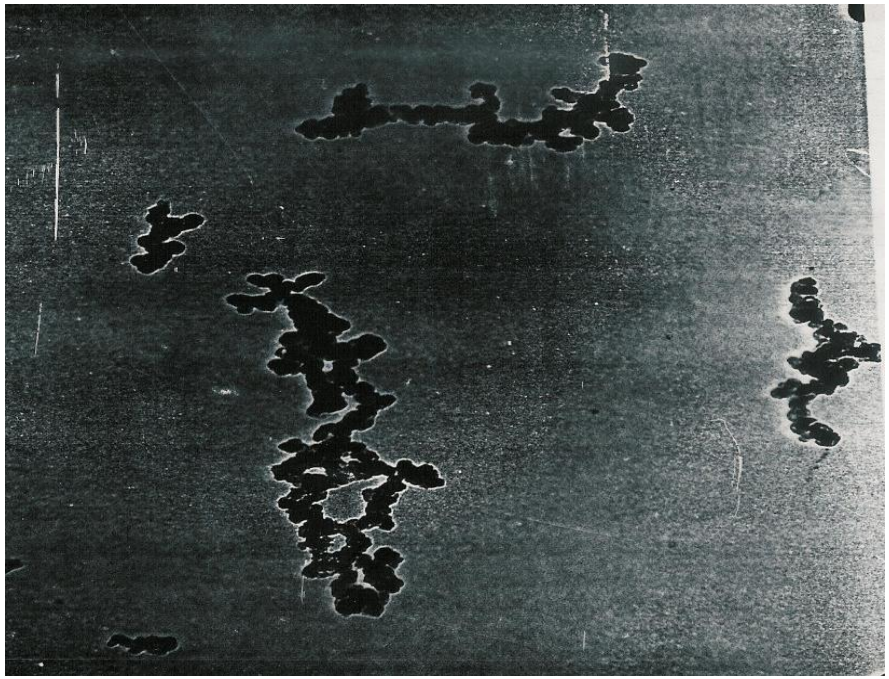

39 vol. %

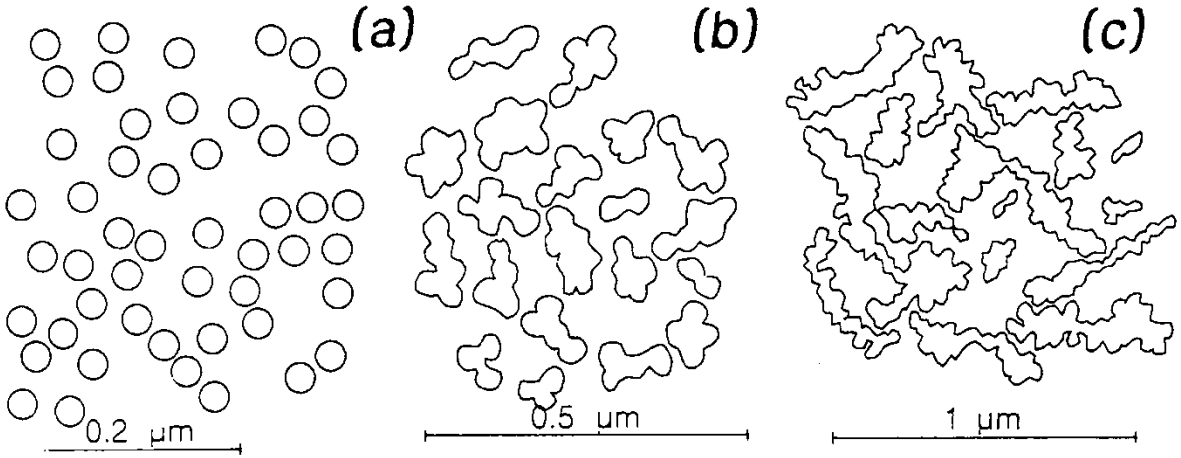

t = 6.4 t = 4 t =1.8

10 wt. %

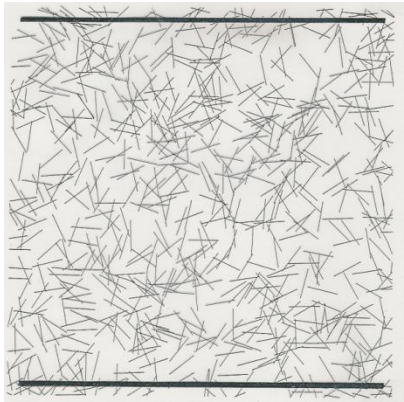

Percolation and Tunneling?

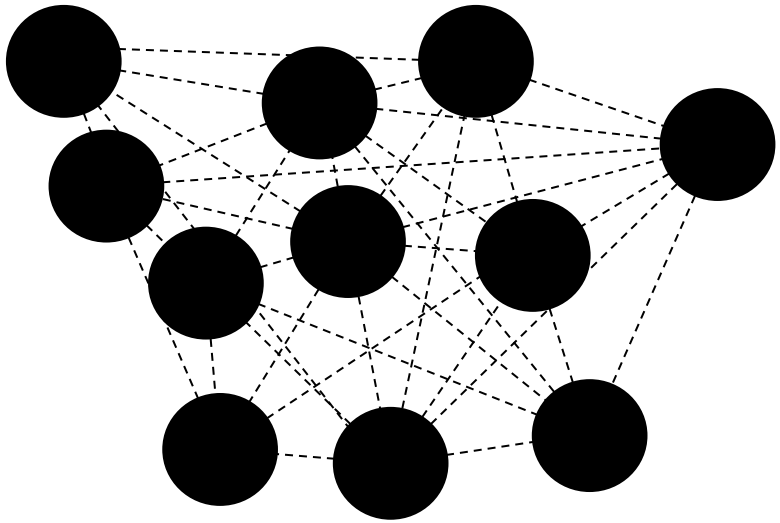

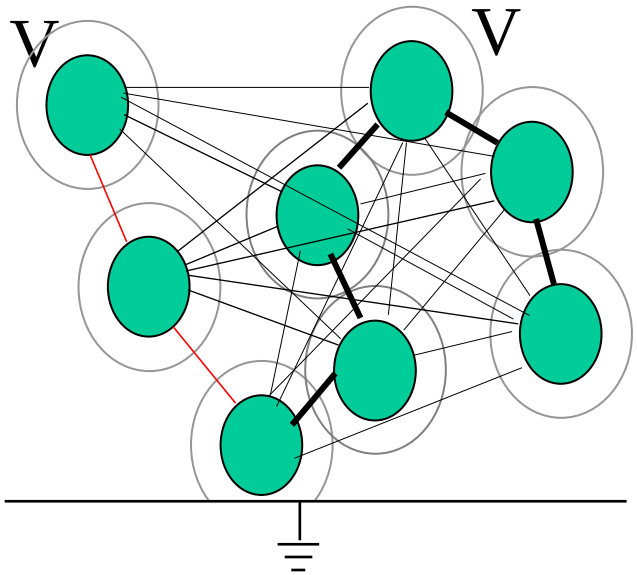

$g(r_{ij}) = g_0 \exp[-2(r_{ij}-D)/\xi]$

What is the meaning of v_c?

Carbon, 40, 139 (2002): 100 Q.

The hopping model (the CPA network)

$B_c=(4\pi/3)[r_c^3-(2b)^3]N$

$g(r_c) = g_0 \exp[-2(r_c-2b)/\xi]$

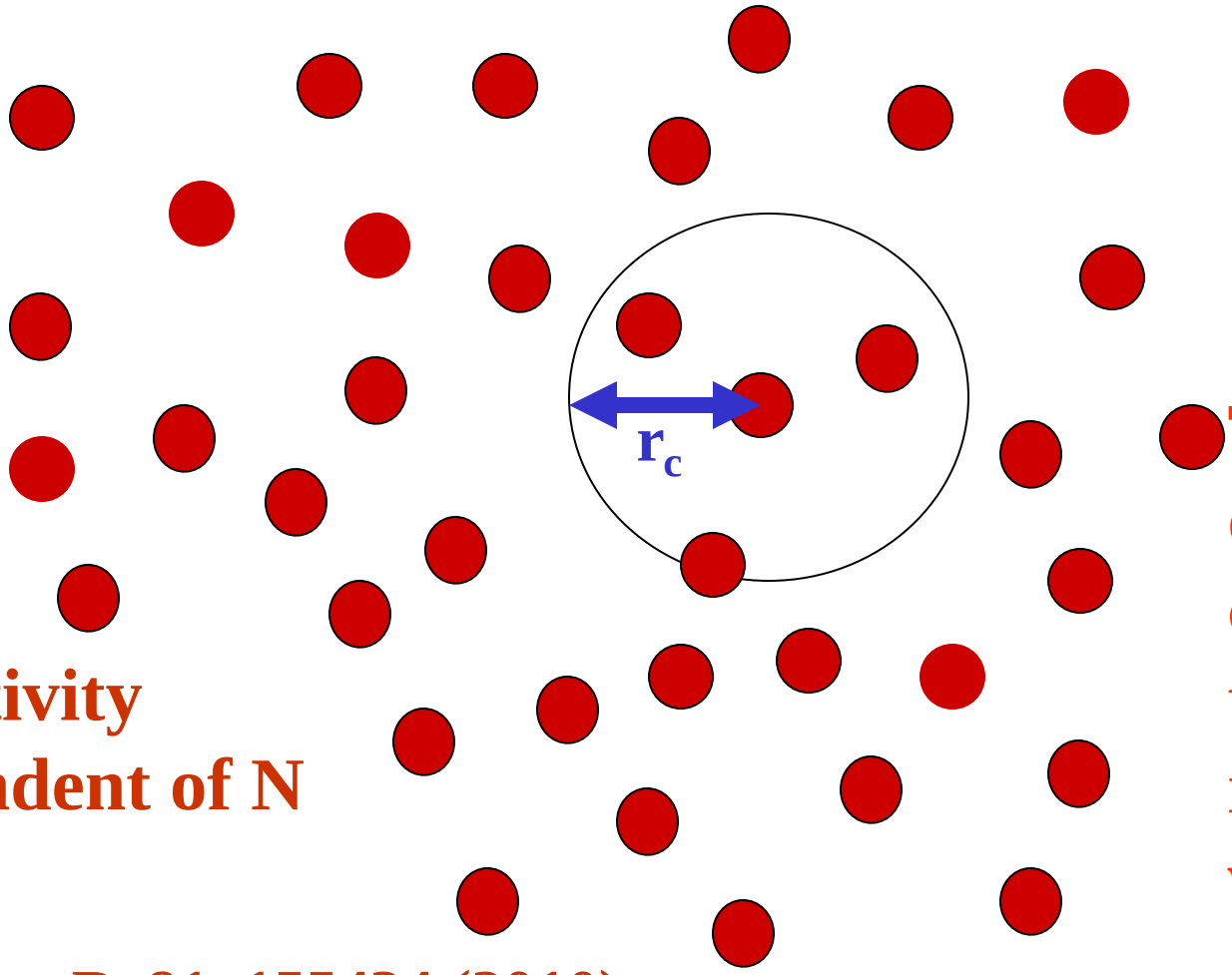

Local connectivity independent of N

The increase of N conserves topology but increase the value of g

Phys. Rev. B, 81, 155434 (2010)

The prediction of the percolation-threshold (critical-resistor, hopping like) model and its relation to the critical-percolation (phase-transition like) model

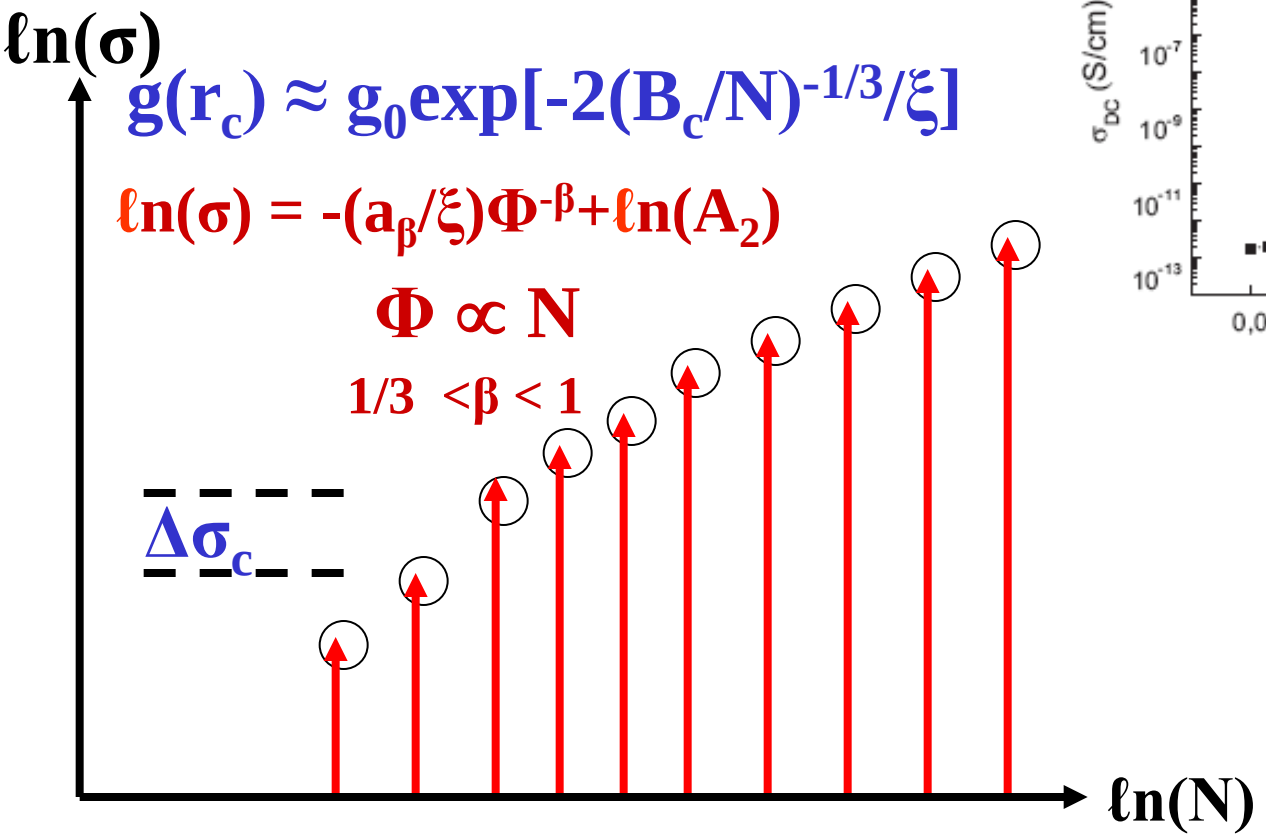

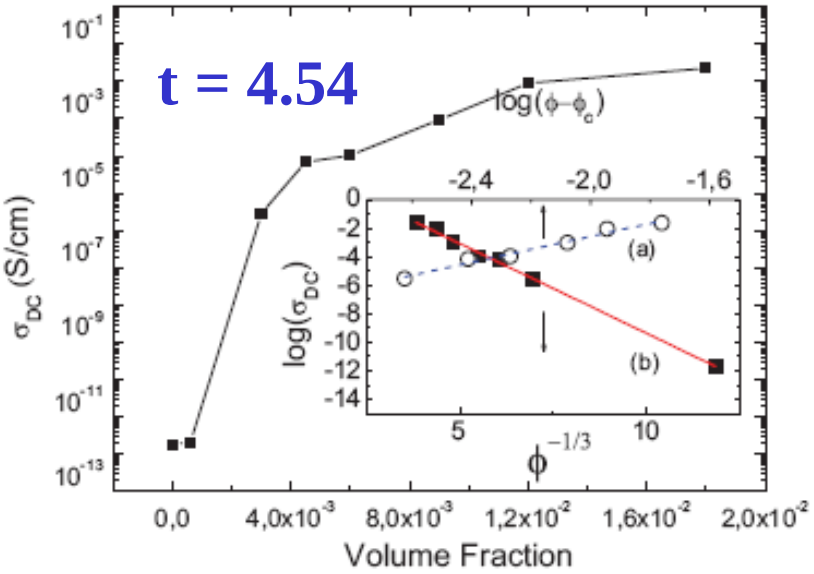

How is it then that in so many cases we see a percolation behavior (even a universal one)?

Phys. Rev. Lett. Comment, 106, 079701 (2011)

The origin of the staircase model

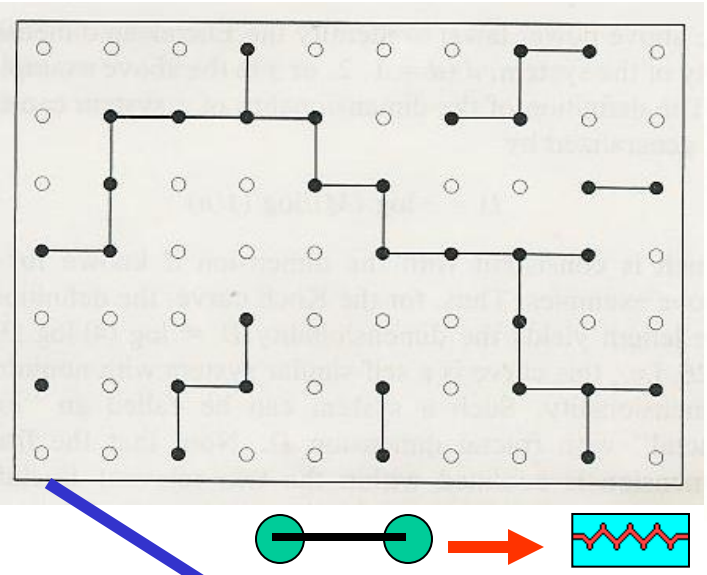

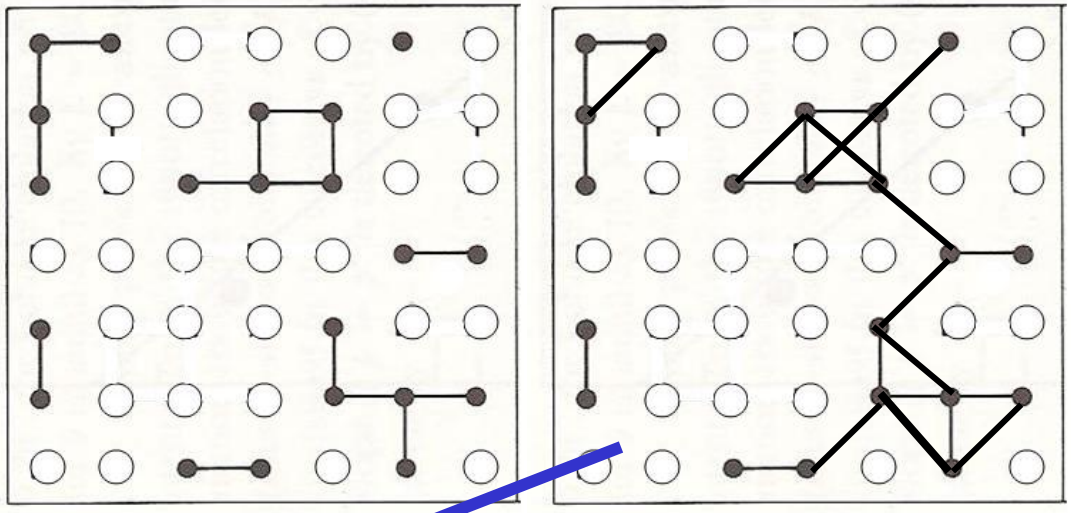

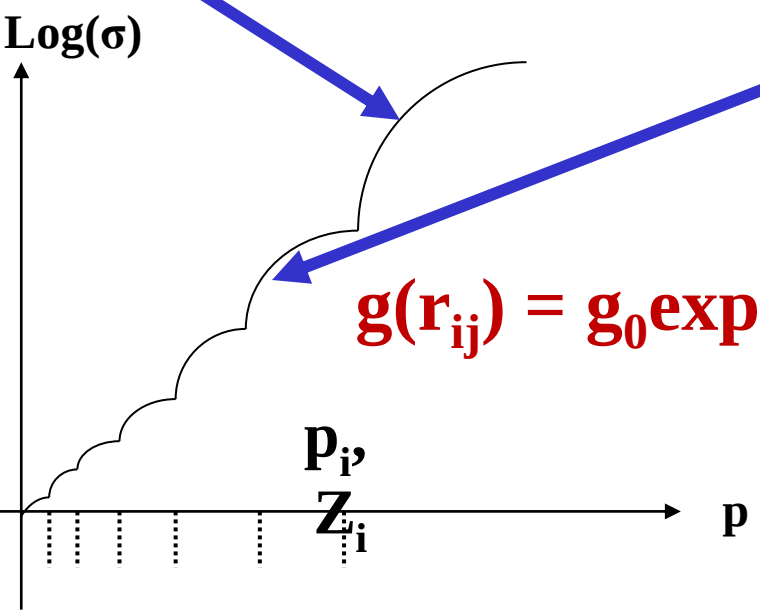

$$g(r_{ij}) = g_0 \exp[-2(r_{ij})/\xi]$$

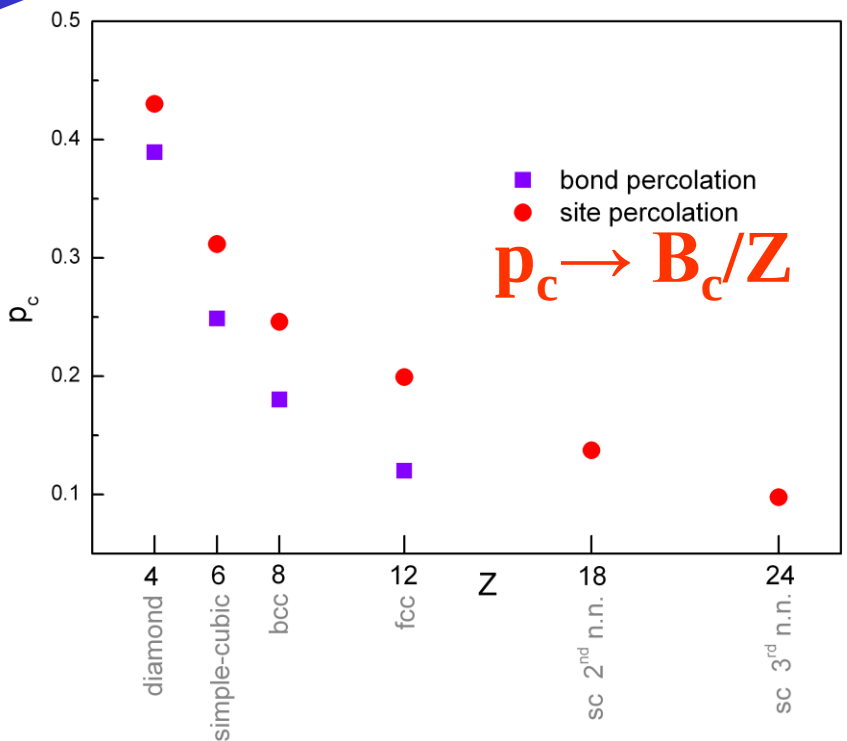

J. Phys. D: 42, 064003 (2009)

The lattice and continuum composite models

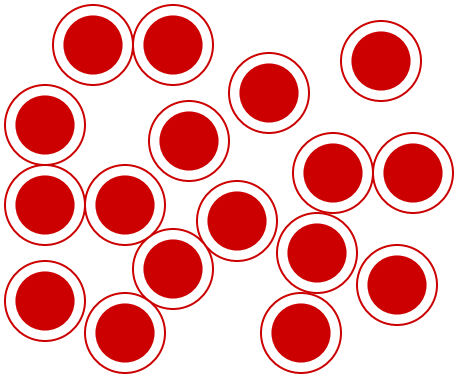

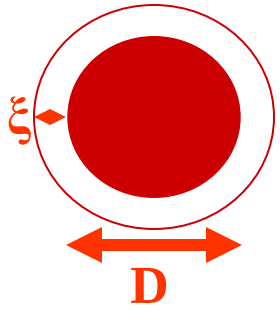

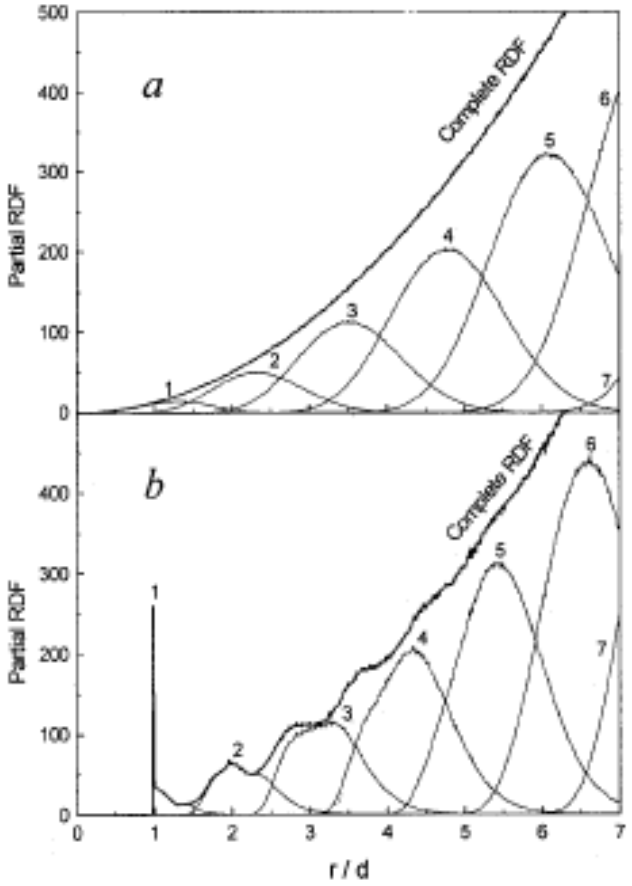

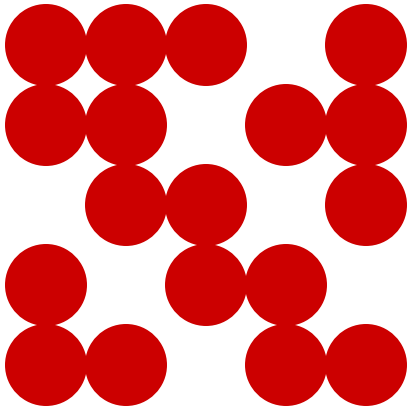

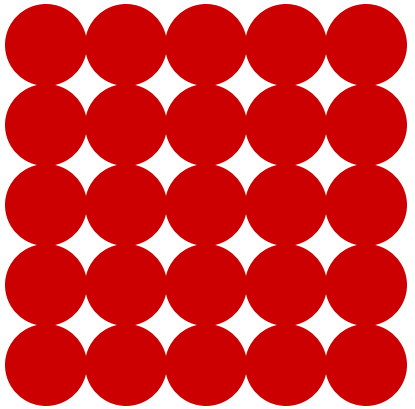

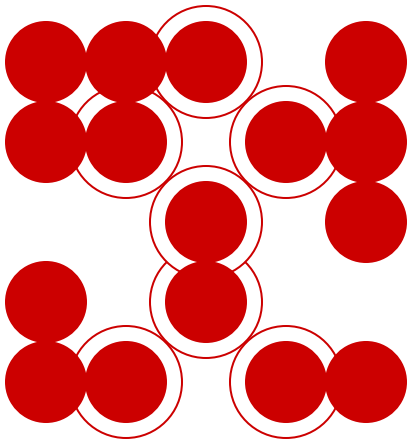

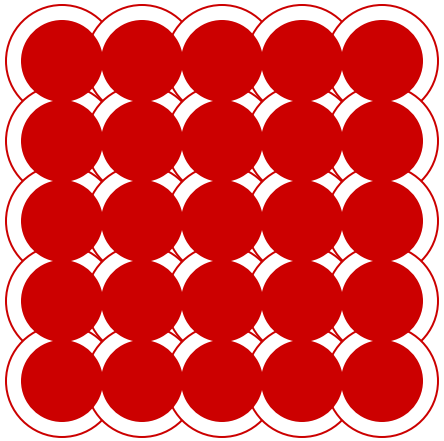

The effect of tunneling in lattices and the continuum

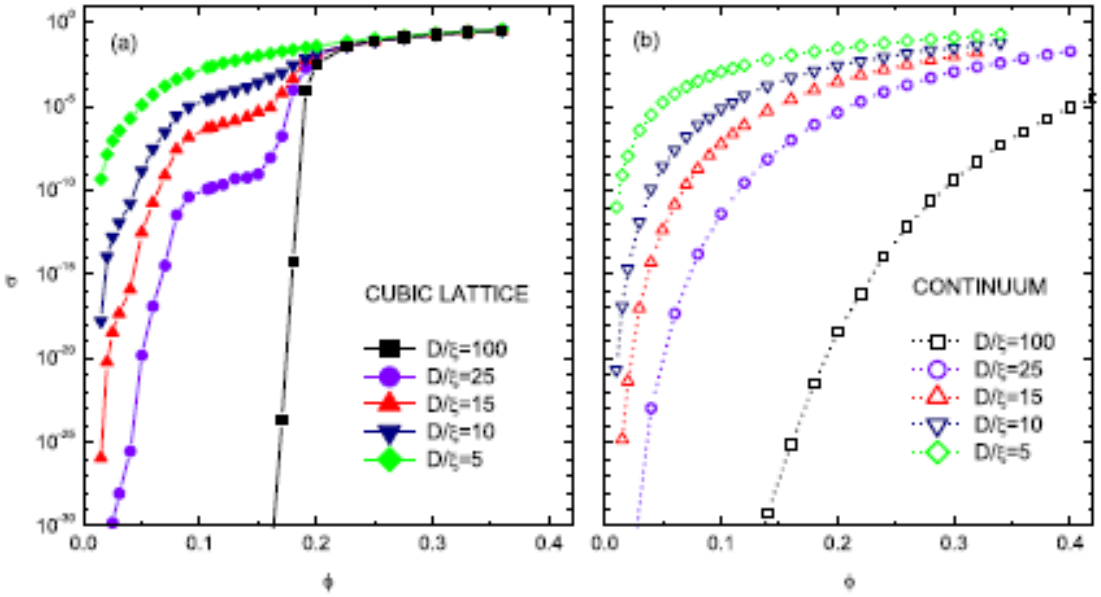

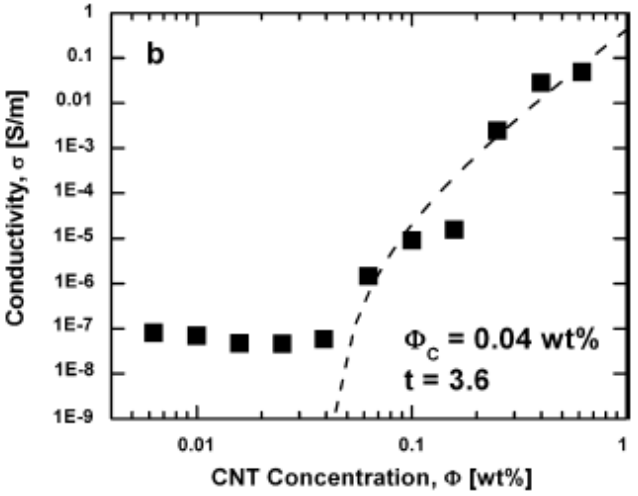

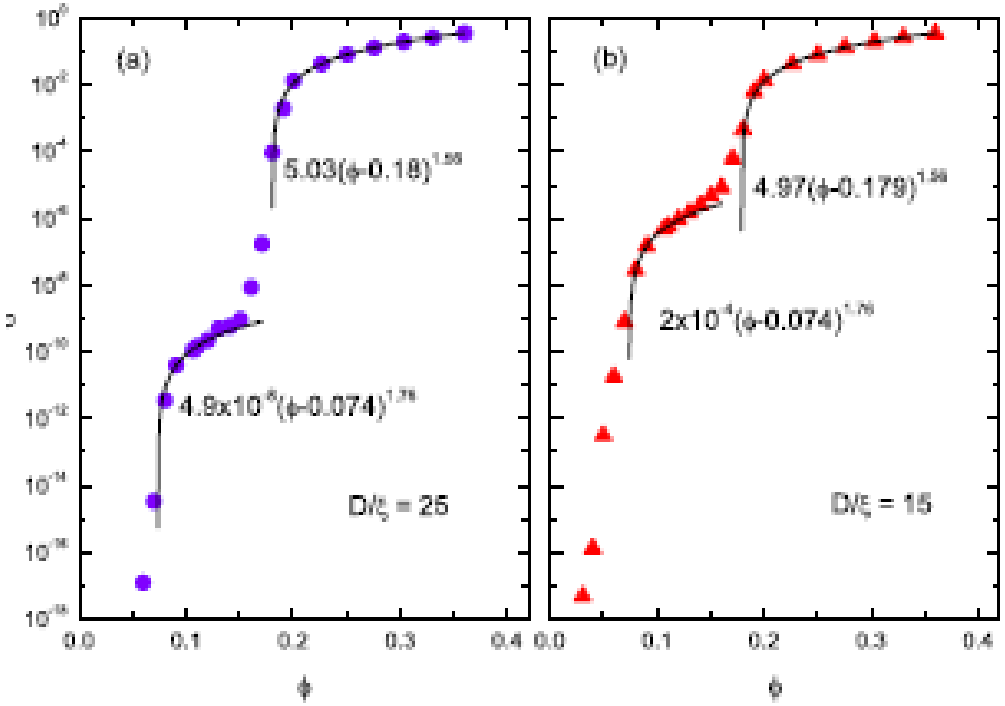

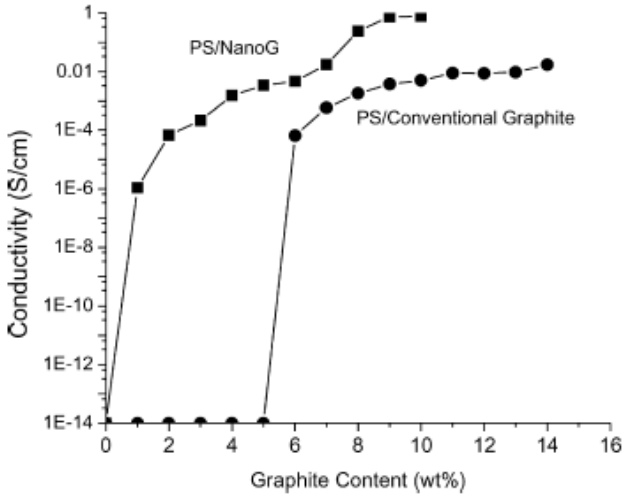

Phys. Rev. B, 82, 134201 (2010)

Staircase observed in N990/Polyethylene Composites

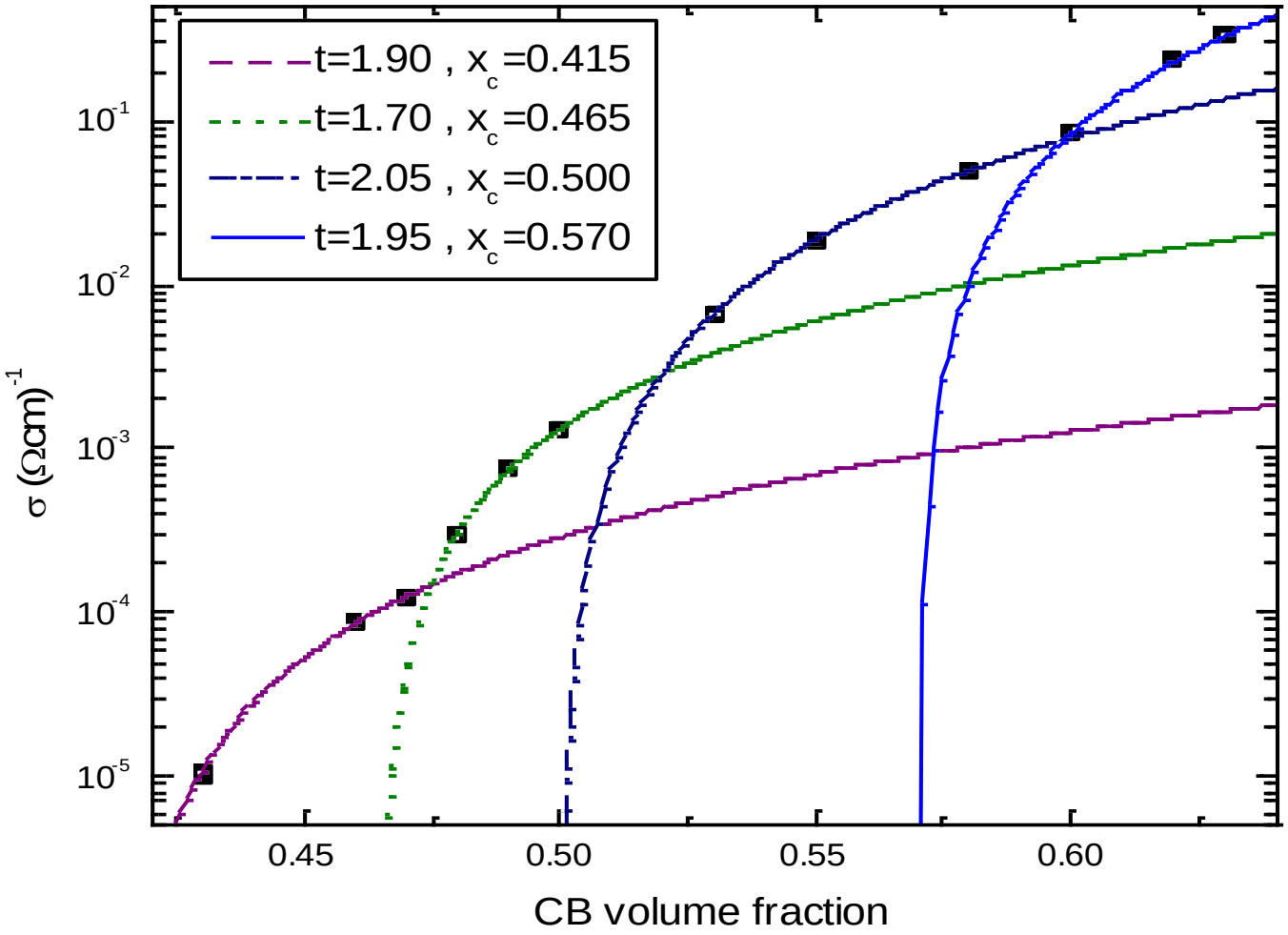

Conclusions

- **The observed σ(Φ) behavior is a series of percolation transitions, the stairs.**

- **In the lattice these have to do with the series of lattice neighbors. In the continuum these have to do with shells of neighbors that result from an RDF with peaks.**

- **In the continuum the σ(Φ) behavior of each stair is that of a universal behavior while the envelope of the stairs yields a non universal percolation behavior which simply presents hopping.**

- **The experimentally observed Φ_c is either of a "universal" stair or a result of the fact that the data do not go to Φ = 0. Percolation is well confirmed if both, a universal behavior and a non hopping behavior are exhibited by the data.**

- **One can get a simple universal percolation behavior if all the resistors are nearly equal (non divergent distribution) and all belong to a random network (as for anisotropic particles).**

The End

RF transmission (“AC Conductivity”) at 80 MHz

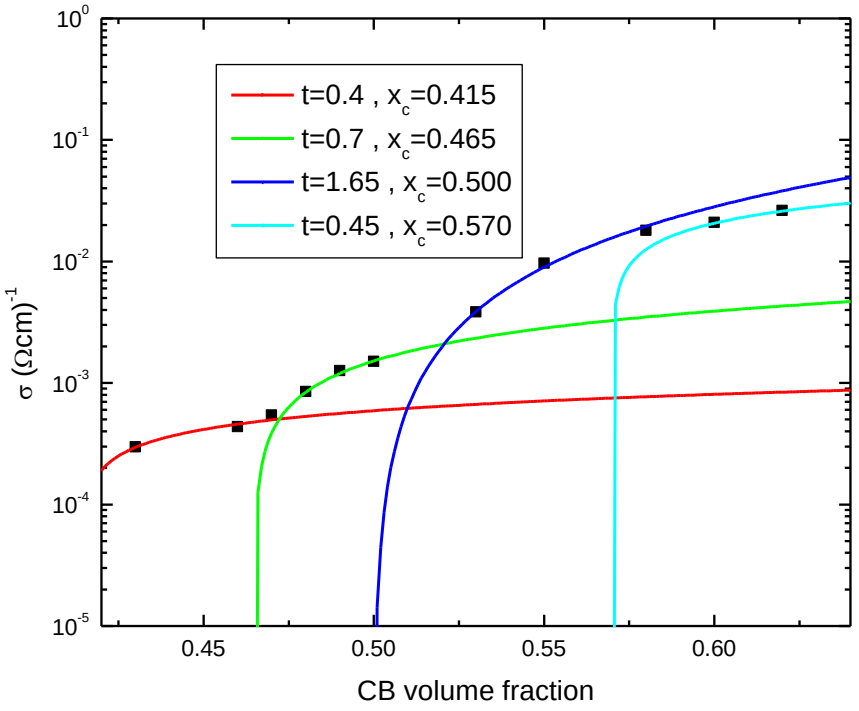

What if we have a distribution of (or $r_0 = 1/g$) values?

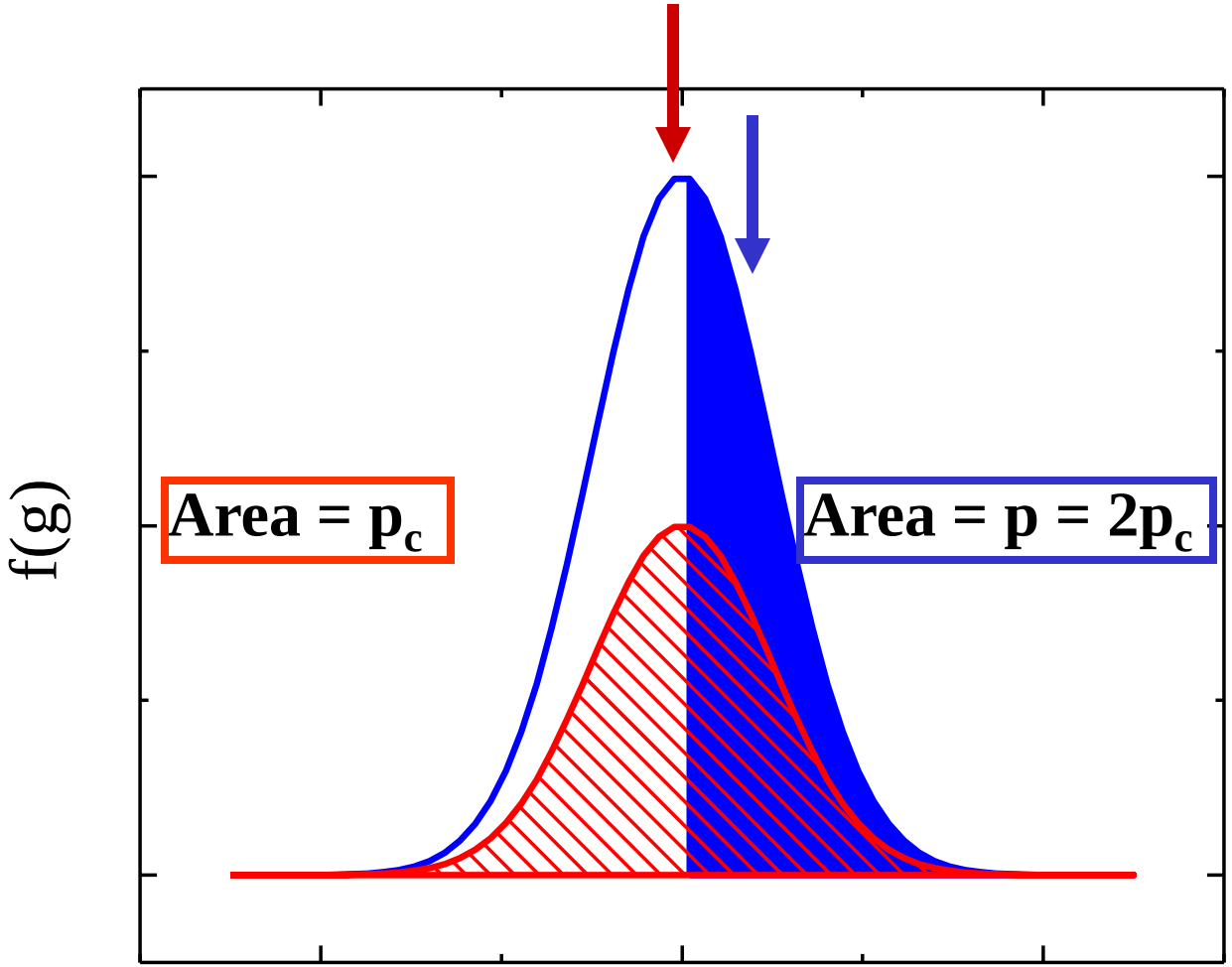

$R_L \propto \langle r \rangle (p-p_c)^{-tun}$

$\langle r \rangle = {}_{gc}\int^{1} (1/g) f(g) dg.$

$p[{}_{gc}\int^{1} f(g) dg] = p_c$

$f(g) = (1-\alpha) g^{-\alpha}$ yields that:

$g_c = [(p-p_c)/p]^{1/(1-\alpha)}$

$\langle r \rangle \propto (p-p_c)^{-\alpha/(1-\alpha)} \propto (p-p_c)^{-(t-tun)}$

Universal and Hopping Interpretations in XC72-Polyethylene Composite

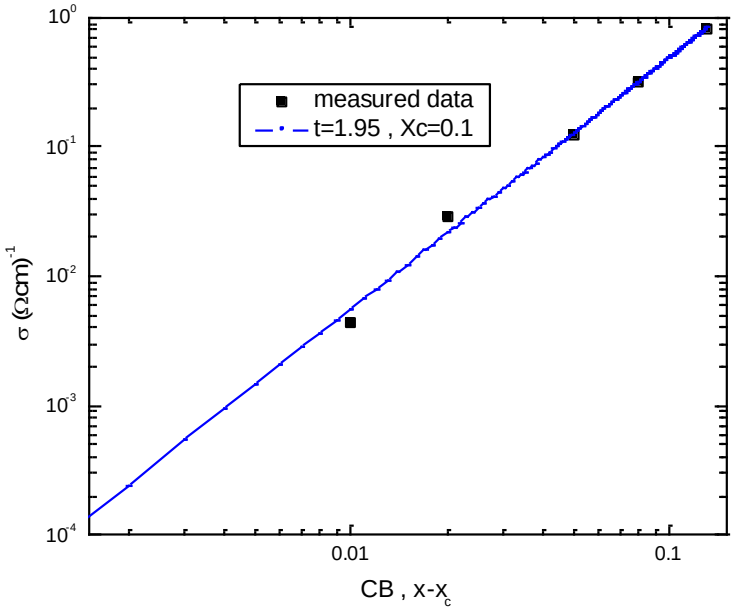

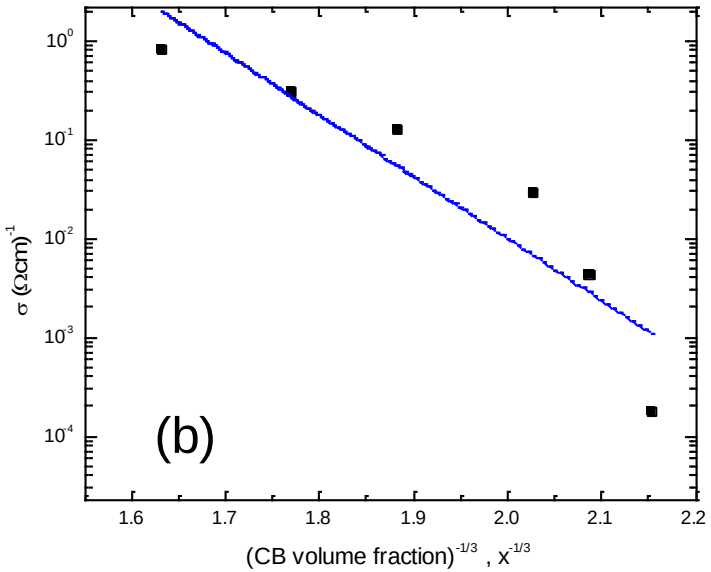

Non-Hopping but Percolation Behavior

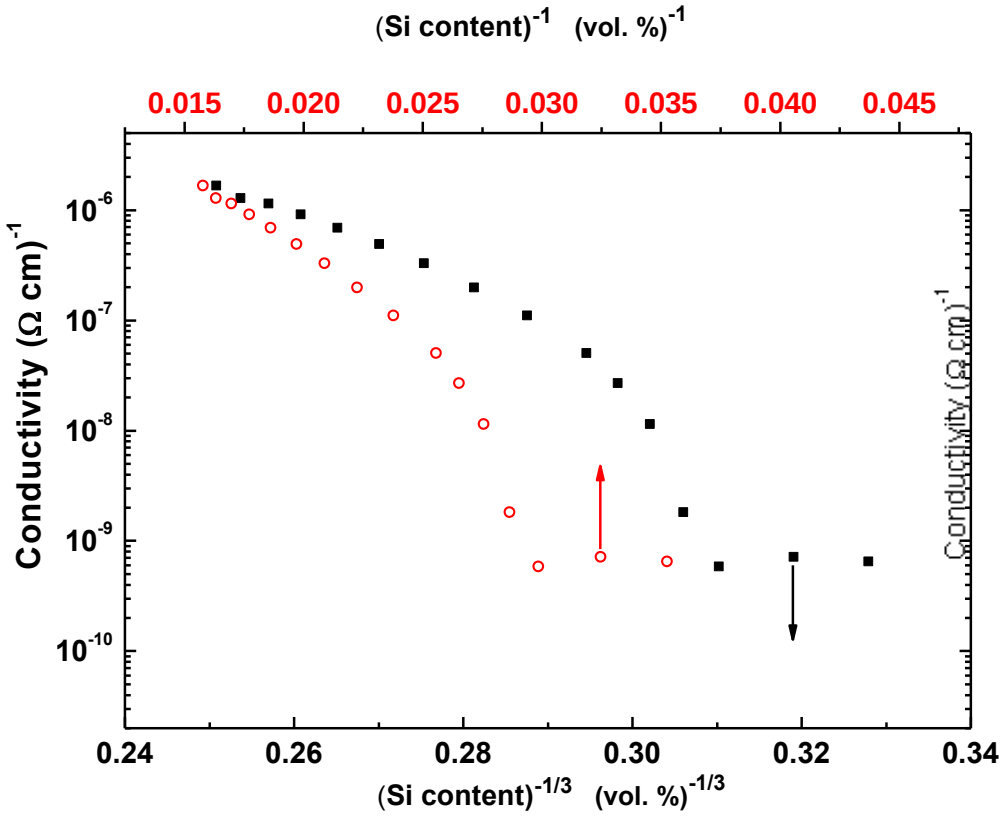

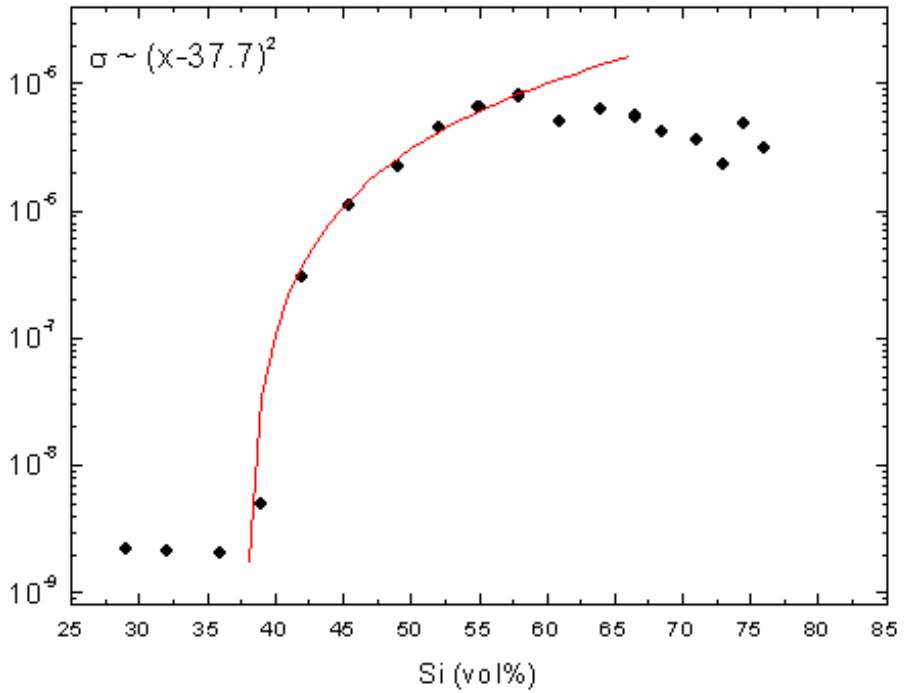

Phys. Rev. B, 83, 035318 (2011)

Percolation Transition

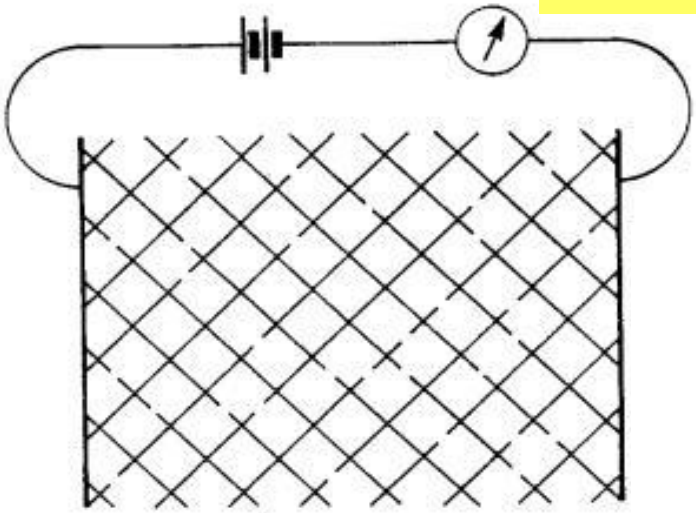

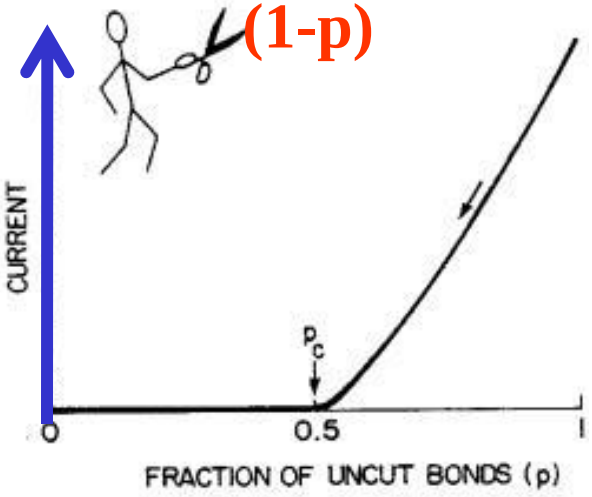

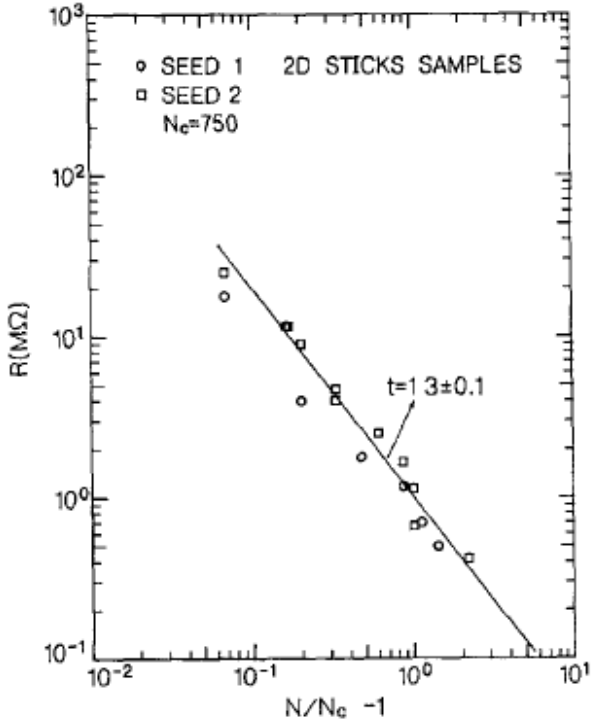

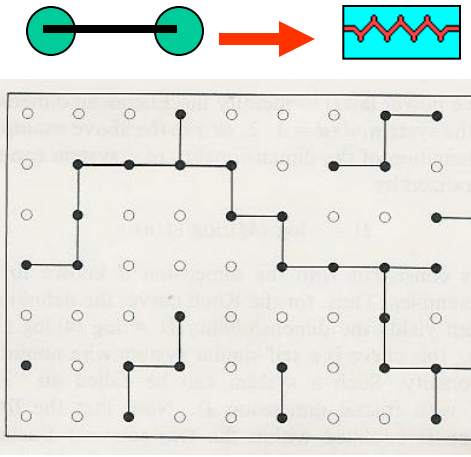

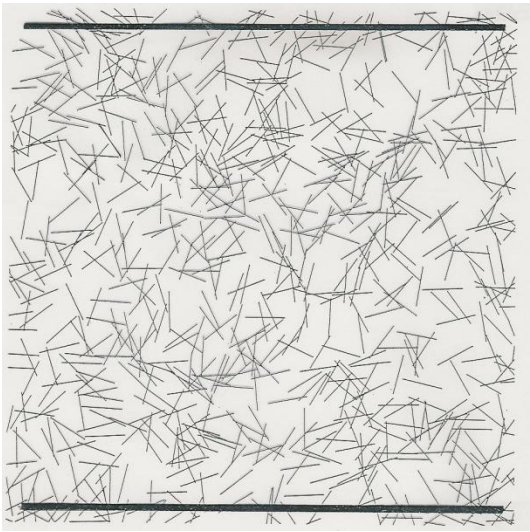

t_{un} (D = 2) ≈ 1.3

$$\sigma \propto (p - p_c)^t$$

t_{un} (D = 3) ≈ 2

$t = t_{un} = (D-2)\nu+\zeta$

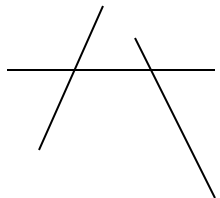

The LNB Model of the backbone

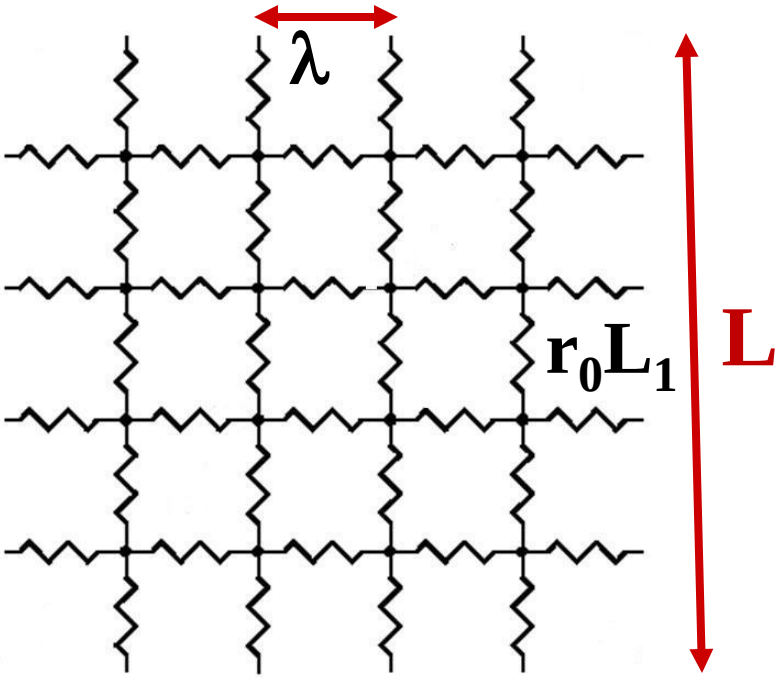

S&A 1992

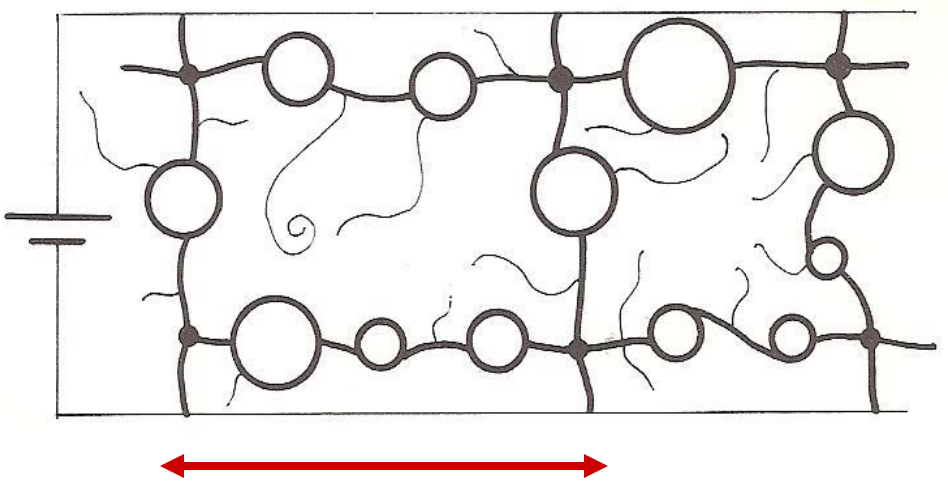

$\lambda \propto (p-p_c)^{-\nu}$

$R_L = R_\lambda (L/\lambda)/(L/\lambda)^{D-1}$ $\quad \zeta \geq 1$ $\quad R_\lambda (\geq r_0 L_1)$

$R_L \propto (p-p_c)^{-[\zeta+(D-2)\nu)]} \propto (p-p_c)^{-t_{un}}$ $\quad L_1(p-p_c)/p_c = 1 \rightarrow L_1 \propto (p-p_c)^{-1}$

The electrical conductance in composites and the analysis of the conductance network

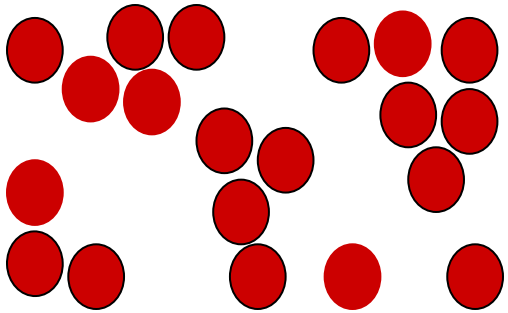

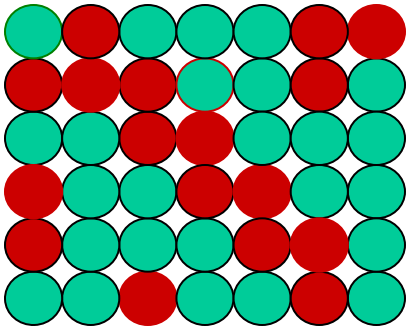

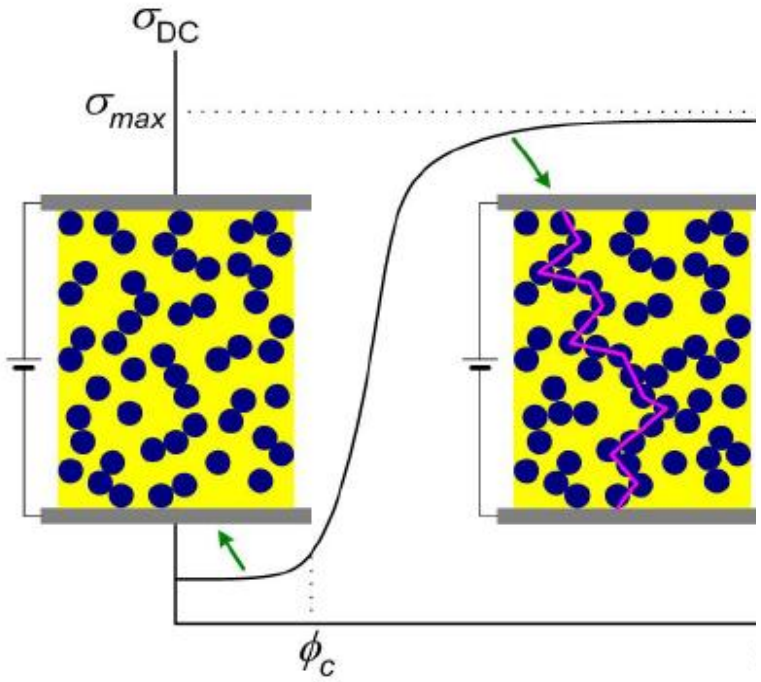

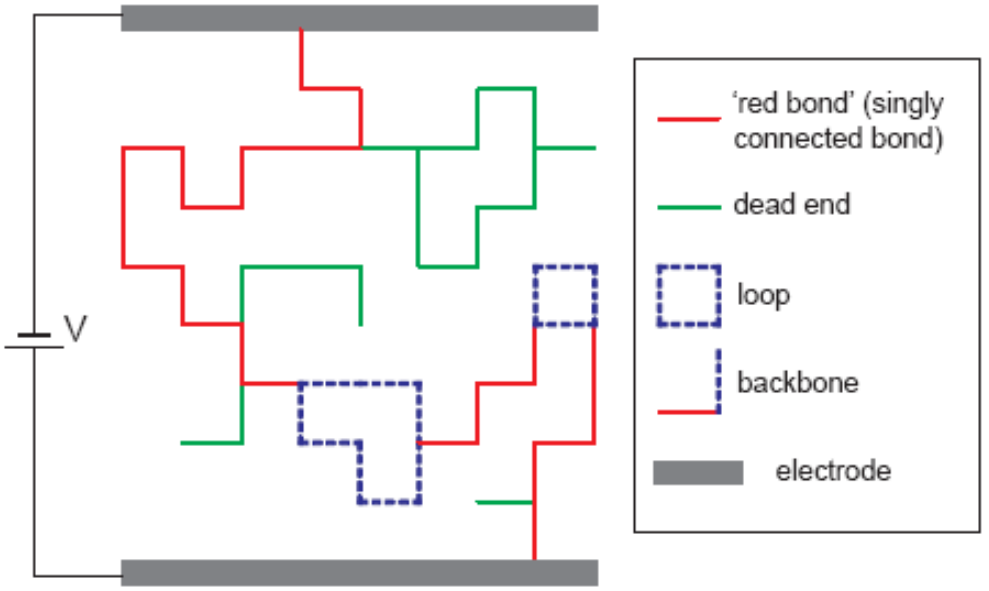

One expects intuitively and we can show rigorously that
$V-V_c = (N-N_c)(v_{HC})$ (vol.%) in the continuum, is equivalent to $p^s-p^s_c$ in lattices

TUNNELING (Wiesendanger, 1994)

$$\sigma(r) = \sigma_0 \exp[-2r/L]$$

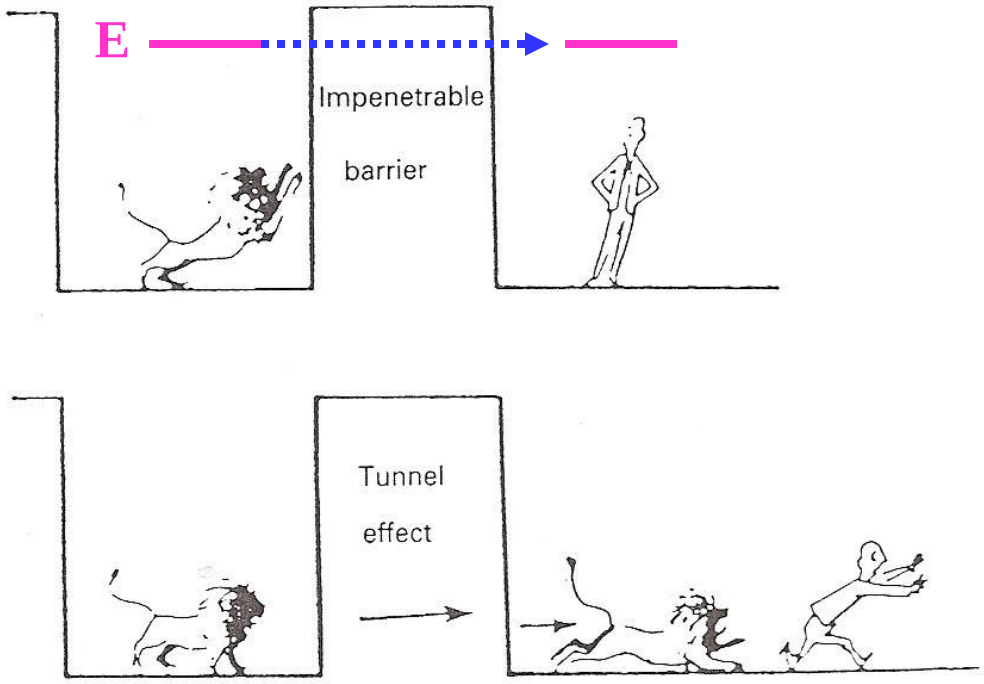

Fig. 1.1. The difference between classical theory and quantum theory, illustrating tunneling through a potential barrier (Bleaney, 1984).

L ≤ 10 nm

Resistors Equivalent Network

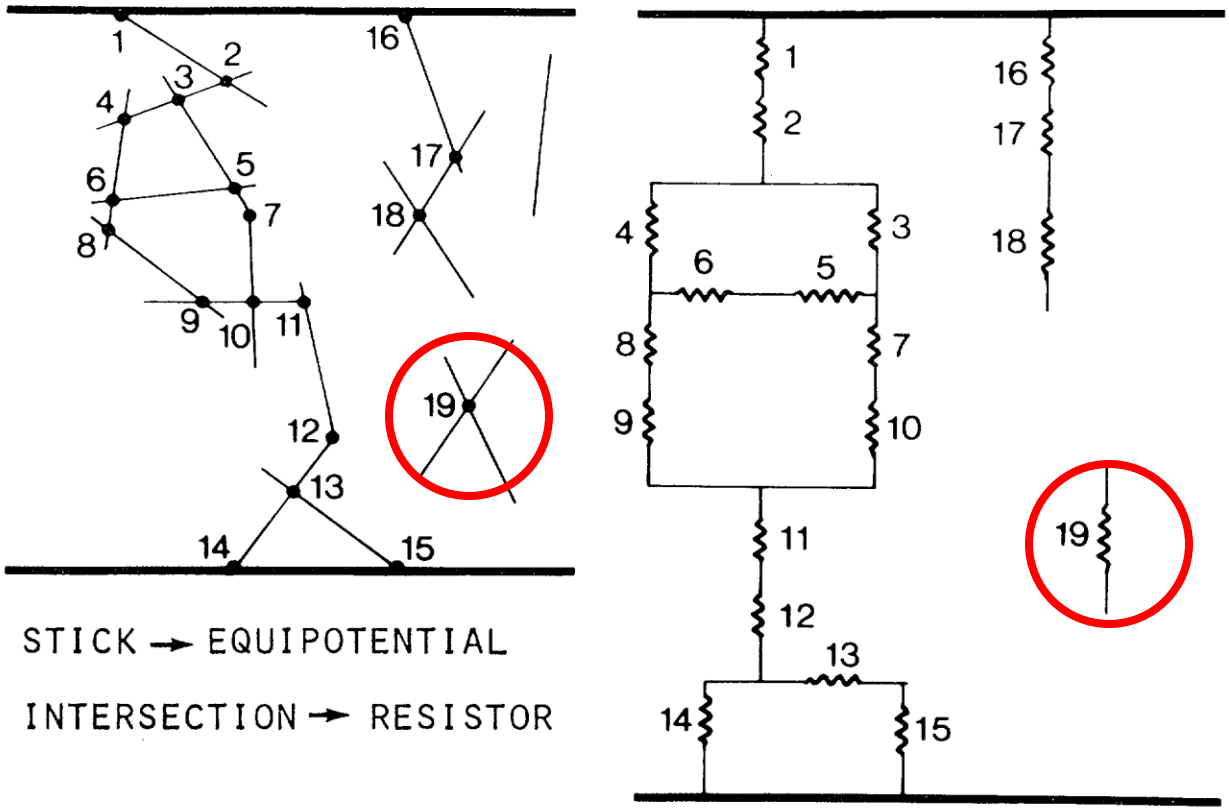

$(I_i) = (g_{ij})(v_i - v_j)$ $\quad (I) = G\,(v)$ $\quad I_1 = -I_N = I,\ I_i\ (i \neq 1,N) = 0$

$R = (v_1 - v_N)/I$ $\quad (v) = G^{-1}(I)$ $\quad G_{ii} = \Sigma g_{i,j},\ G_{ij} = -g_{ji}$

Phys. Rev. B, 28, 3799 (1983): 162 Q

The critical behavior of the resistance of pencil generated line-segments system

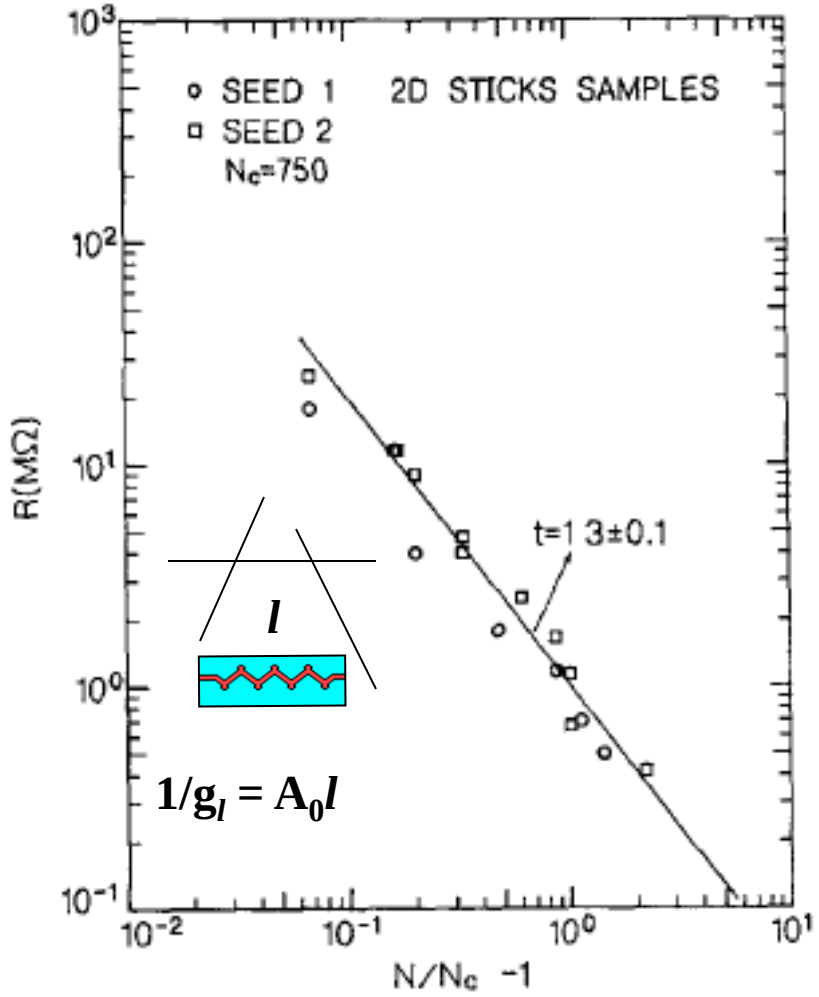

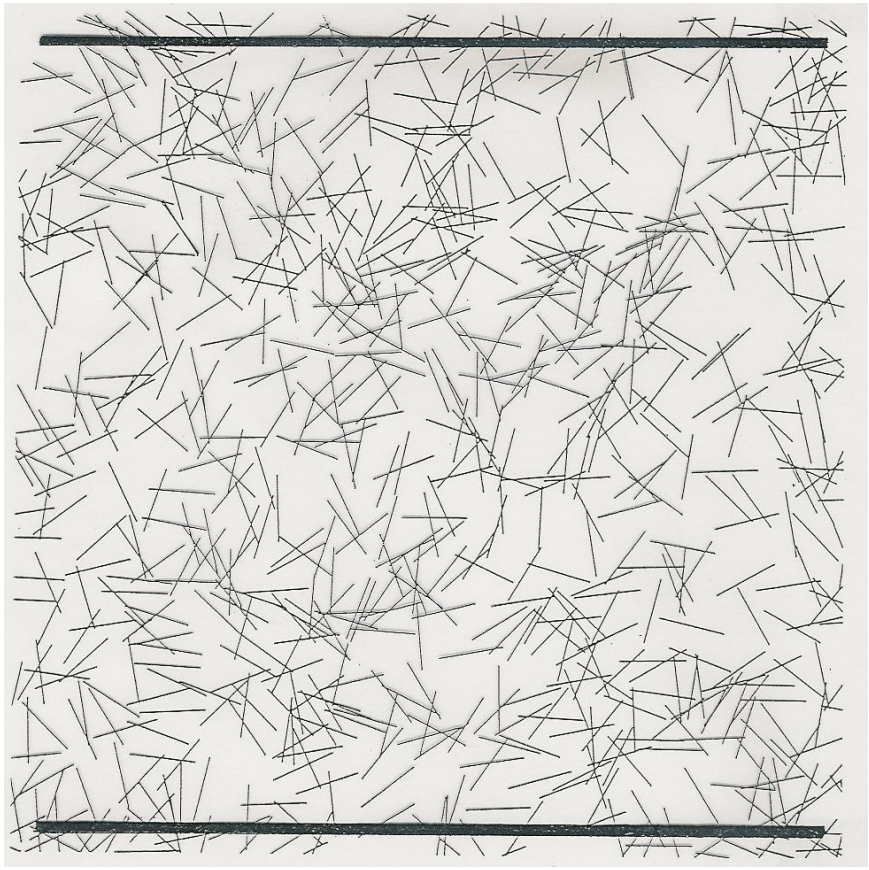

J. Water Resources Research 29, 775 (1993) : 101 Q

Non Universal and Hopping Interpretations

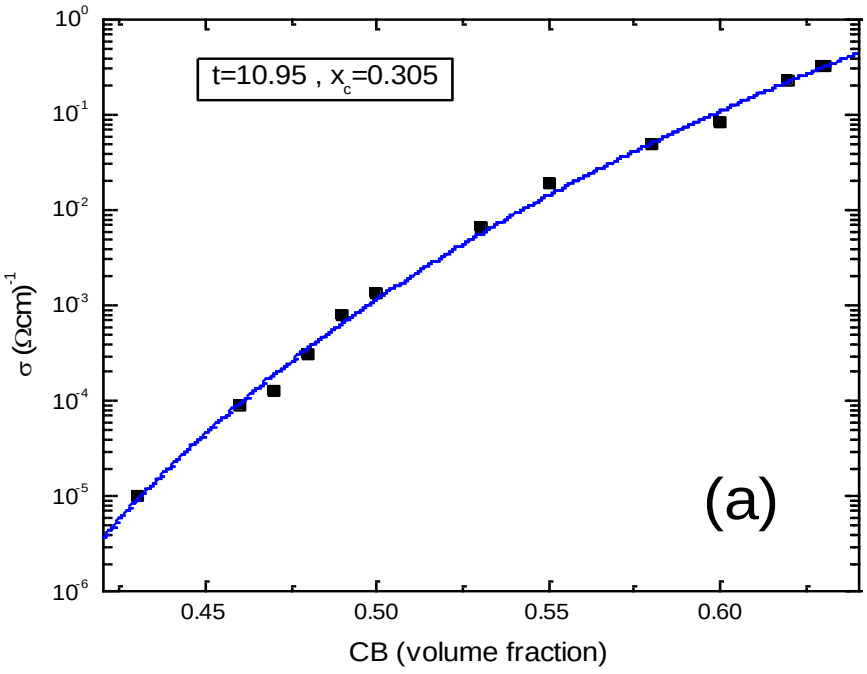

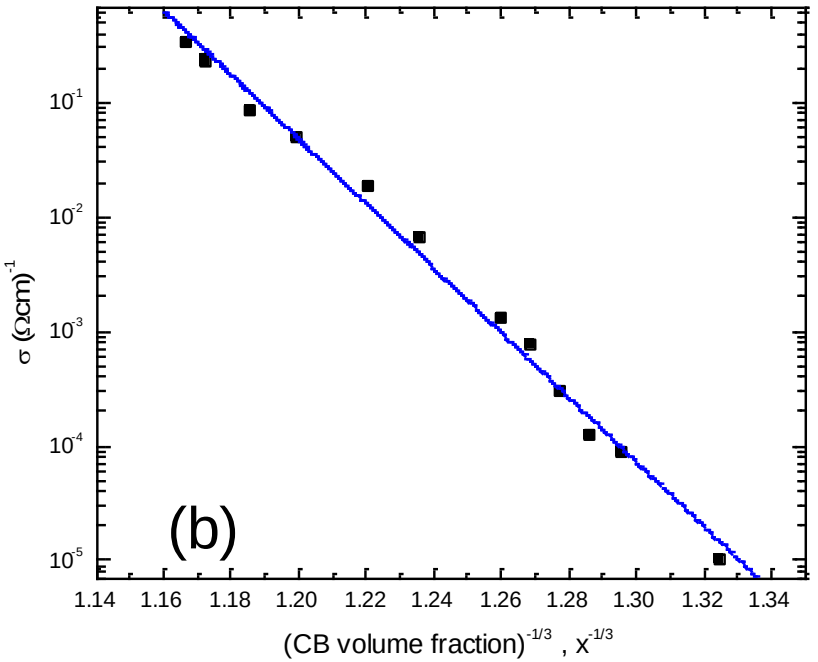

The model of Kogut and Straley

$$f(g) = (1-\alpha)g^{-\alpha}$$

- $\langle r \rangle = \int_{g_c}^{1} [f(g)/g]dg \propto |(g_c^{-\alpha} - 1)|, \; g_c = [(p-p_c)/p]^{1/(1-\alpha)}$
- we have here the three types of $\langle r \rangle = \mathcal{F}(g_c)$ behaviors; strongly-diverges for $0 < \alpha < 1$, logarithmically diverges for $\alpha = 0$ and it will not diverge for $\alpha < 0$.
- Correspondingly: $\langle r \rangle \propto (p-p_c)^{-\alpha/(1-\alpha)}$,
- $\langle r \rangle \propto |\log(p-p_c)|$ and $\langle r \rangle = [(1-\alpha)/(-\alpha)] = \text{const}$.

The basics of non-universal behavior

$$R_L \propto \langle r \rangle (p-p_c)^{-t_{un}}$$

$$\langle r \rangle = \int_{g_c}^{1} (1/g) f(g) dg.$$

$$p\left[\int_{g_c}^{1} f(g) dg\right] = p_c$$

Example (K&S, 1979): $f(g) = (1-\alpha)g^{-\alpha}$ yields that:

$$g_c = [(p-p_c)/p]^{1/(1-\alpha)}$$

$$\langle r \rangle \propto (p-p_c)^{-\alpha/(1-\alpha)} \propto (p-p_c)^{-(t-t_{un})}$$

$$(\langle r \rangle = [(1-\alpha)/(-\alpha)])$$

“RDF” of the polymer shells

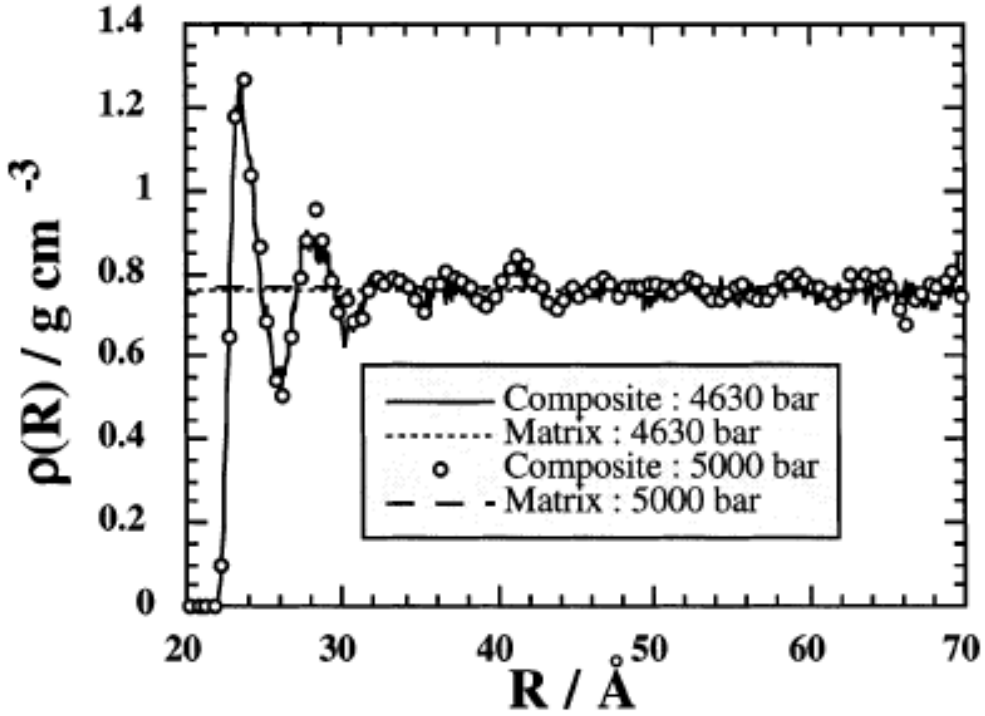

Figure 1. Mass density of the polymer as a function of R, the distance from the center-of-mass of the silica particle. The dotted and dashed lines give the limiting, large R, densities as determined from the pure polymer matrix simulations at the pressures shown.

“RDF” of the polymer shells

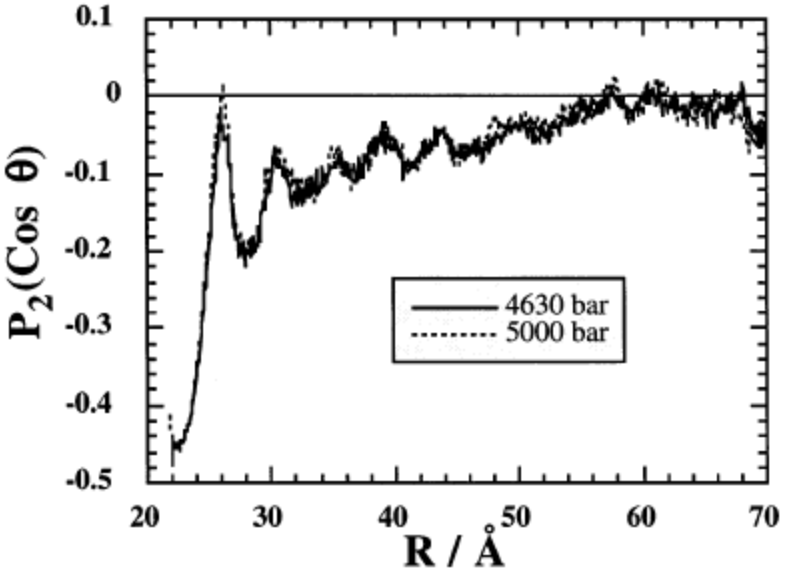

Figure 3. Mean values of $P_2(\cos\theta)$ plotted as a function of R for the composite system at the two pressures shown. θ is the angle between the local polymer chain axis and the outwardly pointing vector normal to the nanoparticle surface. An alignment of the chains parallel to the nanoparticle surface implies a value of $-1/2$ (small R). A random alignment corresponds to a value of zero (large R).

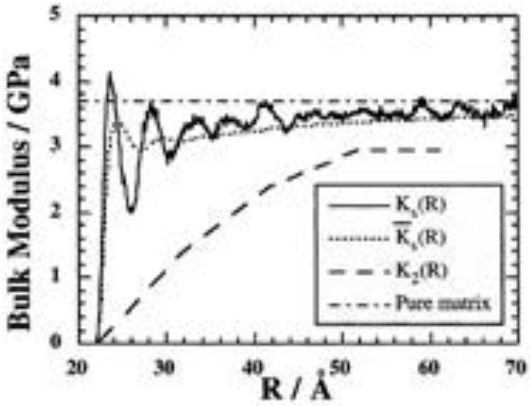

Figure 8. Smooth approximation to the radial dependent bulk modulus $K_s(R)$ for the interphase region of the polymer matrix as determined from eq 14. Also shown is the mass-weighted running average of this function, $\bar{K}_s(R)$, and the corresponding bulk modulus based on the micromechanical calculations, $K_2(R)$.

Evidence for stairs in MWCNT-polymer composites

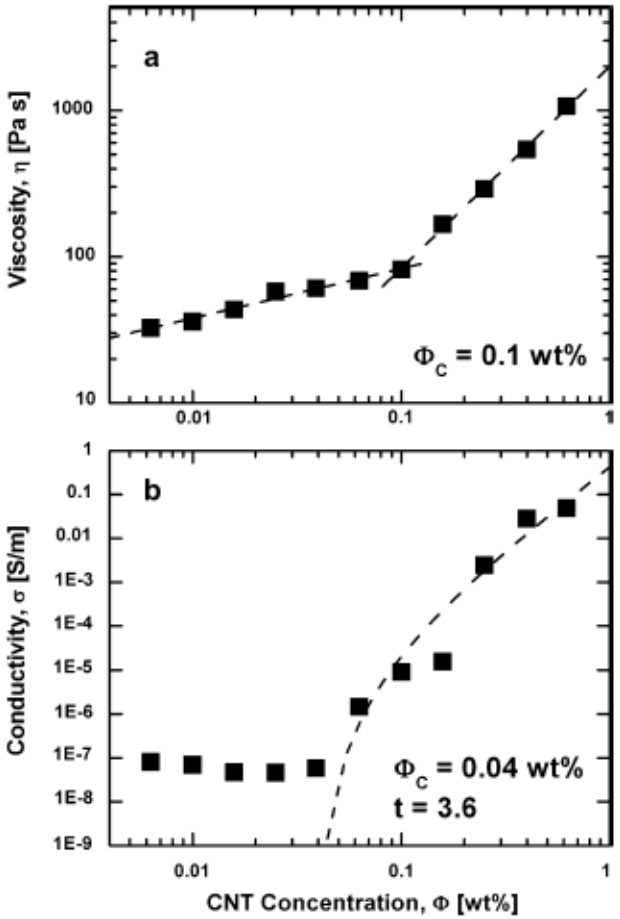

Fig. 4. Simultaneous measurement of the nanocomposite (MWCNT/epoxy) viscosity (a) and electrical conductivity (b) as function of the nanotube weight fraction, performed in the liquid state prior to curing at 0.1 s^{-1} and 20 °C. The rheological percolation threshold is located at 0.1 wt% and the electrical one at 0.04 wt%.

Some idea about the materials

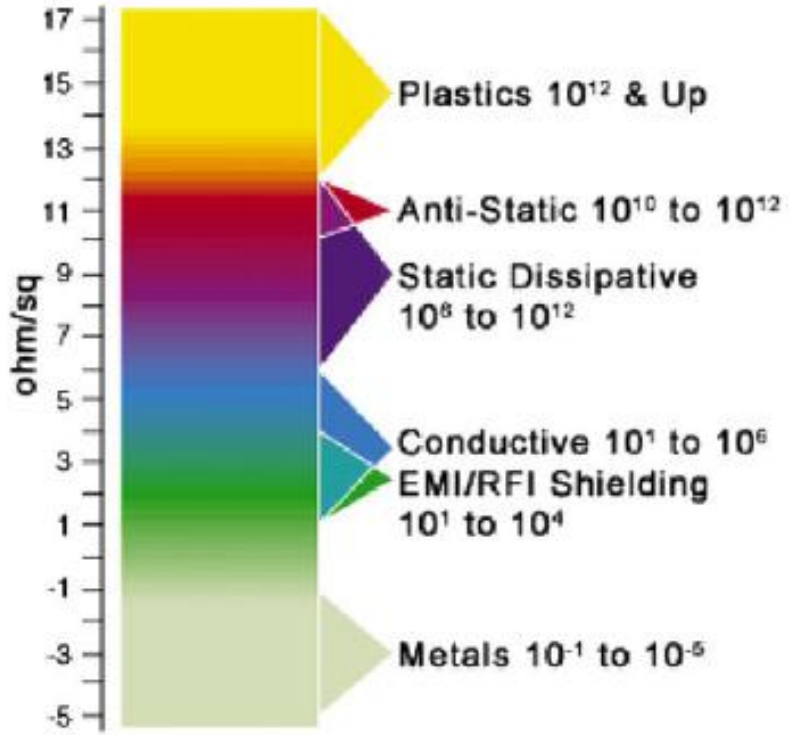

Fig. 1 – Classification of materials according to their surface resistivity and application ranges. (Note: [cited 2007 July]; Available from: http://www.rtpcompany.com/products/conductive/index.htm.)

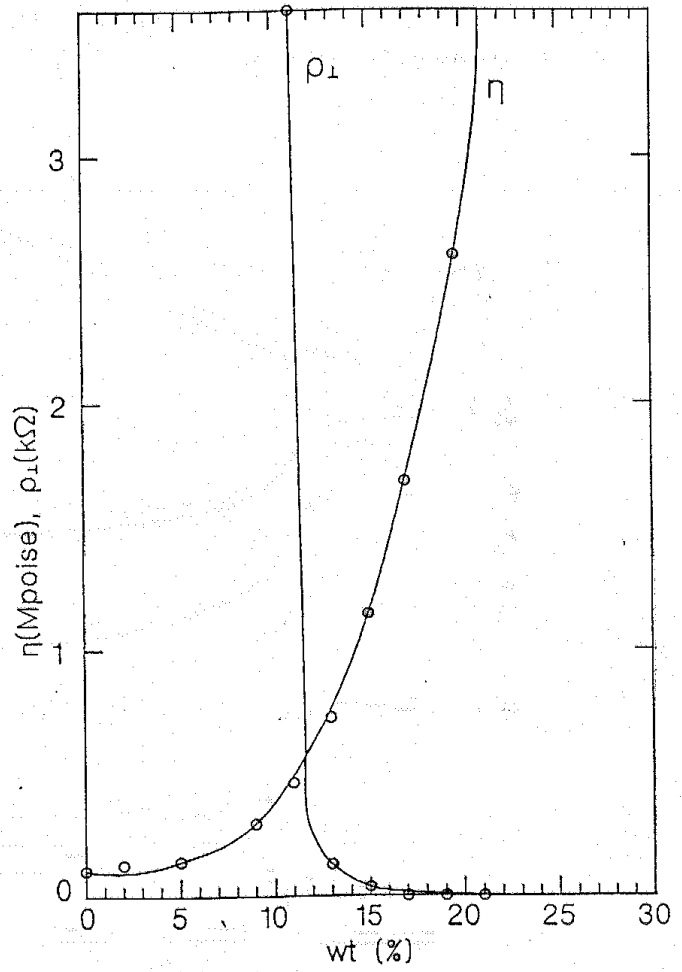

Evidence for stairs in MWCNT-polymer composites

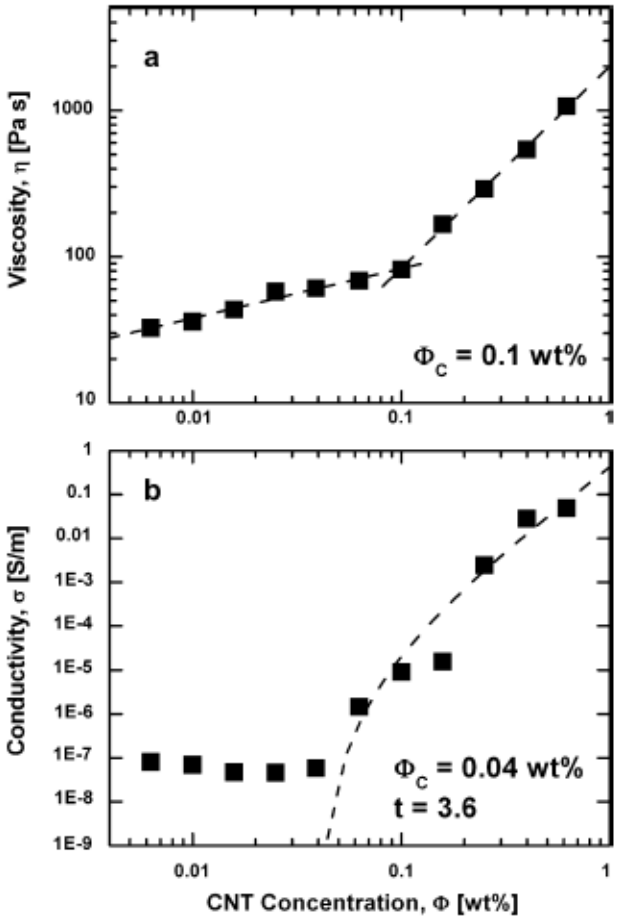

Fig. 4. Simultaneous measurement of the nanocomposite (MWCNT/epoxy) viscosity (a) and electrical conductivity (b) as function of the nanotube weight fraction, performed in the liquid state prior to curing at 0.1 s^{-1} and 20 °C. The rheological percolation threshold is located at 0.1 wt% and the electrical one at 0.04 wt%.

Conductivity and viscosity

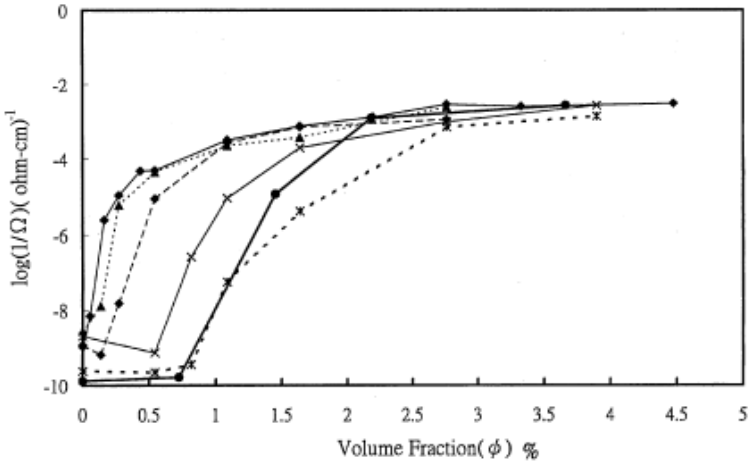

Fig. 1 Dependence of the electrical conductivity on the volume fraction of carbon black dispersed in PDMS liquids with various viscosities. *Diamonds on solid line* 10 cp, *triangles* 100 cp, *diamonds on dotted line* 500 cp, *crosses* 1000 cp, *asterix* 60 000 cp, *circles* silicon rubber

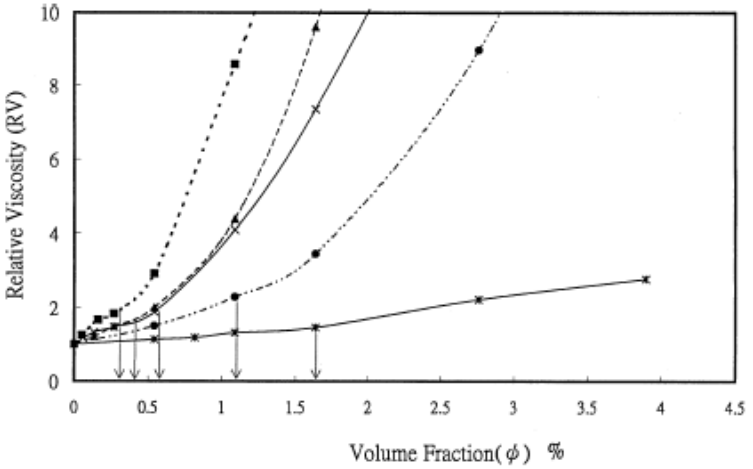

Fig. 3 Dependence of relative viscosity (RV) on the volume fraction of carbon black dispersed in PDMS liquids with various viscosities. *Squares* 10 cp, *triangles* 100 cp, *crosses* 500 cp, *circles* 1000 cp, *asterix* 60 000 cp

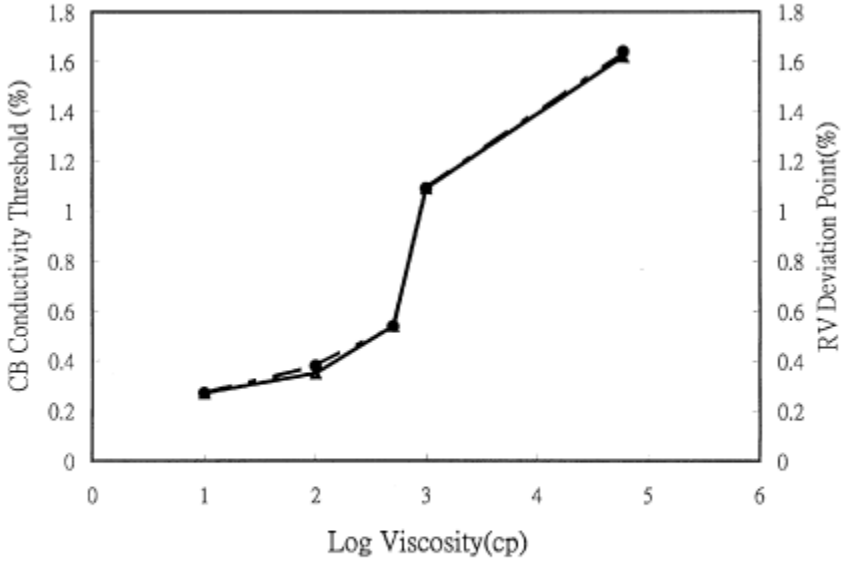

Fig. 5 Dependence of the RV deviation point and threshold conductivity on PDMS viscosity. *Triangles* CB conductivity threshold, *circles* RV deviation point

Conductivity and viscosity

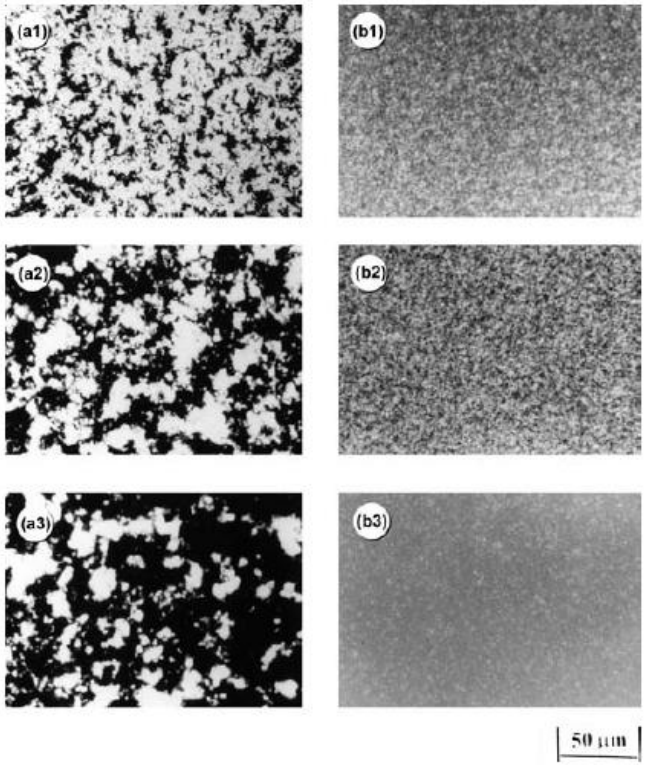

Fig. 2a, b Optical micrographs for carbon black aggregates dispersed in PDMS liquids. Dispersion of 0.13%, 0.27%, and 0.54% carbon black by volume into 500 cp PDMS are shown in **a.**1 to **a.**3. The correspondent conductivities are 6.36×10^{-10}, 1.50×10^{-8}, and 9.04×10^{-6} $(\Omega\text{-cm})^{-1}$, respectively. In contrast, dispersion of 0.81%, 1.09%, and 1.64% carbon black by volume into 60 000 cp PDMS are shown in **b.**1 to **b.**3. The correspondent conductivities are 3.56×10^{-10}, 5.63×10^{-8}, and 4.21×10^{-6} $(\Omega\text{-cm})^{-1}$, respectively

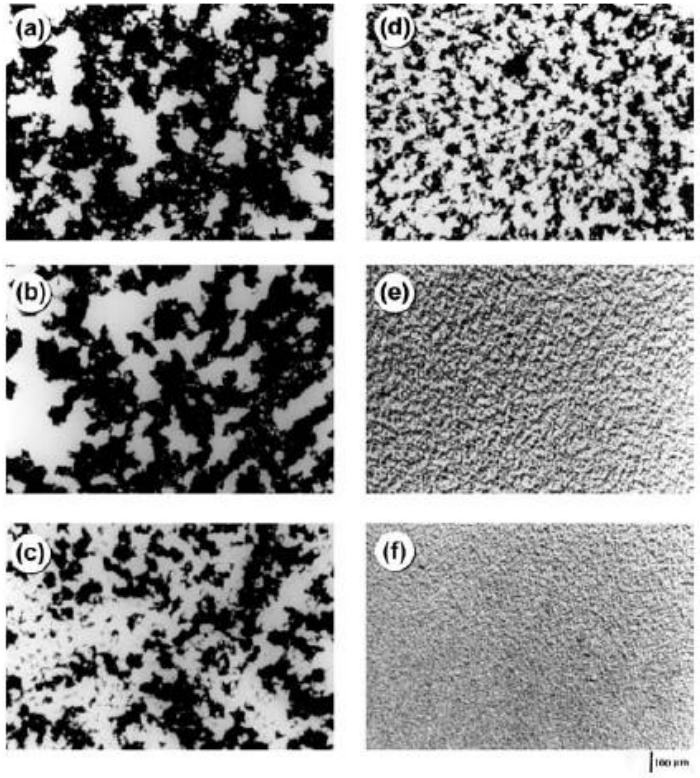

Fig. 4a–f Optical micrographs for 0.43% volume fraction of carbon black dispersed in PDMS liquids with various viscosities: **(a)** 10 cp **(b)** 100 cp **(c)** 500 cp **(d)** 1000 cp **(e)** 10 000 cp **(f)** 60 000 cp

RDF and Cumulative coordination number

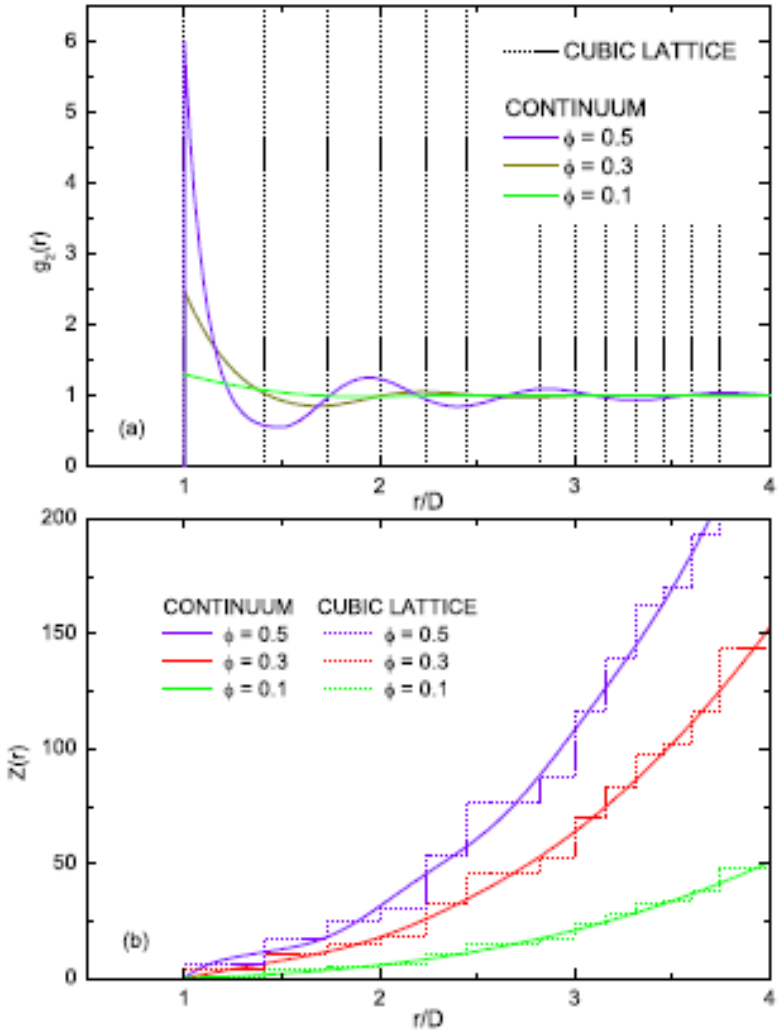

RDF in the Continuum

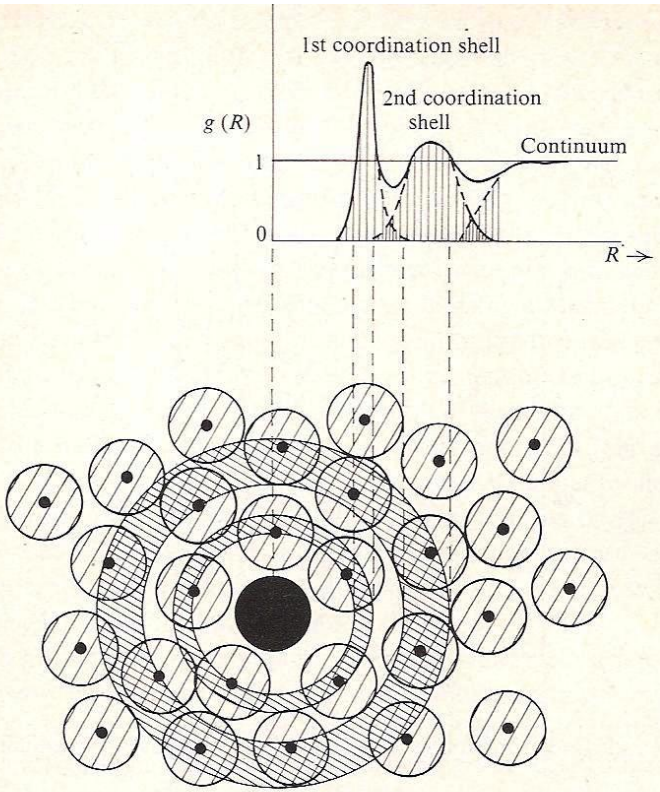

Fig. 2.27. 'Features' of the radial distribution function.

Statistics of the t values in CNT-polymer composites

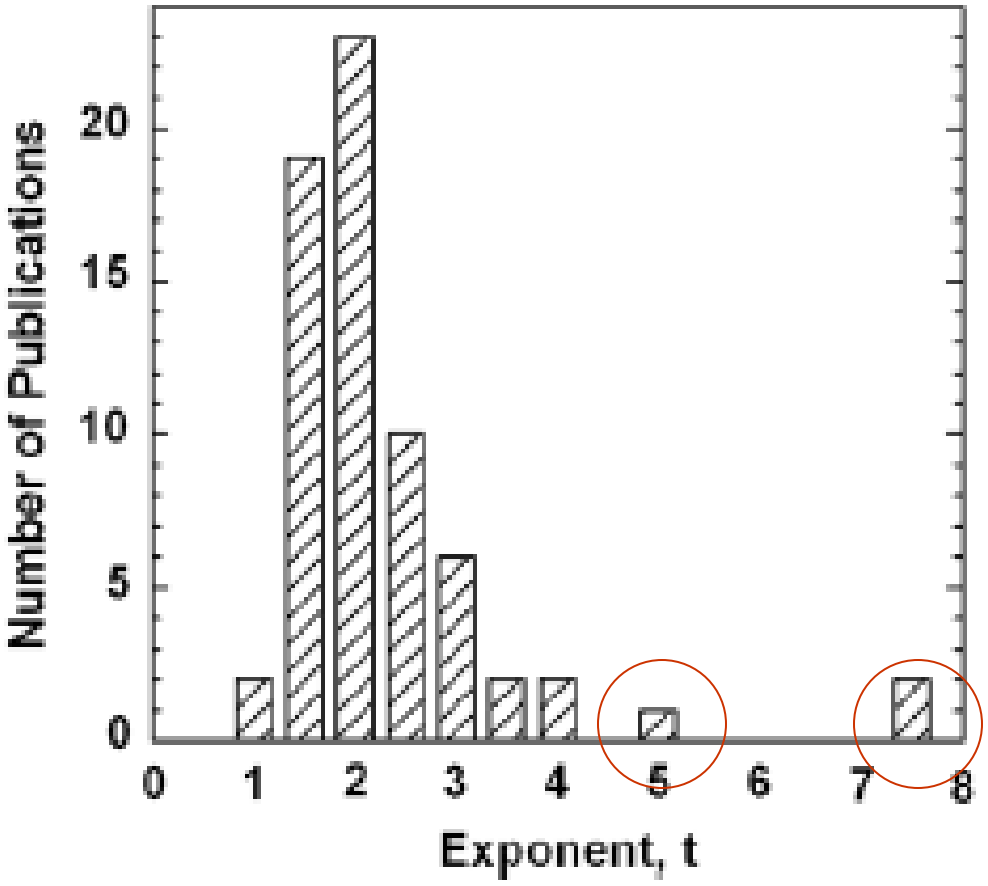

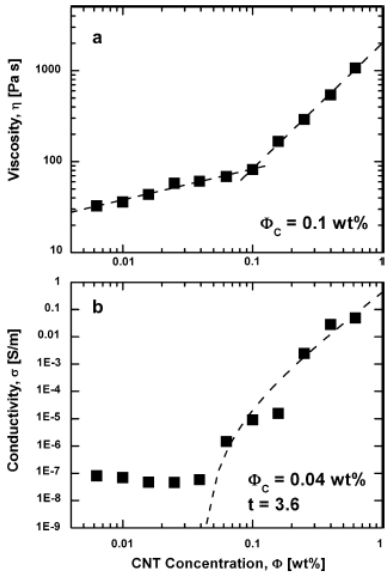

Fig. 4. Simultaneous measurement of the nanocomposite (MWCNT/epoxy) viscosity (a) and electrical conductivity (b) as function of the nanotube weight fraction, performed in the liquid state prior to curing at 0.1 s^{-1} and 20 °C. The rheological percolation threshold is located at 0.1 wt% and the electrical one at 0.04 wt%.

Fig. 7. Plot of the power law exponent t as a function of (a) the maximum conductivity and (b) the percolation threshold for all data in Table 1. The horizontal lines denote $t = 1.3$ and 4. Fig. 7 (c) shows a histogram of t values.

Two presentations of the same data

Percolation interpretation

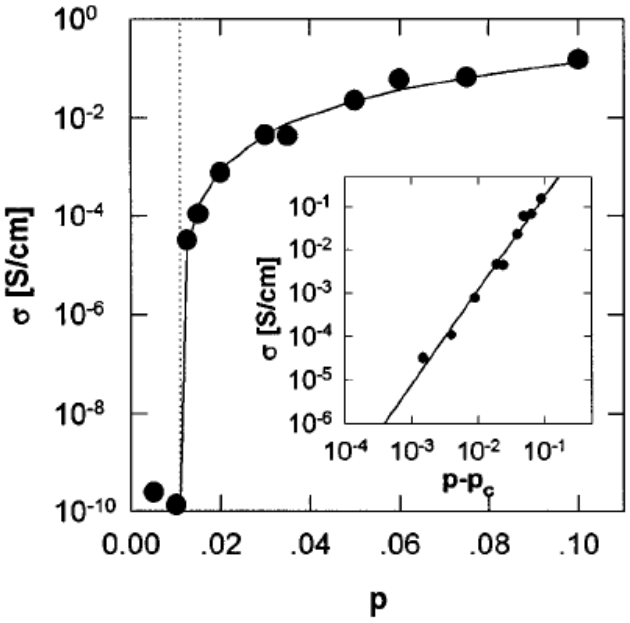

FIG. 1. Plot of σ as a function of carbon black volume content, p of composites; the critical concentration p_c has been determined using Eq. (1) ($p_c = 1.1\%$); inset: log-log plot of σ as a function of $p - p_c$; ($t = 2.17$).

"hopping" interpretation

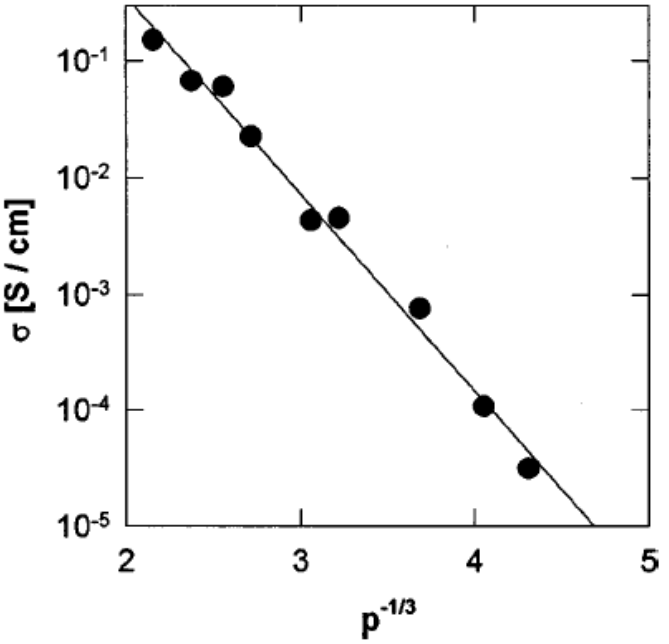

FIG. 2. Linear variation of $\ln\sigma$ vs $p^{-1/3}$.

Non Universal and Hopping Interpretations

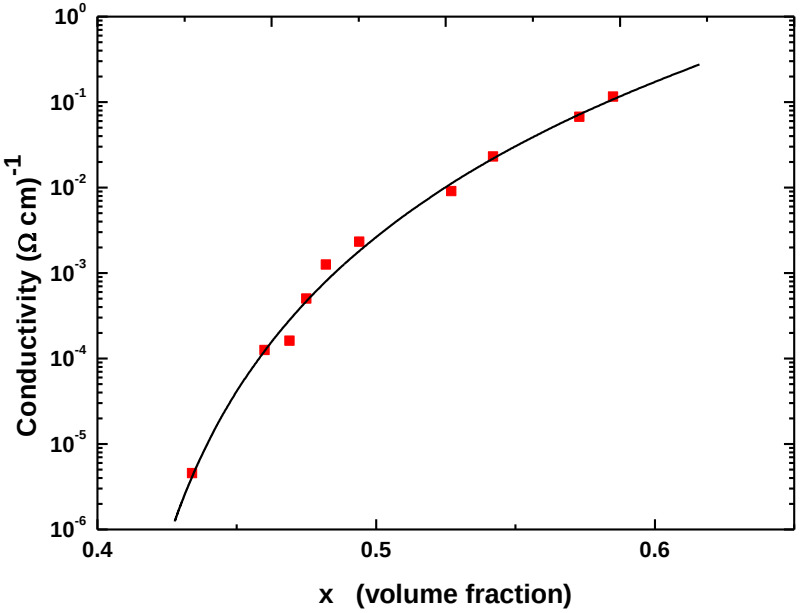

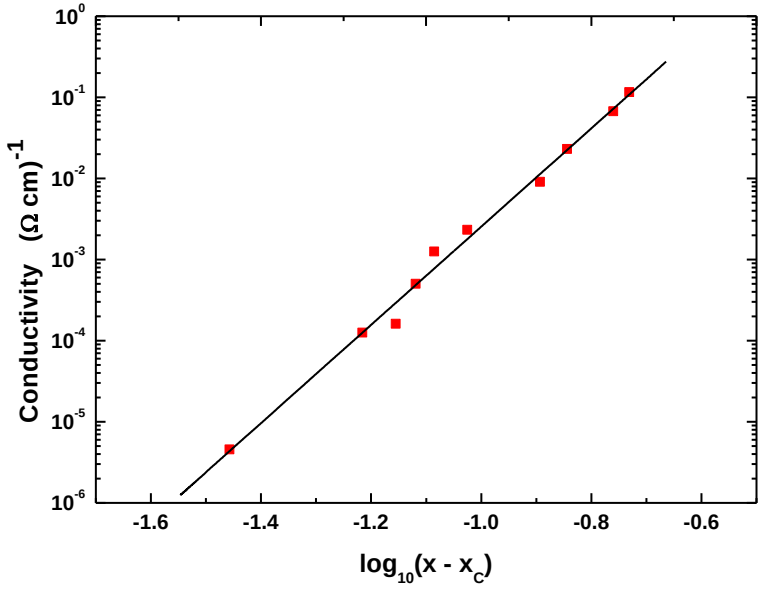

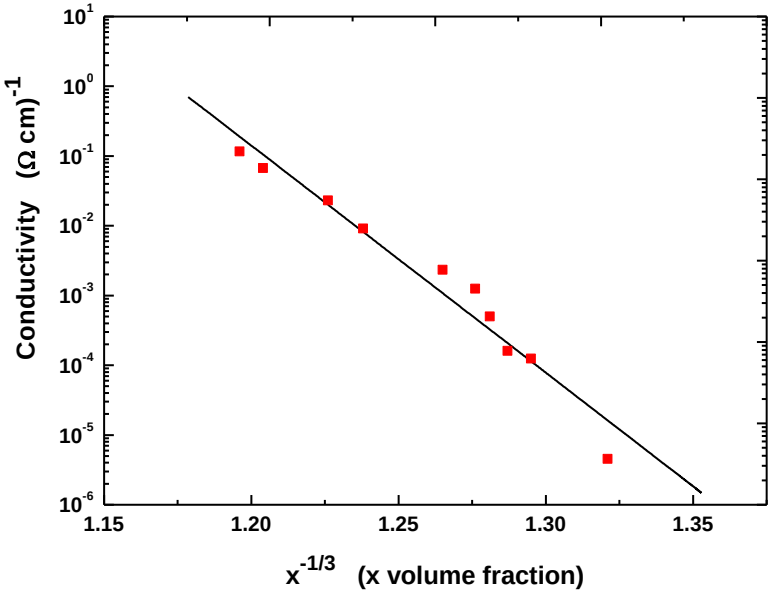

The physical and mathematical resemblance of the percolation and (CPA) hopping behaviors:

In the classical hopping (CPA) model :

$$\log \sigma = -\delta_c/\xi + \log A_1 = -(a_\beta/\xi)x^{-\beta} + \log A_1 \qquad 1/3 \le \beta \le 1$$

In our percolation model: $\log \sigma = t \log(x-x_c) + \log A_2$

and we saw (from the Excluded volume argument) that

$t = t_{un} + d/\xi - 1$ **so that for** $t >> t_{un}$ **we have that** $t \approx -(x^{-\beta})/\xi$

where $1/3 \le \beta \le 1$ **and** $\log (x-x_c) < 0$.

- **The two models yield then quite a similar dependence on x. Experimentally; since usually** $x >> x_c$ **these two are usually non distinguishable. Can we still distinguish between them?**

Presentation of the CPA results in the case of spheres

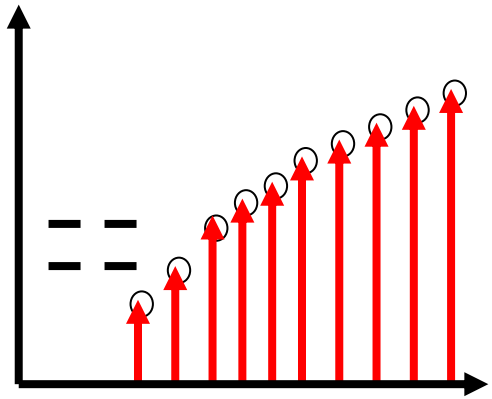

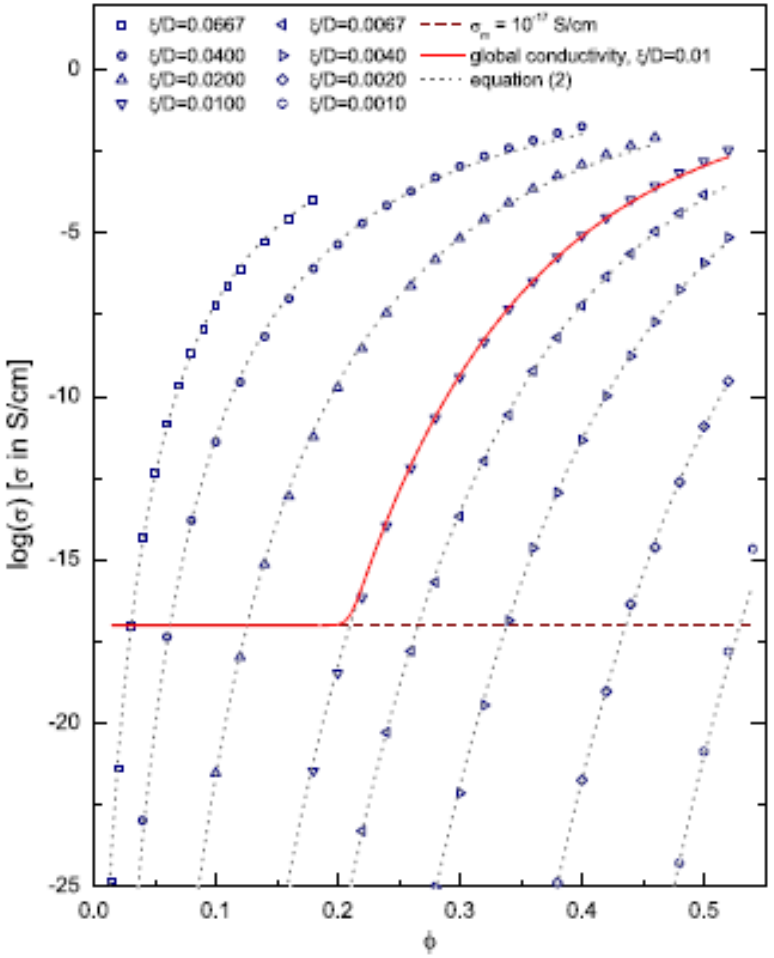

FIG. 1. (Color online) Tunneling conductivity in a system of spheres with different characteristic tunneling distance to spheres diameters ratio ξ/D as a function of the volume fraction ϕ. The matrix intrinsic conductivity for $\sigma_m=10^{-17}$ S/cm and the overall conductivity for the $\xi/D=0.01$ case are shown. Results from Eq. (2) with $\sigma_0=0.115$ S/cm are displayed by dotted lines

CB-polymer composites

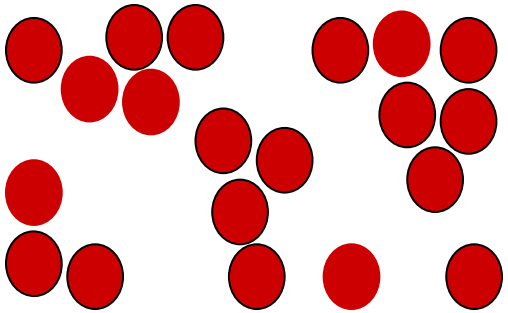

R_λ ($\geq r_0 L_1$)

$R_L = R_\lambda (L/\lambda)/(L/\lambda)^{D-1}$

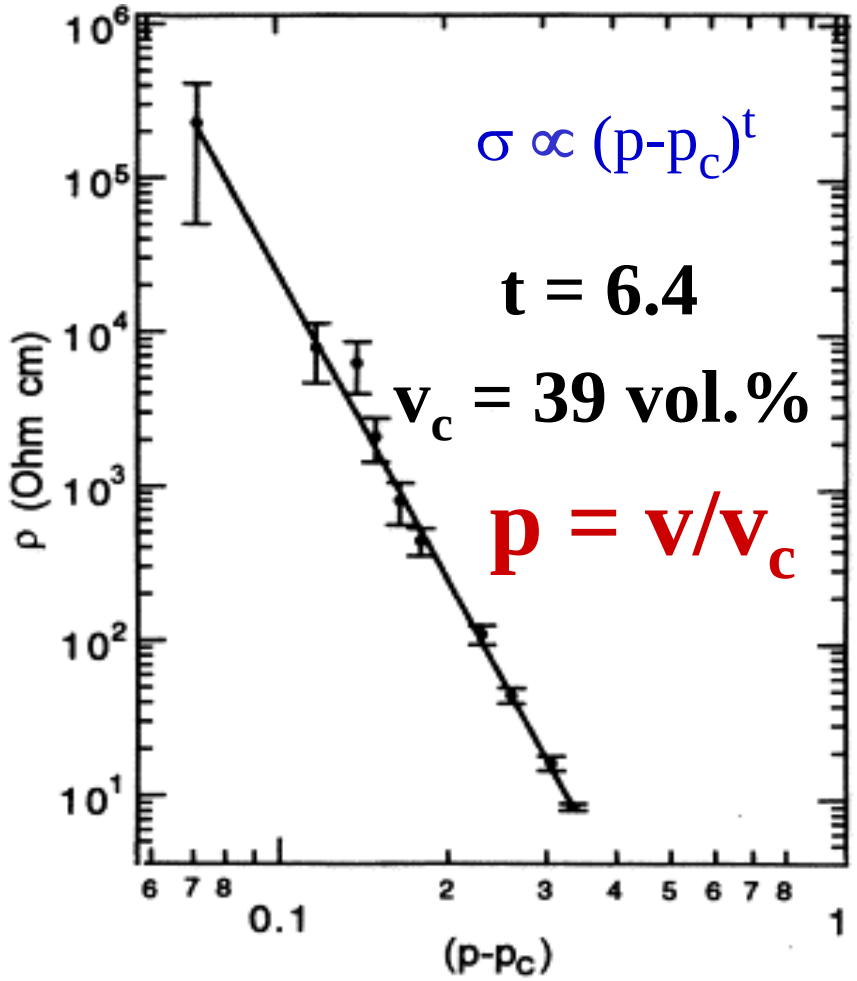

$\sigma \propto (p-p_c)^t$

t = 6.4

v_c = 39 vol.%

$p = v/v_c$

- Non universal value of t ≈ 6 for low structured CB composites

Phil. Mag. B, 56, 991 (1987): 142Q

Non Spherical Fillers

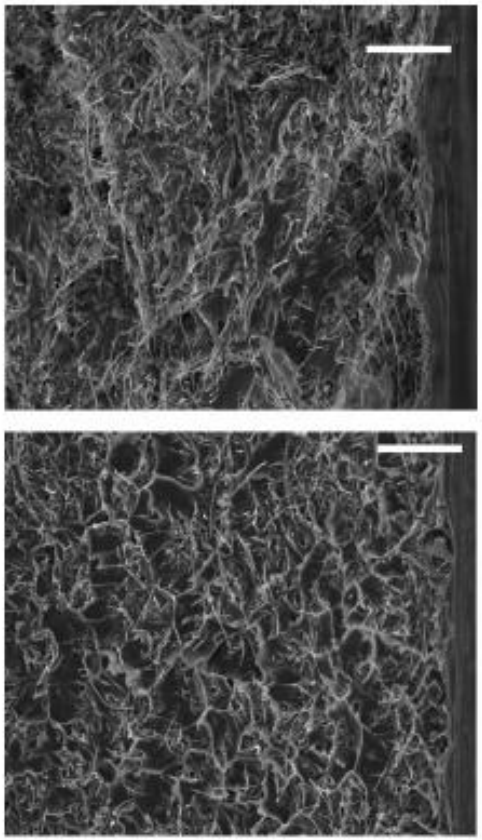

Figure 1. Scanning electron micrographs of the freeze-fractured surfaces of 5PCNF (top) and 5FCNF (bottom) systems, displaying the CNF dispersion throughout the film thickness. The scale bar is 10 μm.

Graphene composites

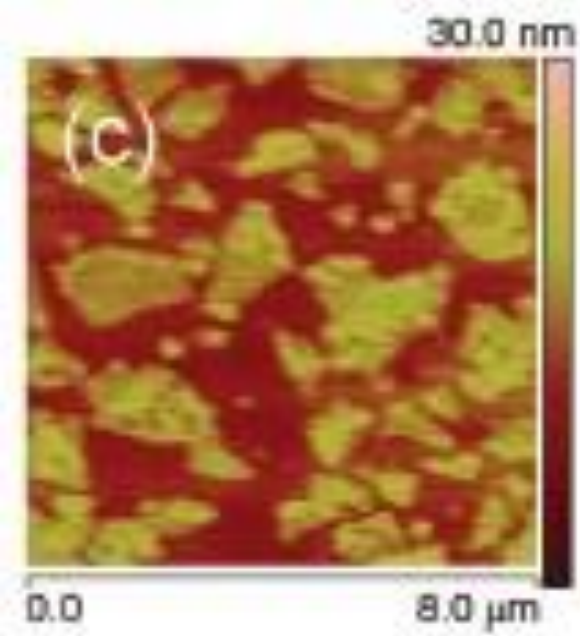

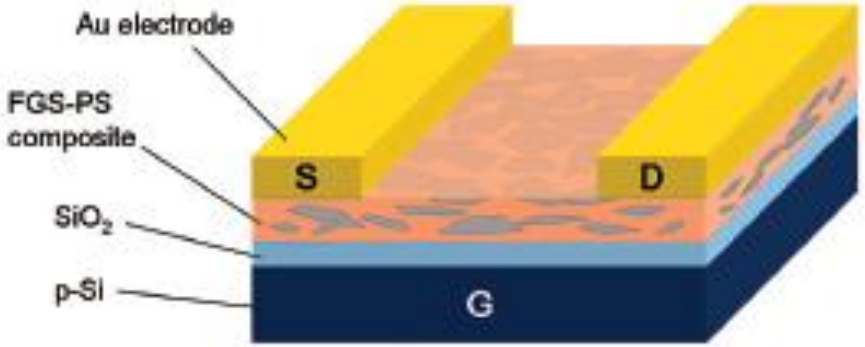

GTN for colloidal conductor-insulator composites

effects of particle shape asymmetry: spheroids (ellipsoids of revolution)

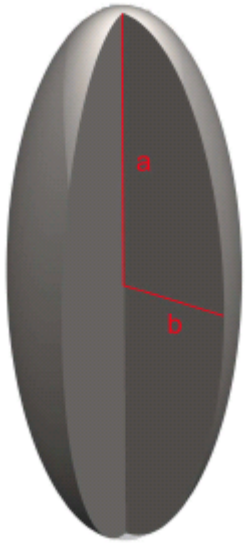

prolate spheroid (a/b >1)

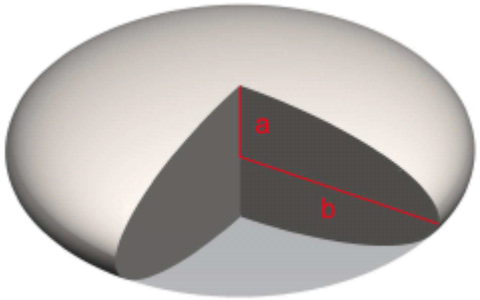

oblate spheroid (a/b <1)

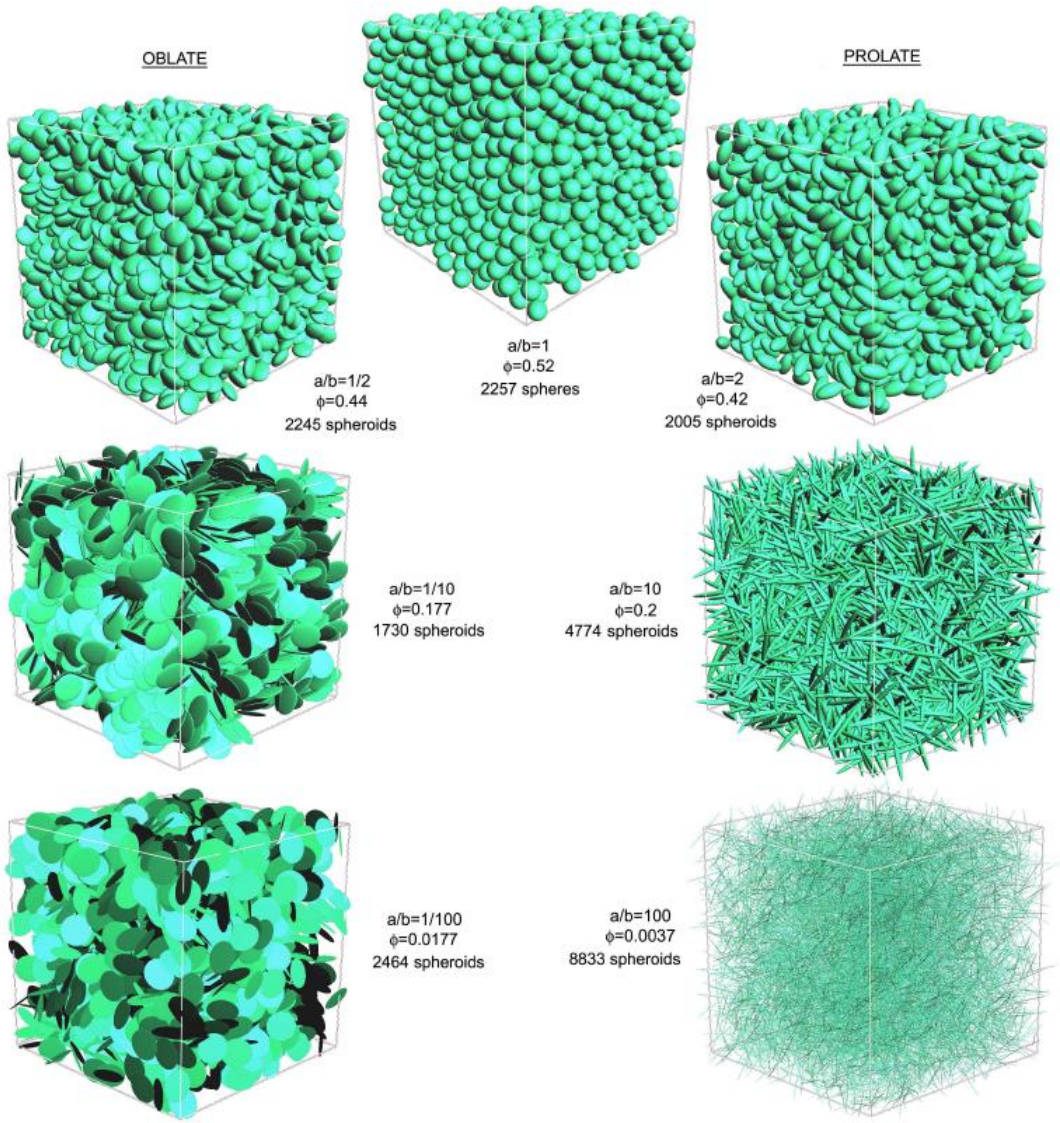

σ(v) behaviors

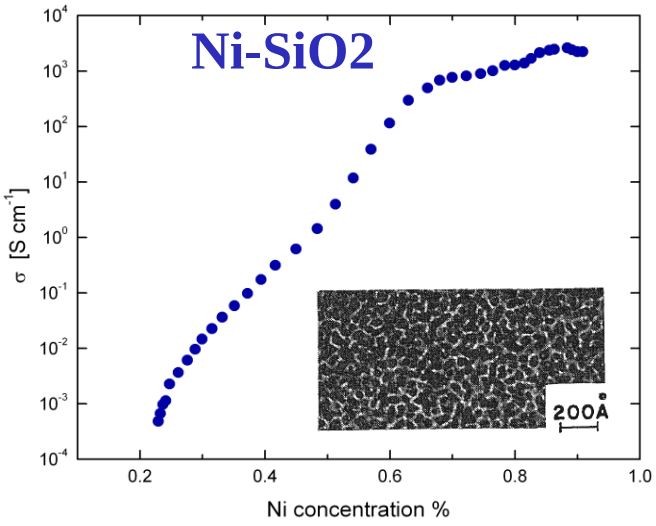

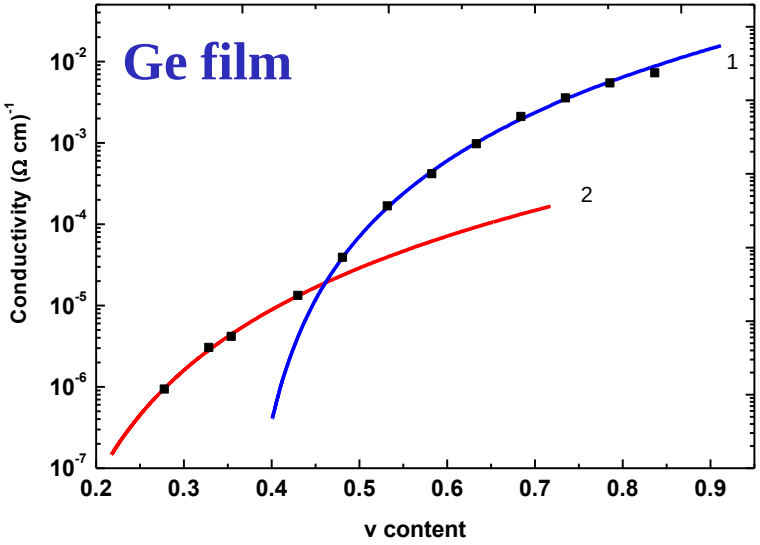

Typical behavior of all composites

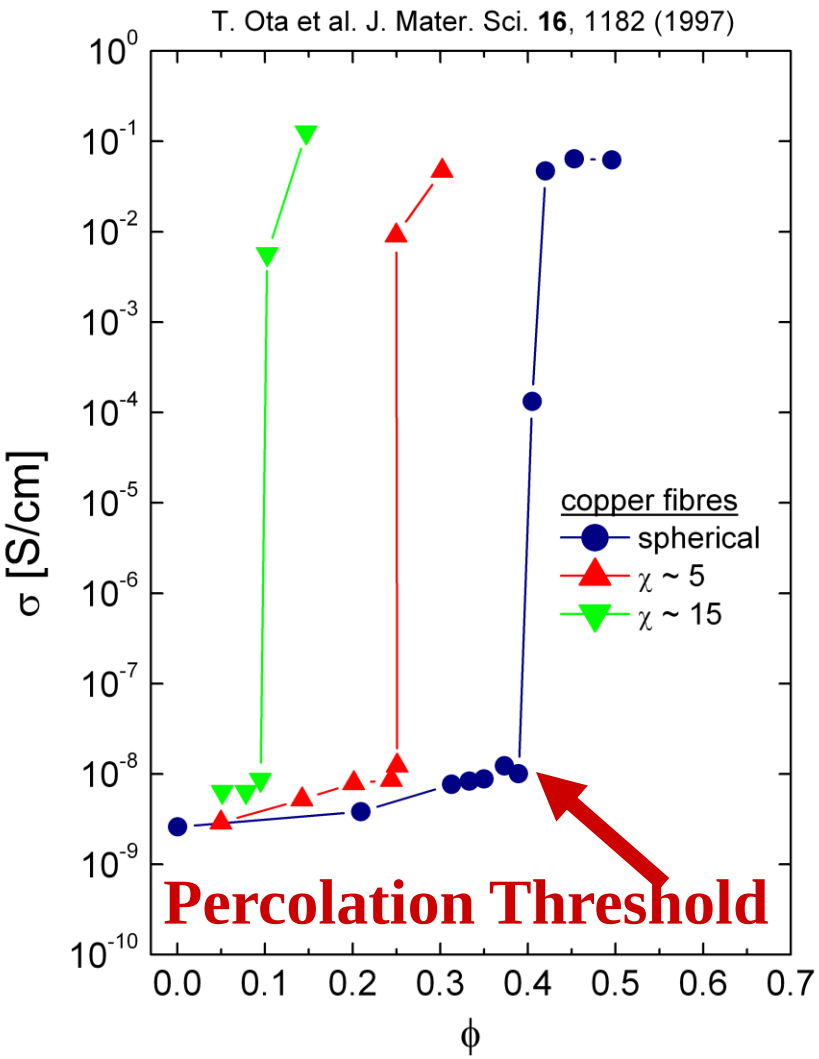

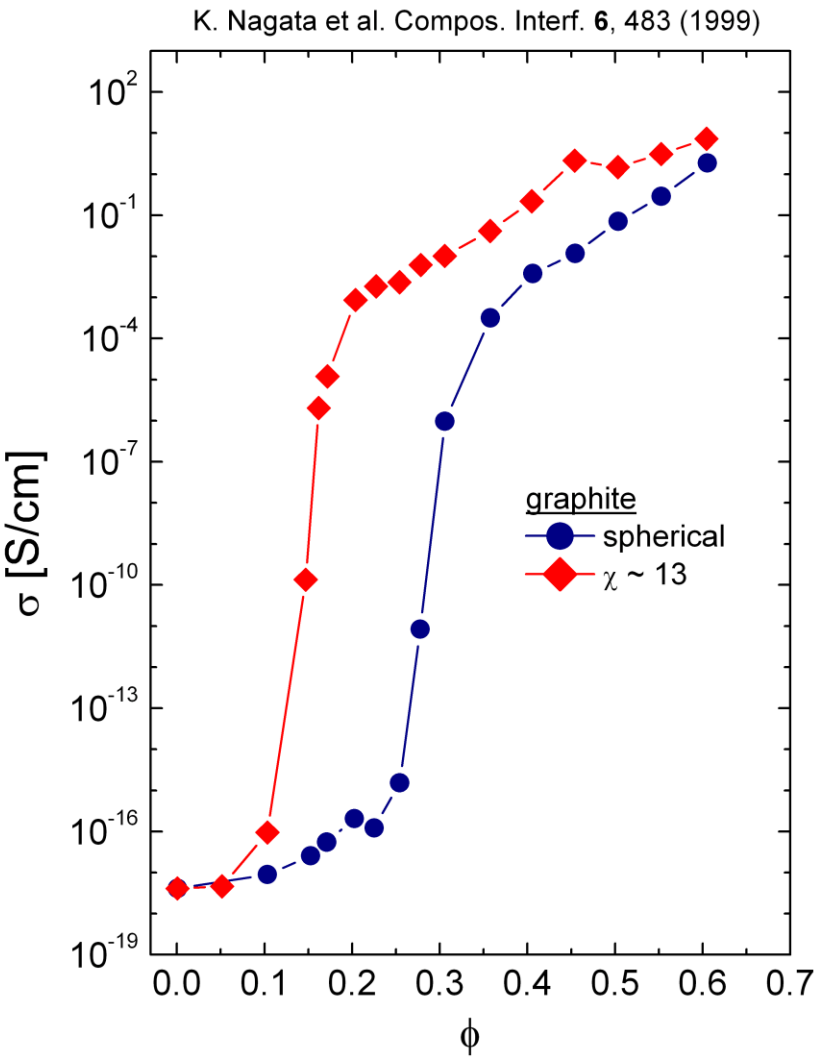

Graphene-based composite materials

Sasha Stankovich[1]*, Dmitriy A. Dikin[1]*, Geoffrey H. B. Dommett[1], Kevin M. Kohlhaas[1], Eric J. Zimney[1], Eric A. Stach[3], Richard D. Piner[1], SonBinh T. Nguyen[2] & Rodney S. Ruoff[1]

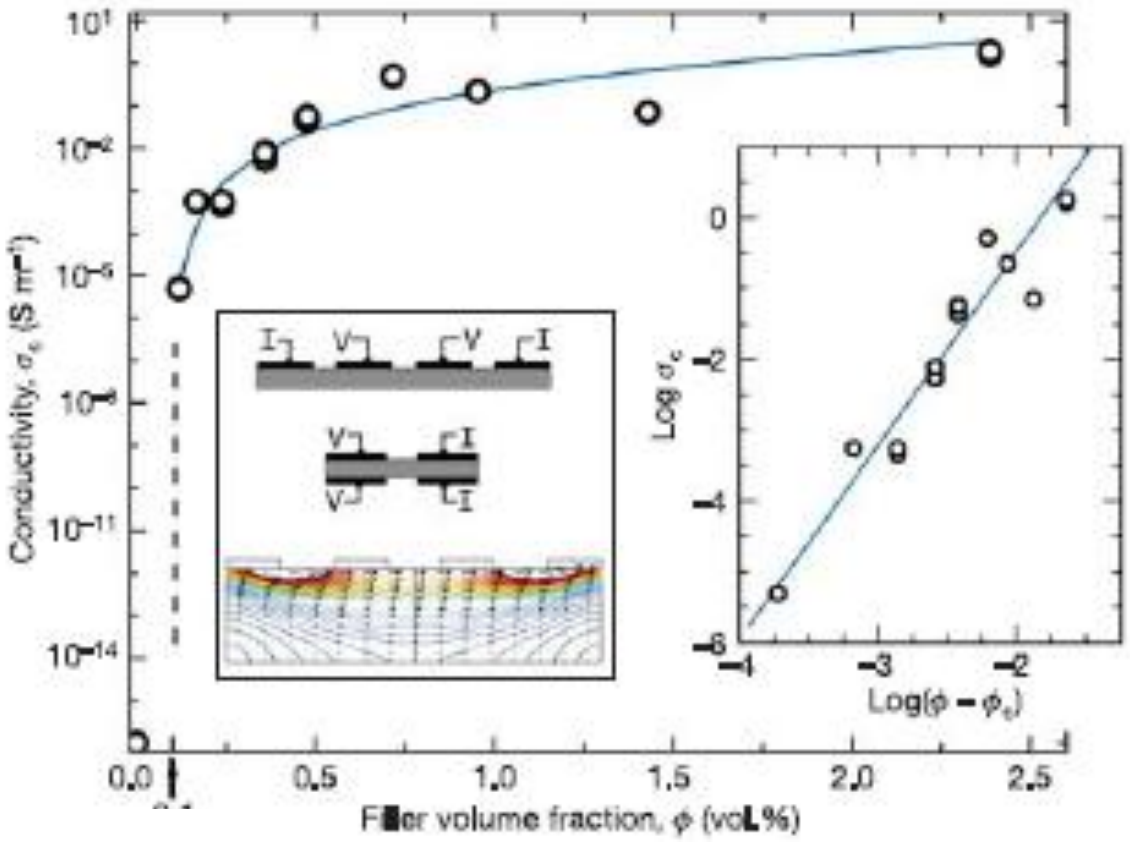

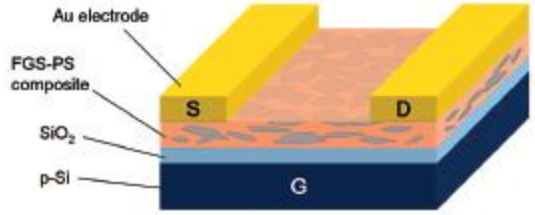

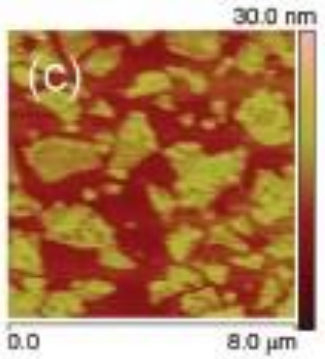

Non Universal behavior

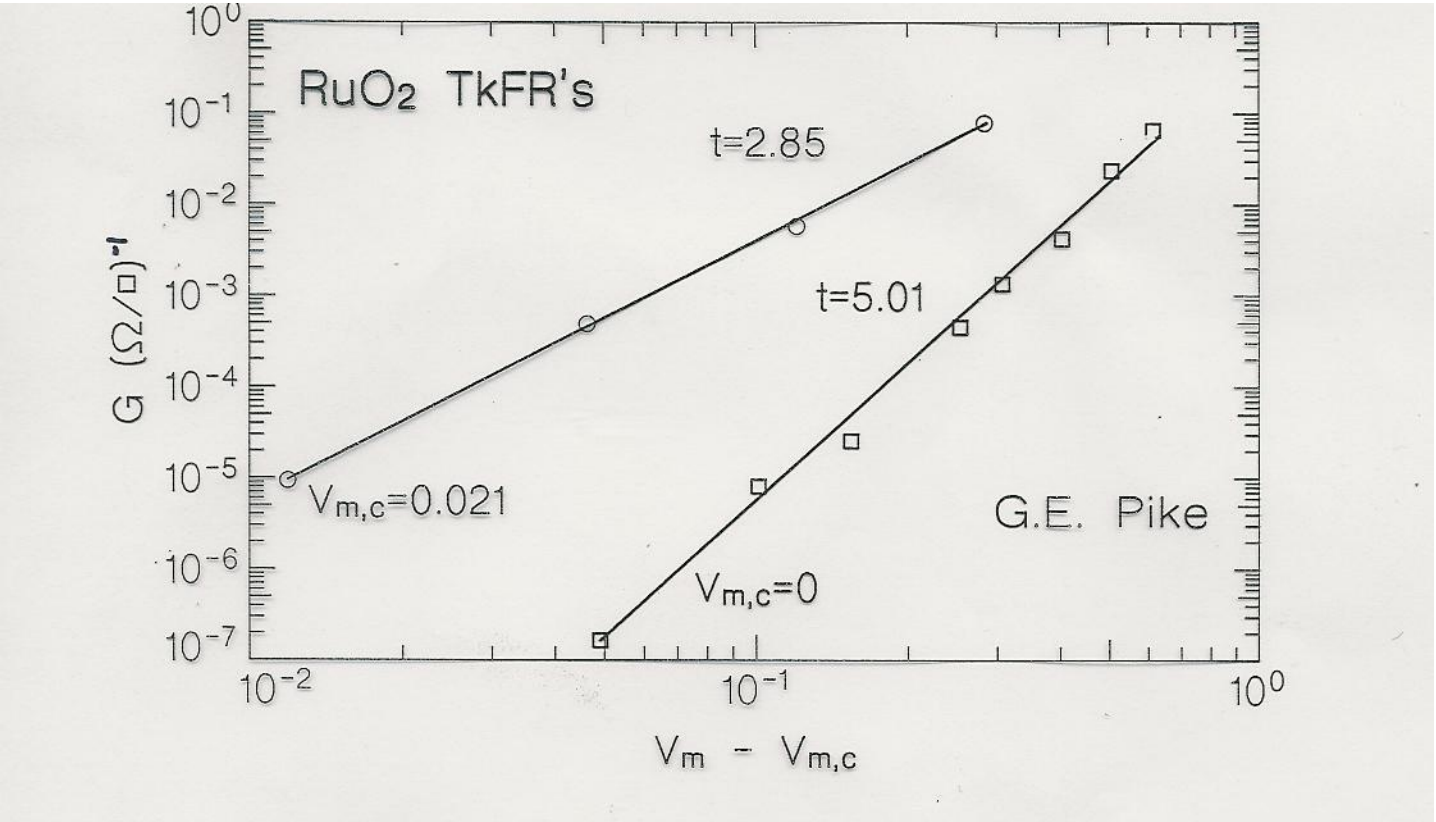

Geometry of Local Resistors

IRV-like (microemulsions)

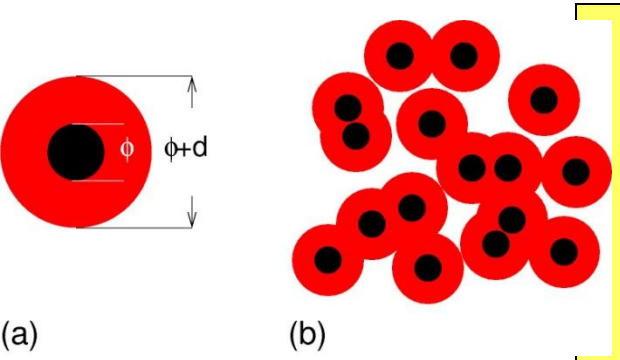

IRV (porous media, impurities in SC model)

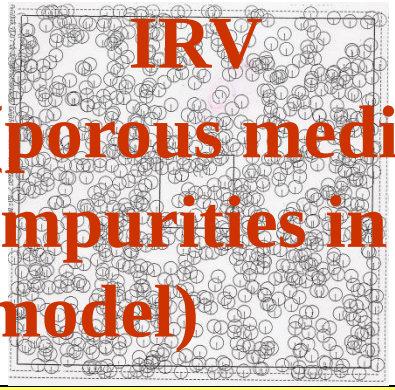

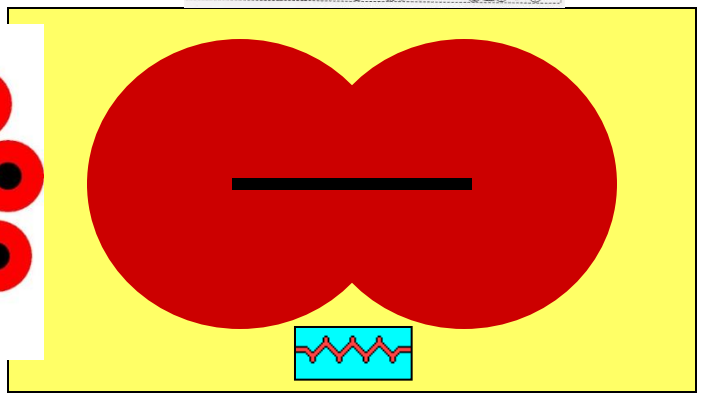

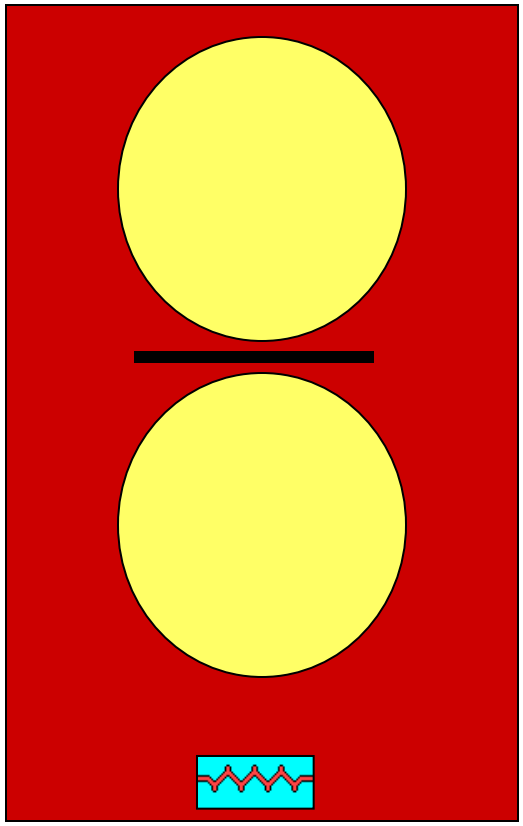

RV

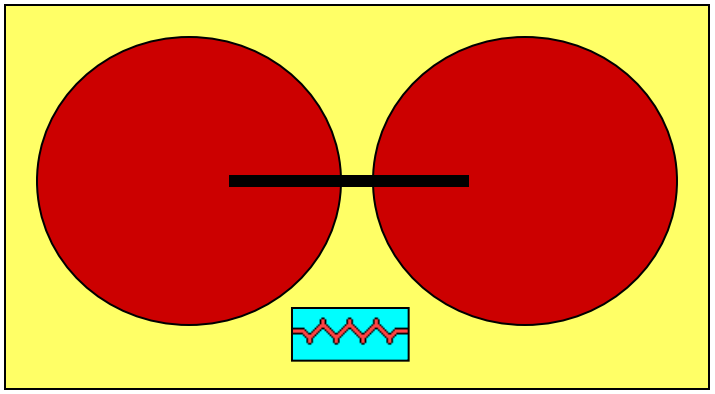

PT

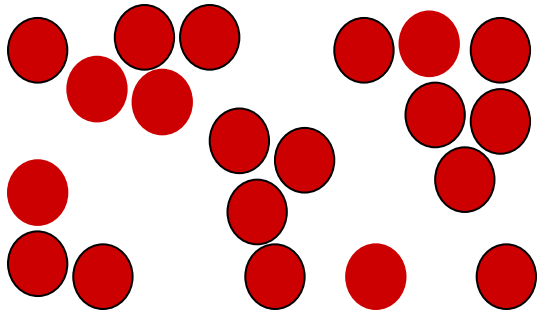

Local connectivity criterion?

A percolation threshold (critical resistor) system vs. a critical percolation (phase transition like) system

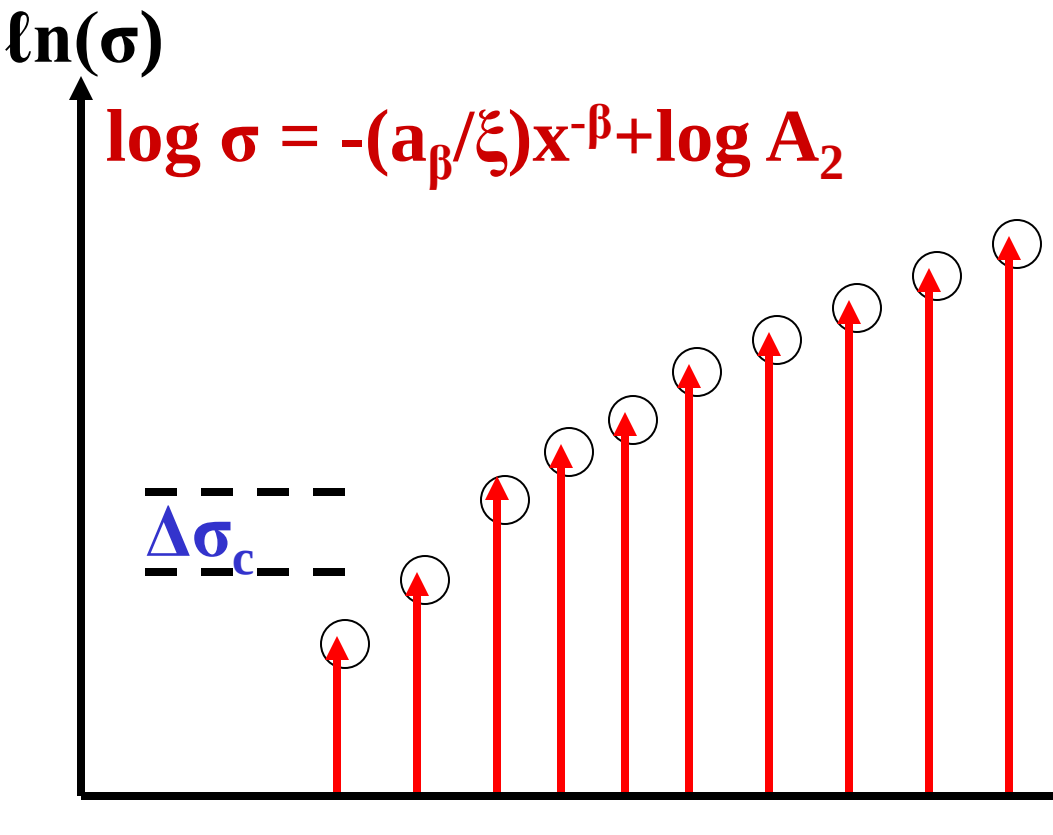

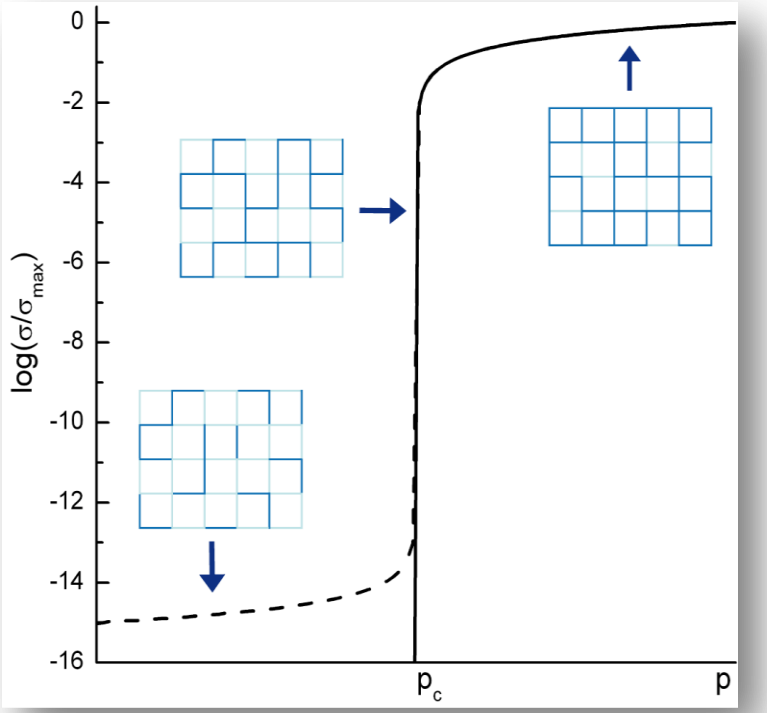

Critical Path Analysis

One labels the conductances (the interparticle distances) in the system in descending order until one gets percolation i.e., one finds the thinnest soft shell δ/2 that still provides percolation for a given Φ.

Actually, we implant hard core particles and then attach to each a shell of thickness δ/2. We check then how many particles, or how high a Φ is needed in order to get a percolation path.

The agreement of the CPA with simulation of the resistors network suggests that one finds the largest σ(Φ) without having to calculate the entire resistor networks.

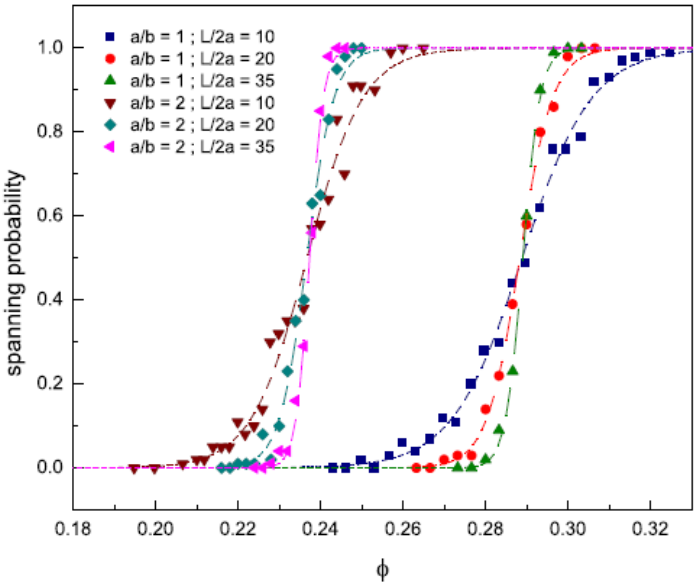

$$\sigma \simeq \sigma_0 e^{-2\delta(\Phi)/\xi},$$

This works because of the very wide resistor distribution values

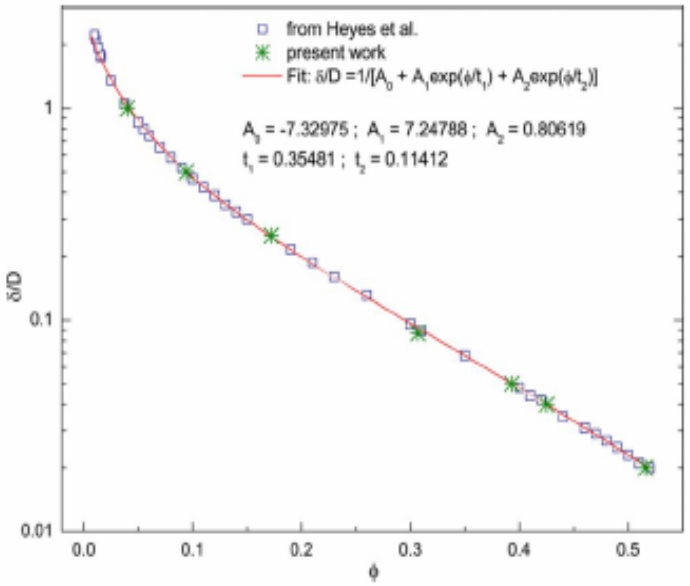

The effect of tunneling in lattices and the continuum

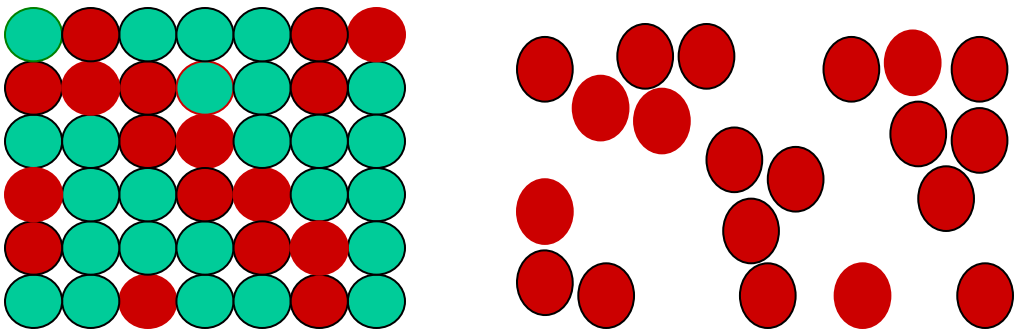

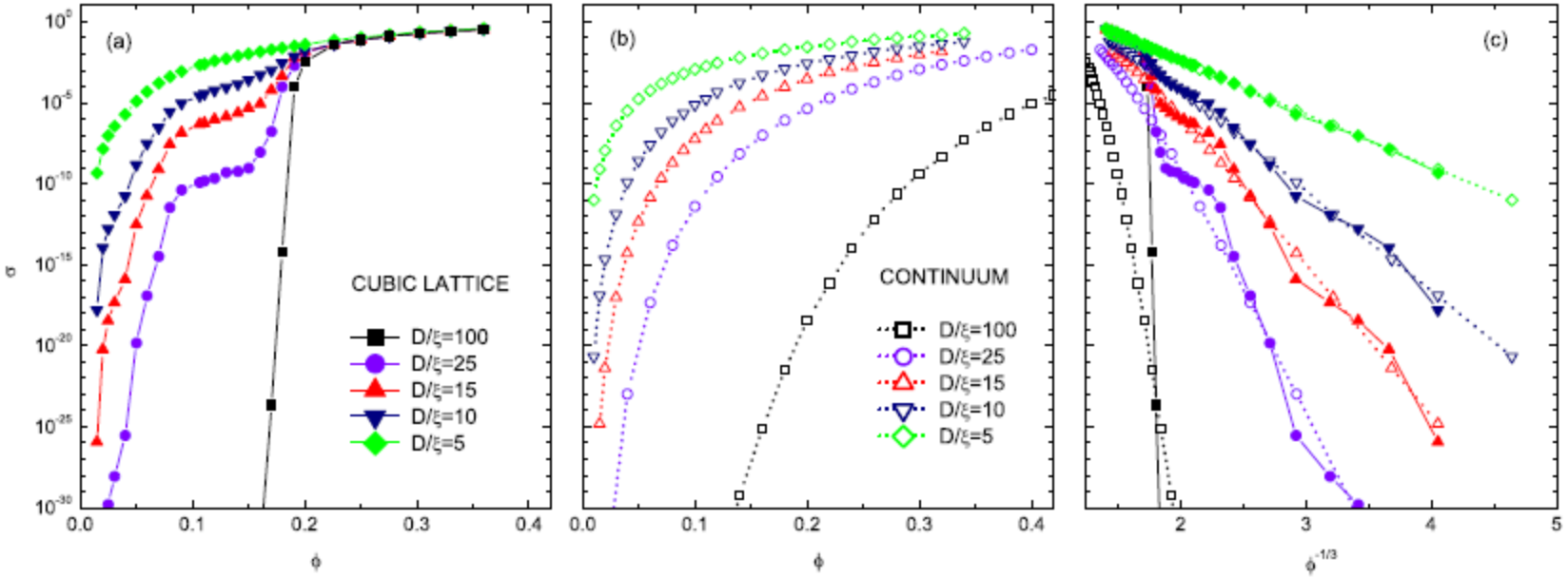

FIG. 3. (Color online) Monte Carlo conductance for (a) the cubic lattice model and (b) the continuum model for different values of D/ξ. (c) The same results of (a) and (b) plotted as a function of $\phi^{-1/3}$.

The tunneling percolation staircase

J. Mod. Phys. B, 18, 2091 (2004): 52 Q

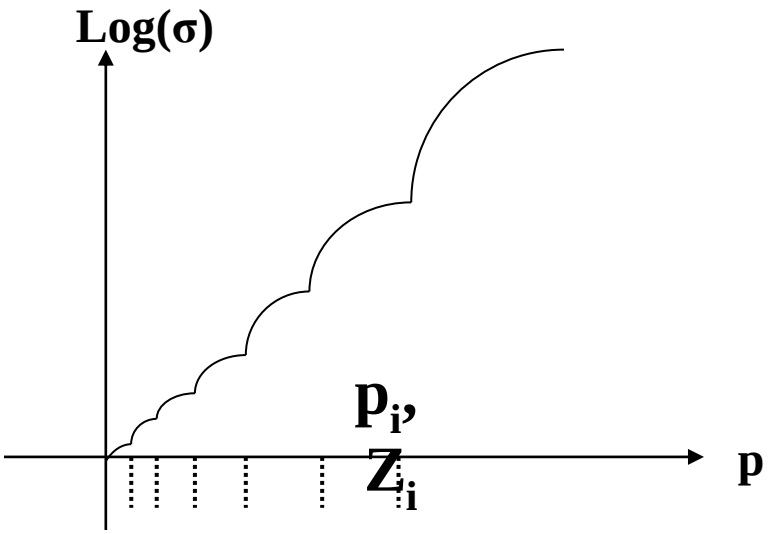

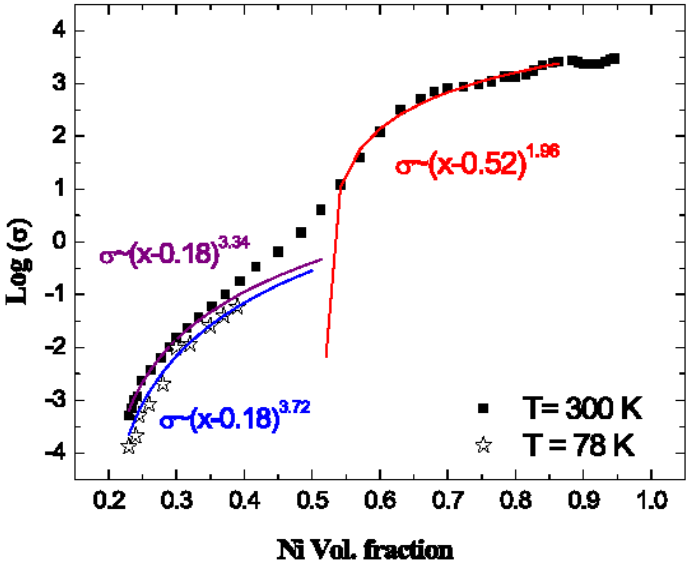

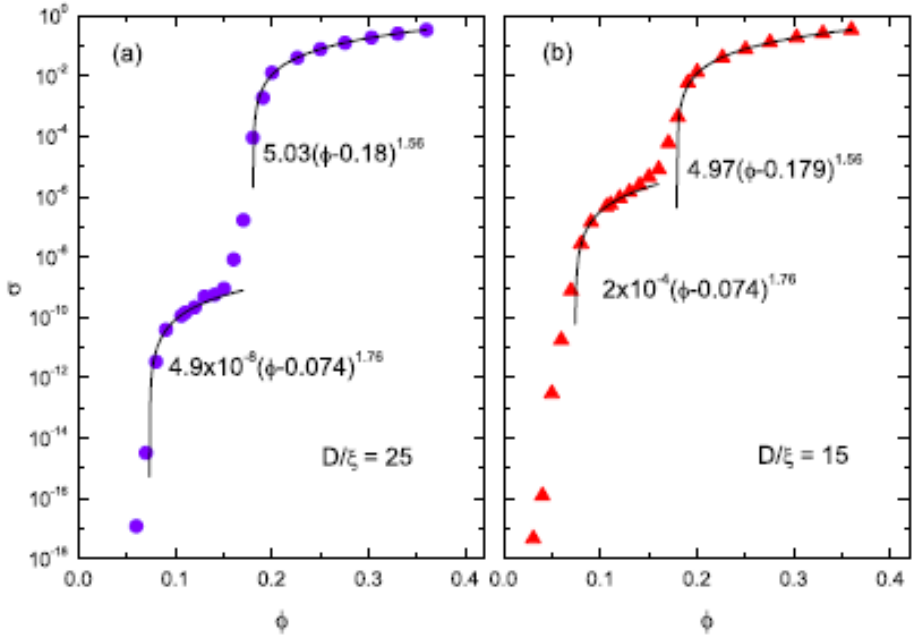

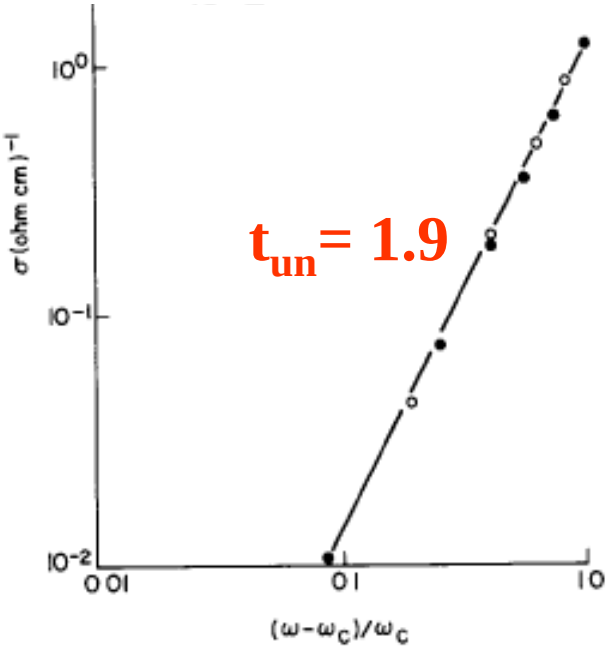

$t_{un} = 1.9$

The tunneling percolation staircase

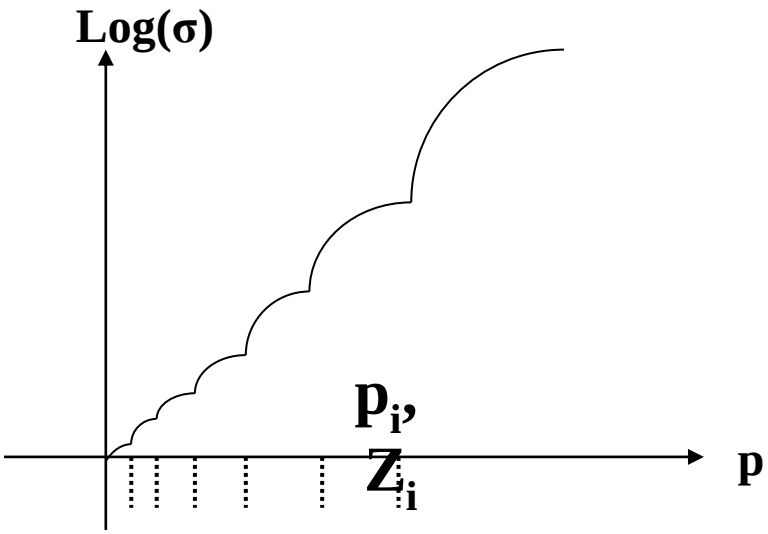

Int. J. Mod. Phys. B, 18, 2091 (2004): 52 Q

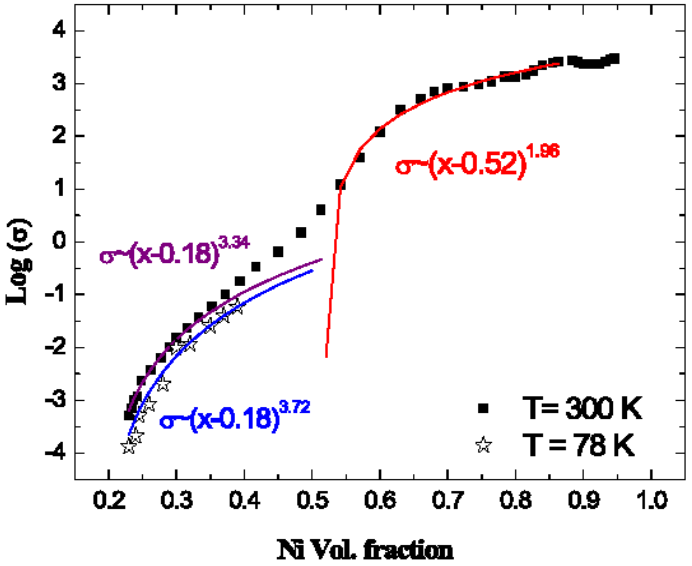

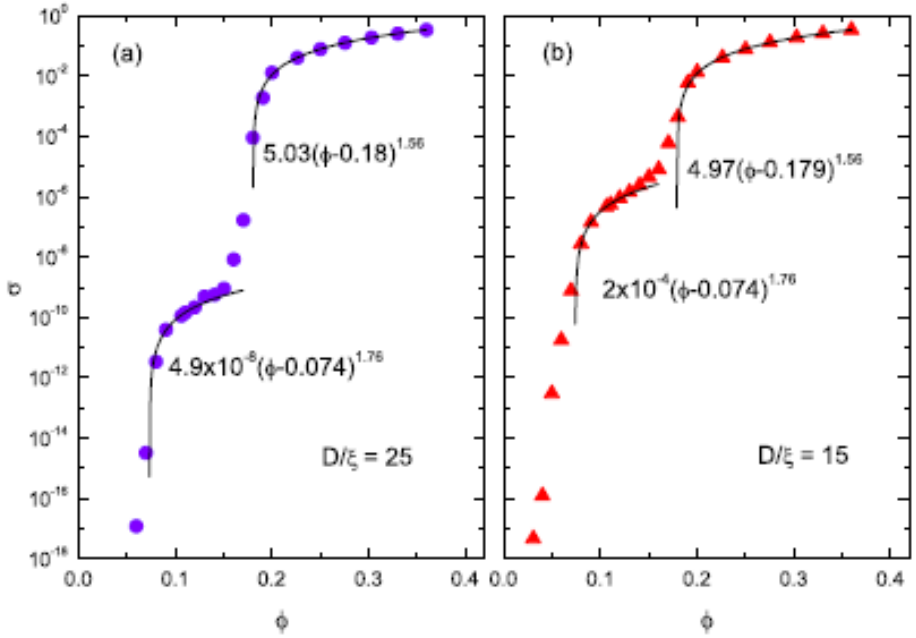

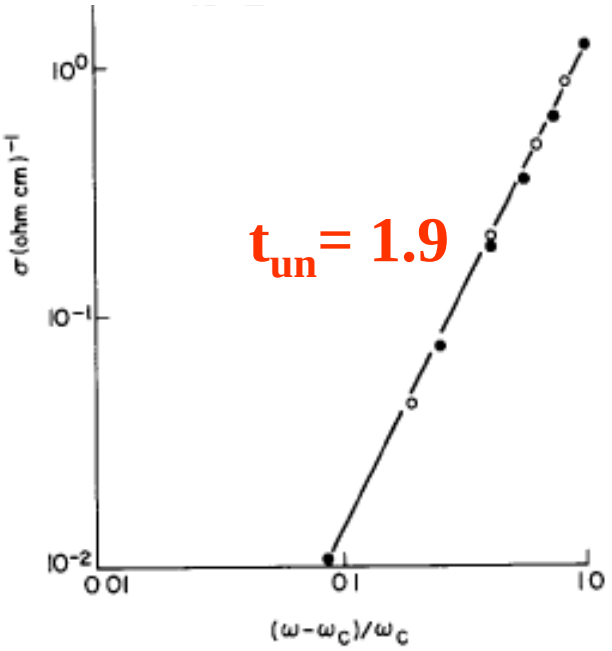

$t_{un} = 1.9$

Two interpretations of the full set of data points

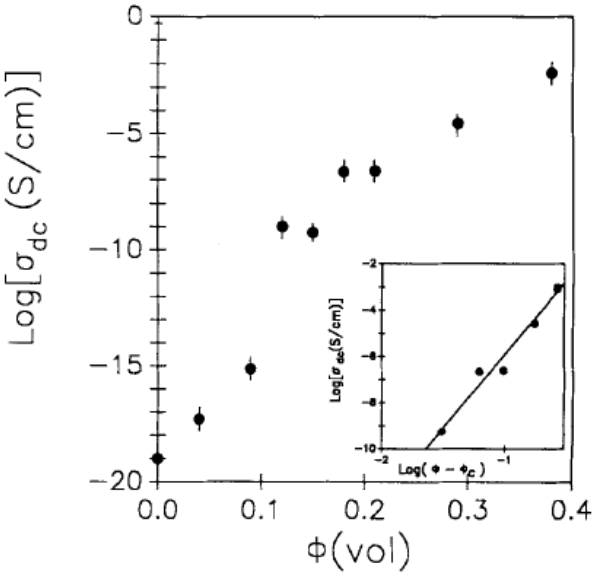

Fig. 1. DC conductivity as a function of the volume concentration of graphite. The insert represents Log σ vs. Log $(\Phi - \Phi_c)$. The slope has a value of 6.27.

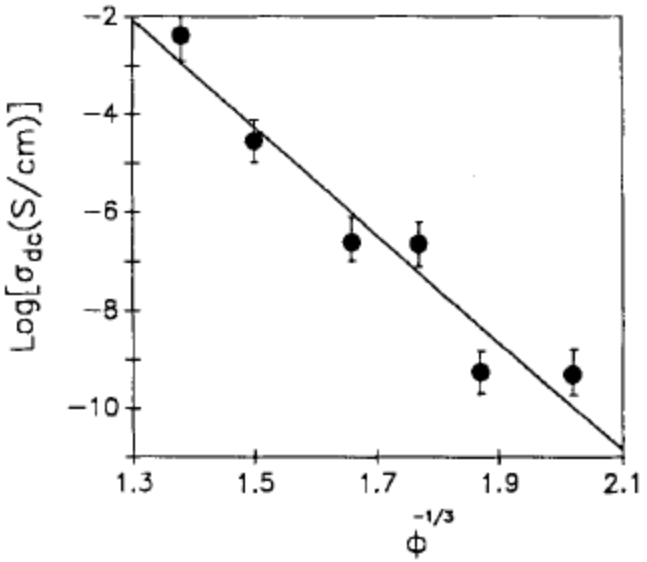

Fig. 3. Variation of Log σ_{dc} vs. $\Phi^{-1/3}$ (see text).

LATTICE PERCOLATION

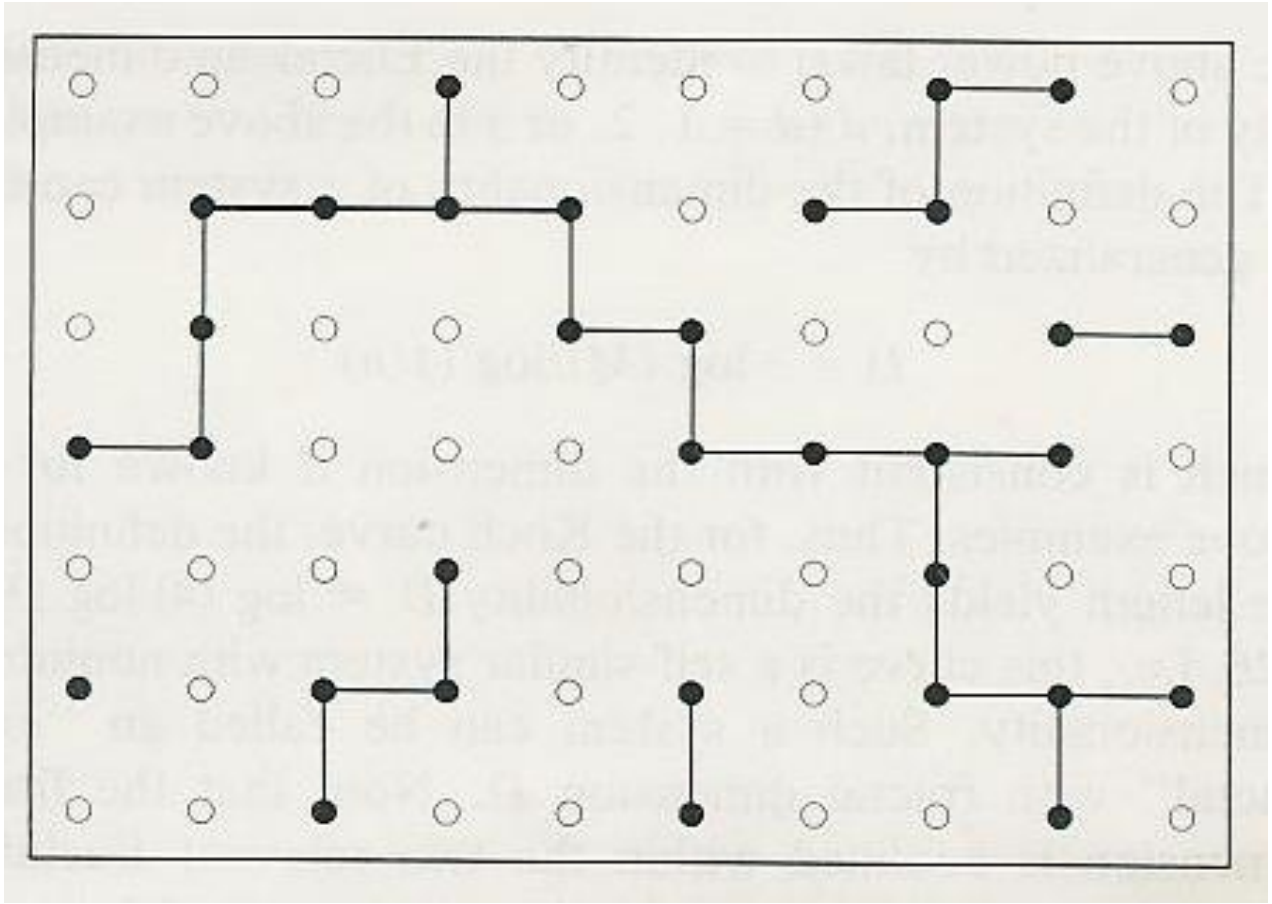

p^s
p^b
S
ξ
p_c

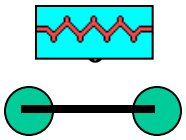

J. Water Resources Research 29, 775 (1993) : 101 Q

A typical continuum system

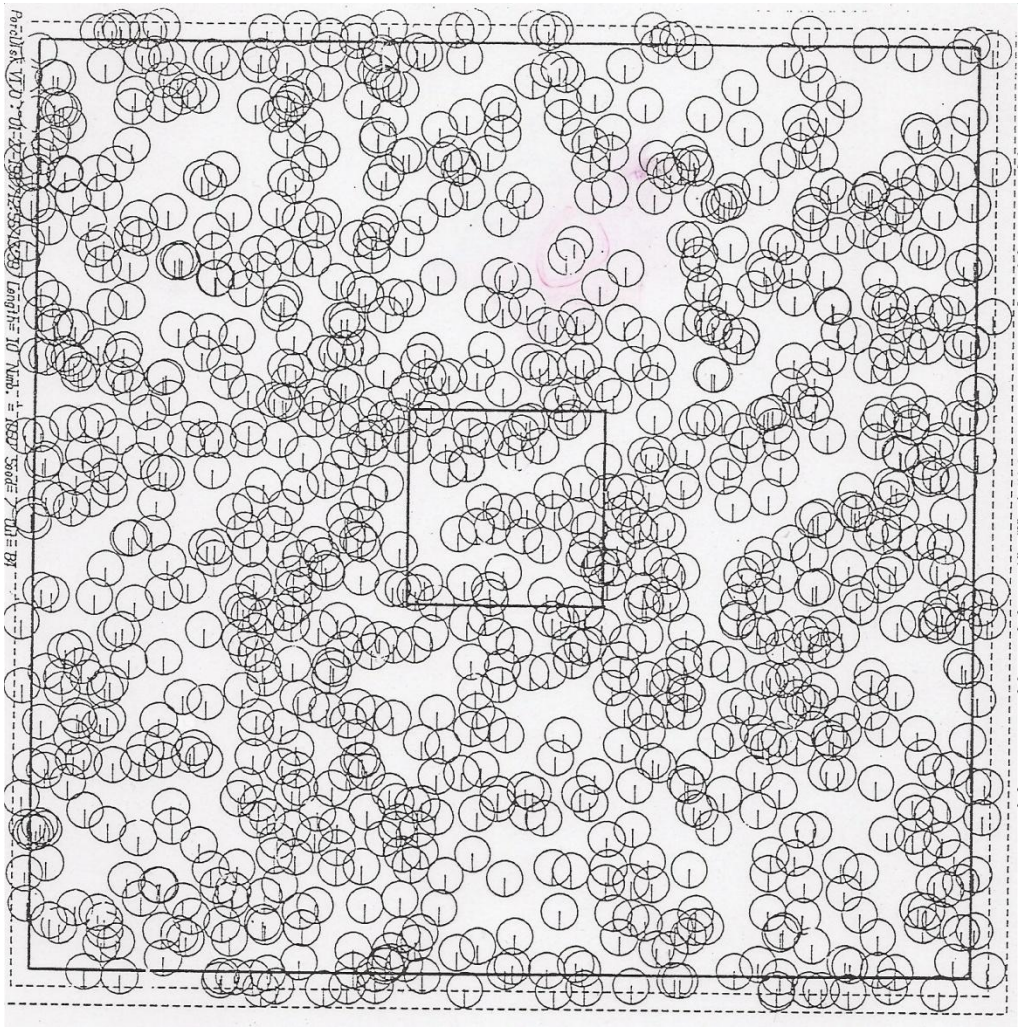

Local connectivity by partial overlap

No p here

The End

The Staircase in the AC measurements

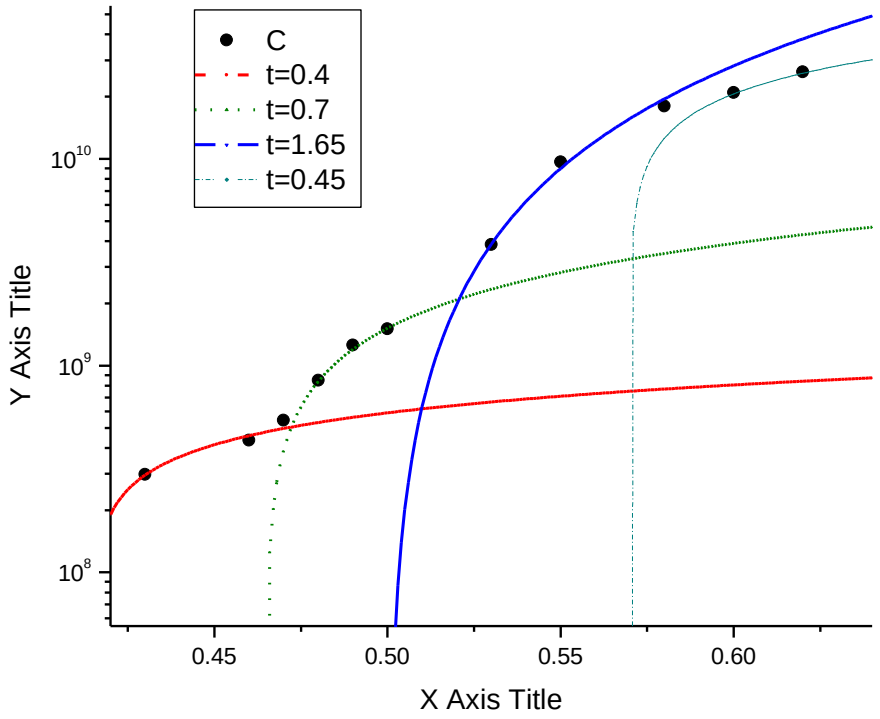

Fluctuations in “experimental “ data

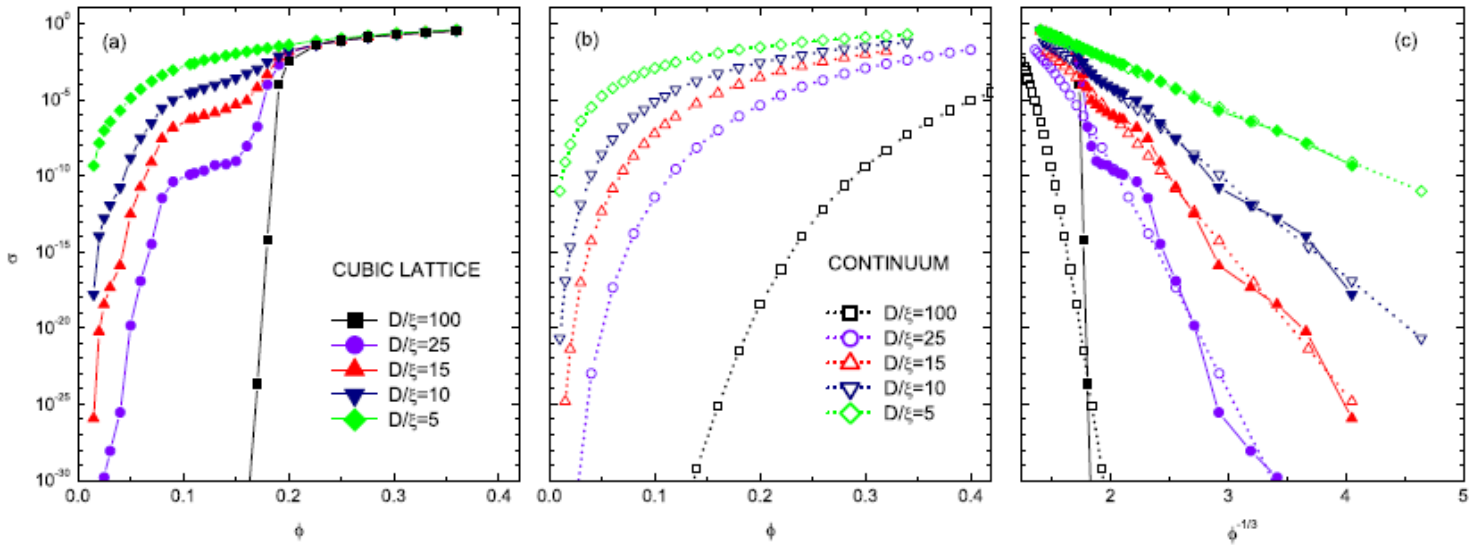

FIG. 3. (Color online) Monte Carlo conductance for (a) the cubic lattice model and (b) the continuum model for different values of D/ξ. (c) The same results of (a) and (b) plotted as a function of $\phi^{-1/3}$.

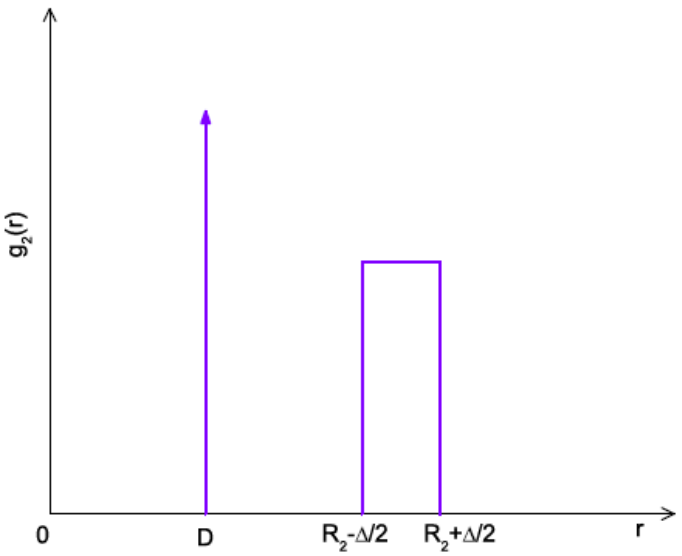
g2(r)
0
D
R2-Δ/2
R2+Δ/2
r

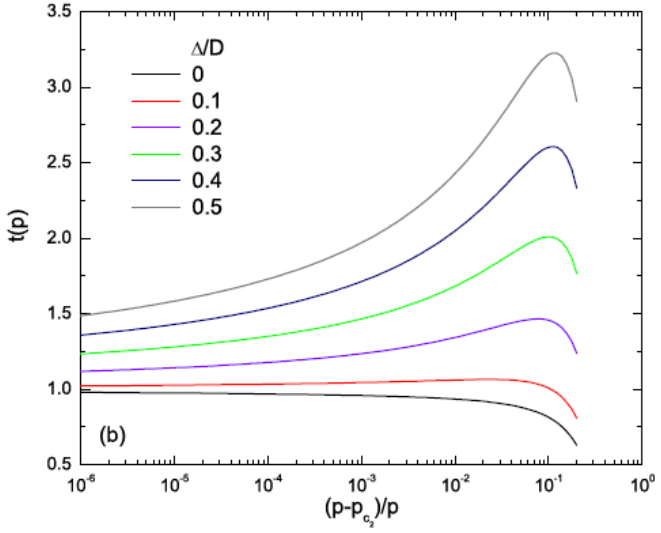
Δ/D
0
0.1
0.2
0.3
0.4
0.5
t(p)
(b)
(p-pc2)/p

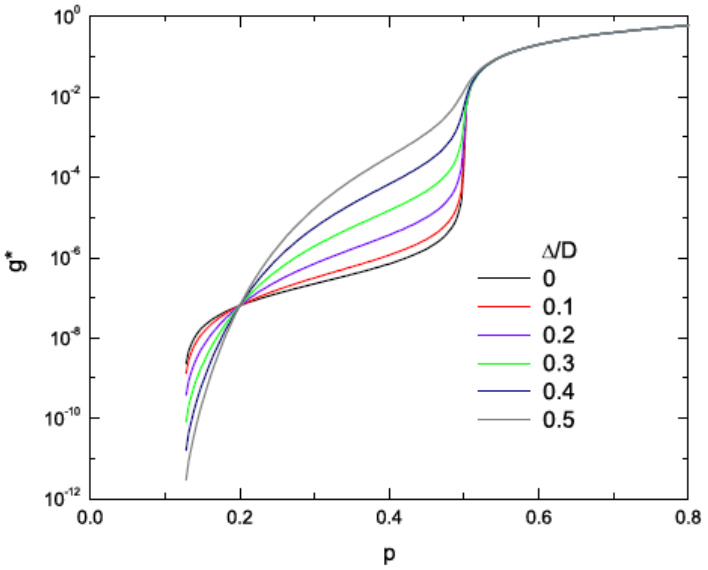
Δ/D
0
0.1
0.2
0.3
0.4
0.5
g*
p

Two presentations of the same data

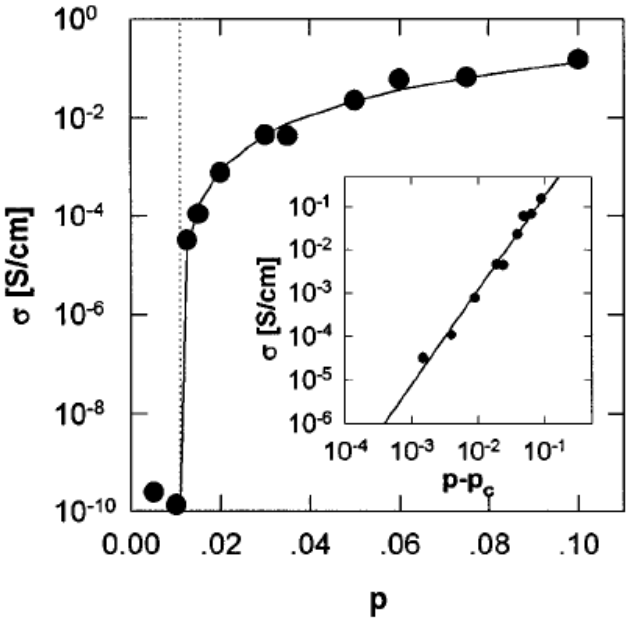

FIG. 1. Plot of σ as a function of carbon black volume content, p of composites; the critical concentration p_c has been determined using Eq. (1) ($p_c = 1.1\%$); inset: log-log plot of σ as a function of $p - p_c$; ($t = 2.17$).

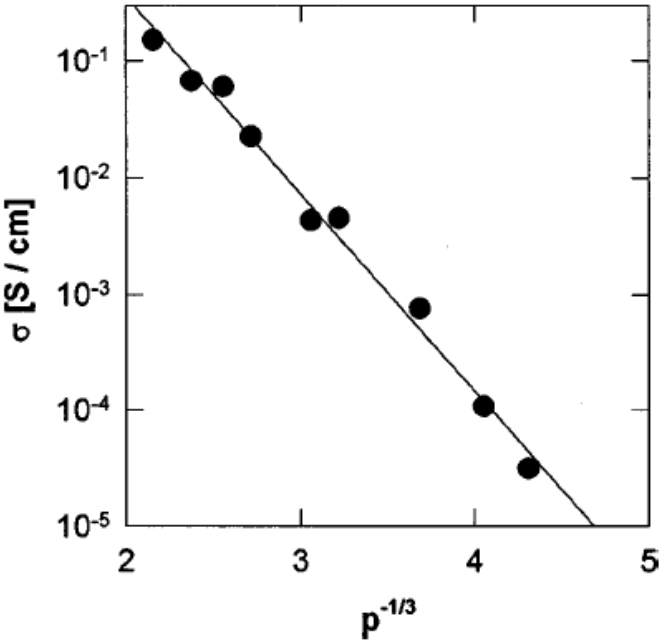

FIG. 2. Linear variation of $\ln\sigma$ vs $p^{-1/3}$.

Two presentations of the same data

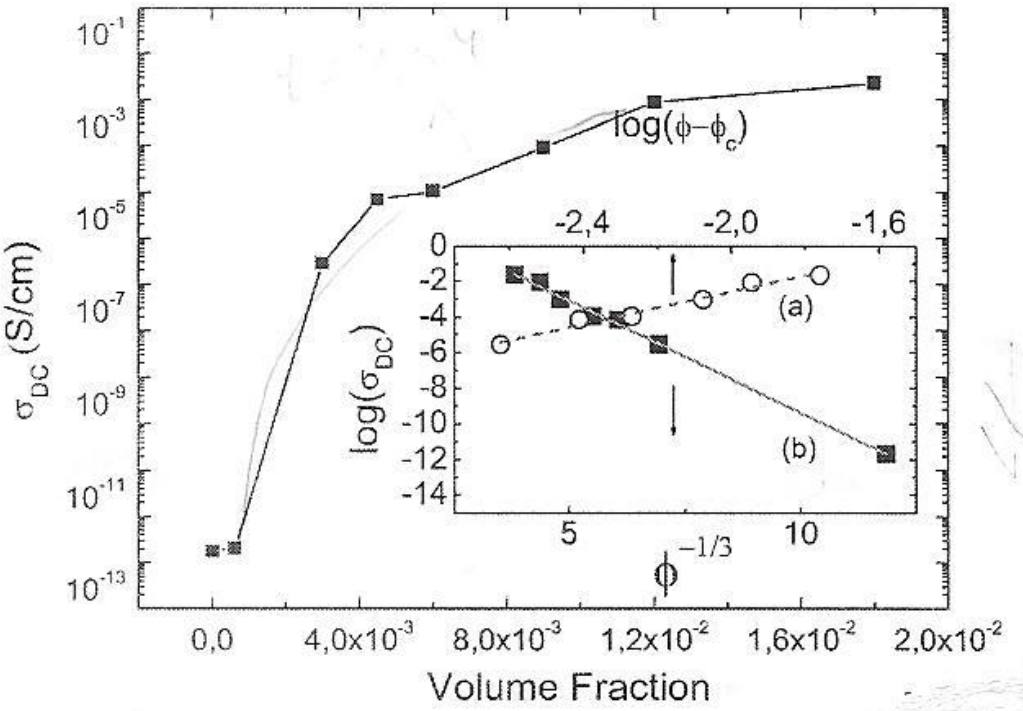

Figure 3 (online colour at: www.pss-a.com) DC conductivity *versus* volume fraction displayed in a log–linear scale. Inset (a): fit of the percolation law $\sigma_{eff} = \sigma_{conductor}(\Phi - \Phi_c)^t$. Inset (b): fit of a single tunneling junction expression in a log–linear plot.

The volume and excluded volume of the capped cylinders

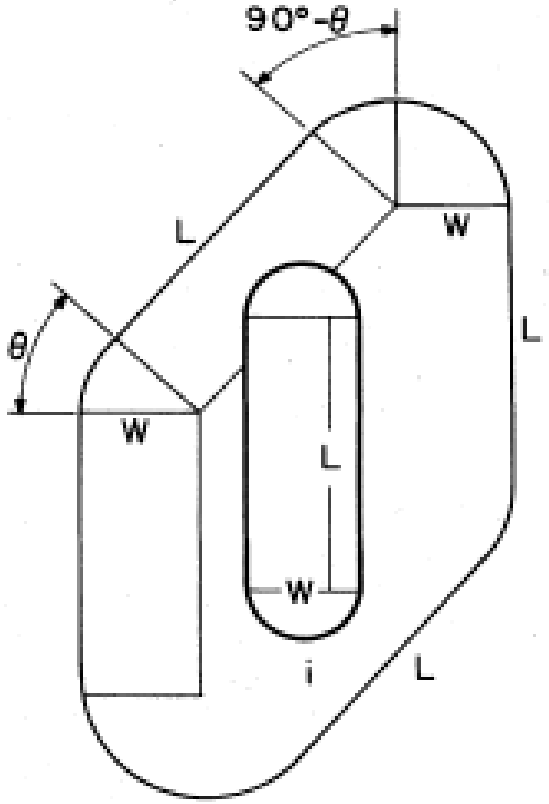

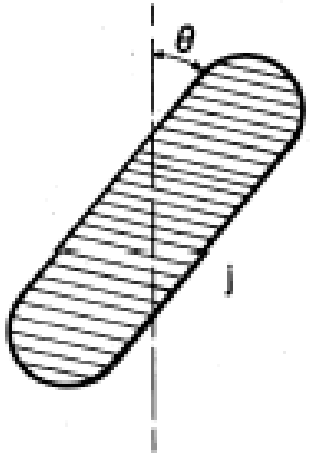

$$N_c = (B_c/v)v/\langle V_{ex}\rangle \propto (B_c/v)(W/L)$$

when $L \gg W$ $(0 \le \theta \le \pi)$

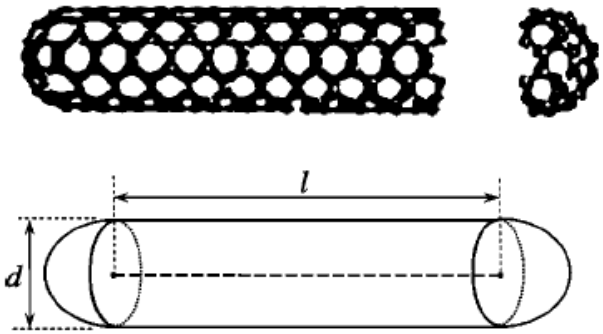

FIG. 1. Carbon nanotube and its representation as a capped cylinder.

$$v = (4\pi/3)(W/2)^3+\pi(W/2)^2L$$

$$\langle V_{ex}\rangle = (32\pi/3)(W/2)^3+8\pi(W/2)^2L+4(W/2)L^2\langle\sin\theta\rangle$$

$$\langle\sin\theta\rangle = \pi/4$$

Phys. Rev. Lett. 52, 1465 (1984): 186 Q

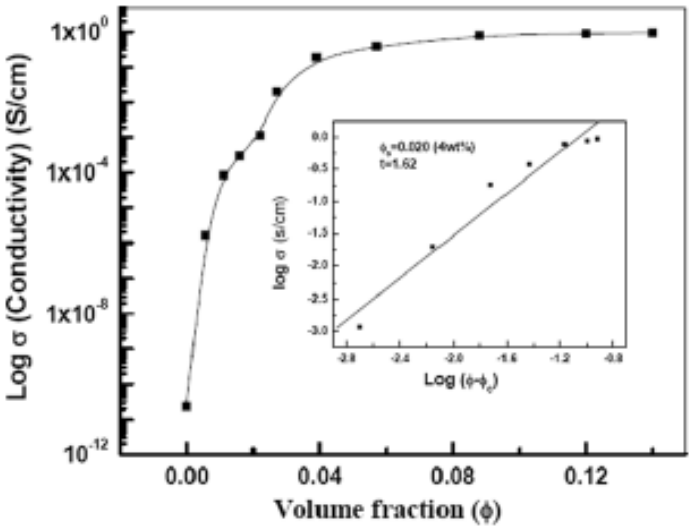

Fig. 2. Electrical conductivity (σ) of SAN–GS composites as a function of GS volume fraction (ϕ).

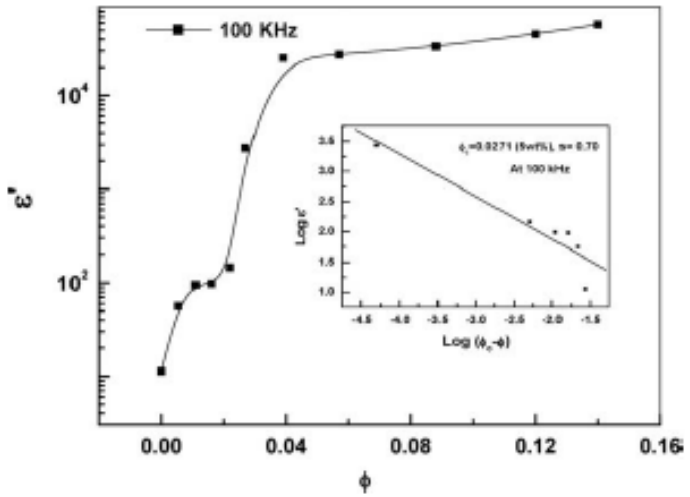

Fig. 3. Dielectric constant (ε') of SAN–GS composites as a function of ϕ at 100 kHz.

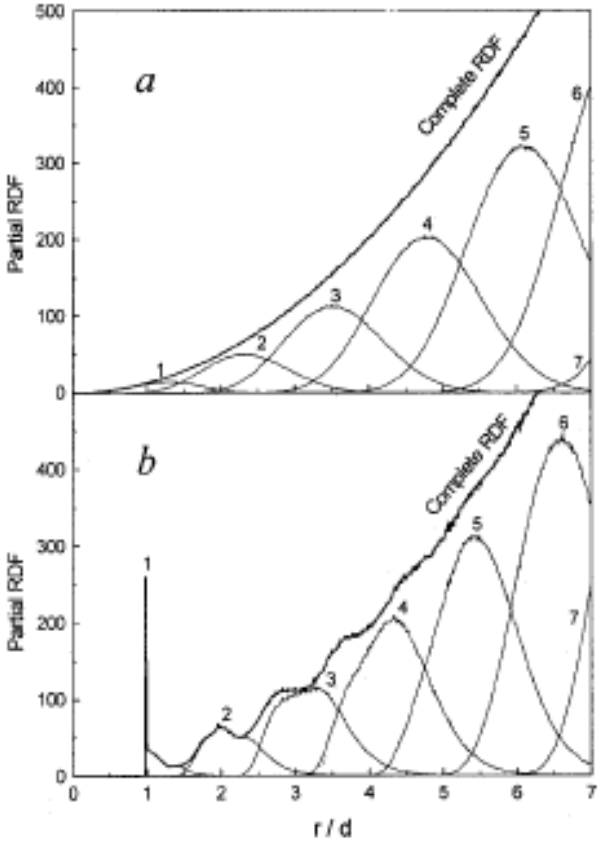

FIG. 2. Radial distribution function. (a) Points, (b) hard spheres $\eta = 0.5$, (1–7) partial densities of the probability of distribution of neighbors, respectively, for neighbors 1, 2, etc.

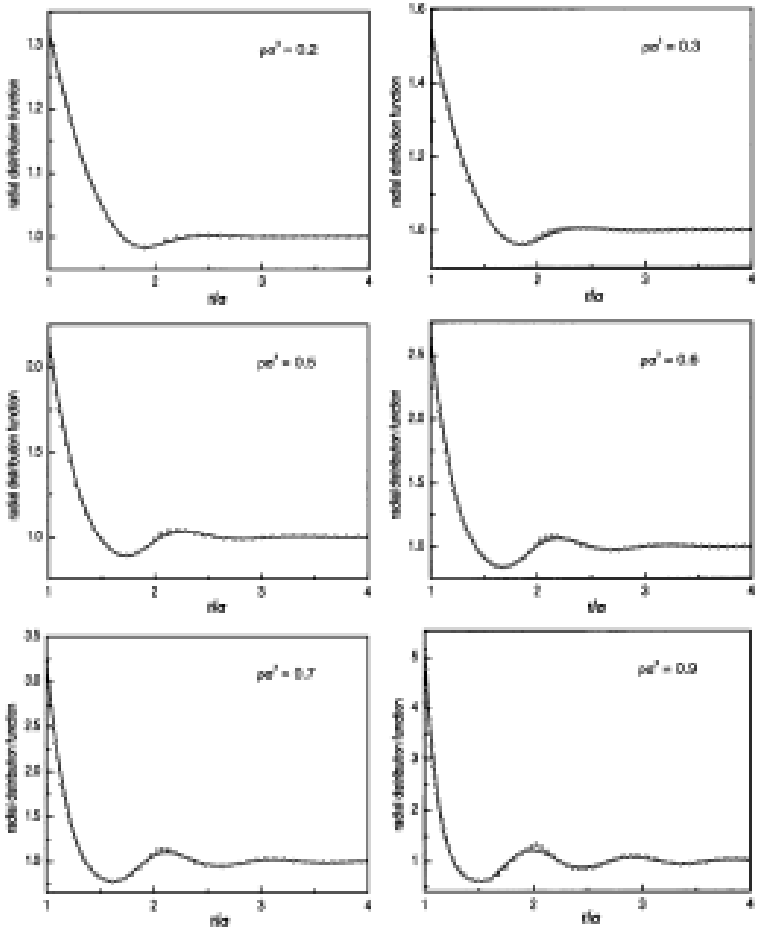

FIG. 4. The hard-sphere RDF evaluated using Eqs. (14)–(16) (thin solid line) and the corresponding MC data (symbols) at different densities.

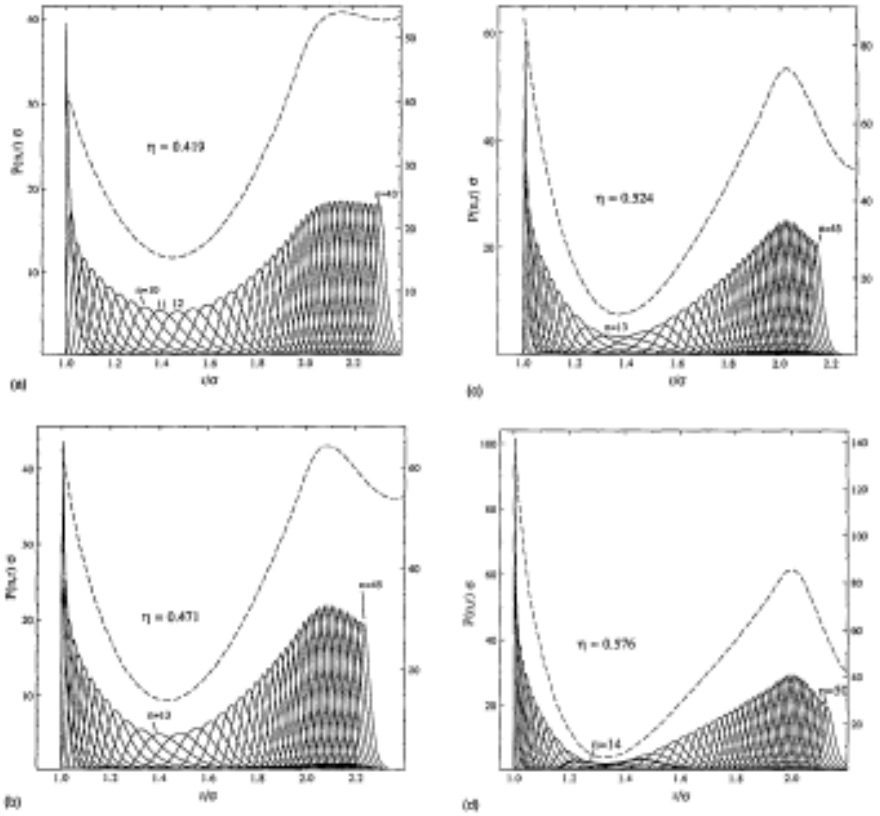

FIG. 4. (a)–(d) Neighborship distributions $P(n,r)$ (solid lines) for hard spheres at the indicated volume fractions. For comparison, $G(r)$ (dashed line) is plotted on the right-hand scale.

Electro-Thermal Switching: the 'global' effect

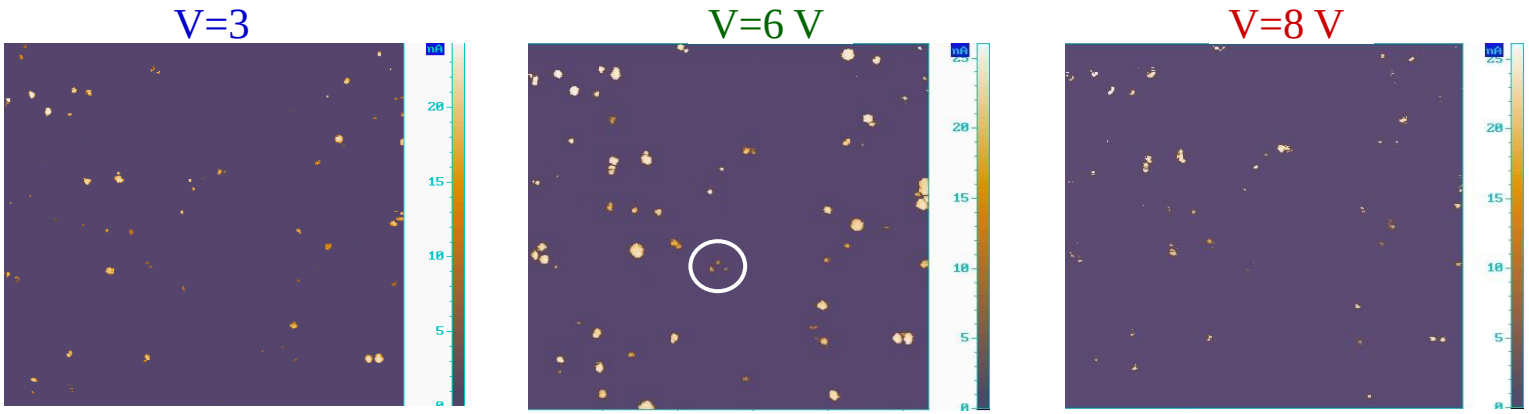

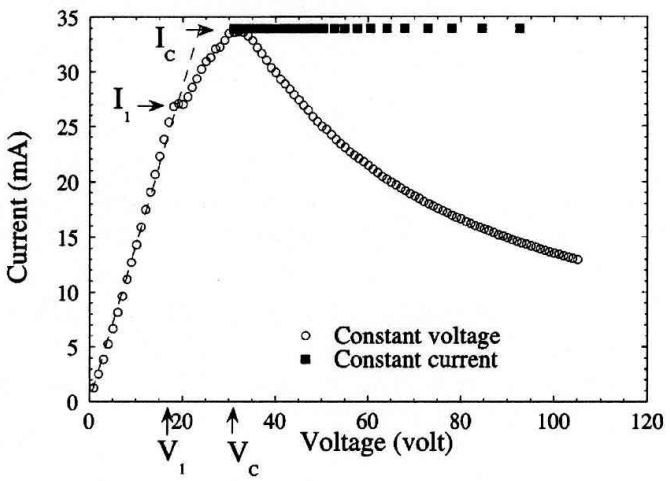

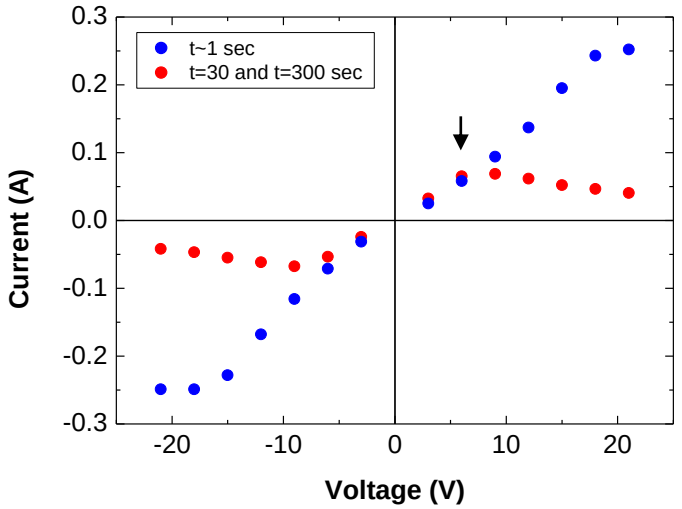

- an increase of the *macroscopic* resistance above a threshold bias
- a stationary "switched" state is reached within 30 sec

Phys. Rev. Lett. 90, 236601 (2003): 20 Q.

Making the Audio Disc

MAKING A RECORD. Sounds are carried by air. In the past, once the sound waves died out, that particular sound was gone forever. If you wanted to hear something, you had to be listening at the same moment the sound was being made. But, with the invention of the record player and the tape recorder, people could not only carry music around with them, captured on a record or tape, but they could hear it over and over again, when and where they wanted.

In the recording studio, the microphone changes the music to electrical signals which are amplified, and then recorded on tape. The musicians and studio technicians listen to the tapes. They adjust the balance of the instruments and voices, and sometimes add more music to the tape.

Finally, the master tape is played into the record cutting machine. The vibrations of the signals make the needle vibrate from side to side. As the plastic disc turns, the vibrating needle cuts a wavy spiral groove into it from the outside in. This groove is a physical "record" of the music.

Metal molds made from the master disc press out the plastic record that you buy in a store.

HISTORY

- 1982 RCA Laboratories, Princeton, USA
- Request: High conductivity, High elasticity.

- Question: Carbon Black supplier?

- A) Cabot Corporation, Boston USA
- B) Akzo Chemicals, Amersfoort, The Netherlands

Low structure or high structure ?

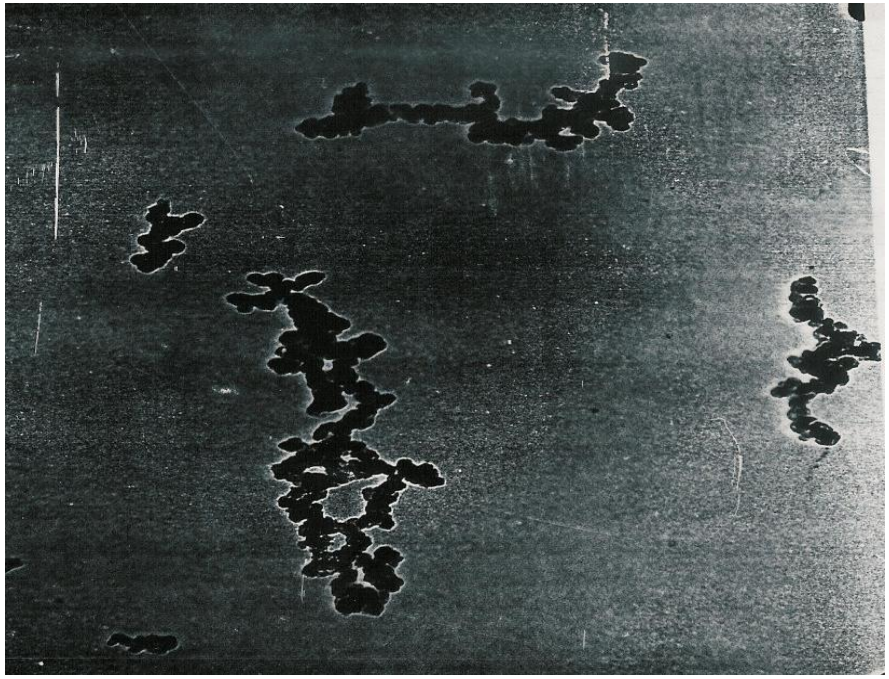

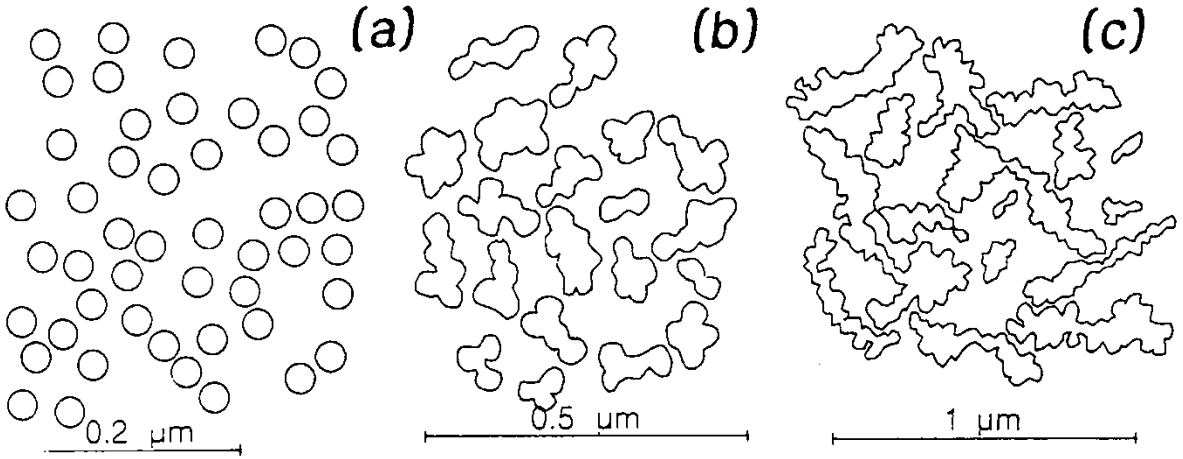

The “lost” signal (Percolation Threshold and Anisotropy)

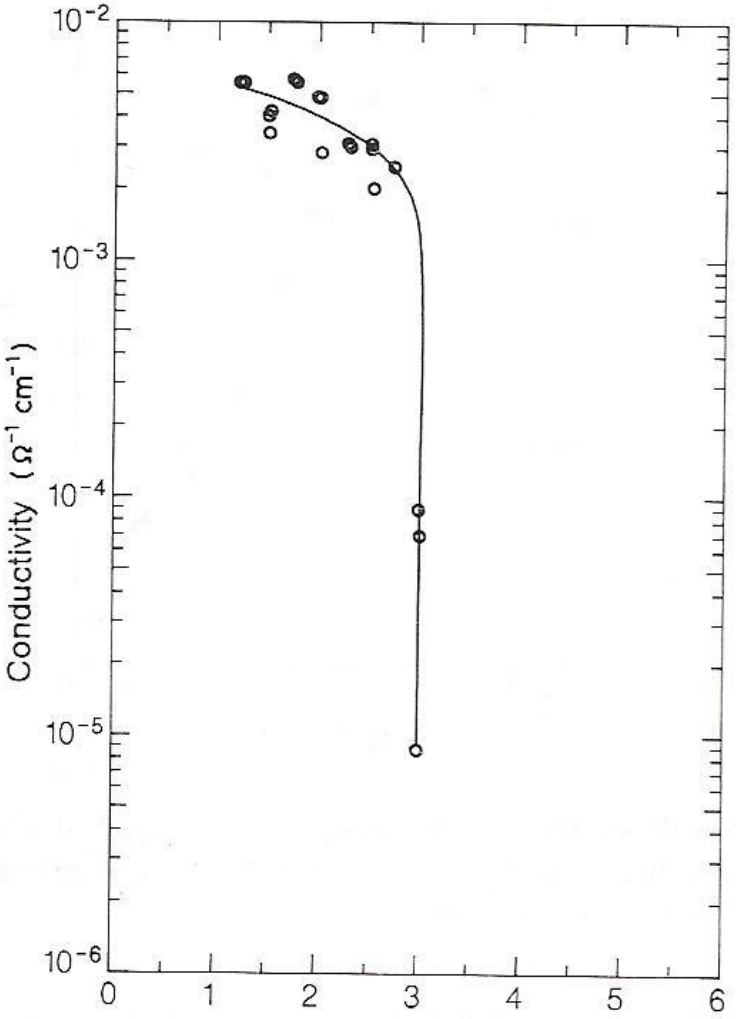

Phil Mag. B, 56, 991 (1987): 142 Q.

Overcoming the “Anisotropy”

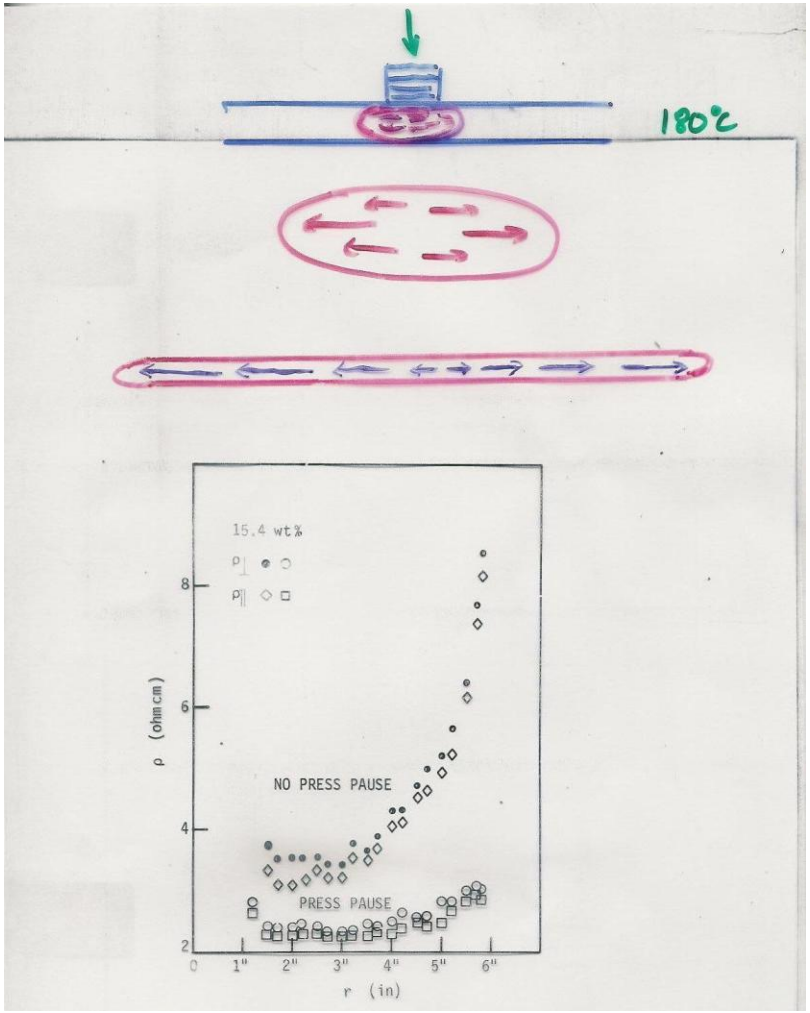

The Question is:

How to express conceptually and mathematically the feeling that elongated, not parallel, particles will yield a higher conductivity (i.e. connectivity) for the same CB content?

Cylinder like objects

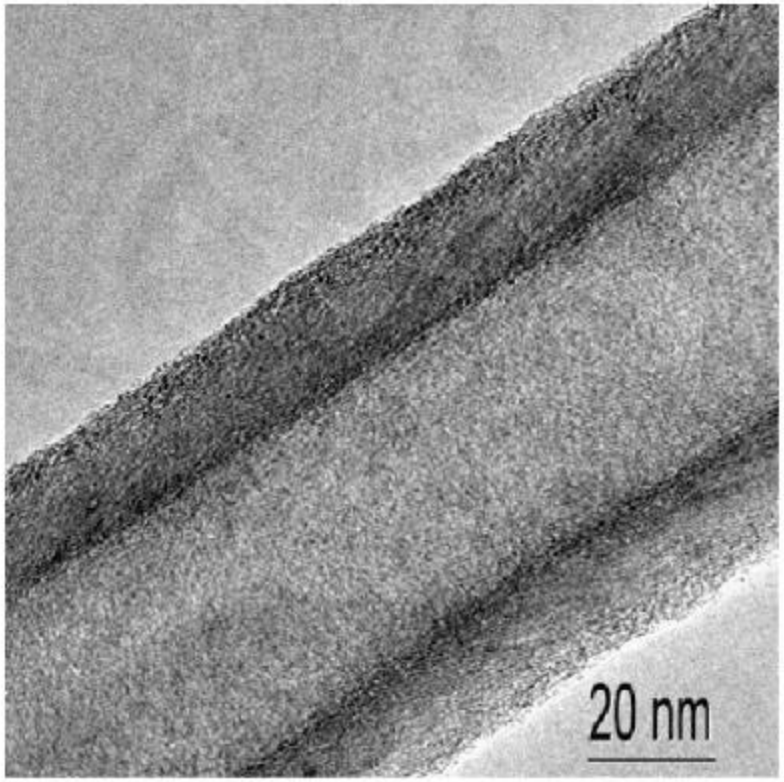

Fig. 2 – TEM micrograph of VGCNF [20].

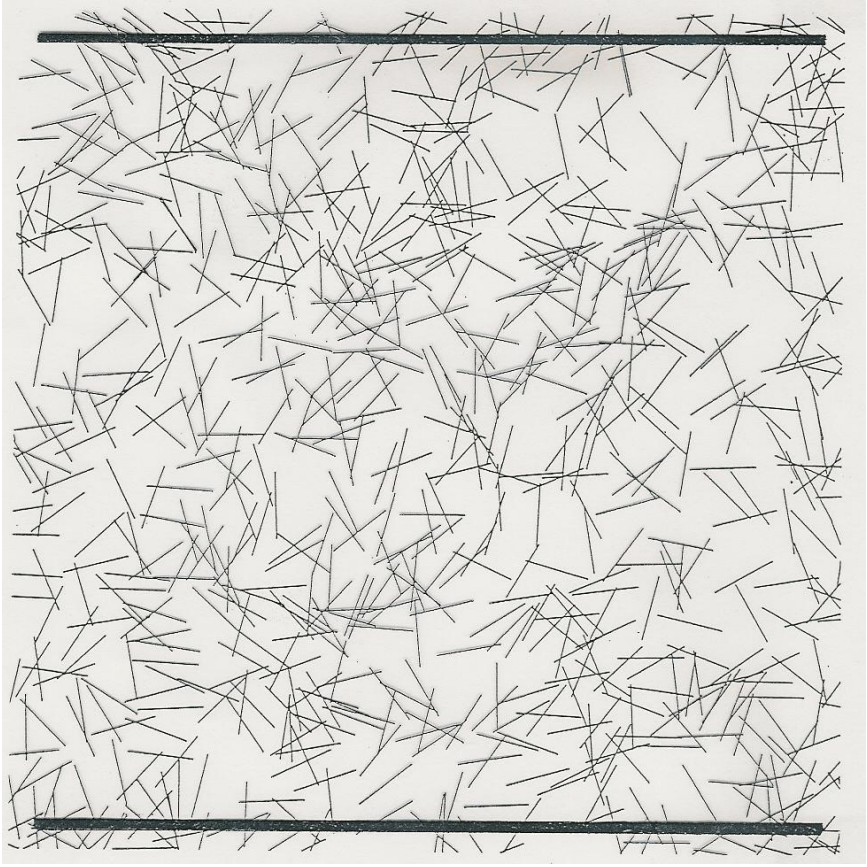

Phys. Rev. B, 28, 3799 (1983): 156 Q

Behavior of three types of composites that are based on elongated carbon particles

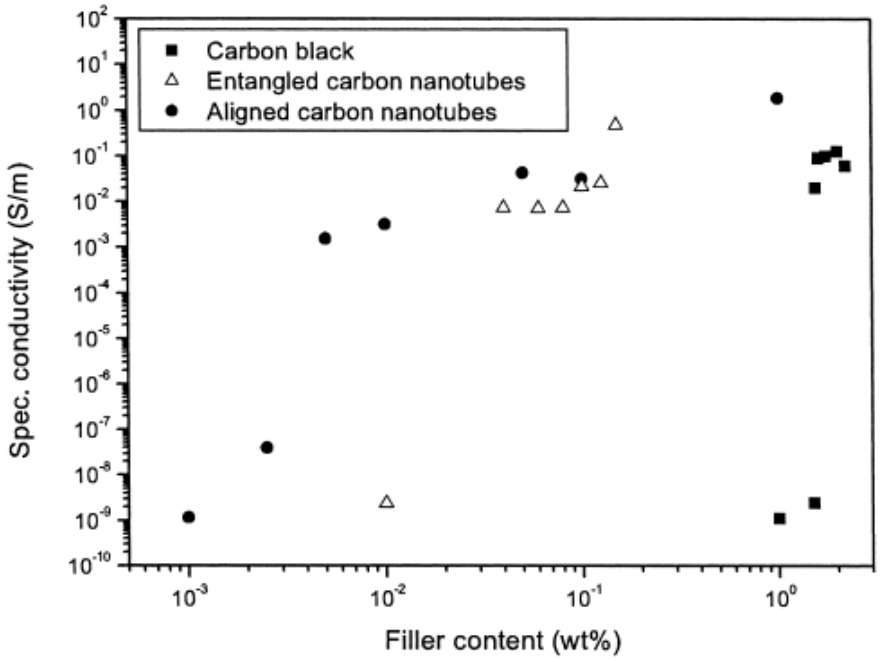

Fig. 6. Epoxy composite conductivity as a function of filler weight fraction for the aligned CVD-grown multi-wall carbon nanotubes compared to results previously achieved with entangled nanotubes and carbon black particles [4].

Table 1 – Typical properties of VGCNF, SWNT, MWNT and CF

Property	VGCNF[a]	SWNT[b]	MWNT[b]	CF[c]
Diameter (nm)	50–200	0.6–1.8	5–50	7300
Length (μm)	50–100			3200
Aspect ratio	250–2000	100–10,000	100–10000	440

Typical behavior of all composites

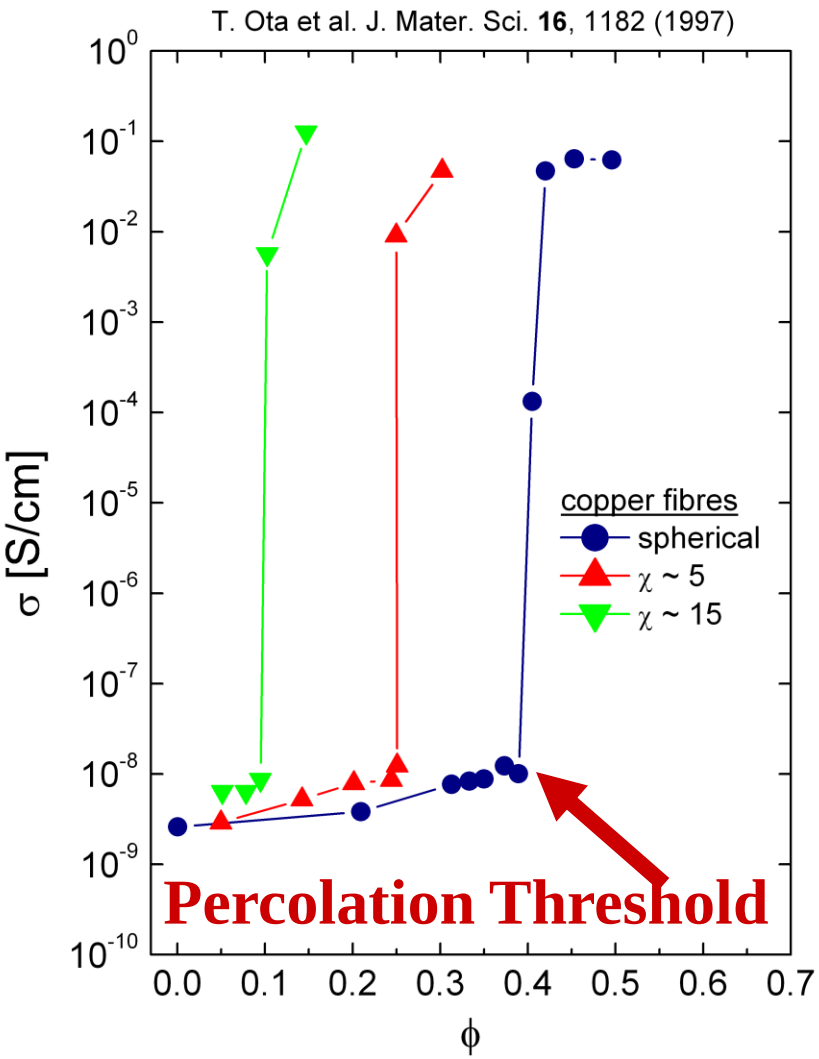

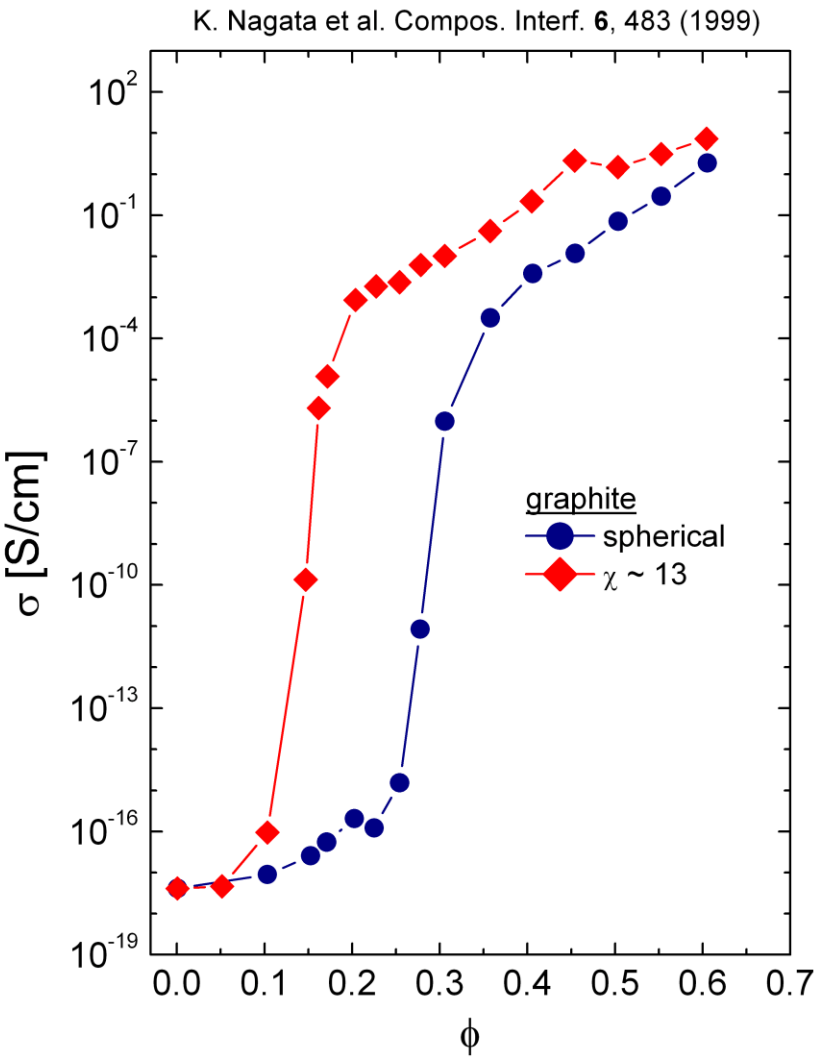

Typical behavior of all composites

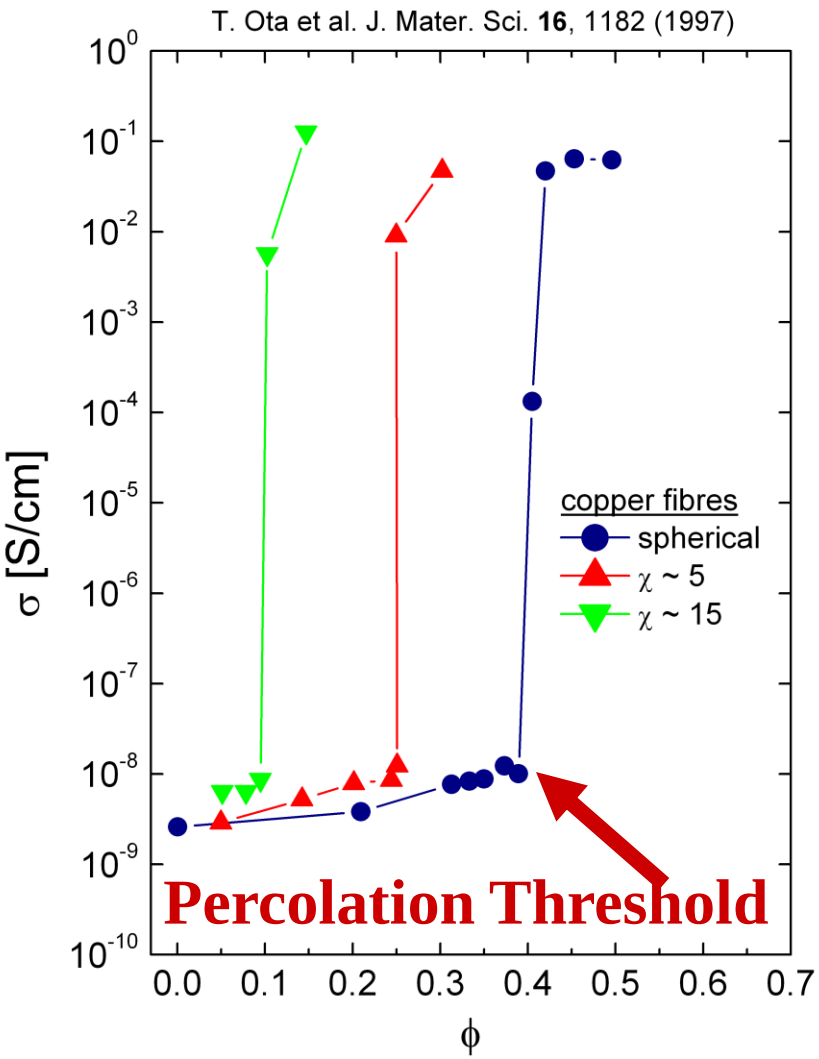

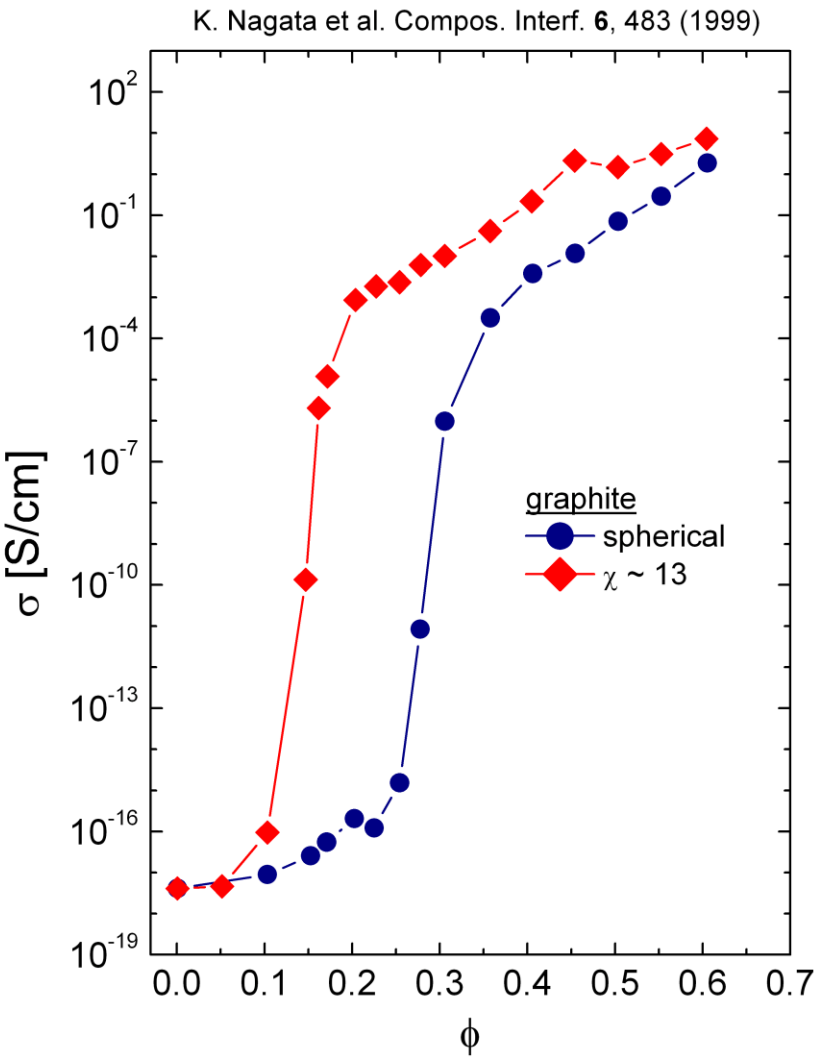

percolation versus tunneling

the percolation picture implies the presence of a sharp cut-off, but tunneling does not

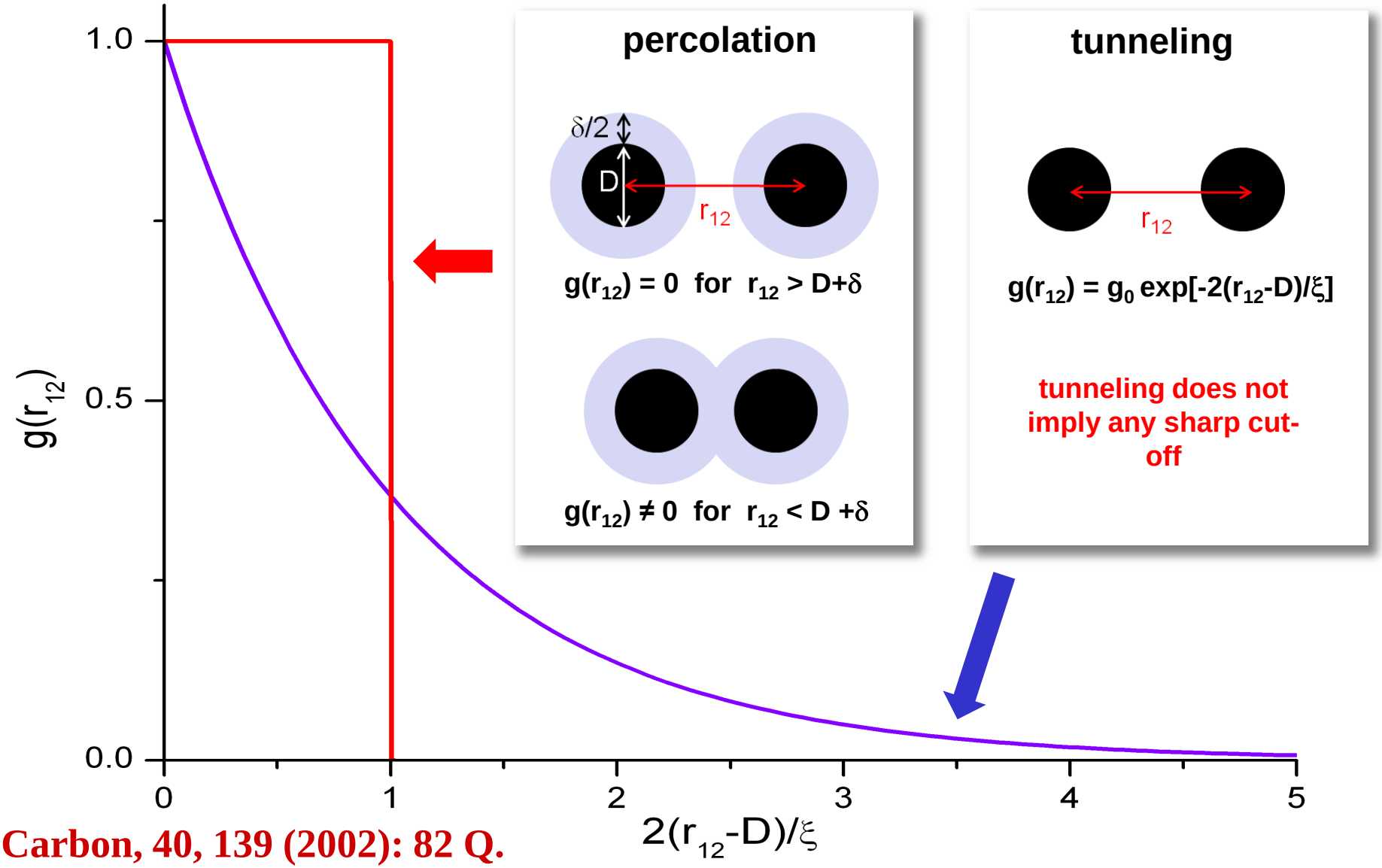

percolation

$g(r_{12}) = 0$ for $r_{12} > D+\delta$

$g(r_{12}) \neq 0$ for $r_{12} < D+\delta$

tunneling

$g(r_{12}) = g_0 \exp[-2(r_{12}-D)/\xi]$

tunneling does not imply any sharp cut-off

Carbon, 40, 139 (2002): 82 Q.

The concept of "excluded volume"

We generalized $v2^D$ to other objects calling it "Excluded Volume"

NV_{ex} = B: the average number of overlapping objects, i.e. the average number of bonds per object. B_c is expected then to be a topological invariant.

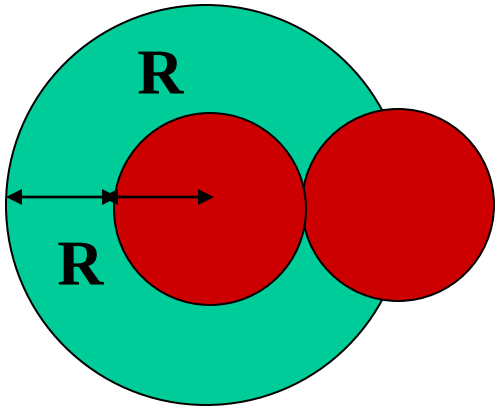

$$V_{ex} = v2^D$$

$$vN_c = (v/V_{ex})(V_{ex}N_c) = (v/V_{ex})B_c$$

The Excluded Volume is the volume in which the center of the "other object" has to be in order for the two objects to, at least partially, overlap

Phys. Rev. B, 30, 3933 (1984): 290 Q

Note: 2^D = smallest V_{ex}/v for permeable objects

History of percolation Thresholds in the Continuum (Sastry, PRE 2007)

Table 2. Key percolation studies in three dimensional random fibrous materials

Authors	Year	Reference	Arrangement	Objects	Contribution	Approach
Balberg, Binenbaum and Wagner	1984	27	isotropic	capped cylinders	First study of percolation of random objects in three dimensions	Monte Carlo simulations
Balberg, Anderson, Alexander et al.	1984	26	isotropic	capped cylinders	Presented the conjecture that percolation threshold for a system of identical objects in three dimensions is inversely proportional to excluded volume of one object	Monte Carlo simulations
Bug, Safran and Webman	1985	28	isotropic	capped cylinders	Confirmed excluded volume rule and showed constant of proportionality equals one in slender rod limit	cluster expansion
Neda, Florian and Brechet	1999	29	isotropic	capped cylinders	Performed Monte Carlo simulations of 3D stick systems using correct isotropic distribution and confirmed excluded volume theory	Monte Carlo simulations
Yi and Sastry	2004	30	isotropic	ellipsoids	Presented analytical approximation for the percolation threshold of two- and three- dimensional arrays of overlapping ellipsoids	series expansion
Yi, Wang, and Sastry	2004	31	Uniform distribution in x-y plane. Range of distributions from parallel to random in z-direction	ellipsoids	Provided comparisons of cluster sizes, densities, and percolation points for two- and three-dimensional systems of overlapping ellipsoids to investigate the range of applicability of a 2D model for predicting percolation in thin three-dimensional systems	Monte Carlo simulations

The generalization to the hard core case

$$V = \frac{4\pi}{3}R^3 + \pi R^2 L.$$

For L >> R

$V_{ex} \approx 4L^2R\langle \sin\Theta \rangle$

$\Delta V_{ex} \approx 4L^2\delta\langle \sin\Theta \rangle$

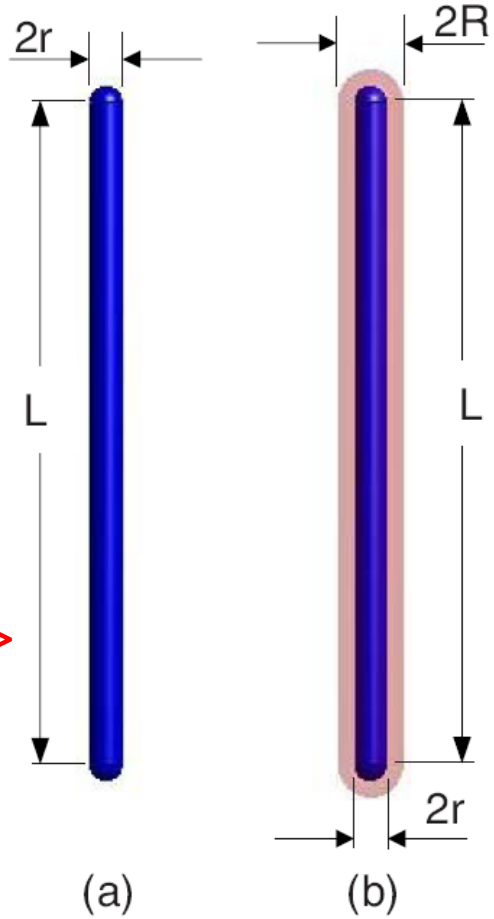

In considering tunneling, the tunneling range is R-r = δ

The important observation is that :

$\Phi_c = N_c v \propto (B_c/\Delta V_{ex})v \propto r^2L/[L^2(R-r)] \propto [r/(R-r)](r/L)$

If δ = (R-r) we have that

$\Phi_c \propto (r/\delta)(r/L)$

For Oblate Particles

For discs of radius a and thickness b

$V_{ex} \propto a^3$

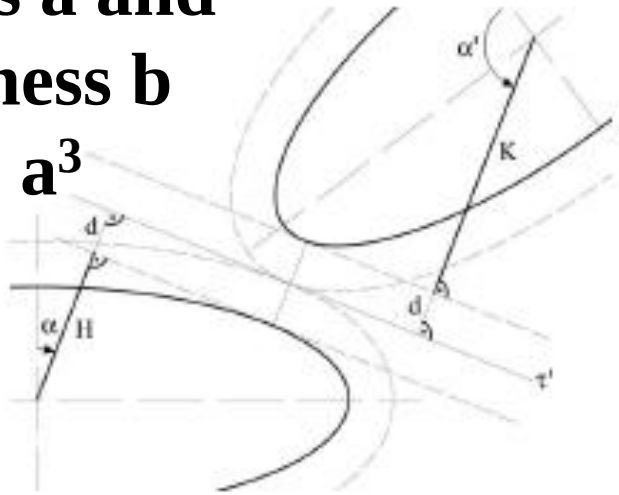

FIG. 8. Two oblate spheroids surrounded with shells of constant thickness which are in contact (2D representation).

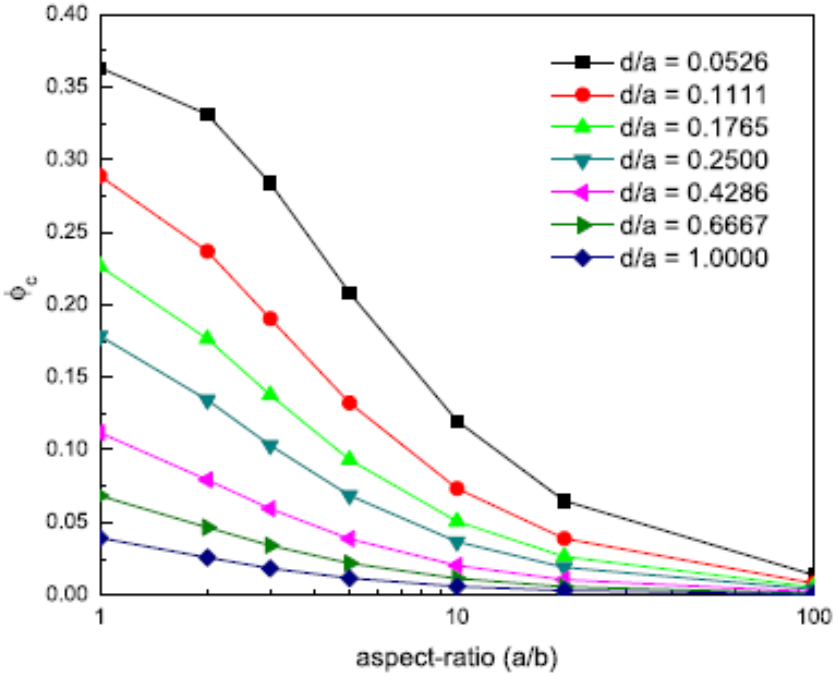

FIG. 3. (Color online) Percolation threshold ϕ_c variation as a function of the aspect ratio for different shell thicknesses.

Asymptotically for a >> b, d and isotropic distribution:

$$\Delta V_{ex} \propto [(a+d)3 - a3] \approx (a^2 d),\ v = \pi a^2 b,\ \Phi_c \propto b/d = (a/d)(b/a)$$

From the simulations:

$$\Phi_c \propto v/V_{ex} \propto \approx (a/d)(b/a)^{1/2}$$

Phys. Rev. B, 81,155434 (2010).

Resistors Equivalent Network

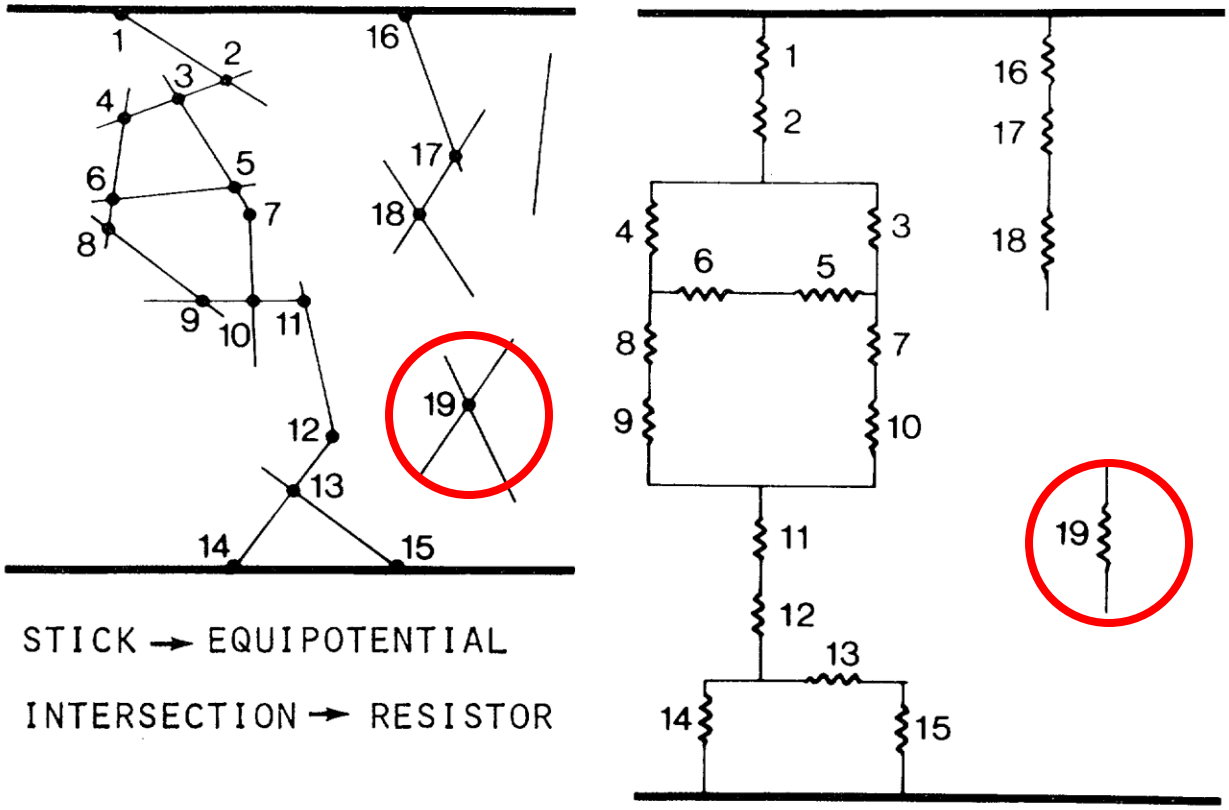

The tunneling percolation staircase

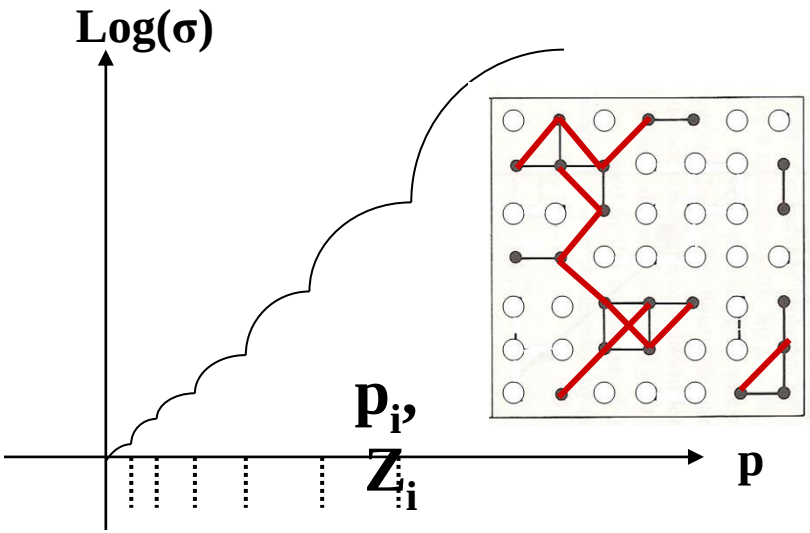

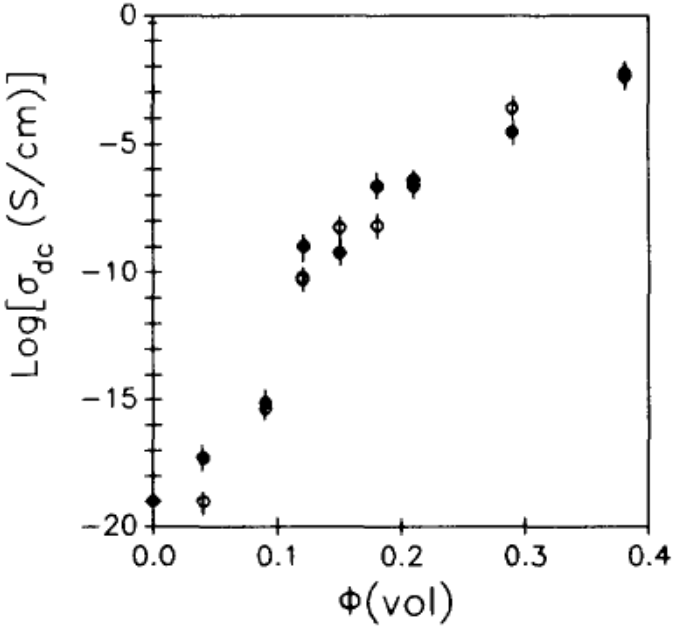

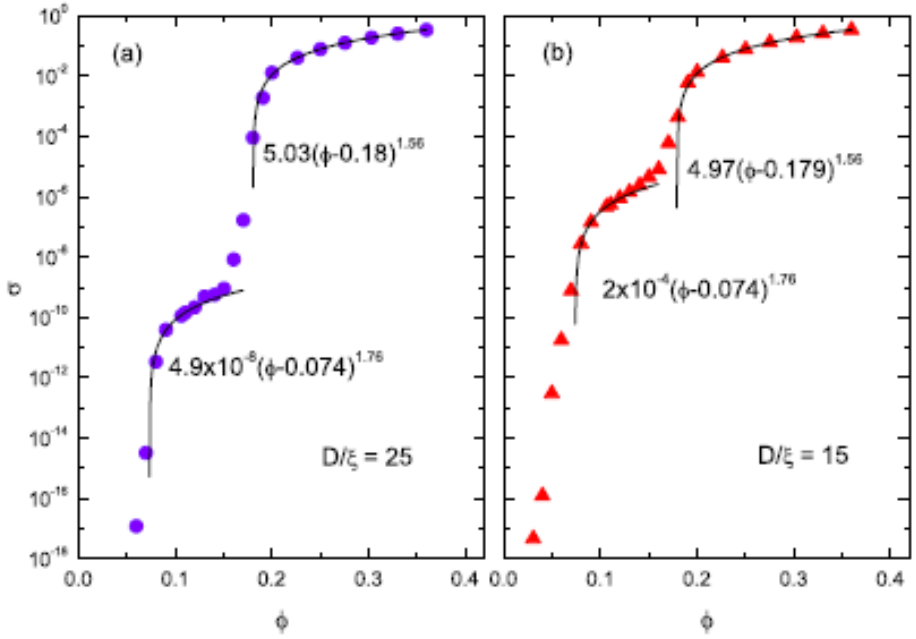

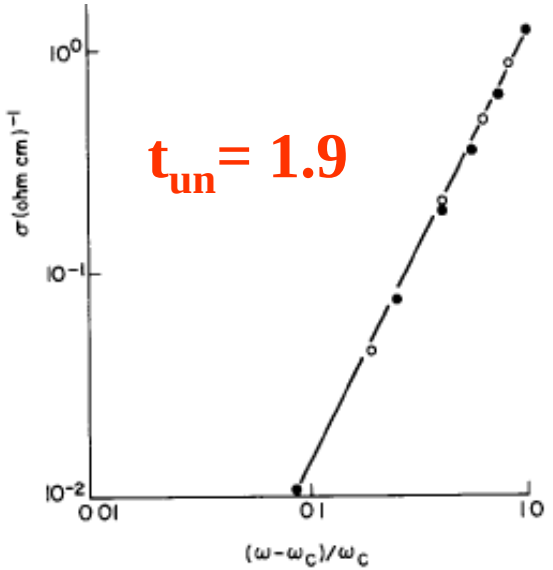

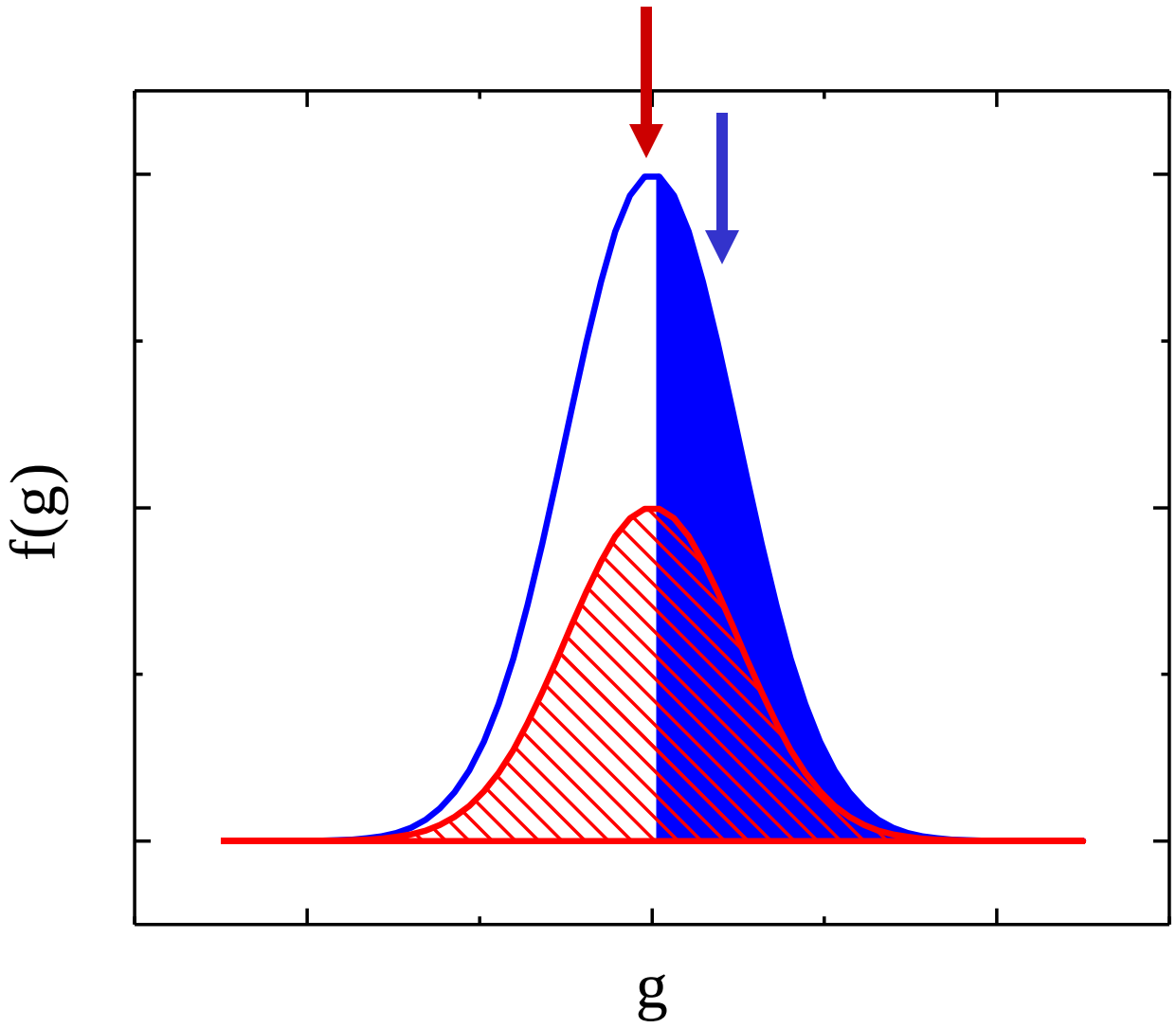
f(g)
g

The RDF

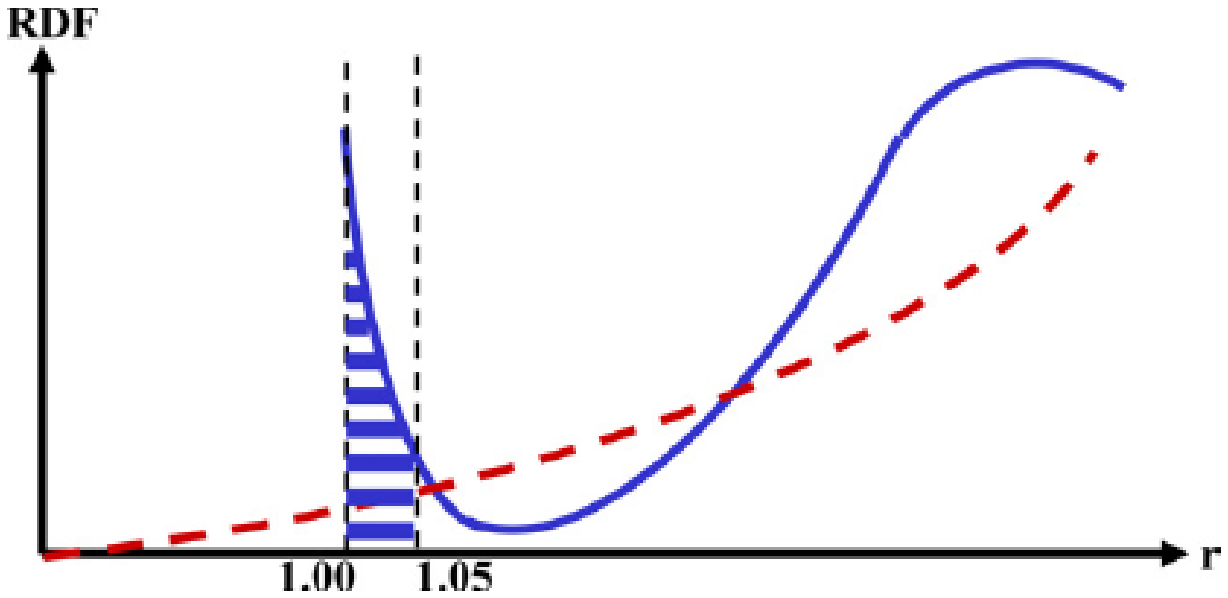

Figure 7. The main features of the RDF of non-interacting hard spheres (see figure 6) for a typical critical density of $x = 0.4$ (see [59, 60]). The solid curve represents the envelope of the contribution of the various nearest neighbours. In particular note that the integrated area between 1 and 1.05 sphere diameters (that has contributions up to the third nearest neighbours) provides, on the average, the critical two 'needed' near neighbours for a given particle. Also illustrated (by the dashed curve) is the parabolic RDF for the uniform concentration distribution (see figure 3) that is applicable to spheres with a diameter $2b$ that is negligible in comparison with the average nearest neighbours distance $2a$.

The effect of a tunneling like distribution of conductances

$$\sigma \propto (p - p_c)^t$$

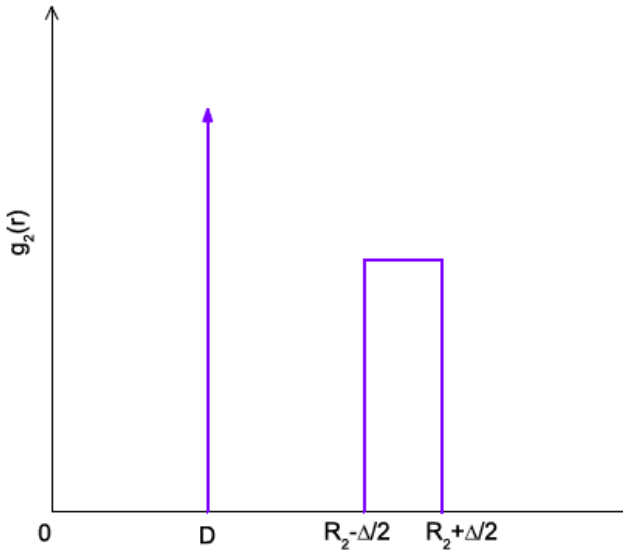

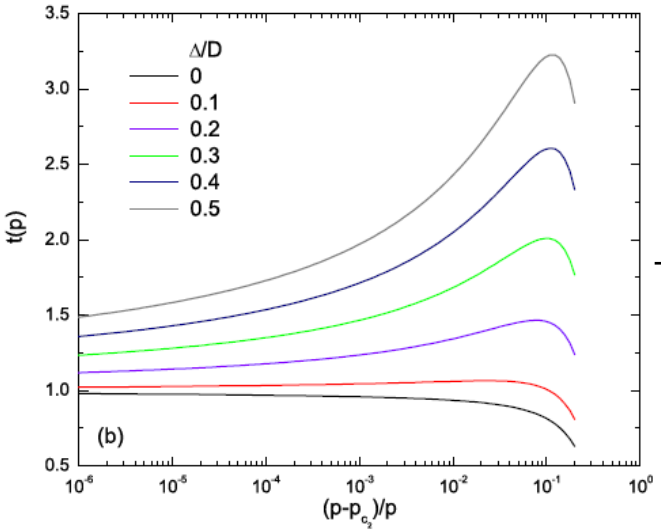

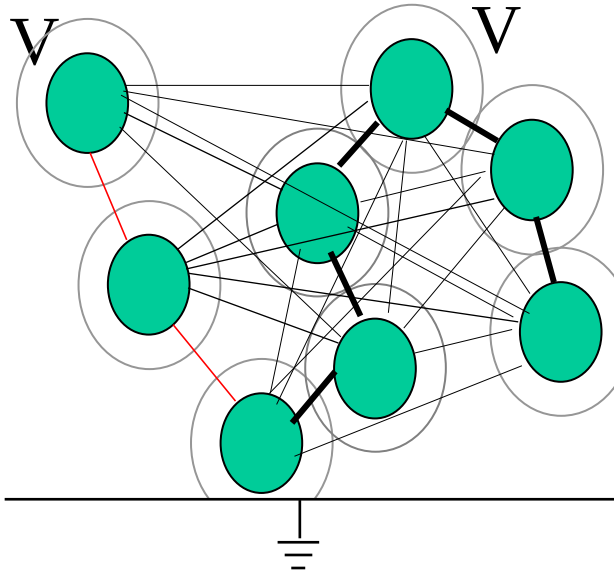

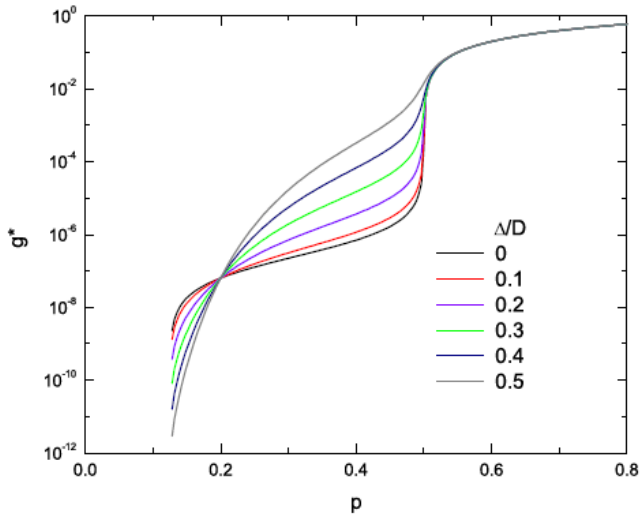

$$f(g) = (1-\alpha)g^{-\alpha}$$

$$\langle r \rangle \propto (p-p_c)^{-\alpha/(1-\alpha)}$$

$$f(g) \propto g^{(\xi/d-1)}$$

$$t = t_{un} + (d/\xi) - 1$$

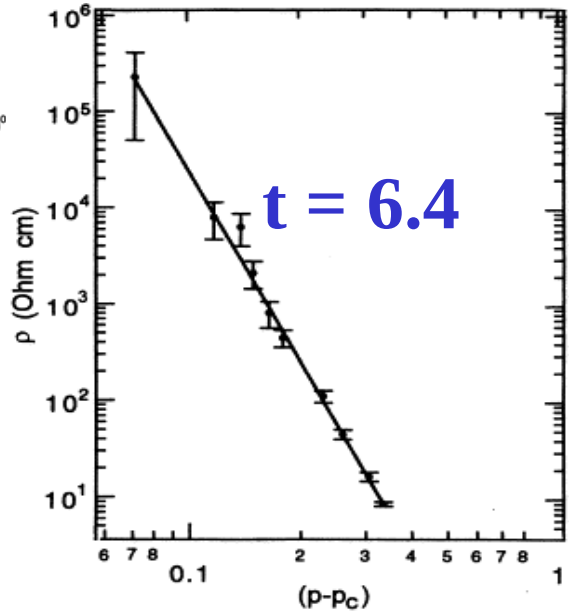

Resistors Equivalent Network

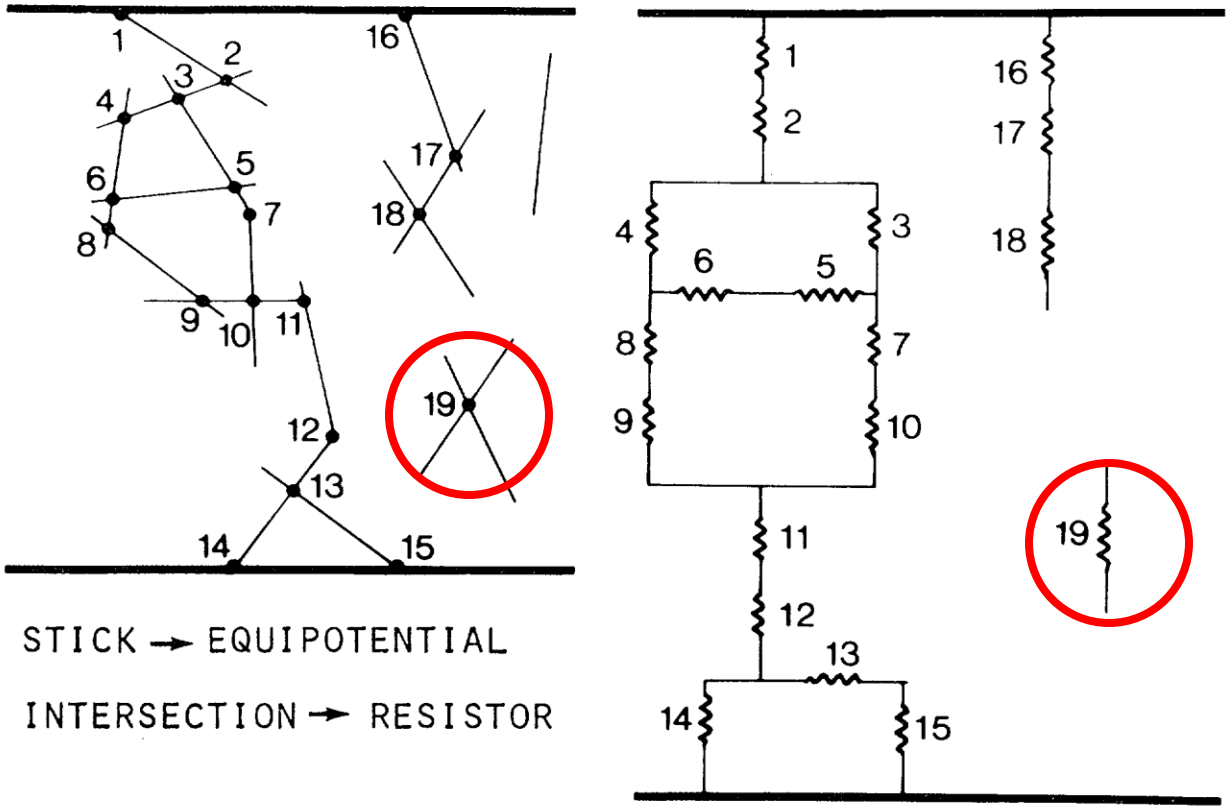

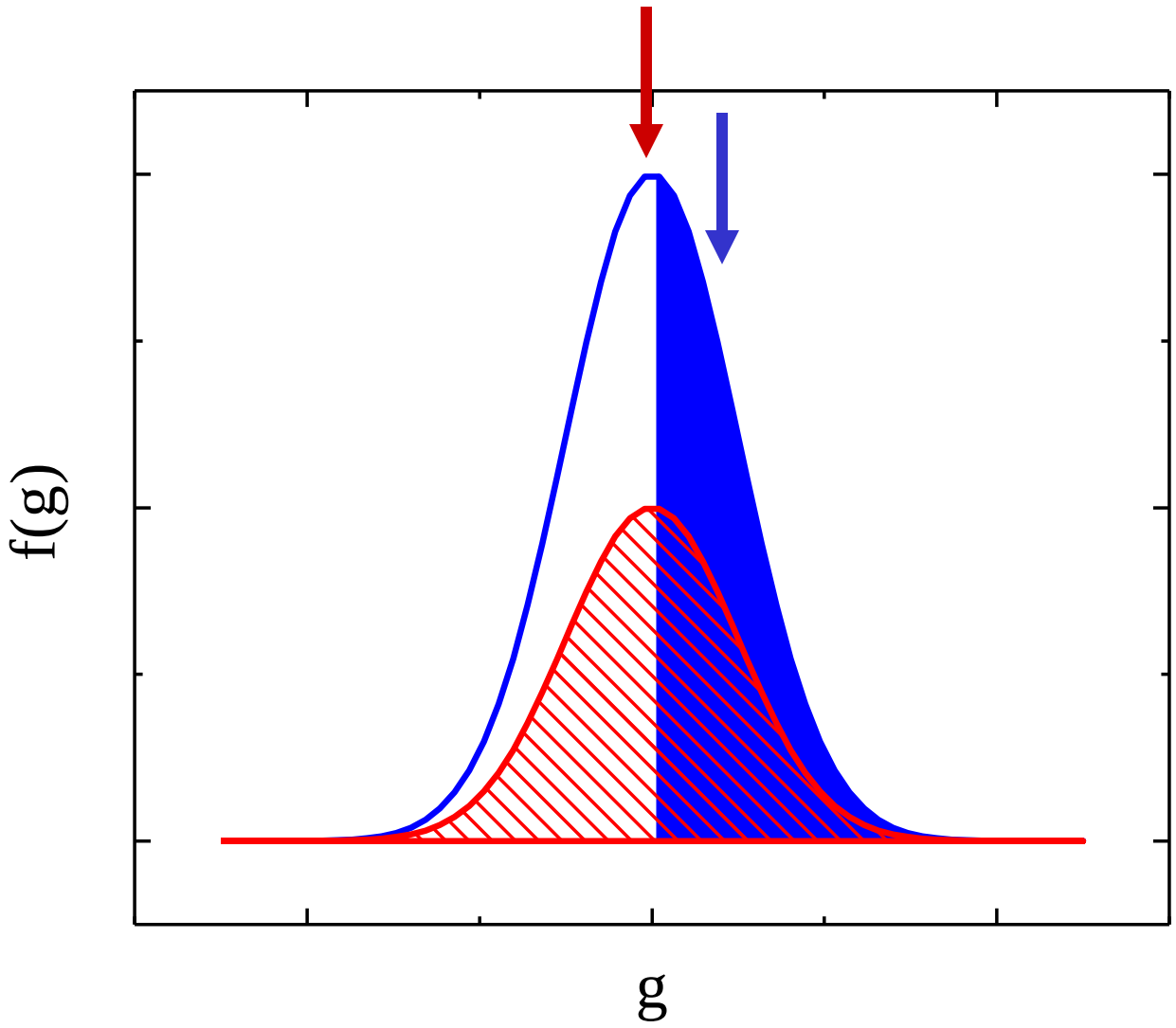
f(g)
g

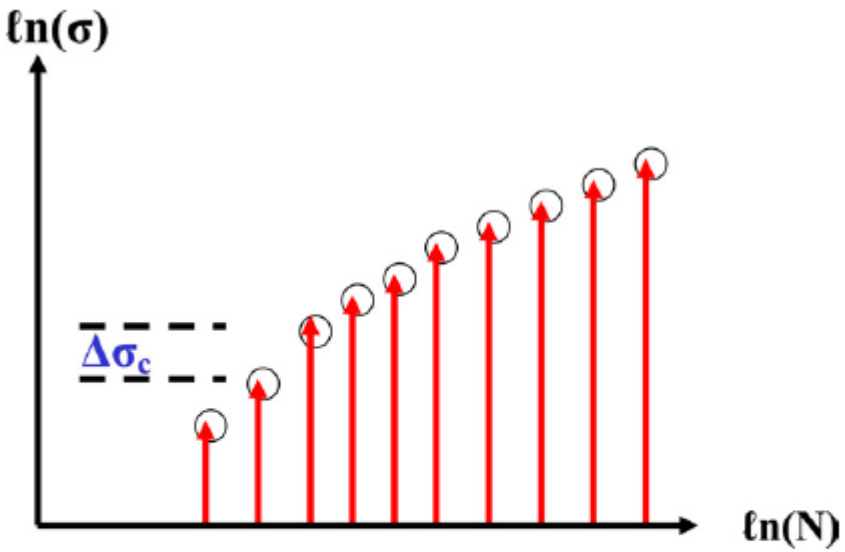

Figure 4. The dependence of the conductivity on the particle concentration in the critical sub-network of the (nearest neighbour) hopping model for a system such as the one that is shown in figure 3. The curve that is described by the open circles indicates primarily the change in the values of the critical resistors in the network. The jump in the critical conductance $\Delta\sigma_c$, with an increase in the density by ΔN is indicated in the figure.

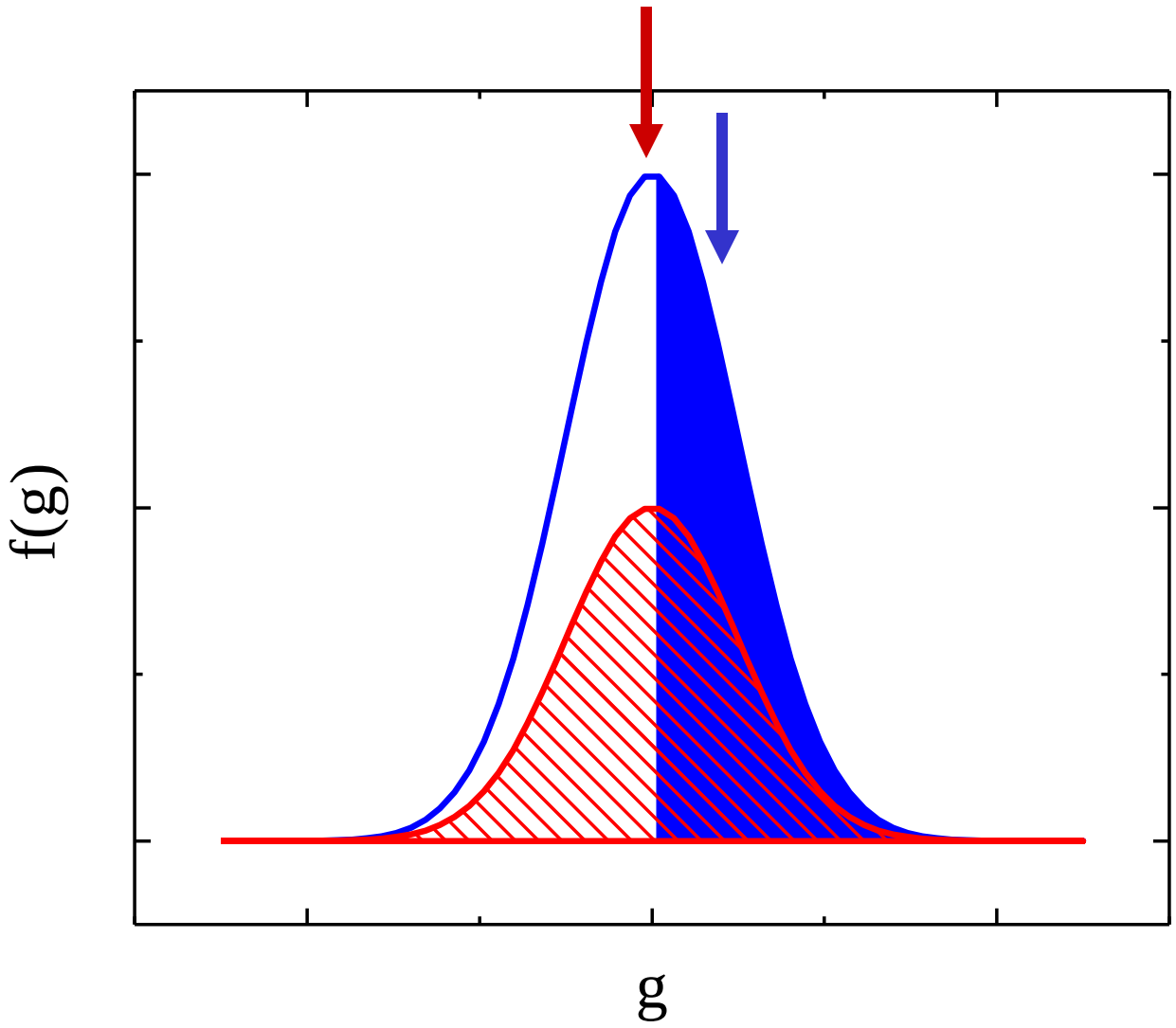
f(g)
g

A percolation threshold (critical resistor) system vs. a critical percolation (phase transition like) system

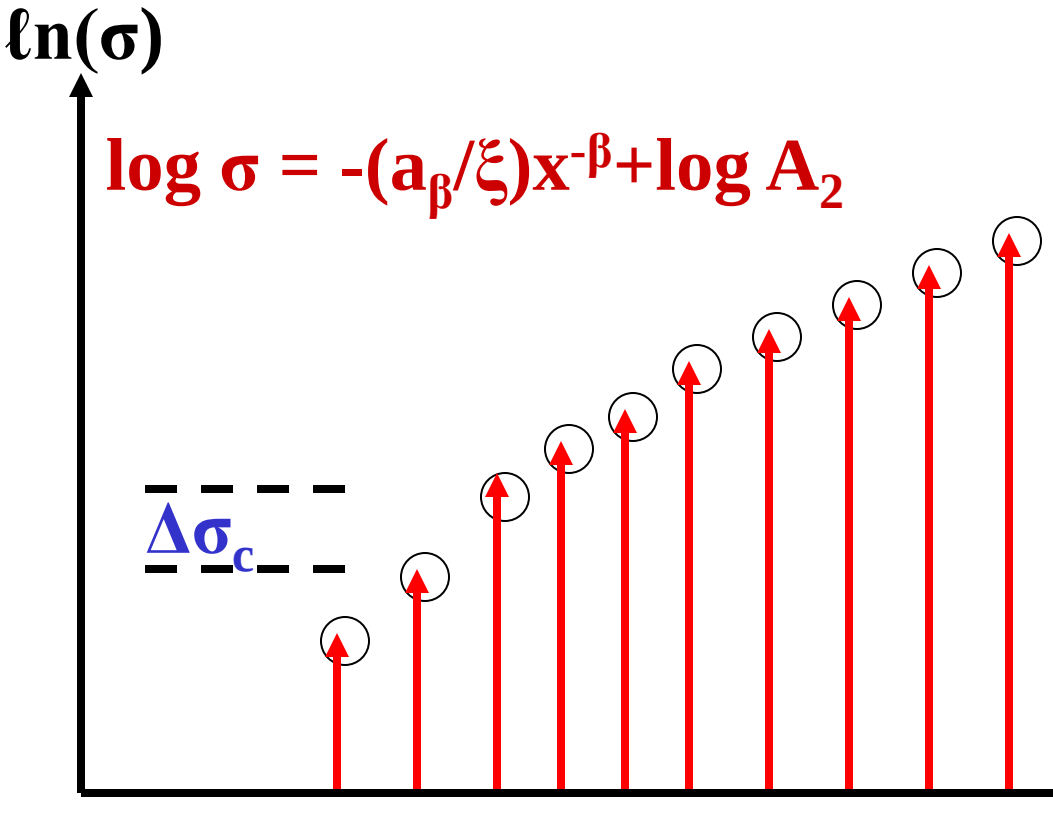

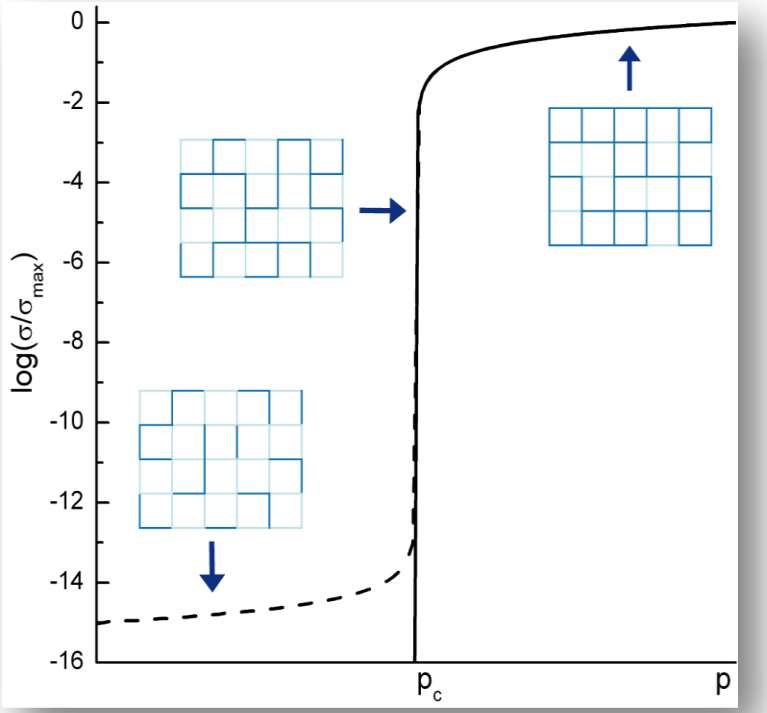

Critical Path Analysis

One labels the conductances in the system in descending order until one gets percolation i.e., one finds the largest soft shell δ that is needed to get percolation for a given Φ.

Actually, one implants hard core particles and then attaches with a shell δ/2. One checks then how many particles, or how high a Φ is needed in order to get percolation.

The agreement of the CPA with simulation of the resistors network suggests that one finds the largest σ(Φ) without having to calculate resistor networks.

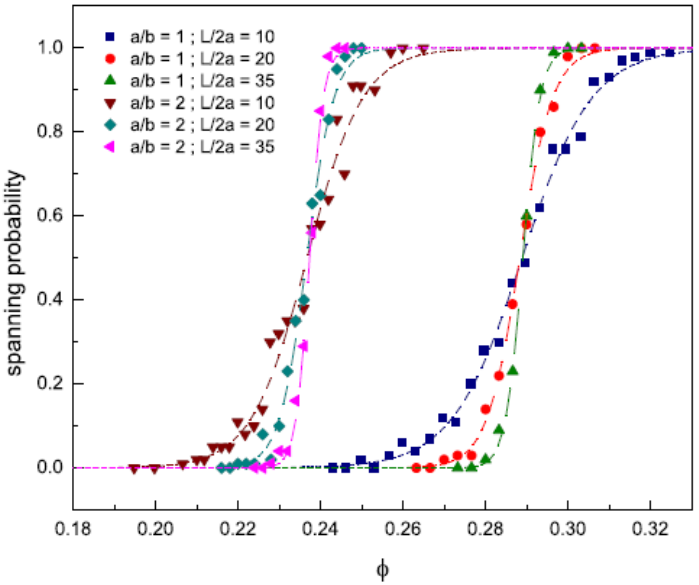

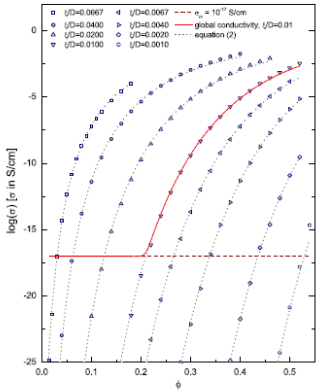

FIG. 1. (Color online) Tunneling conductivity in a system of spheres with different characteristic tunneling distance to spheres diameters ratio ξ/D as a function of the volume fraction ϕ. The matrix intrinsic conductivity for $\sigma_m=10^{-17}$ S/cm and the overall conductivity for the $\xi/D=0.01$ case are shown. Results from Eq. (2) with $\sigma_0=0.115$ S/cm are displayed by dotted lines

This works because of the very wide distribution of resistor values

$$\sigma \simeq \sigma_0 e^{-2\delta(\phi)/\xi},$$

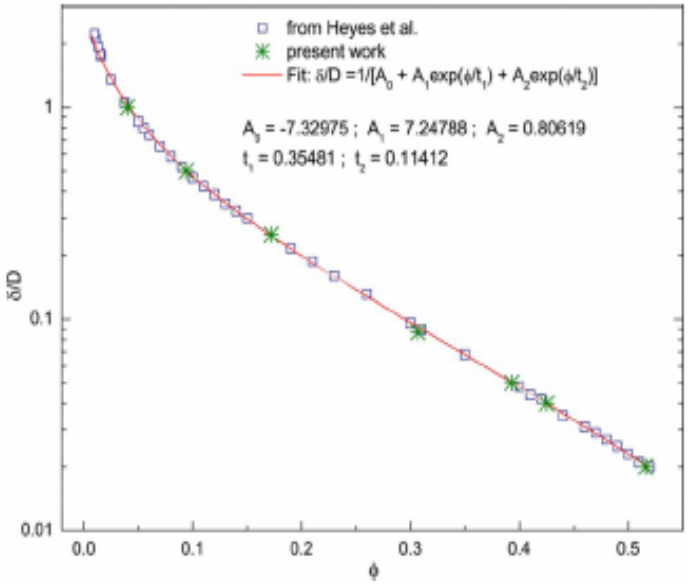

Presentation of the CPA results in terms of percolation

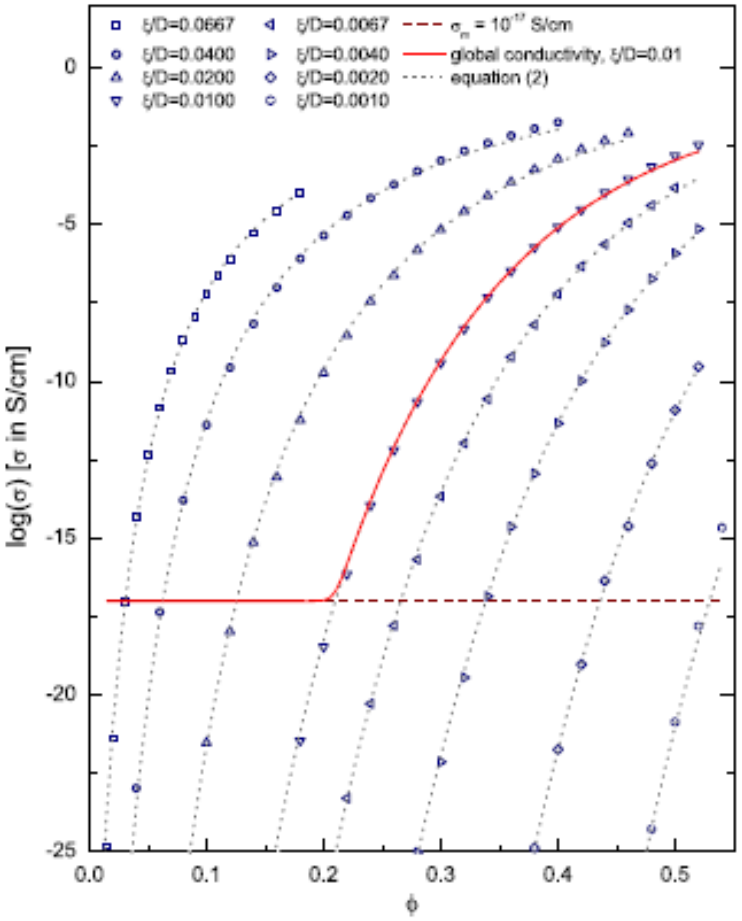

FIG. 1. (Color online) Tunneling conductivity in a system of spheres with different characteristic tunneling distance to spheres diameters ratio ξ/D as a function of the volume fraction ϕ. The matrix intrinsic conductivity for $\sigma_m=10^{-17}$ S/cm and the overall conductivity for the $\xi/D=0.01$ case are shown. Results from Eq. (2) with $\sigma_0=0.115$ S/cm are displayed by dotted lines

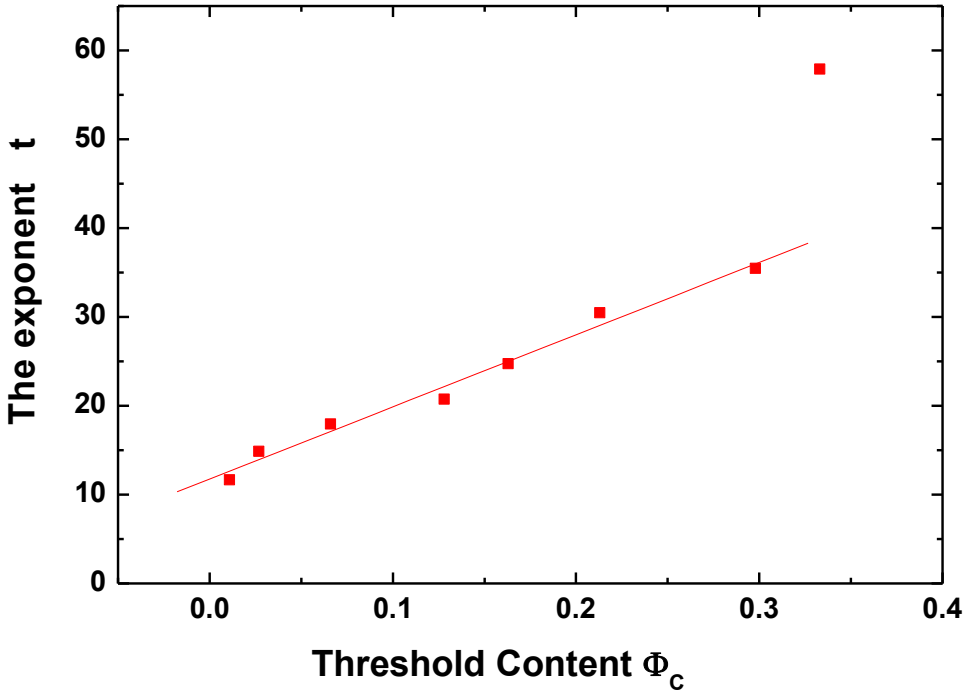

GTN for colloidal conductor-insulator composites

application of CPA formulas to real conductor-polymer nanocomposites

$$\sigma \simeq \sigma_0 \exp\left[-\frac{2\delta_c(\phi)}{\xi}\right]$$

from the knowledge of σ vs ϕ and from the filler geometry [a/b and D=2max(a,b)] one can estimate the value of the tunneling factor ξ

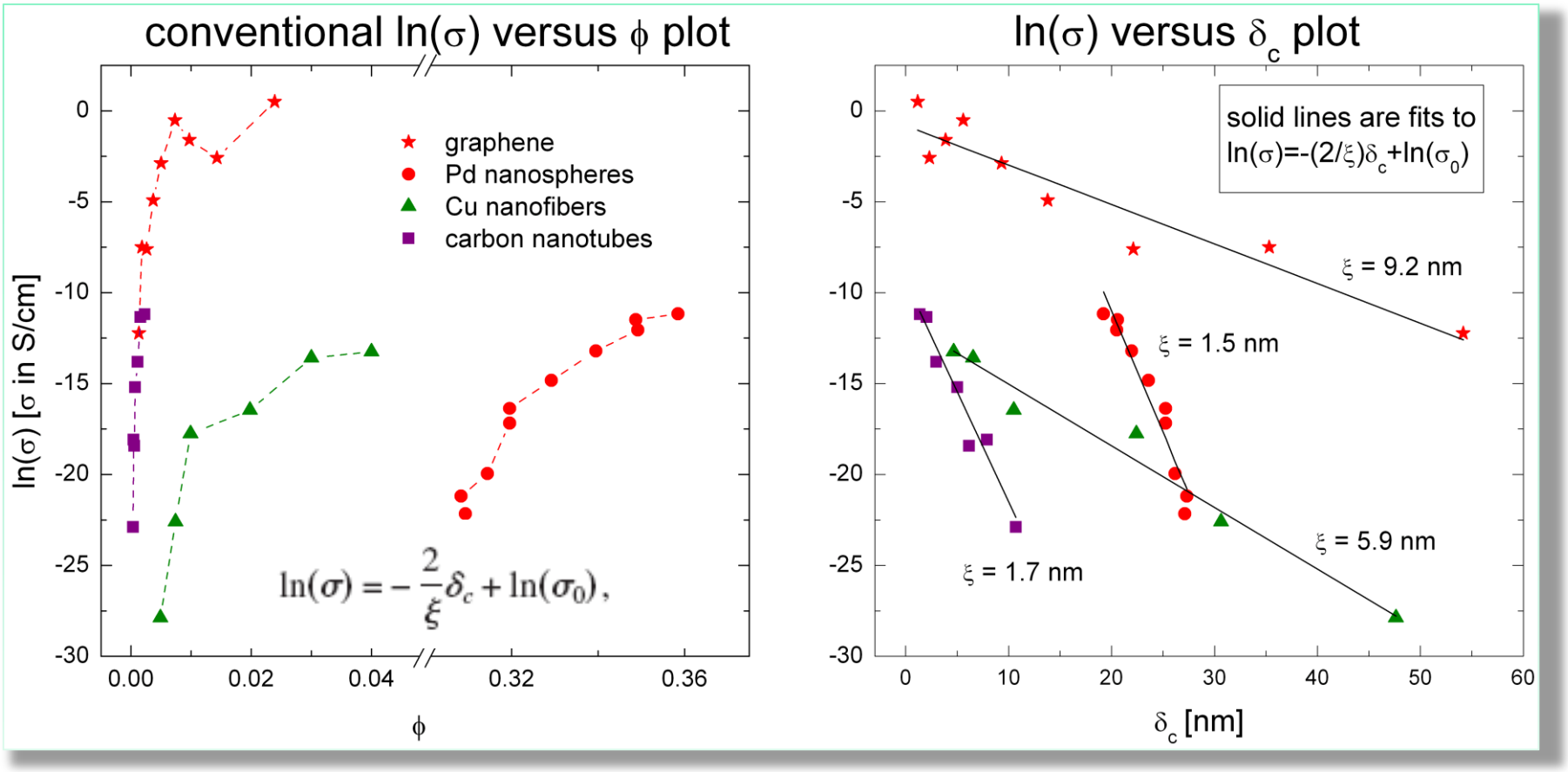

The physical and mathematical resemblance of the percolation and (CPA) hopping behaviors:

In the classical hopping (CPA) model :

$$\log \sigma = -d/\xi = -(a_\beta/\xi)x^{-\beta} + \log A_1 \quad 1/3 \le \beta \le 1$$

In our percolation model: $\log \sigma = t \log(x-x_c) + \log A_2$

we saw (from the Excluded volume argument) that

$t = t_{un} + d/\xi - 1$ **so that for** $t >> t_{un}$ **we have that** $t \approx -x^{-\beta}/\xi$

where $1/3 \le \beta \le 1$ **and** $\log (x-x_c) < 0$.

- **The two dependence yield then quite a similar dependence on x. Experimentally; since usually** $x >> x_c$ **these two are usually non distinguishable. Can we still distinguish between them?**

GTN for colloidal conductor-insulator composites

application of CPA formulas to real conductor-polymer nanocomposites

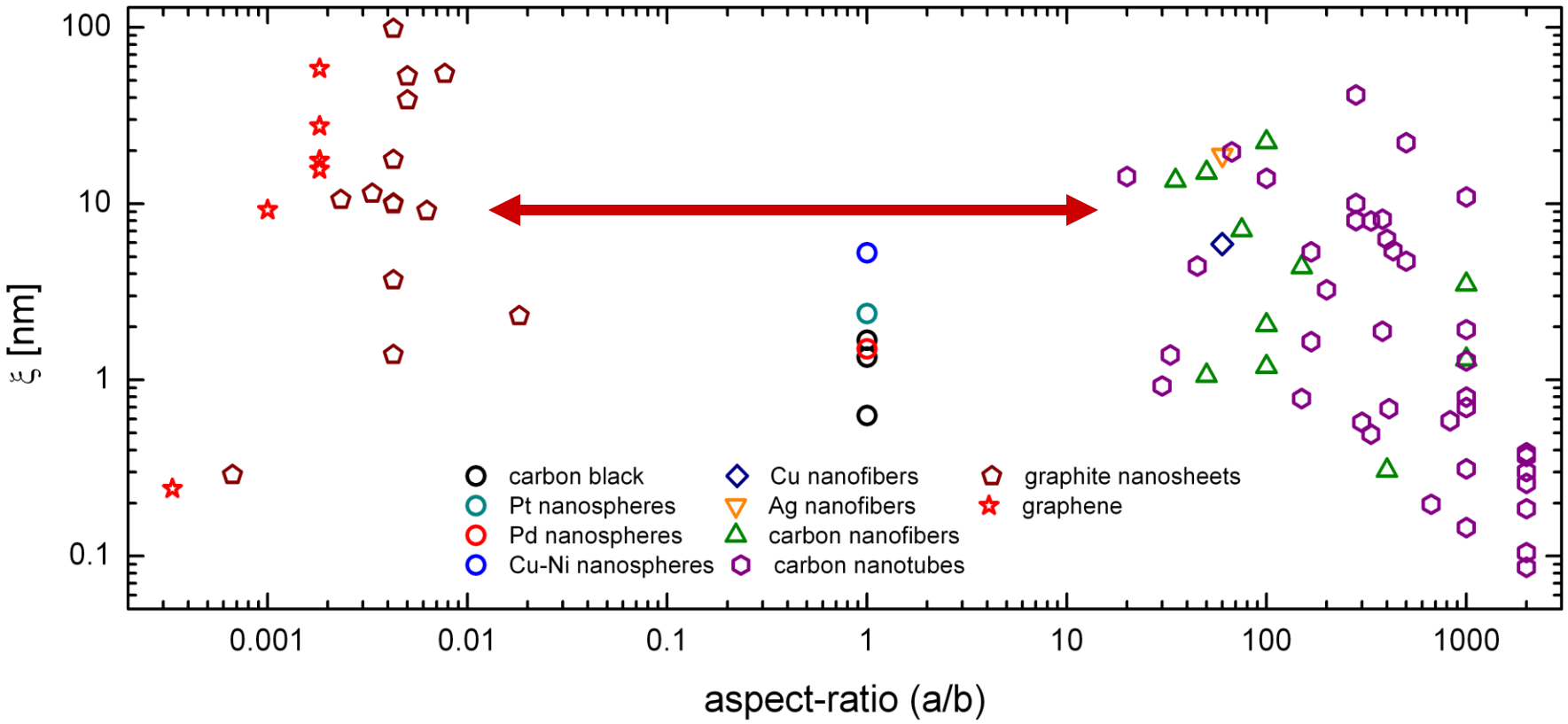

even if a/b changes over 6 orders of magnitude, the tunneling factor is found to be within the expected range 0.1 nm < ξ < 10 nm

[G. Ambrosetti et al. Phys. Rev. B 81, 155434 (2010)]

The effect of tunneling in lattices and the continuum

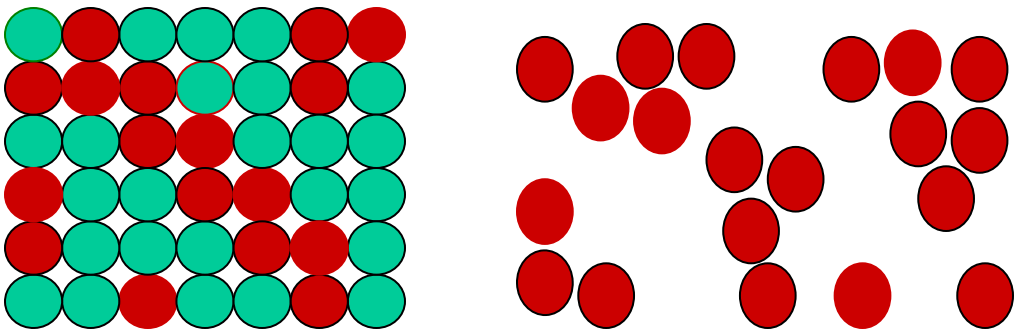

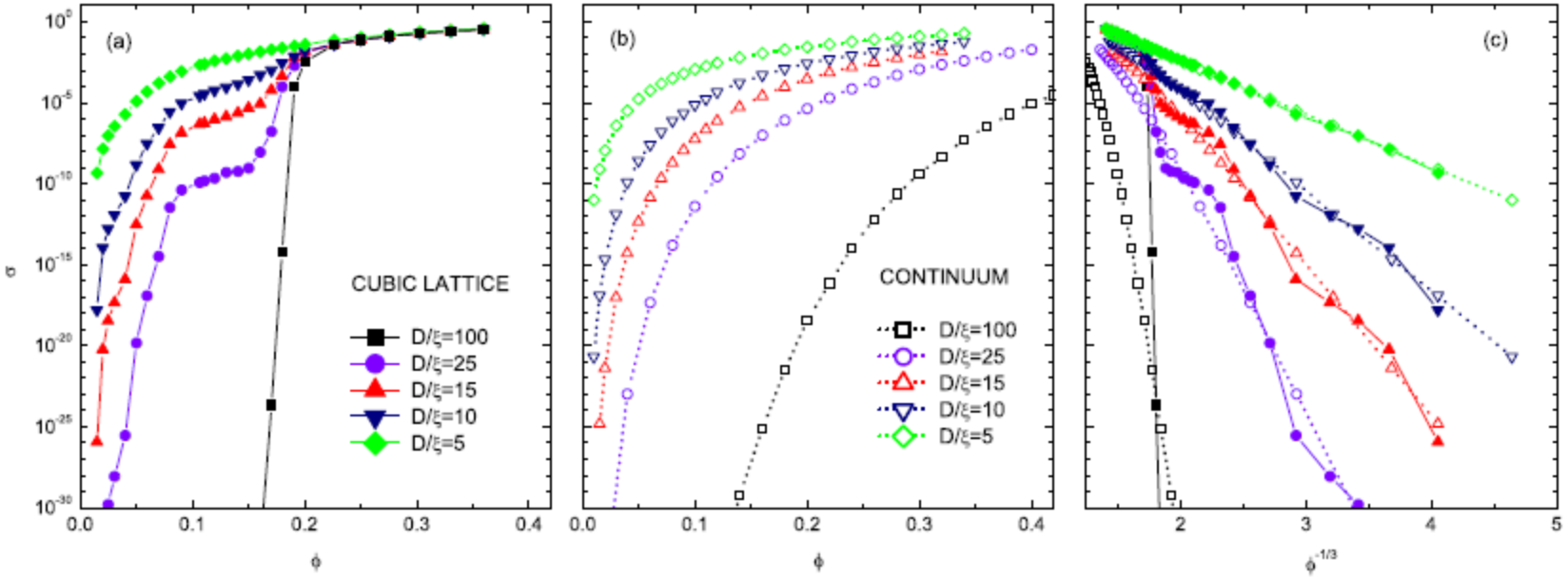

FIG. 3. (Color online) Monte Carlo conductance for (a) the cubic lattice model and (b) the continuum model for different values of D/ξ. (c) The same results of (a) and (b) plotted as a function of $\phi^{-1/3}$.

Analysis of a resistors network

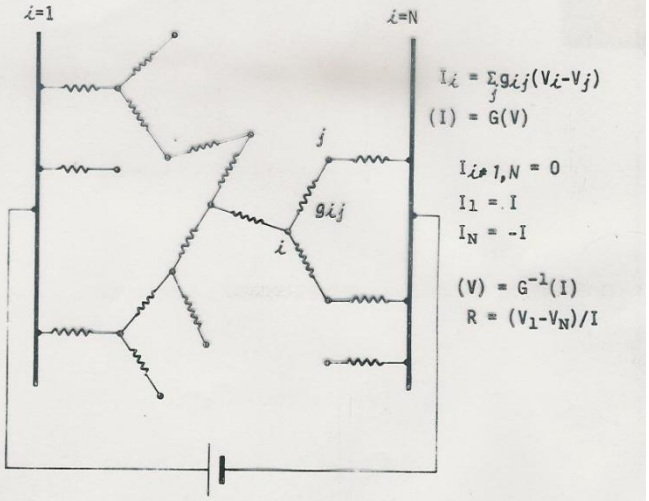

$$G_{ii} = \sum_{\substack{j=1 \\ j \neq i}}^{N} g_{ij}$$

$$G_{ij} = -g_{ij}$$

Critical Path Analysis

One labels the conductances in the system in descending order until one gets percolation.

One takes then the smallest conductance thus found and determines its δ(Φ) value. The agreement with simulation suggests that:

One can simply arrange the δ(Φ) values and find directly the largest needed δ(Φ) without having to calculate resistor networks.

This works because of the very wide distribution of resistor values

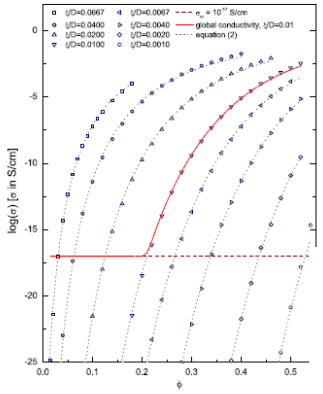

FIG. 1. (Color online) Tunneling conductivity in a system of spheres w different characteristic tunneling distance to spheres diameters ratio ξ/D a function of the volume fraction ϕ. The matrix intrinsic conductivity $\sigma_m=10^{-17}$ S/cm and the overall conductivity for the $\xi/D=0.01$ case are shown. Results from Eq. (2) with $\sigma_0=0.115$ S/cm are displayed by dotted lines

$$\varrho = \varrho_0 e^{-2(s-D)/\xi},$$

$$\sigma \simeq \sigma_0 e^{-2\delta(\phi)/\xi},$$

$$\frac{\delta(\phi_c)}{\xi} = \frac{1}{2}\ln\left(\frac{\sigma_0}{\sigma_m}\right),$$

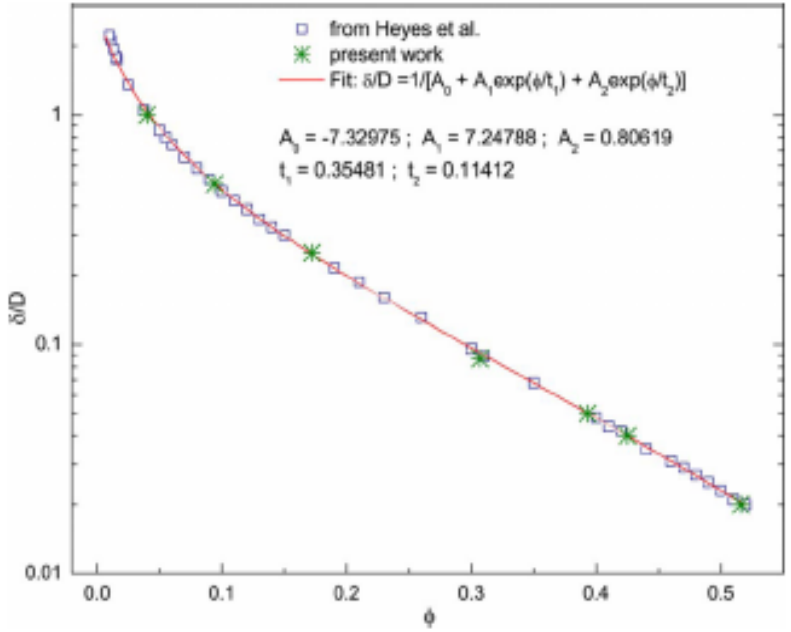

FIG. 2. (Color online) Geometrical percolation threshold of the hard-core-soft-shell model from algorithm of present work and from results of Ref. 16. Shown is the critical interaction distance to sphere diameter ratio δ/D as a function of the hard spheres volume fraction ϕ.

The excluded volume approach

- The parameter that is known experimentally is the critical volume % of the "filler" Φ_c, so the prediction to be made is how does Φc depend on the microscopic parameters.
- For spheres these parameters are D and ξ so:
- $v= (4\pi/3)(D/2)^3$, $\Phi = Nv$, $\Phi_c = N_c v$,
- $B_c = (4\pi/3)(r_c^3-D^3)N$ and $\delta_c = r_c-D$
- Case 1: $r_c >> D \rightarrow B_c = (4\pi/3)(\delta_c^3)N = (4\pi/3)(\delta_c^3)\Phi/v$
- $\rightarrow \delta_c \propto (\Phi/v)^{-1/3} \rightarrow$
- **$\text{Log } \rho = \alpha_1 + \beta_1 \Phi^{-1/3}$.**
- Case 2: $r_c \approx D \rightarrow B_c \approx (4\pi/3)(3\delta_c D^2)N = (4\pi/3)(3\delta_c D^3)N/D = (3\delta_c 8)\Phi/D$
- $\Phi/v \rightarrow B_c = 24\, \delta_c \Phi/D \rightarrow \delta_c = B_c D/24\Phi$
- $\delta_c \propto D\Phi^{-1}$
- **$\text{Log } \rho = \alpha_1 + \beta_1 \Phi^{-1}$.**

The predicted CPA conductivity dependence on Φ

- For capped cylinders:
- $v \approx \pi R^2 L$, $\Phi = Nv = \pi R^2 LN$
- $\Delta V_{ex} \approx \pi L^2 \delta_c \langle \sin\theta \rangle$, $N\Delta V_{ex} = B_c$

- $\delta_c \approx B_c R[(R/L)\langle \sin\theta \rangle]\Phi^{-1} \propto \Phi^{-1}$
- In general then, $\delta_c \propto \Phi^{-\beta}$ where in 3D: $1/3 \leq \beta \leq 1$

CPA for spheres

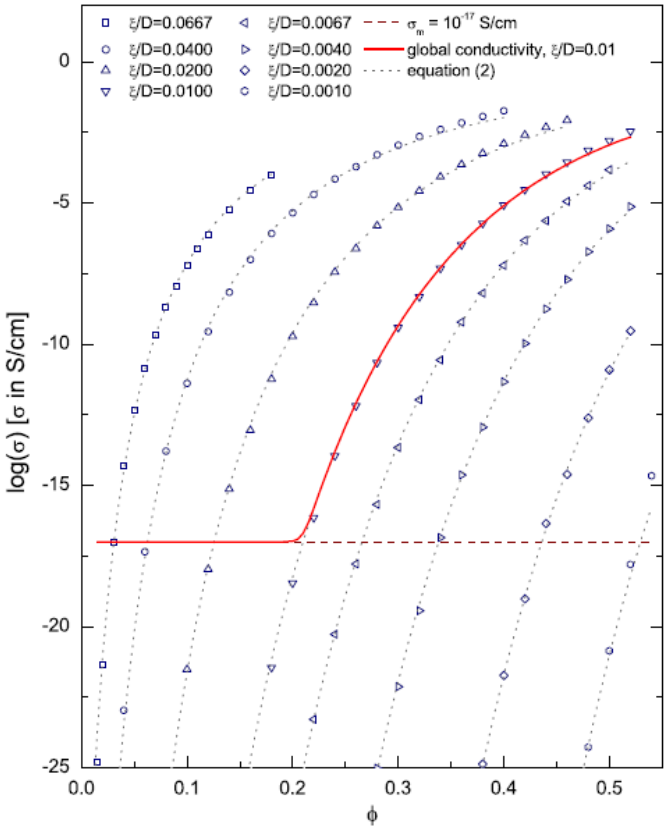

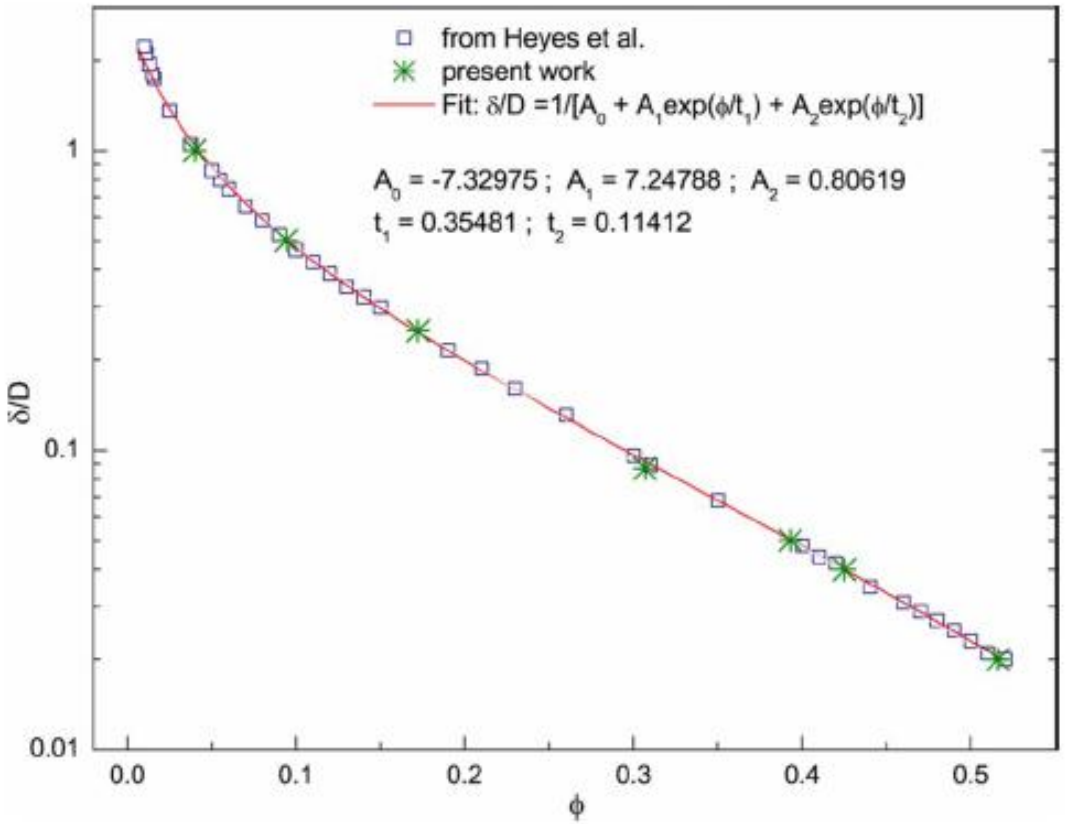

The RDF

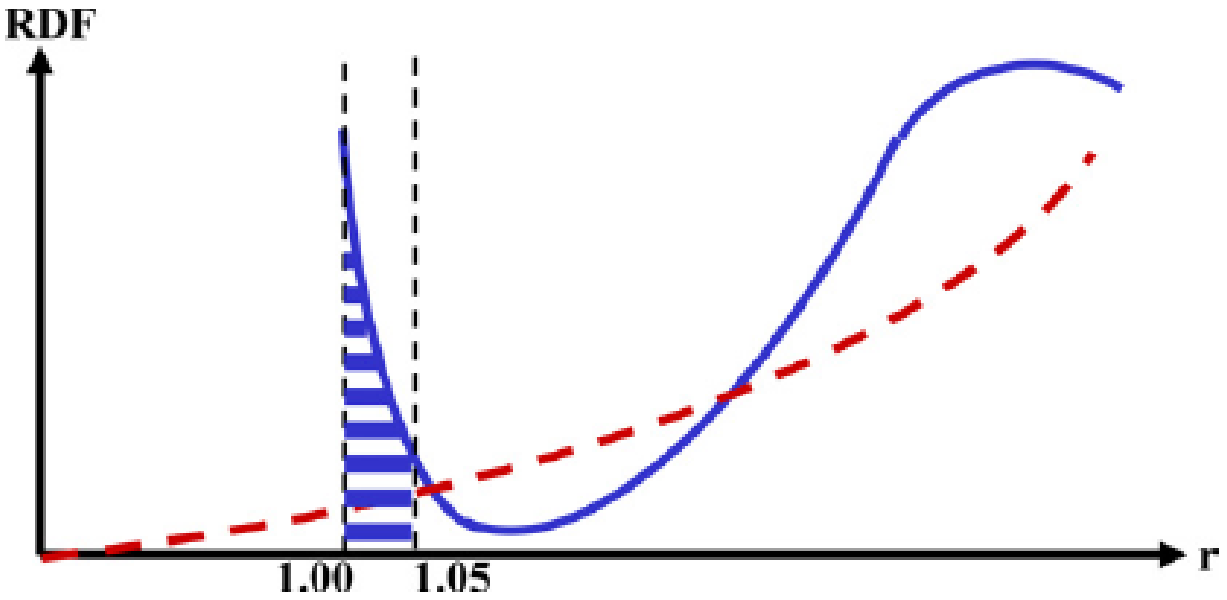

Figure 7. The main features of the RDF of non-interacting hard spheres (see figure 6) for a typical critical density of $x = 0.4$ (see [59, 60]). The solid curve represents the envelope of the contribution of the various nearest neighbours. In particular note that the integrated area between 1 and 1.05 sphere diameters (that has contributions up to the third nearest neighbours) provides, on the average, the critical two 'needed' near neighbours for a given particle. Also illustrated (by the dashed curve) is the parabolic RDF for the uniform concentration distribution (see figure 3) that is applicable to spheres with a diameter $2b$ that is negligible in comparison with the average nearest neighbours distance $2a$.

The End

VISCOSITY vs. CONDUCTIVITY

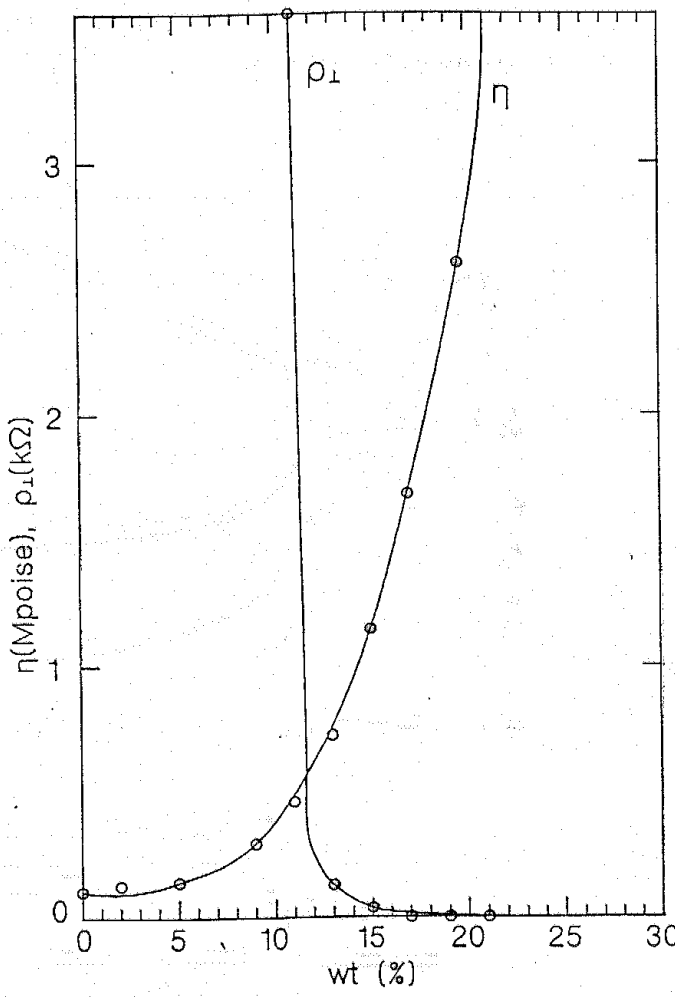

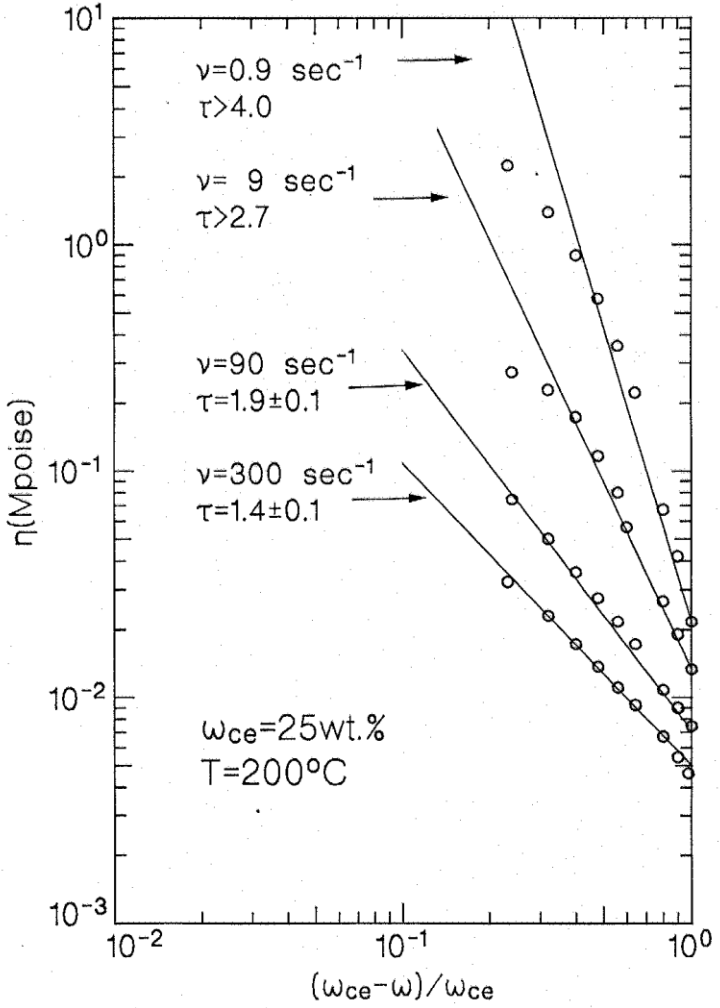

The differences between the different types of elongated Carbon particles

Table 1 – Typical properties of VGCNF, SWNT, MWNT and CF

Property	VGCNF[a]	SWNT[b]	MWNT[b]	CF[c]
Diameter (nm)	50–200	0.6–1.8	5–50	7300
Length (μm)	50–100			3200
Aspect ratio	250–2000	100–10,000	100–10000	440
Density (g/cm^3)	2	~1.3[d]	~1.75[e]	1.74
Thermal conductivity (W/m K)	1950	3000–6000[f]	3000–6000[f]	20
Electrical resistivity (Ω cm)	1×10^{-4}	1×10^{-3}–1×10^{-4}	2×10^{-3}–1×10^{-4}	1.7×10^{-3}
Tensile strength (GPa)	2.92	50–500[g]	10–60[g]	3.8
Tensile modulus (GPa)	240	1500	1000	227

a From Refs. [1,20,62,66].
b From Ref. [2].
c Properties of Akzo Nobel Fortafil 243 PAN-based fibers [67].
d From Ref. [33].
e From Ref. [68].
f From Ref. [69].
g From Ref. [35].

For high structure carbon black the aspect ratio is of the order of 10

The End

Recent results of the RF conductivity and permitivity of Carbon Black composites

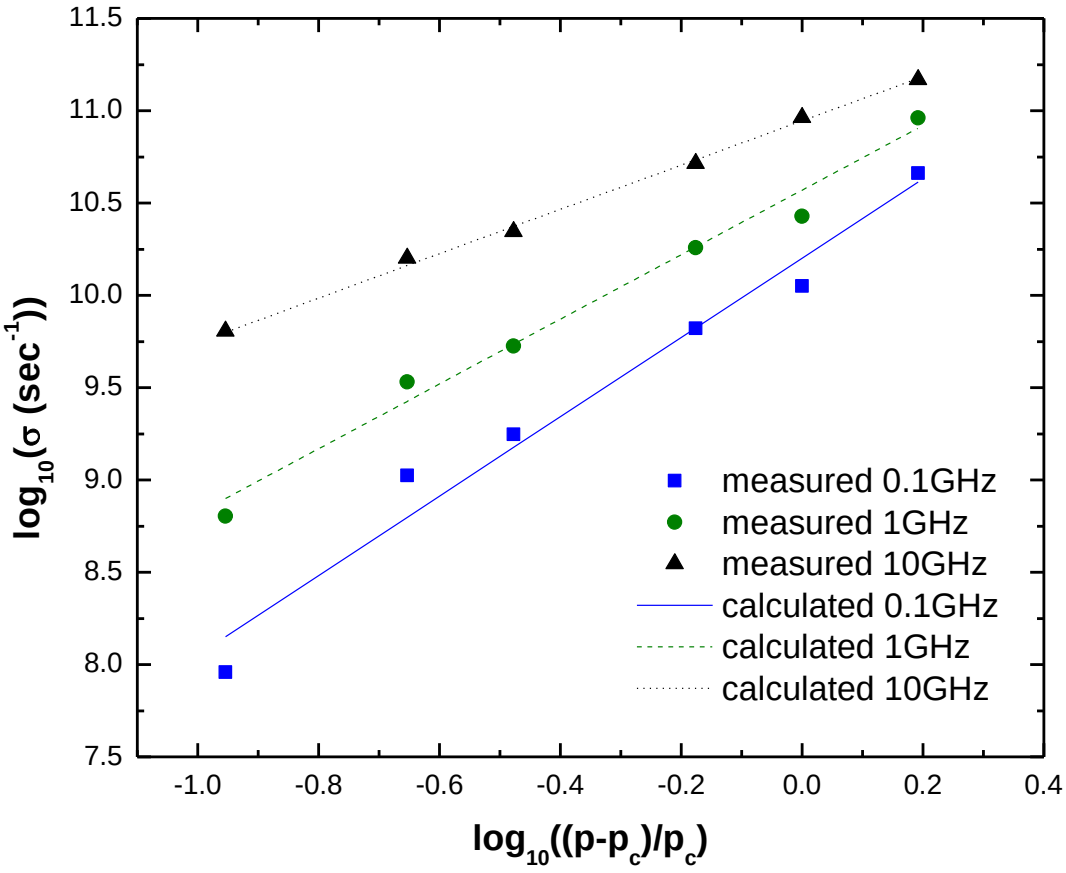
11.5
11.0
10.5
10.0
9.5
9.0
8.5
8.0
7.5
-1.0
-0.8
-0.6
-0.4
-0.2
0.0
0.2
0.4
log10(σ (sec-1))
log10((p-pc)/pc)
measured 0.1GHz
measured 1GHz
measured 10GHz
calculated 0.1GHz
calculated 1GHz
calculated 10GHz

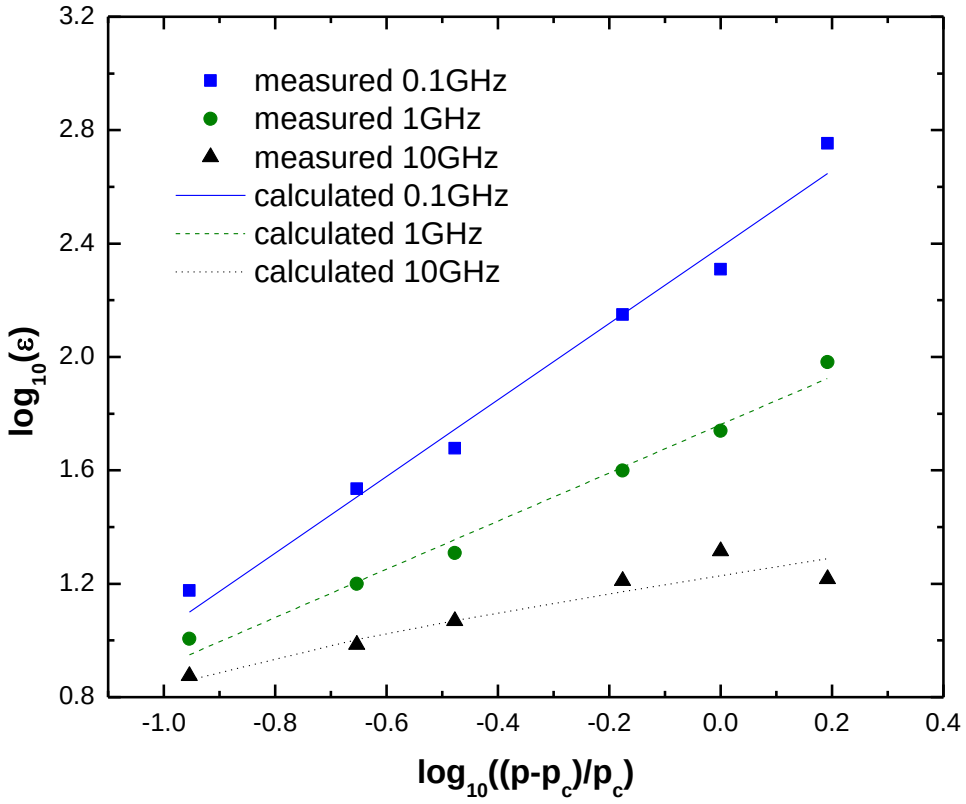
measured 0.1GHz
measured 1GHz
measured 10GHz
calculated 0.1GHz
calculated 1GHz
calculated 10GHz
log10(ε)
log10((p-pc)/pc)
3.2
2.8
2.4
2.0
1.6
1.2
0.8
-1.0
-0.8
-0.6
-0.4
-0.2
0.0
0.2
0.4

Conductivity exponent

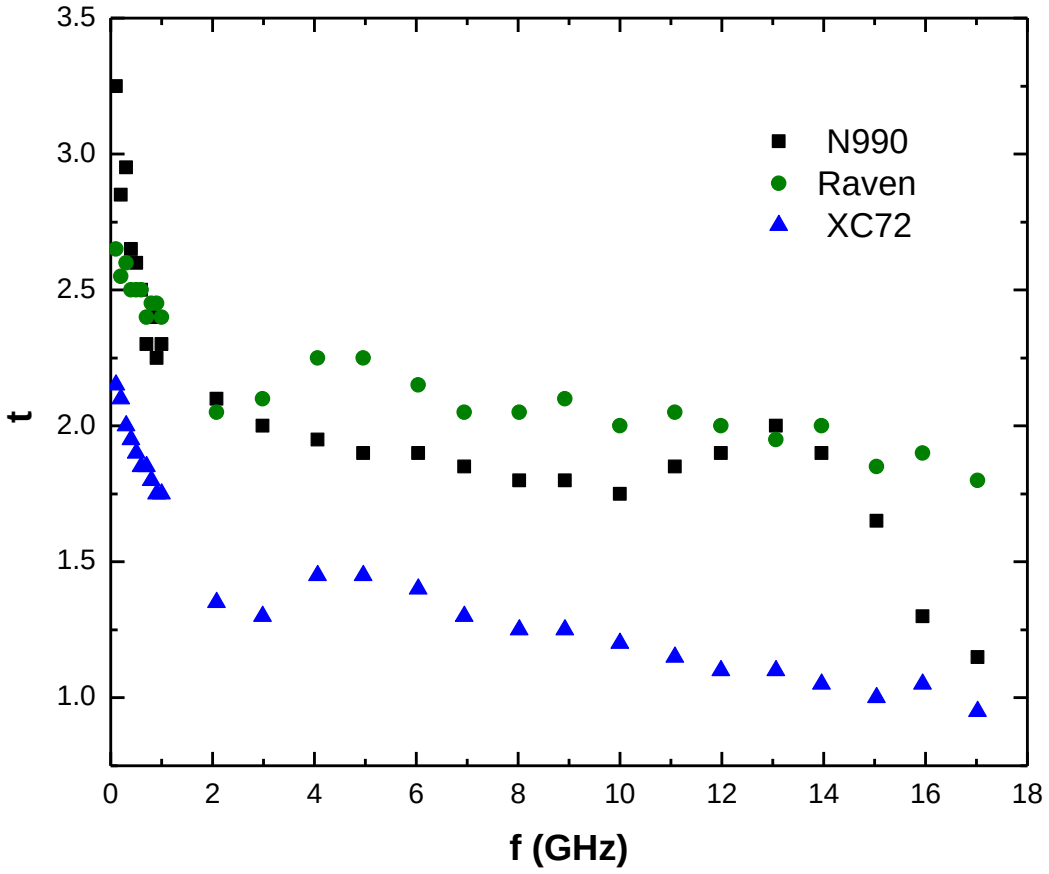

Permitivity exponent

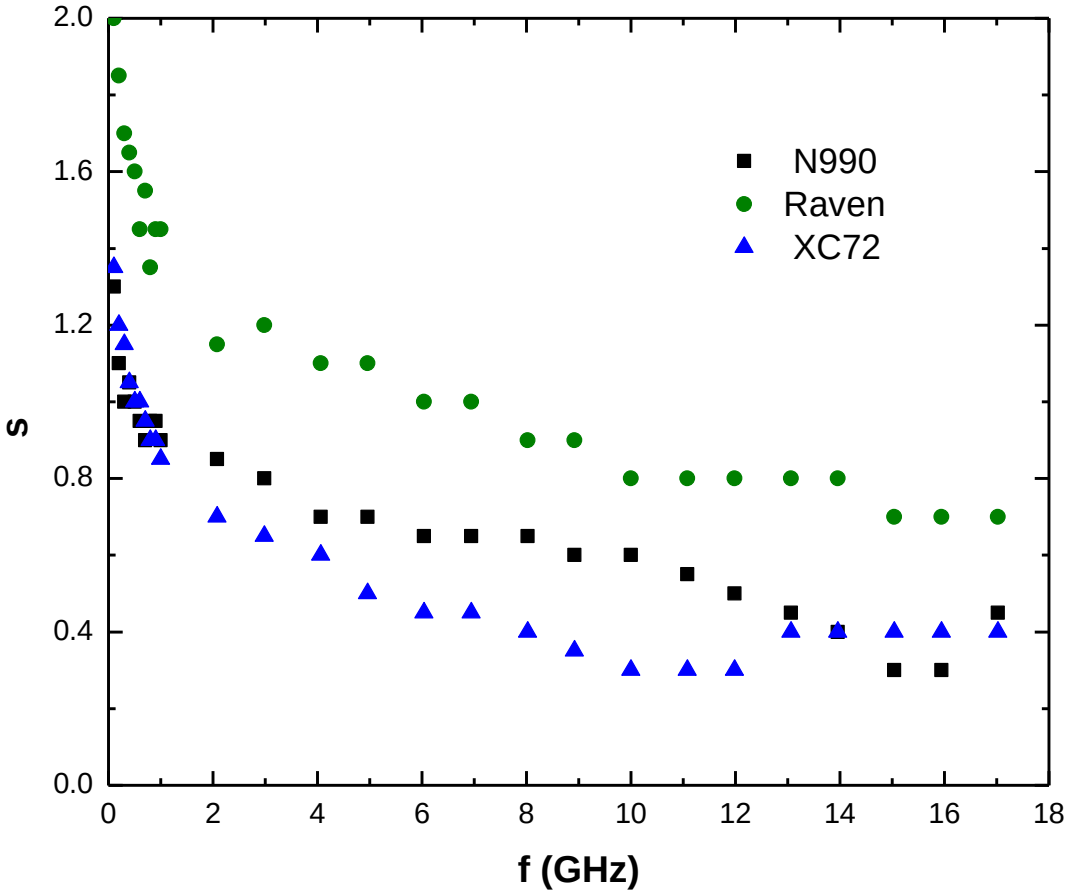

THE ISRAEL VACUUM SOCIETY
Science, Technology & Applications

האגודה הישראלית לואקום
מדע, טכנולוגיה ויישומים

One – Day IVS Symposium & Folman Lecture

Carbon Nanostructures - from fundamentals to applications

Thursday Jan. 13 2011, 8:45 - 17:30

Coler California Visitors Center, Technion, Haifa

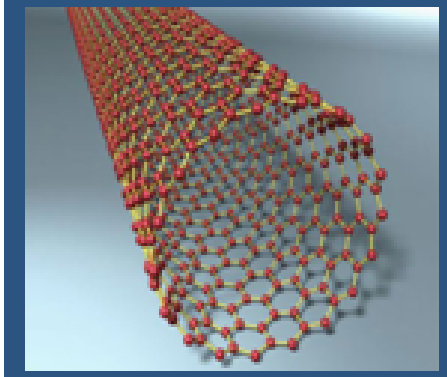

Speakers:

Ernesto Joselevich, Weizmann Institute
Yachin Cohen, Technion
Daniel Wagner, Weizmann Institute
Andrey Kaplan , University of Birmingham , UK
Rafi Kalish, Technion
Isaac Balberg, The Hebrew University of Jerusalem
Yeshayahu Lifshitz, Technion
Oded Hod, Tel Aviv University
Oren Regev, Ben Gurion University of the Negev
Daniel Nessim. Bar Ilan University

14:00-15:00 **Folman Lecture:** Prof. Reshef Tenne, Weizmann Institute
15:00-15:30 Get together

Registration and Information:
www.science.co.il/ivs/conferences/

ORGANIZING AND PROGRAM COMMITTEE
Eli Kolodney, Technion
Alon Hoffman, Technion

IVS - CONFERENCE SECRETARIAT
Galit Weizman:
ivscon09@tx.technion.ac.il
Phone: + 972- 54- 5580727

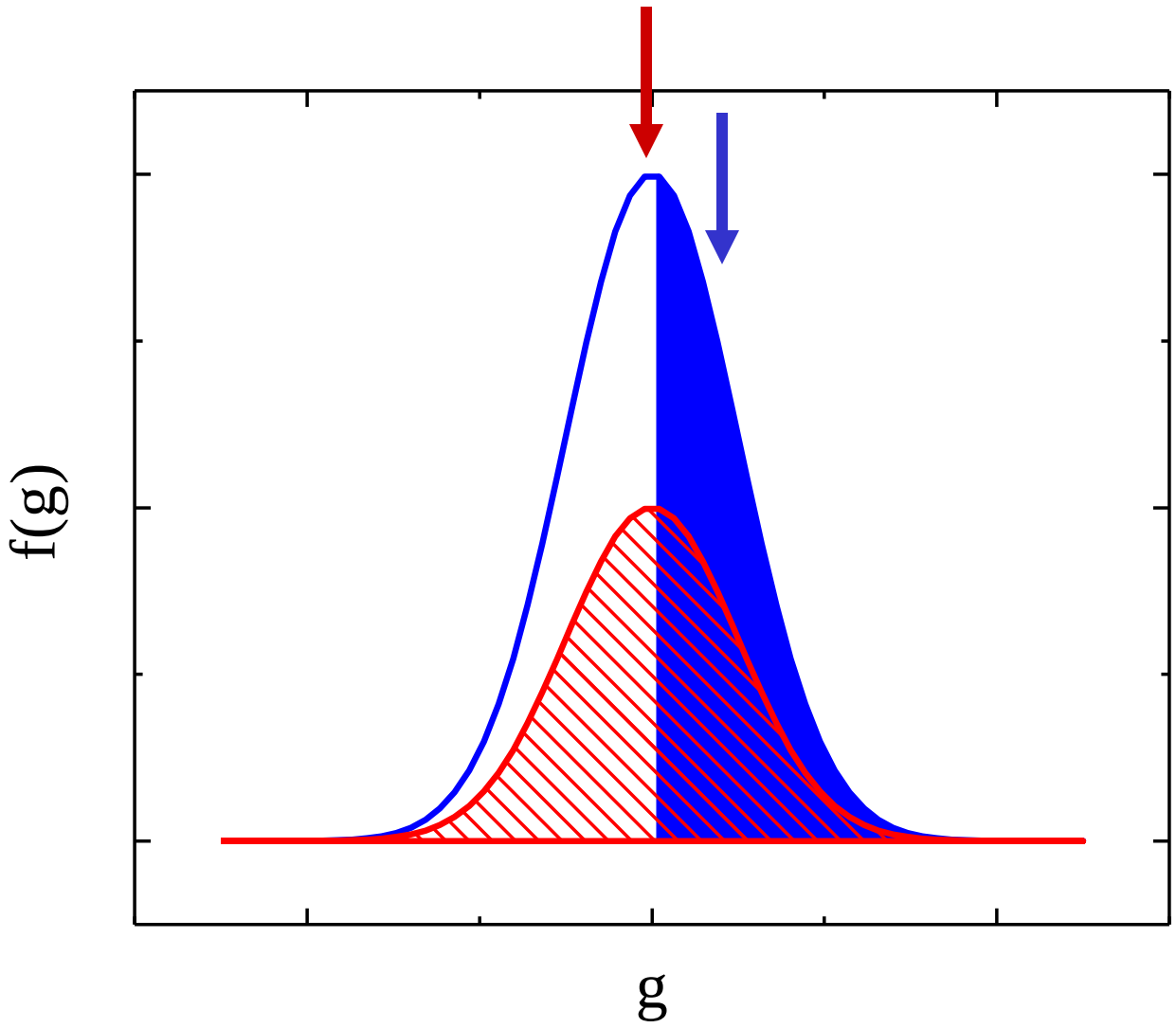
f(g)
g

An illustration of the basic answer

Approach: Keeping p and going from Z_1 to Z_2 in the square lattice

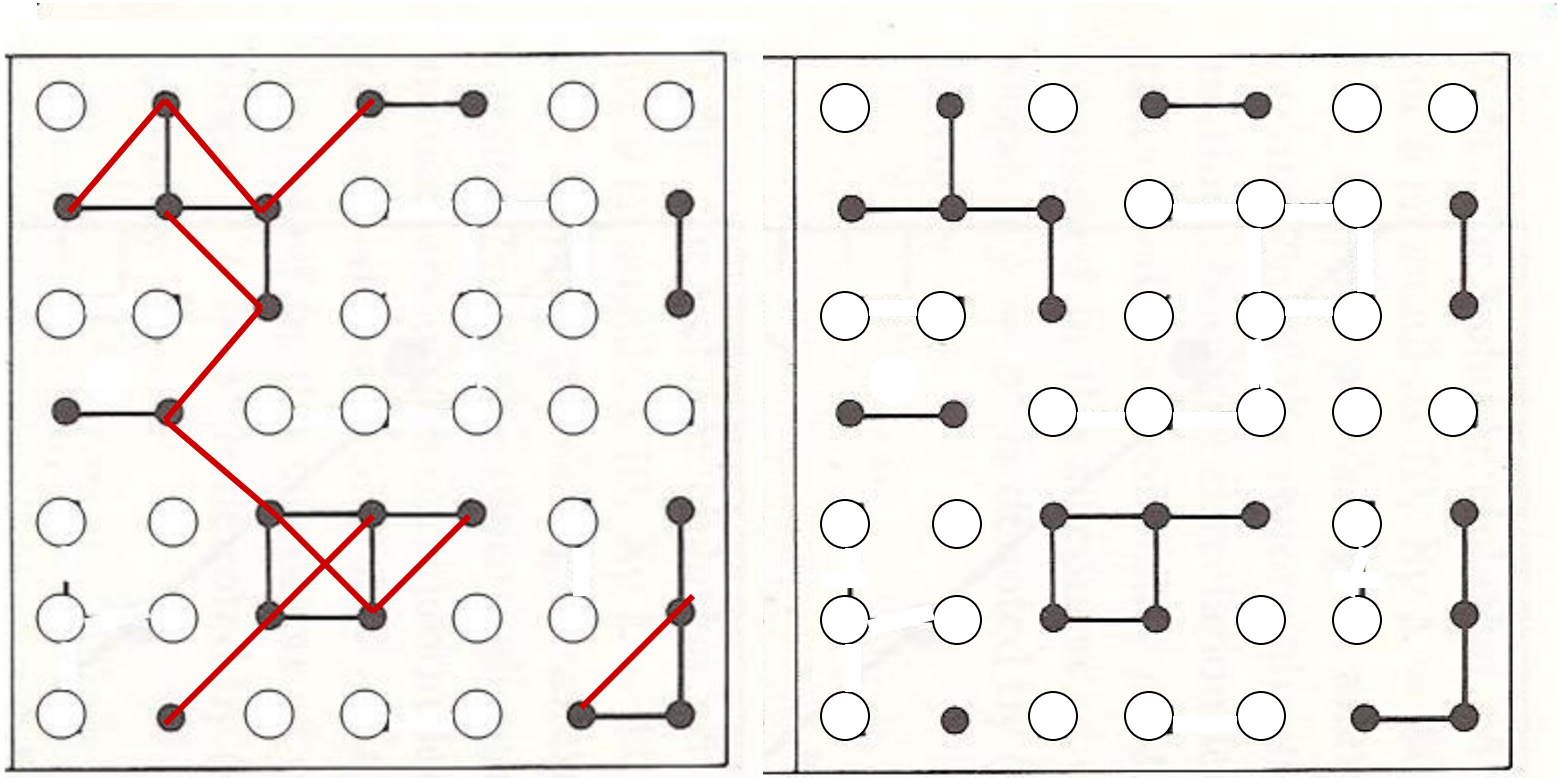

● **Occupied sites**

○ **Empty sites**

$B_c = zp_c = pz_c$

If resistors $R_3 >> R_2 >> R_1$ are attached, the resultant resistance of the system will be dominated by R_2, i.e., for a given p, an R_2 resistor will yield a threshold resistance of the system ($R_1 \rightarrow 0$ and $R_3 \rightarrow \infty$).

The staircase in a lattice

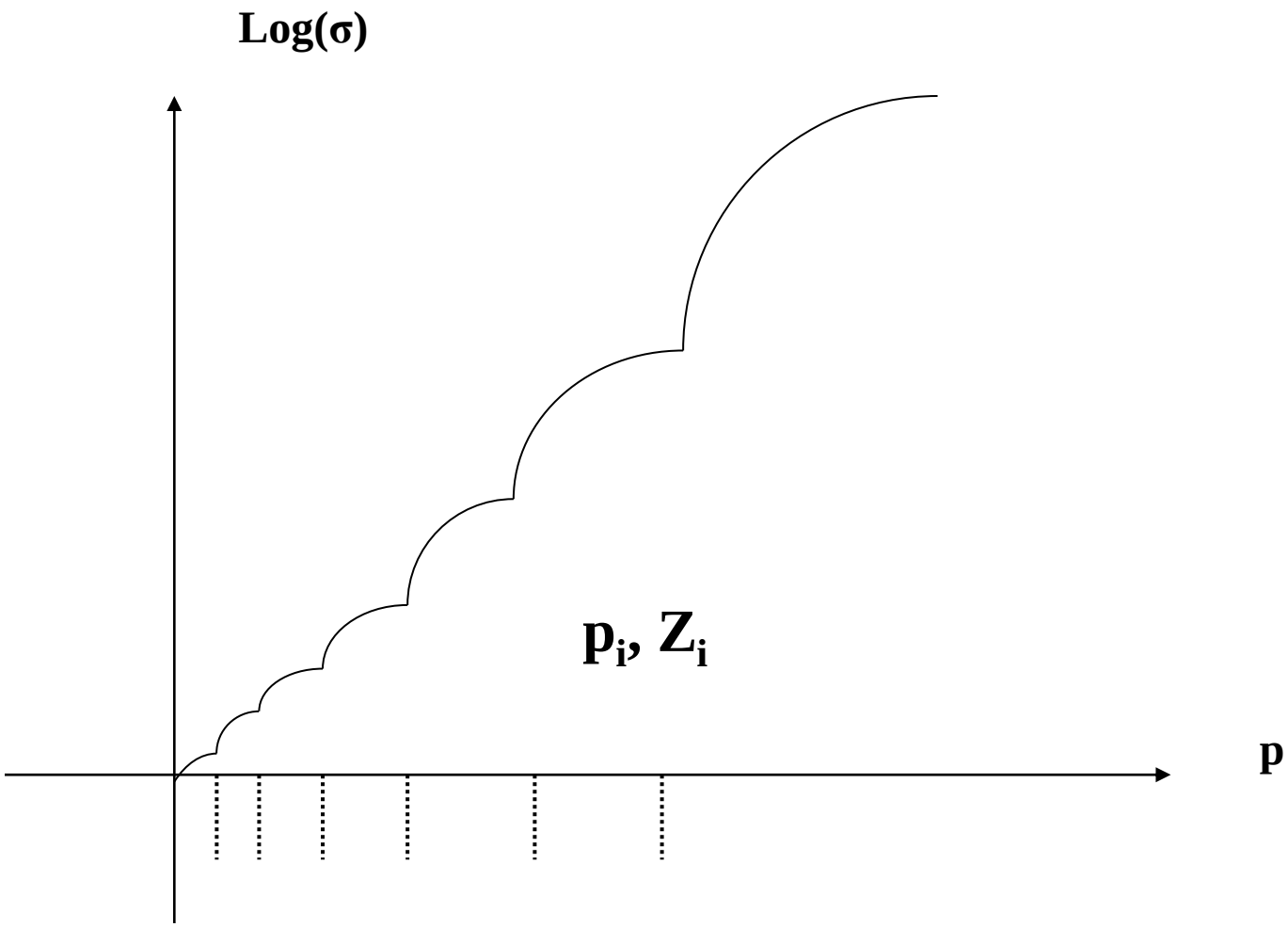

The change of the average local resistance upon threshold approach (the bypassing network)

1) Start from $p > p_c$
2) Consider the g's in descending order
3) The largest p_c of them yield percolation
4) The smallest g in this subset is g_c.
5) If there is a distribution, g_c decreases as $p \rightarrow p_c$.
6) At $p = p_c$ the resistor of smallest g must be included
7) If it is $g \rightarrow 0$ it may result that $\langle \mathbf{r} \rangle \rightarrow \infty$

UPON $p \rightarrow p_c$ NOT ONLY THE NETWORK SHRINKS BUT THE AVERAGE RESISTANCE INCREASES AND MAY DIVERGE

A typical (pencil generated) continuum system

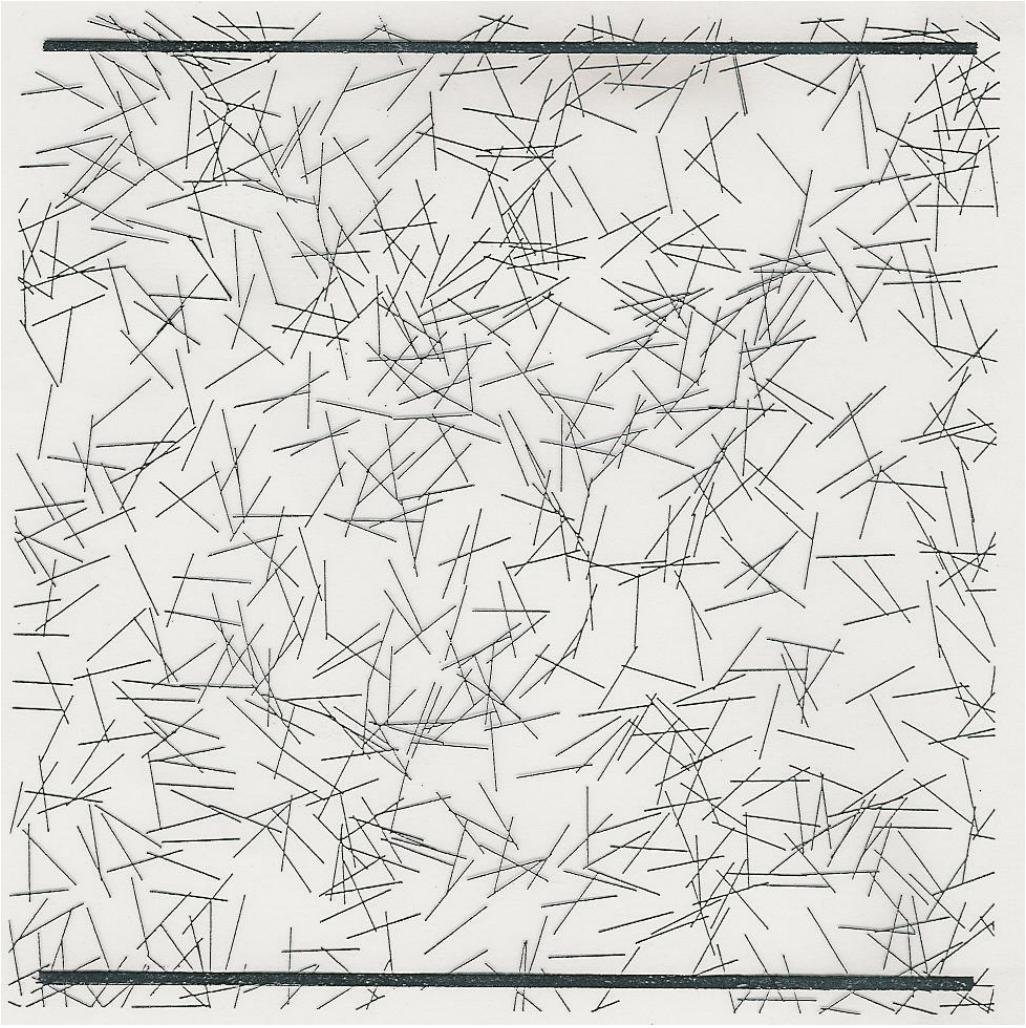

No p
no ϕ.
and N is not informative

Phys. Rev. B, 28, 3799 (1983): 156 Q

The lattice composite model

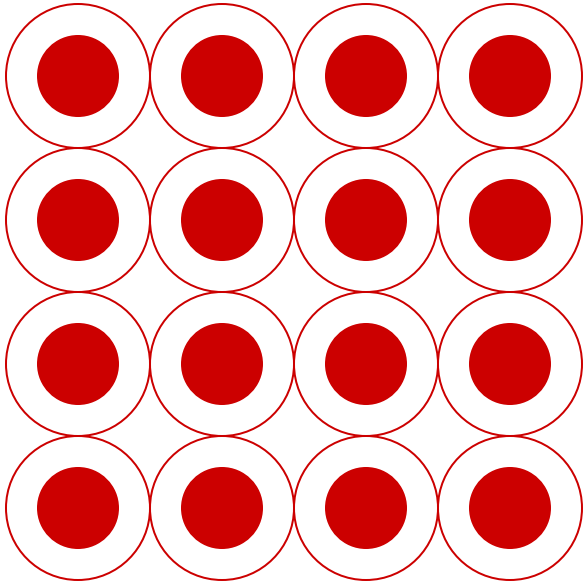

Statistics and conductance of a composite system

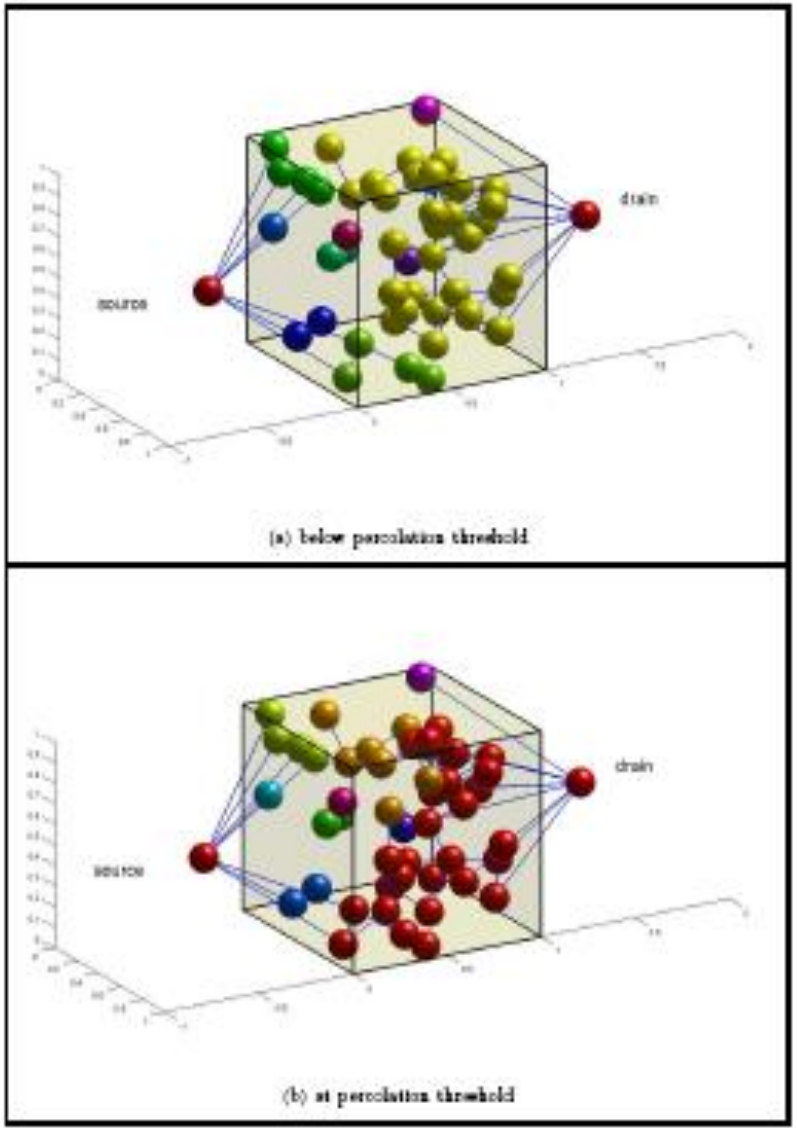

RDF of spherical particles

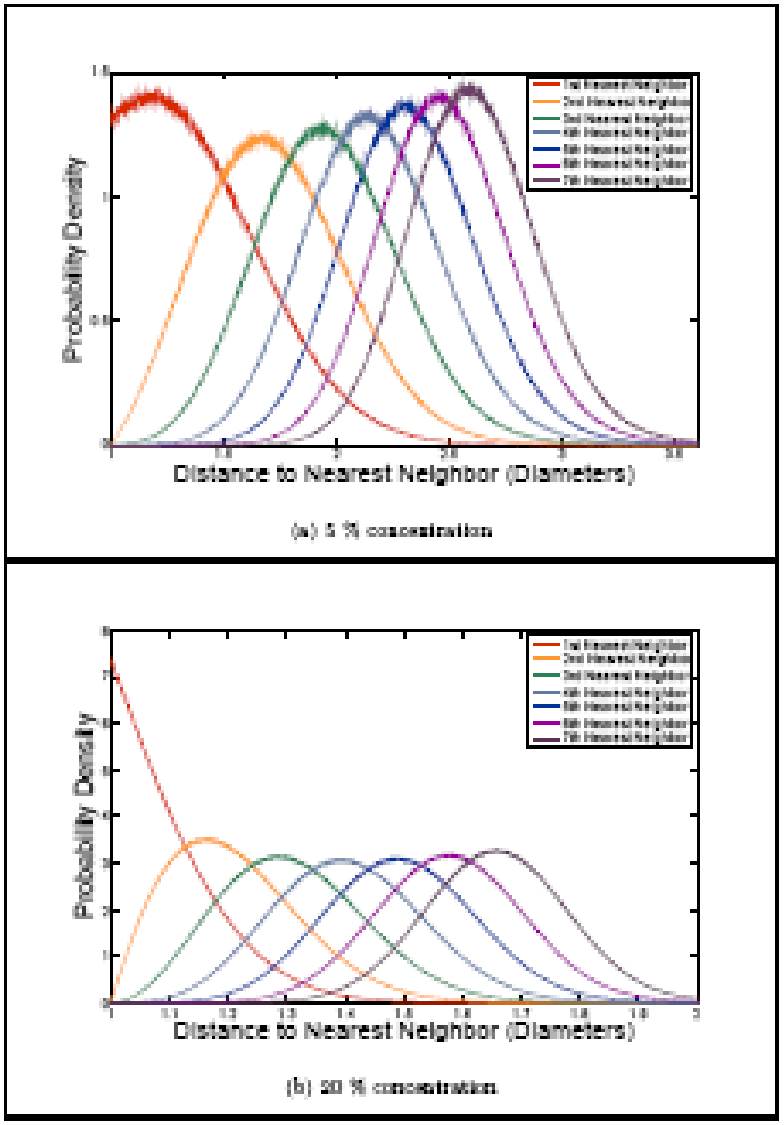

Staircase structure in nano Graphite composites

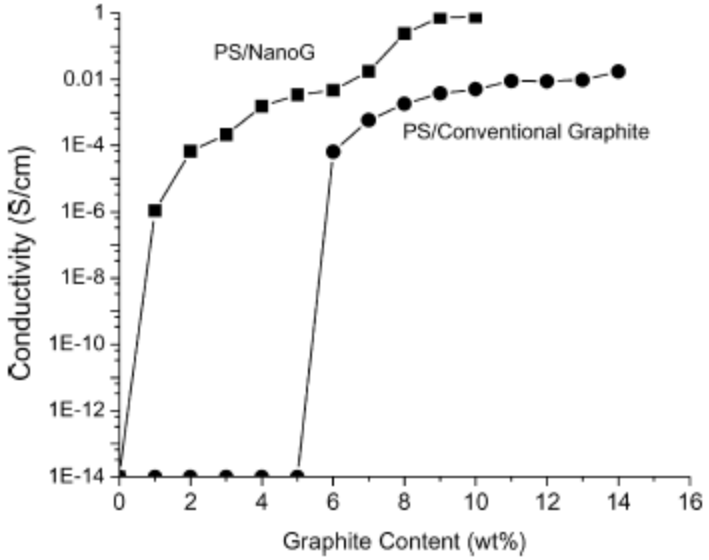

Non Universal and Hopping Interpretations

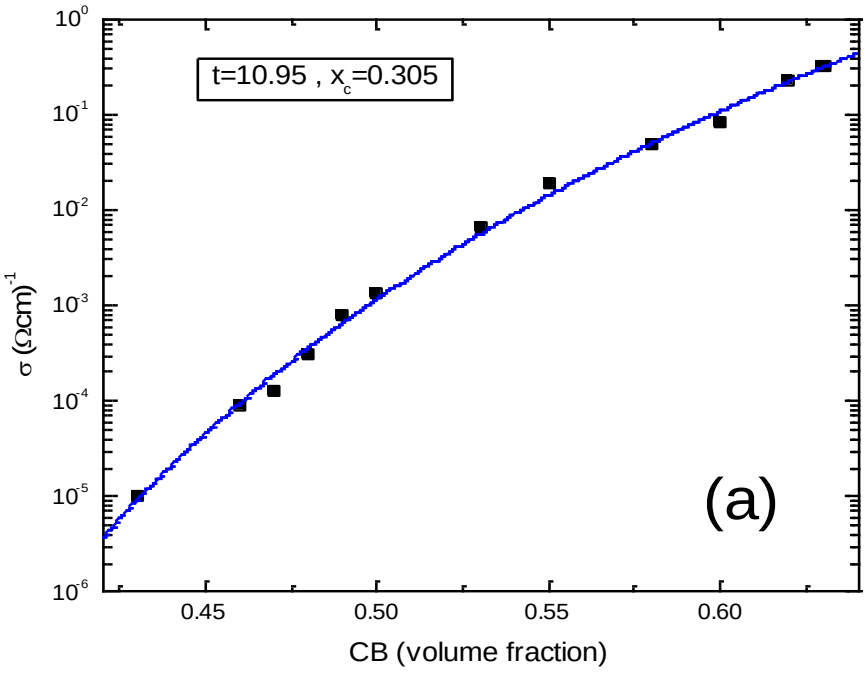

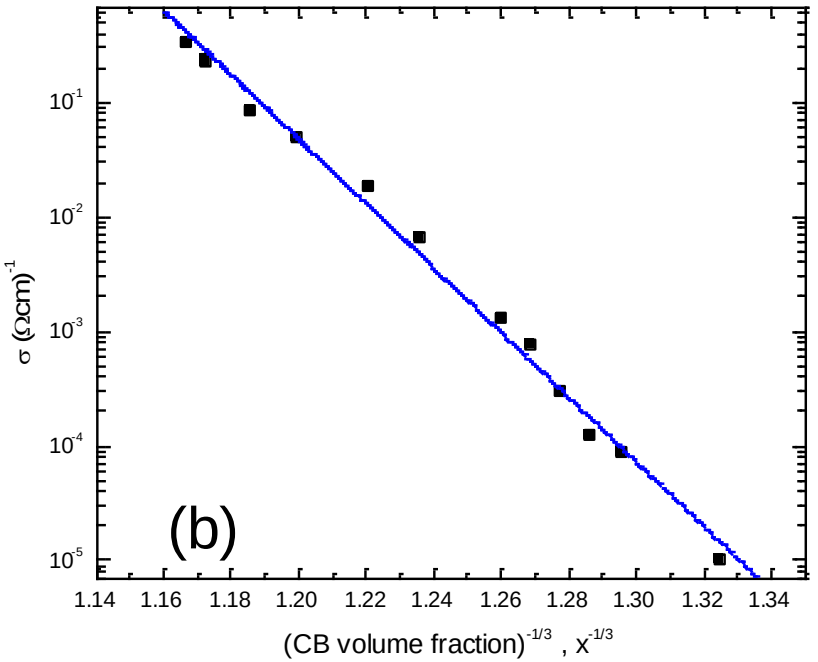

$Ni\text{-}SiO_2$

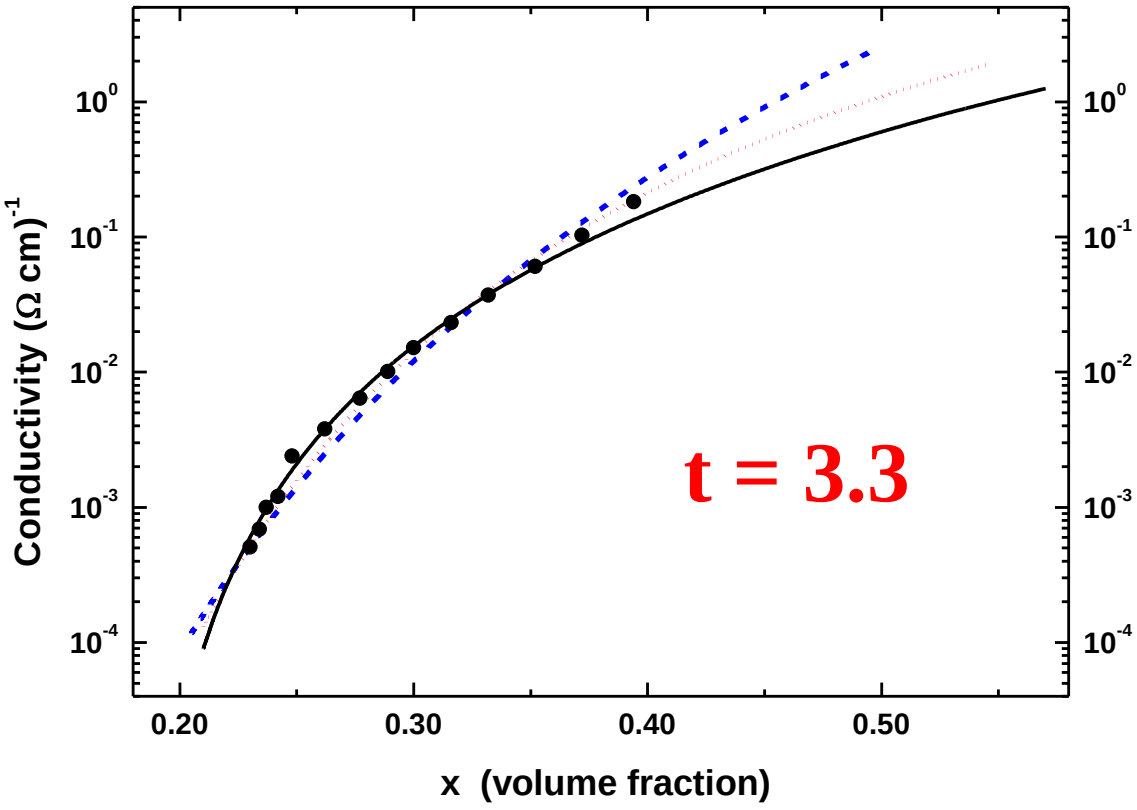
Conductivity (Ω cm)^-1
10^0
10^-1
10^-2
10^-3
10^-4
0.20
0.30
0.40
0.50
x (volume fraction)
t = 3.3

Two fundamental questions

1) What determines the percolation threshold?

2) What determines the shape of the σ(x) dependence?

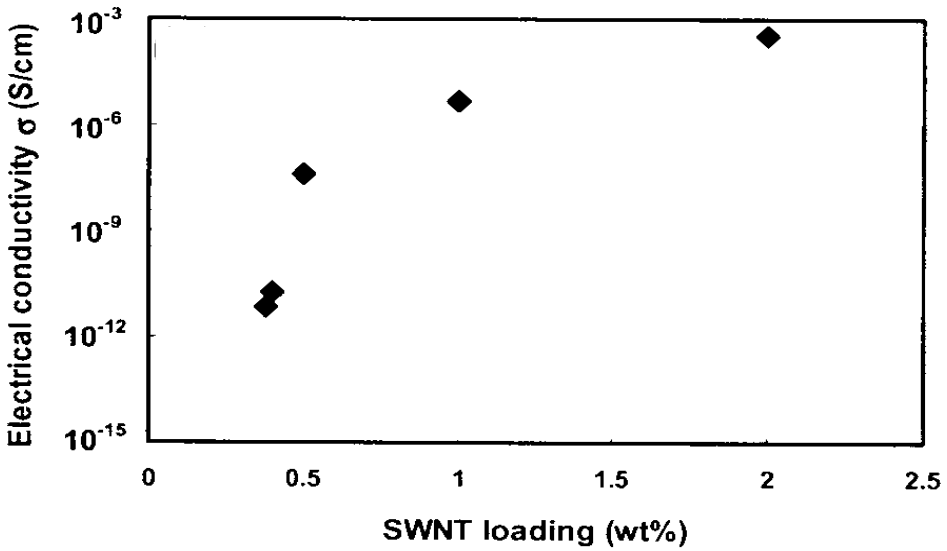

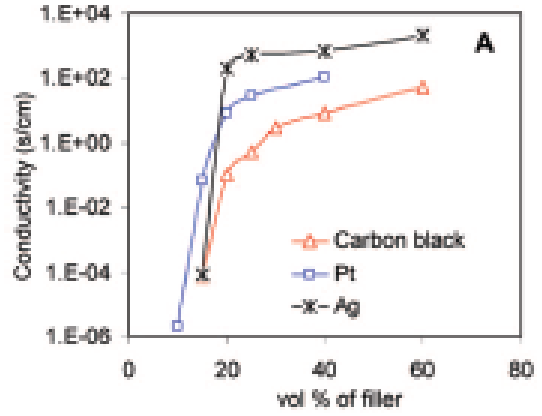

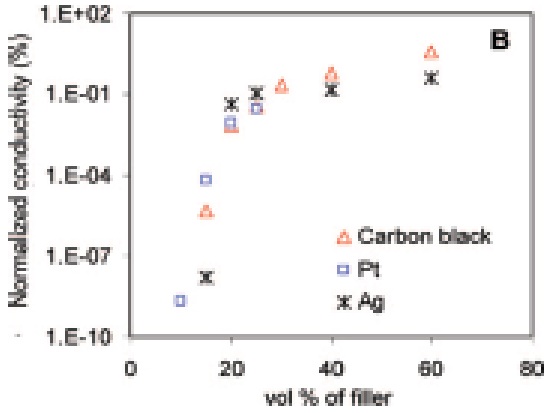

FIGURE 2. (A) Conductivity of polymer/filler composites as functions of volume fraction of fillers. (B) Composite conductivity normalized to that of the bulk fillers as functions of volume fraction of fillers.

Another a priori unexpected behaviors

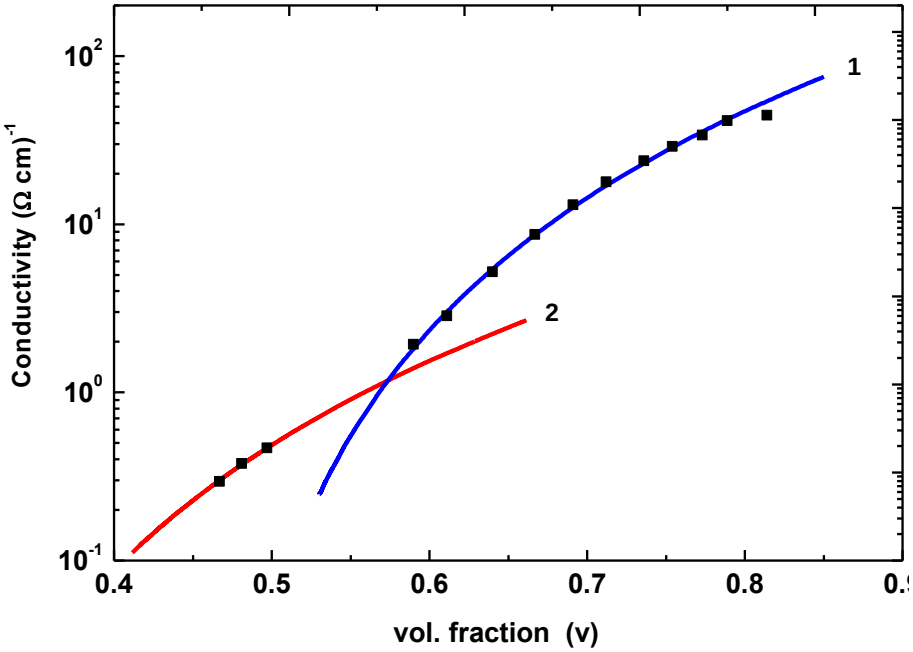

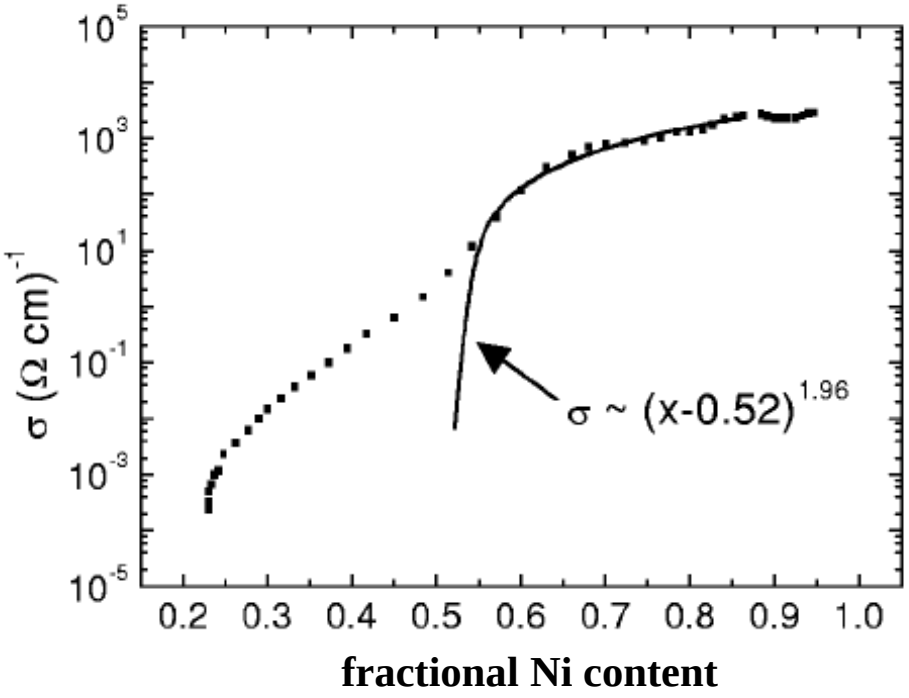

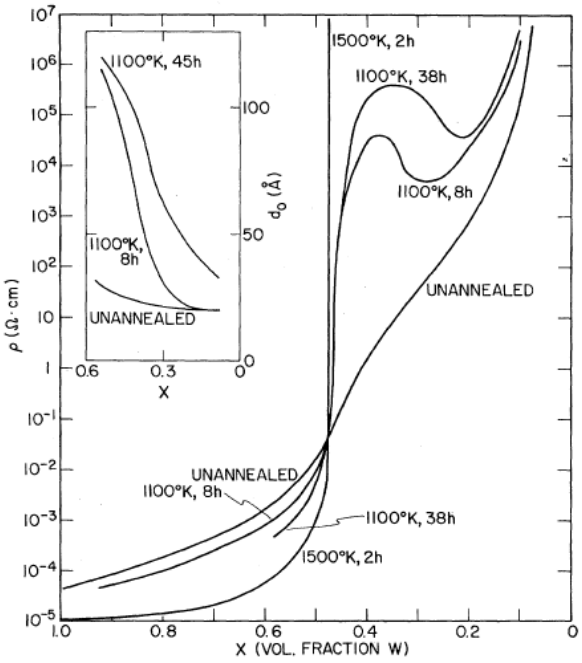

FIG. 2. Resistivity, ρ, of granular W-Al_2O_3 films as a function of volume fraction, x, of W. For the sake of clarity data points are left out and only smoothed curves are shown. The annealing time and temperature are indicated. The inset shows the average W grain size, determined by x-ray diffraction, as a function of x before and after annealing.

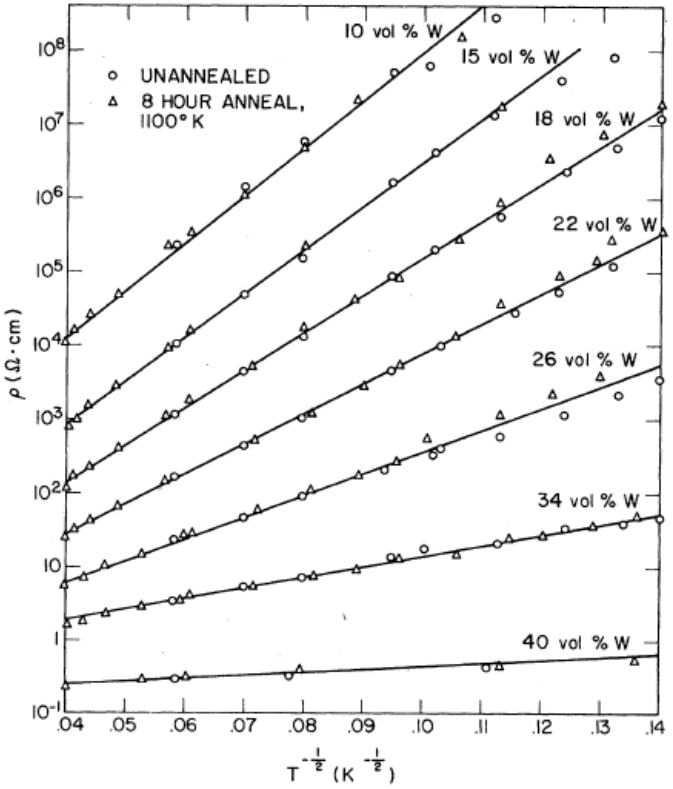

FIG. 4. lnρ versus $1/\sqrt{T}$ for several compositions of W-Al_2O_3, before and after annealing for 8 h at 1100°K. The resistivities of the annealed samples are normalized at 300°K to the resistivity value determined on the same sample before annealing.

Percolation and tunneling -percolation

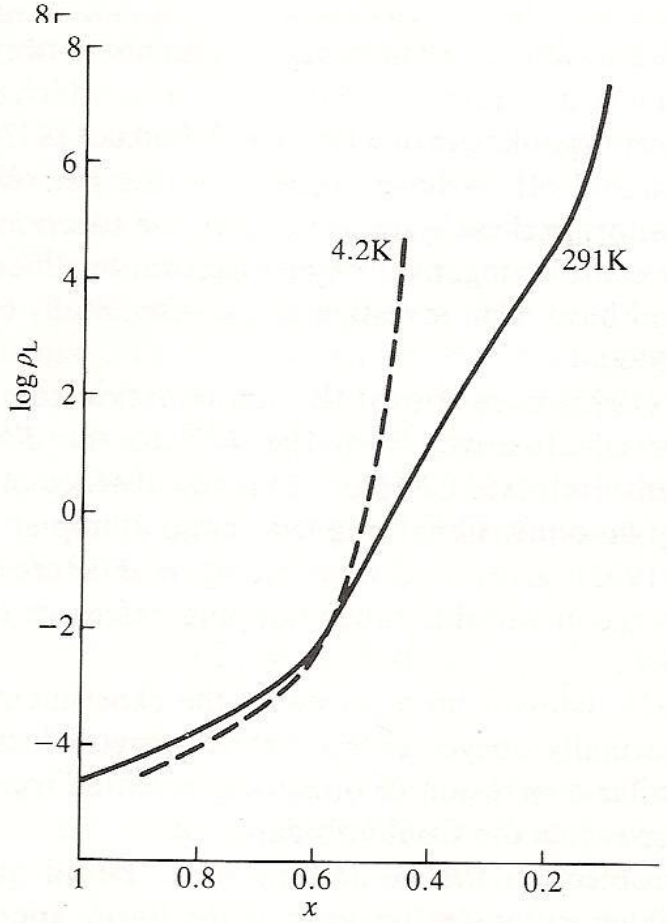

Fig. 3.7. Low-field resistivity ρ_L in Ω cm as a function of volume fraction x of Ni in Ni–SiO_2 sputtered films, at the temperatures shown (Abeles and Ping Shen 1974).

Various carbon blacks

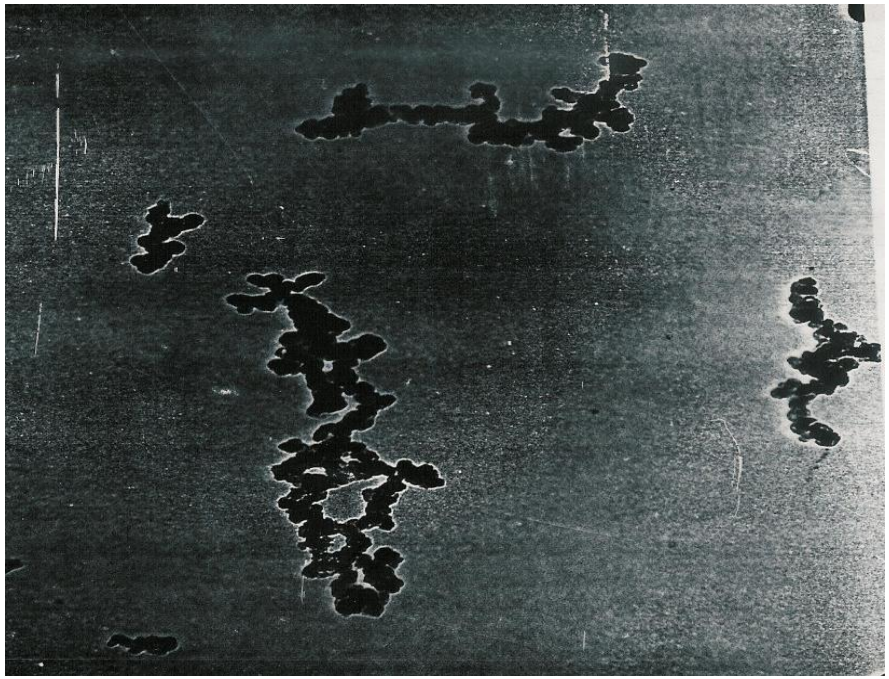

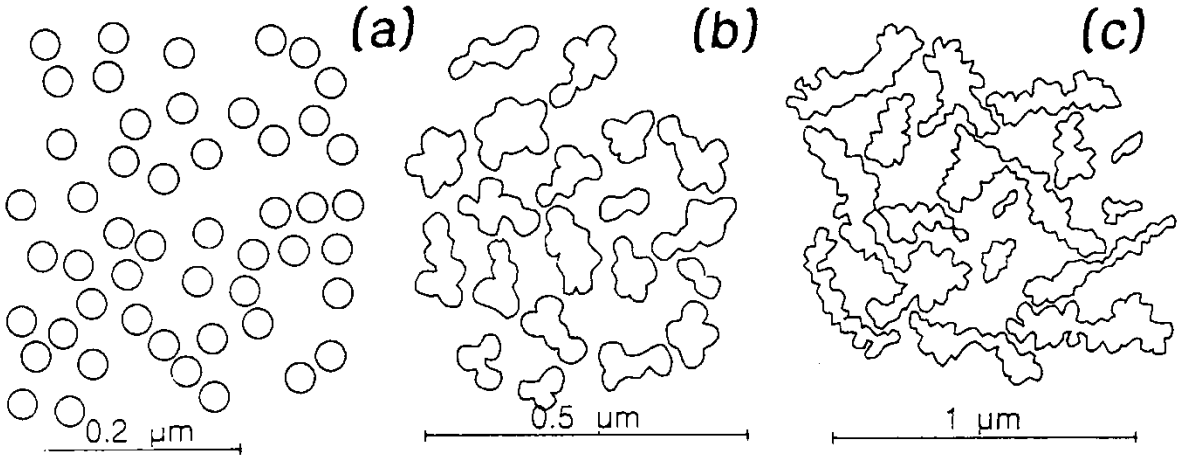

Two Conclusions

The understanding of the conductivity dependence on the content of the carbon filler in terms of percolation theory is based on:

$$\sigma \propto (\Phi - \Phi_c)^t$$

- **1) The larger the aspect ratio and the isotropy the smaller the percolation threshold (the smaller the content of carbon particles needed for the onset of large conductivity), the "excluded volume" argument.**
- **2) The Behavior of the conductivity is determined by the distribution of the tunneling conductances (or interparticle distances) which is manifested by the deviation of the critical exponent t from its universal value.**

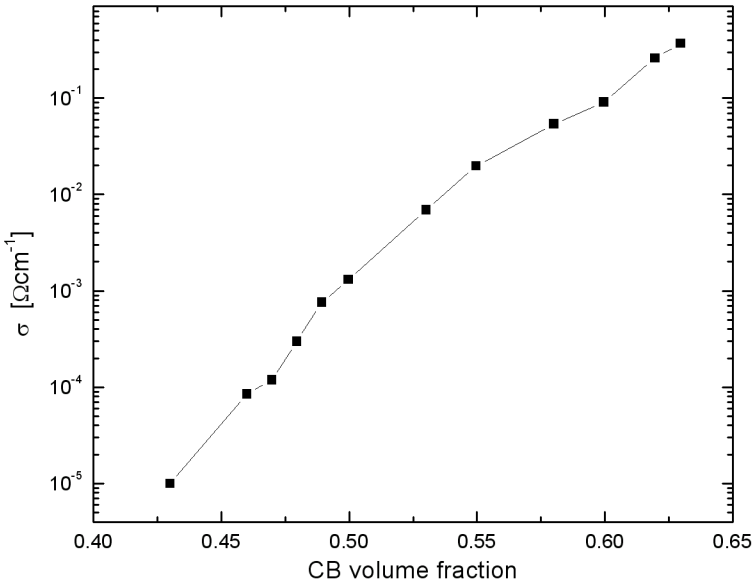
σ [Ωcm-1]
10-1
10-2
10-3
10-4
10-5
0.40
0.45
0.50
0.55
0.60
0.65
CB volume fraction

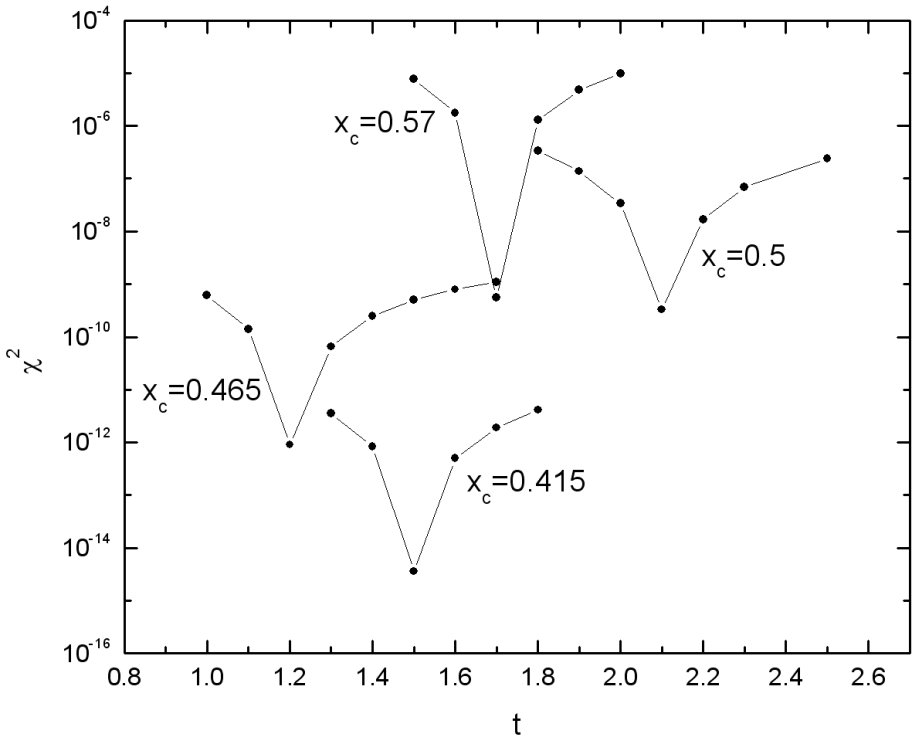
10^{-4}
10^{-6}
10^{-8}
10^{-10}
10^{-12}
10^{-14}
10^{-16}
χ^2
0.8
1.0
1.2
1.4
1.6
1.8
2.0
2.2
2.4
2.6
t
x_c=0.57
x_c=0.5
x_c=0.465
x_c=0.415

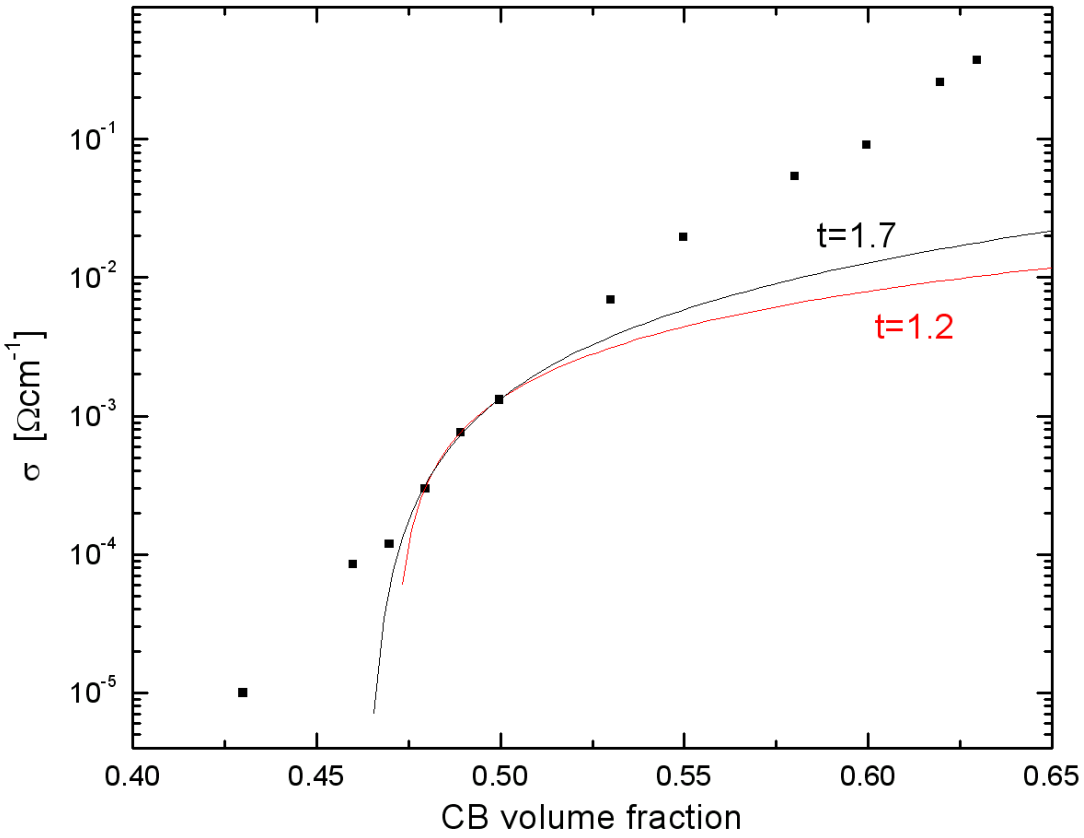
σ [Ωcm-1]
10-1
10-2
10-3
10-4
10-5
0.40
0.45
0.50
0.55
0.60
0.65
CB volume fraction
t=1.7
t=1.2

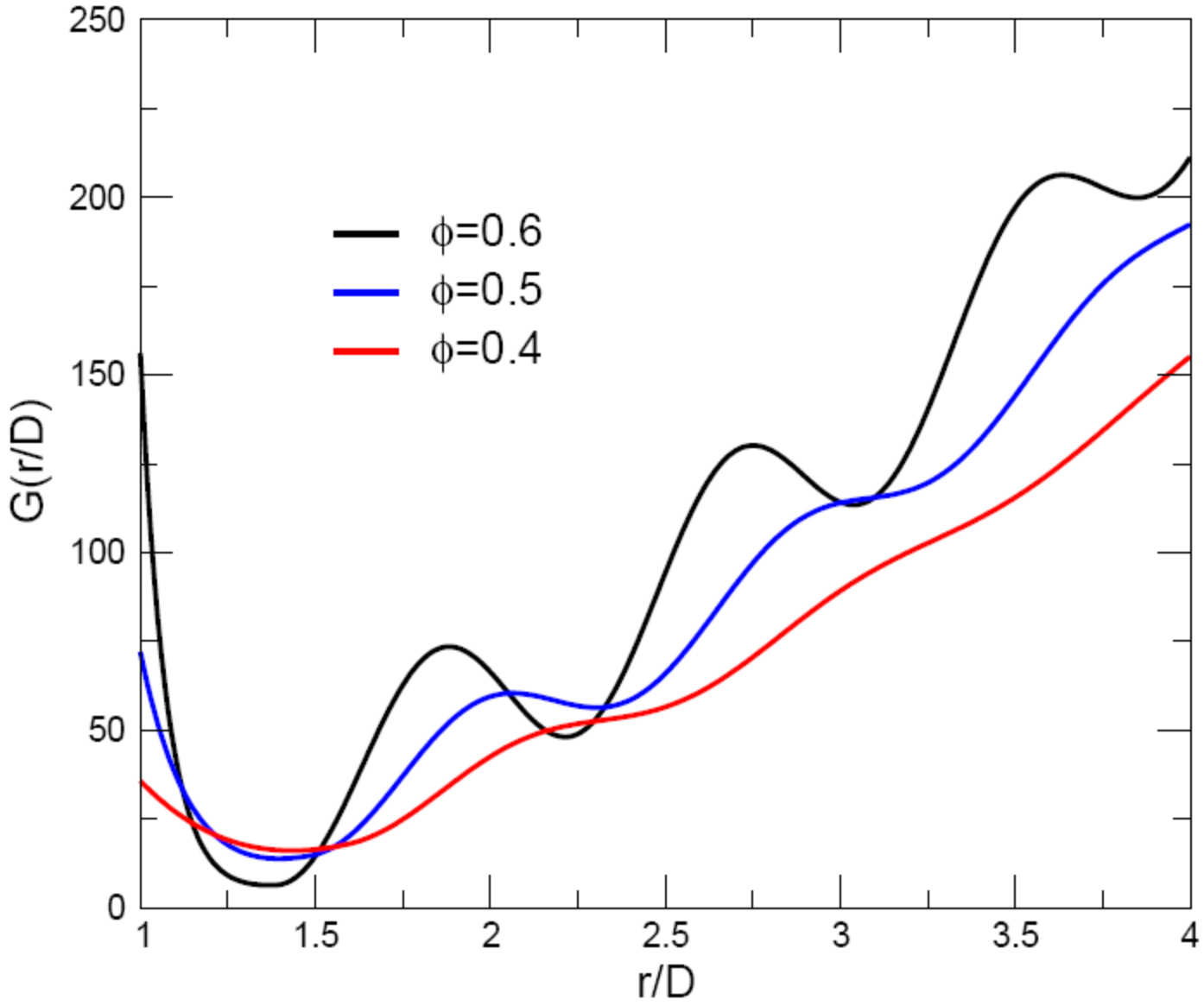
250
200
150
100
50
0
G(r/D)
1
1.5
2
2.5
3
3.5
4
r/D
ϕ=0.6
ϕ=0.5
ϕ=0.4

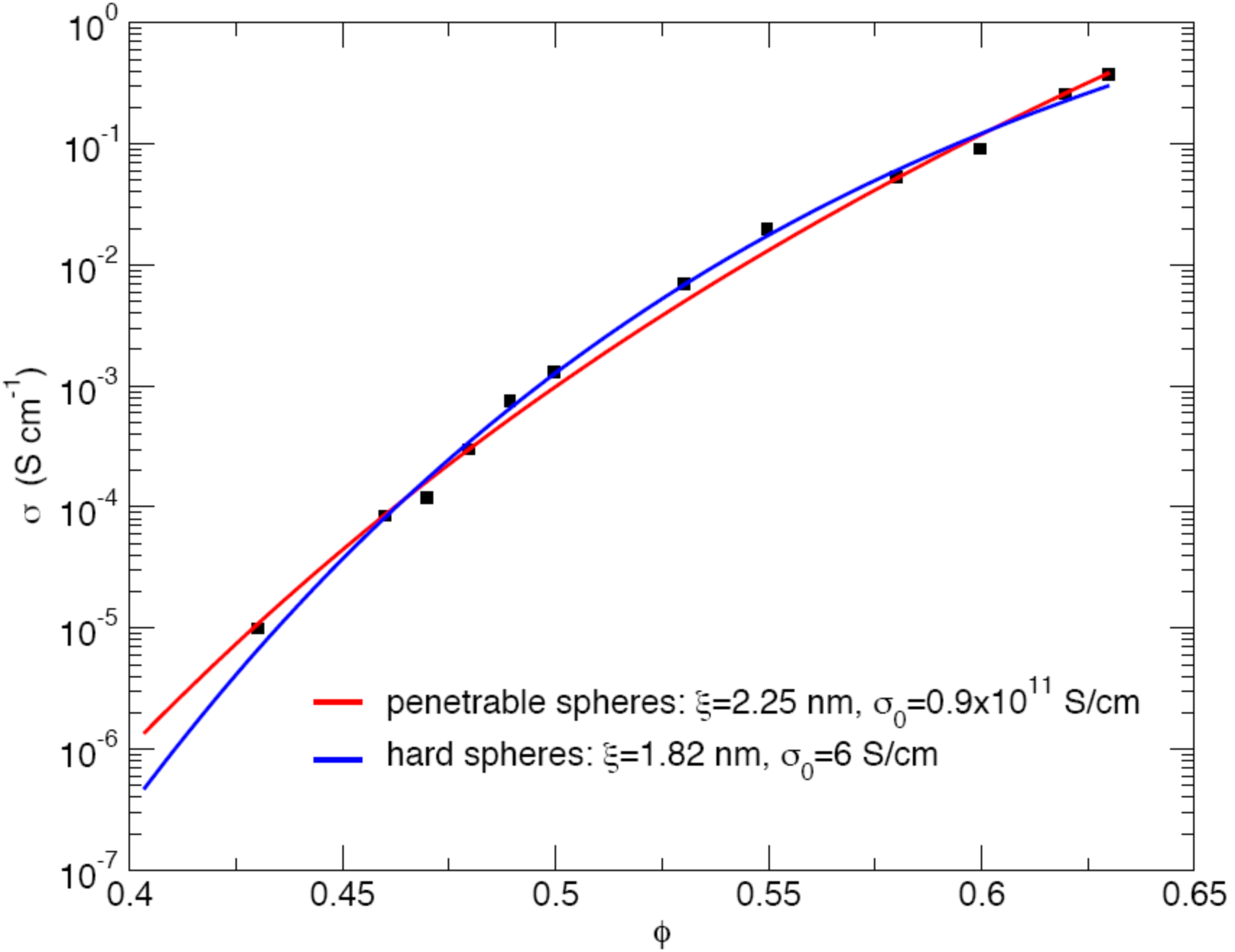
10^{0}
10^{-1}
10^{-2}
10^{-3}
10^{-4}
10^{-5}
10^{-6}
10^{-7}
σ (S cm^{-1})
0.4
0.45
0.5
0.55
0.6
0.65
ϕ
penetrable spheres: ξ=2.25 nm, σ_0=0.9x10^{11} S/cm
hard spheres: ξ=1.82 nm, σ_0=6 S/cm

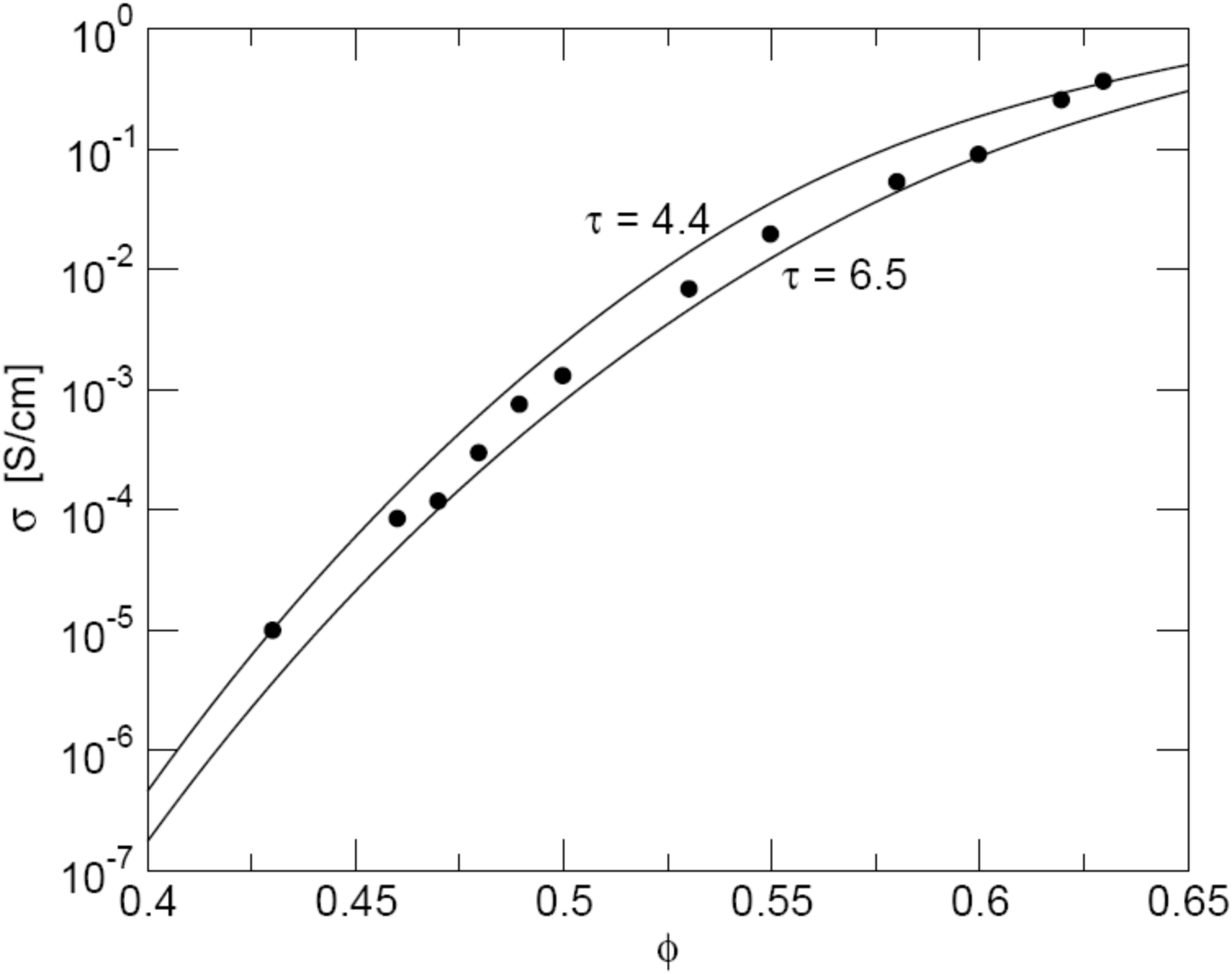
10^0
10^{-1}
10^{-2}
10^{-3}
10^{-4}
10^{-5}
10^{-6}
10^{-7}
σ [S/cm]
τ = 4.4
τ = 6.5
0.4
0.45
0.5
0.55
0.6
0.65
ϕ

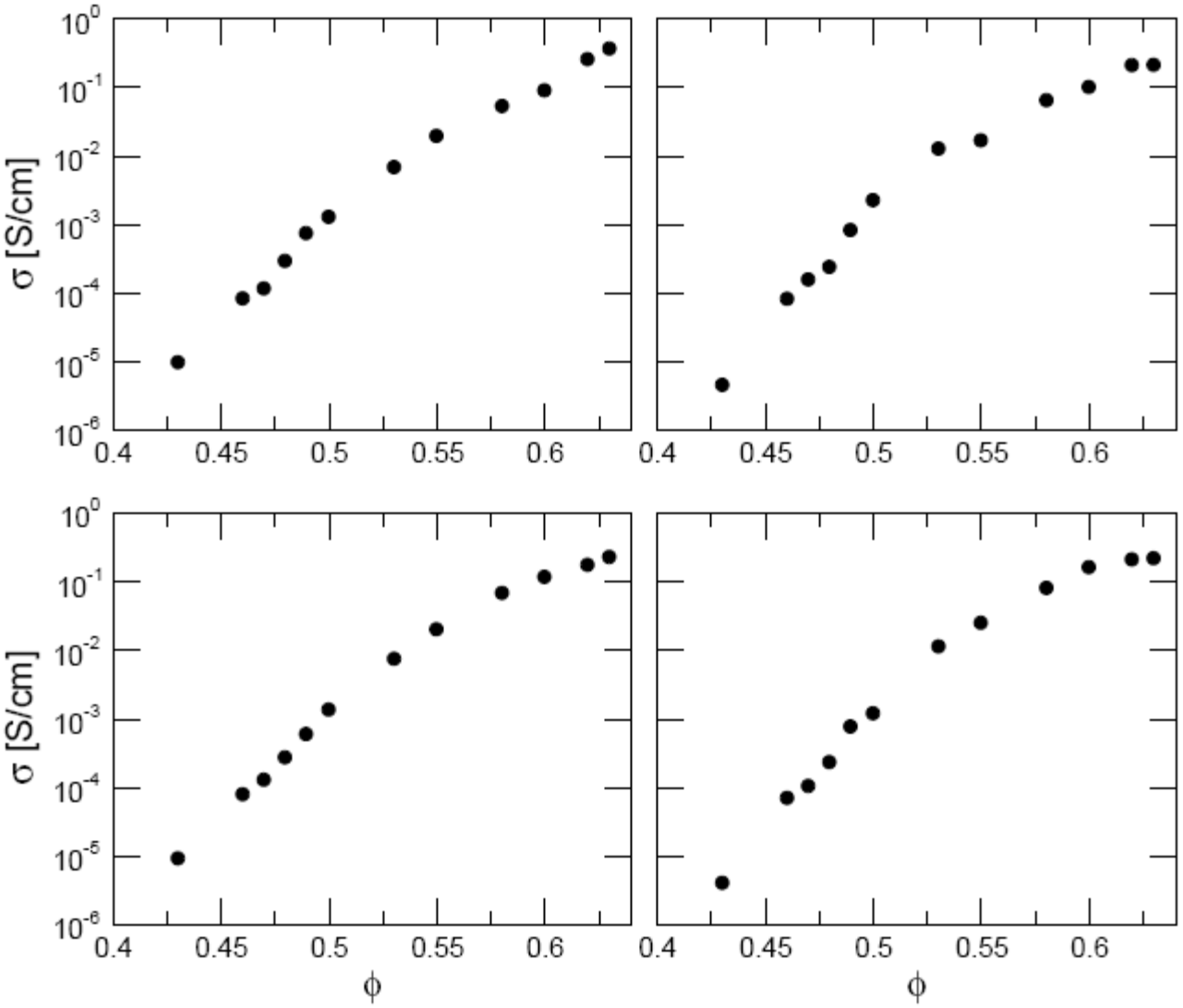
σ [S/cm]
10^0
10^-1
10^-2
10^-3
10^-4
10^-5
10^-6
0.4
0.45
0.5
0.55
0.6
ϕ

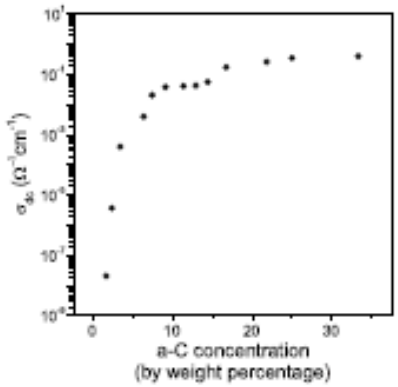

Fig. 8. The d.c. conductivity vs. concentration of a-C.

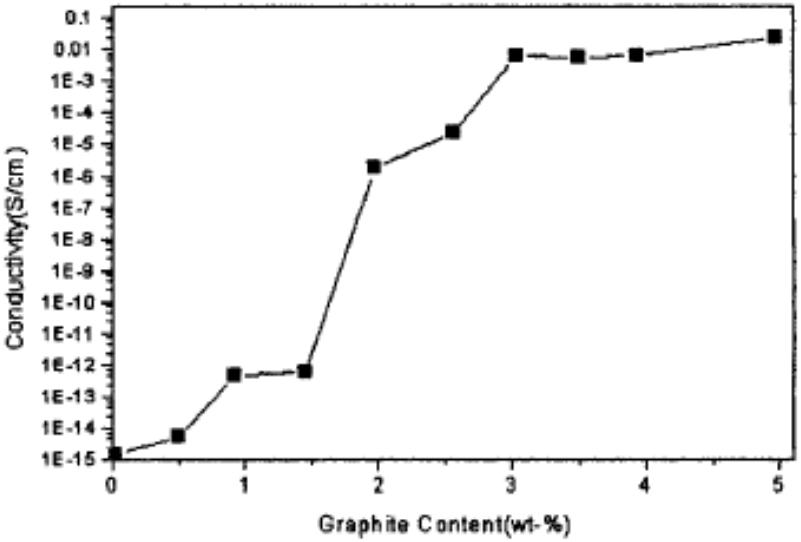

Figure 7. Electrical conductivity of PS–expanded graphite as a function of graphite content.

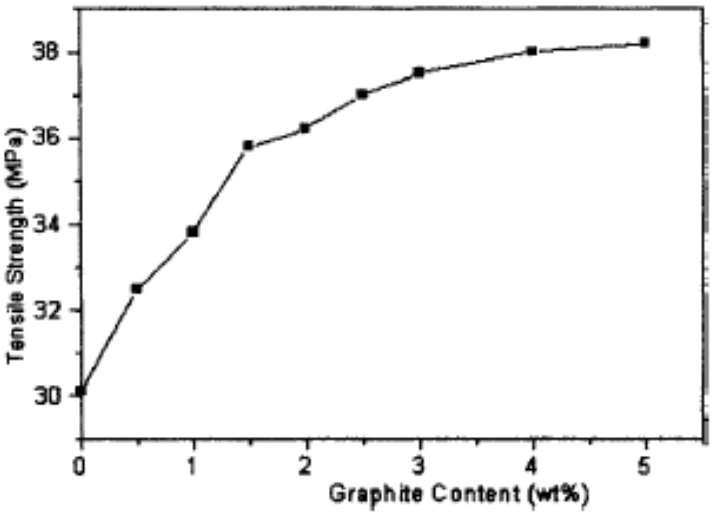

Figure 13. Dependence of the tensile strength of PS–expanded graphite nanocomposite on the graphite content.

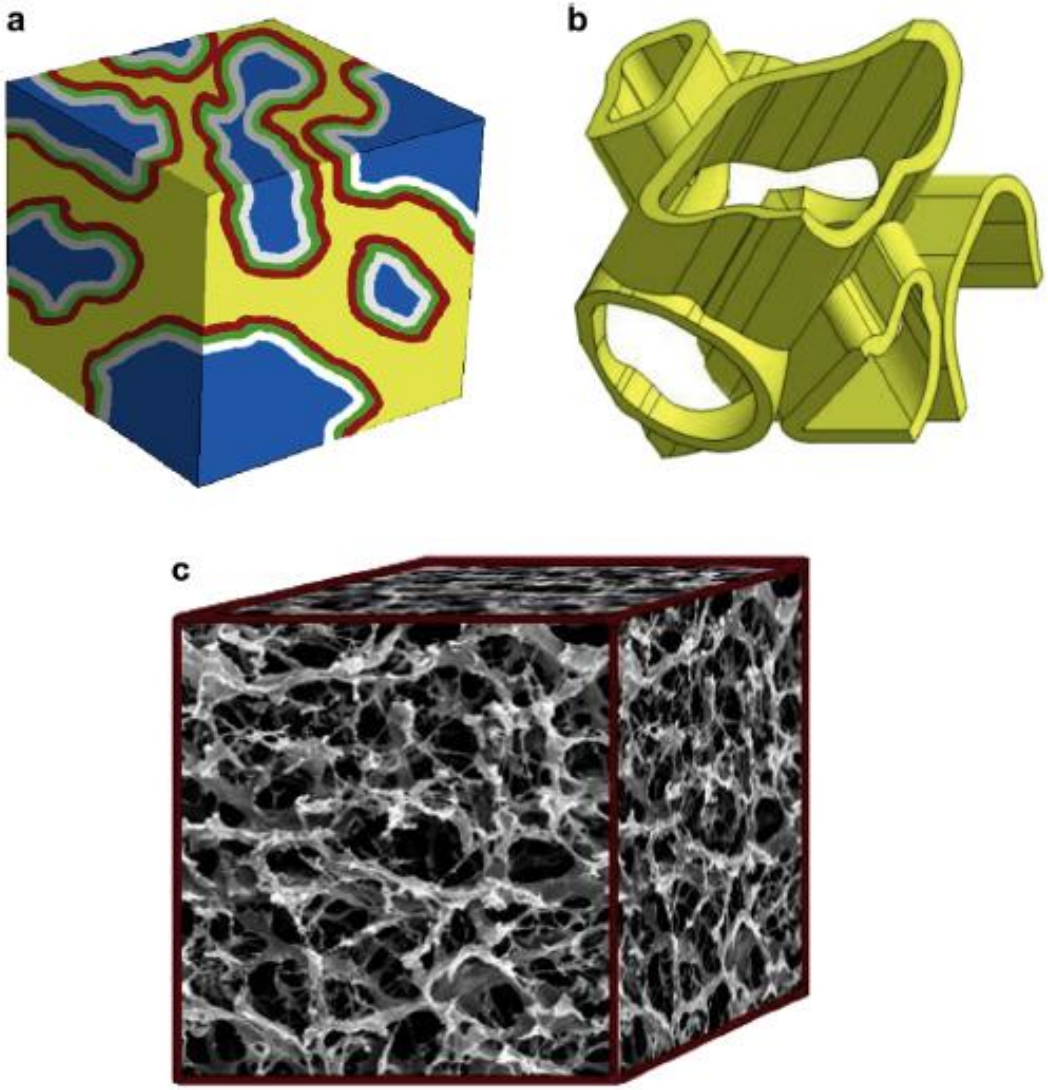

Fig. 12. a) Schematic representation of quinary multi-percolated morphology, the yellow phase is PANI, the blue phase is HDPE, and all other phases are located between them, b) schematic of a PANI network obtained after removal of all phases except PANI, and c) a 3D image constructed from 2D SEM images of the interconnected PANI network in the quinary 15/20/15/25/25 PS/PS-co-PMMA/PMMA/PVDF/PANI blend after extraction of all other phases.

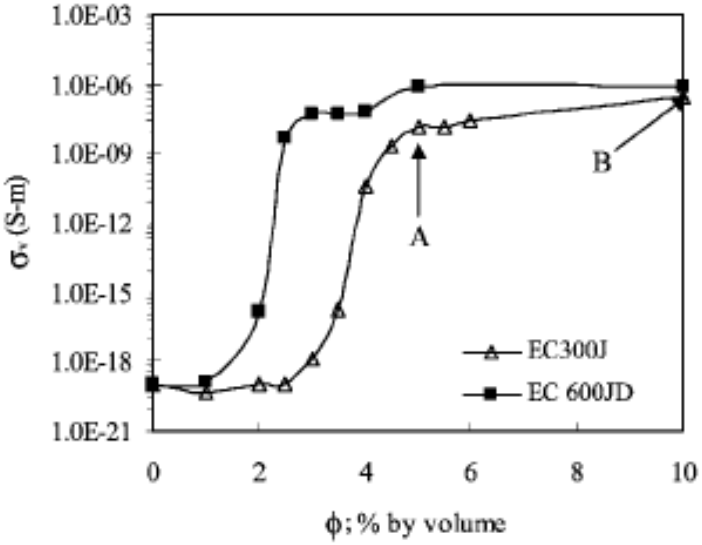

(b) PS/carbon black

Fig. 5. Volume conductivity of (a) PP and (b) PS/carbon black conductive compounds. Sample specimens were prepared by compression molding.

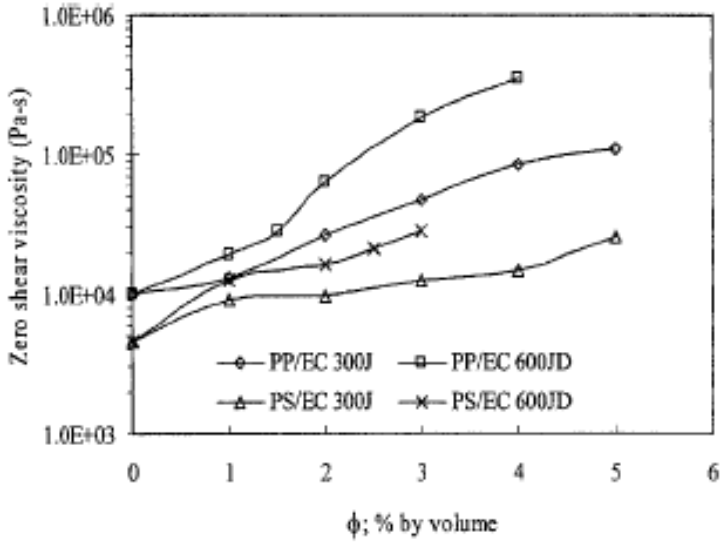

Fig. 6. Zero shear viscosity of PP and PS compounds with EC 300J and 600JD carbon black particles measured at 200°C using ARES Rheometrics cone and plate rheometer.

The origin of the staircase model

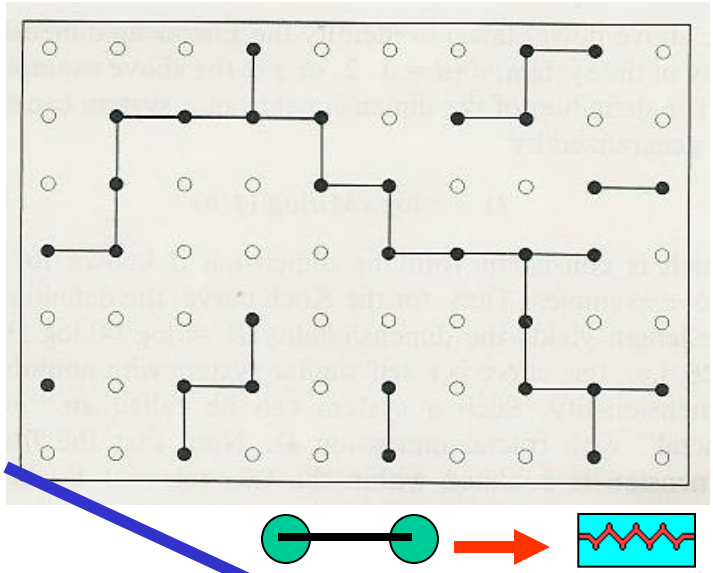

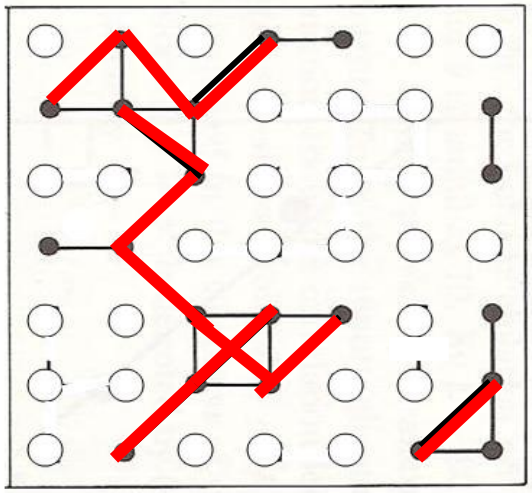

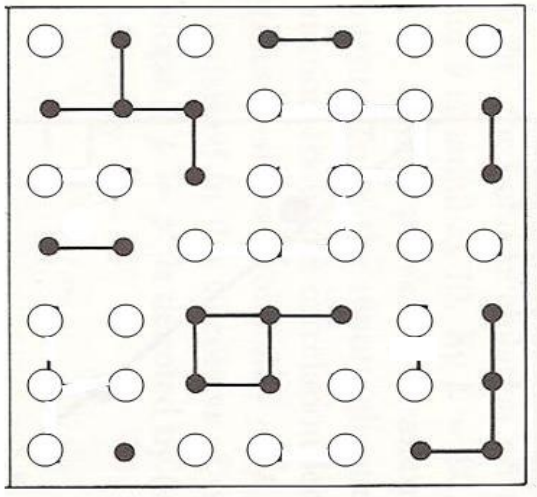

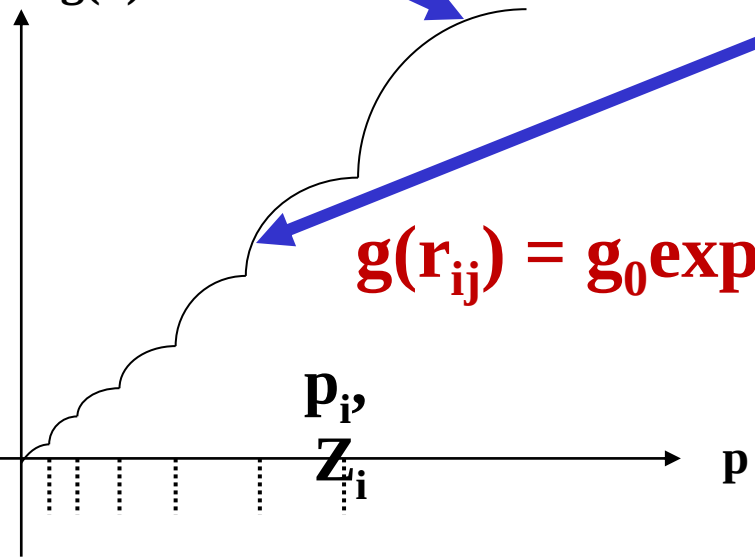

$$g(r_{ij}) = g_0 \exp[-2(r_{ij})/\xi]$$

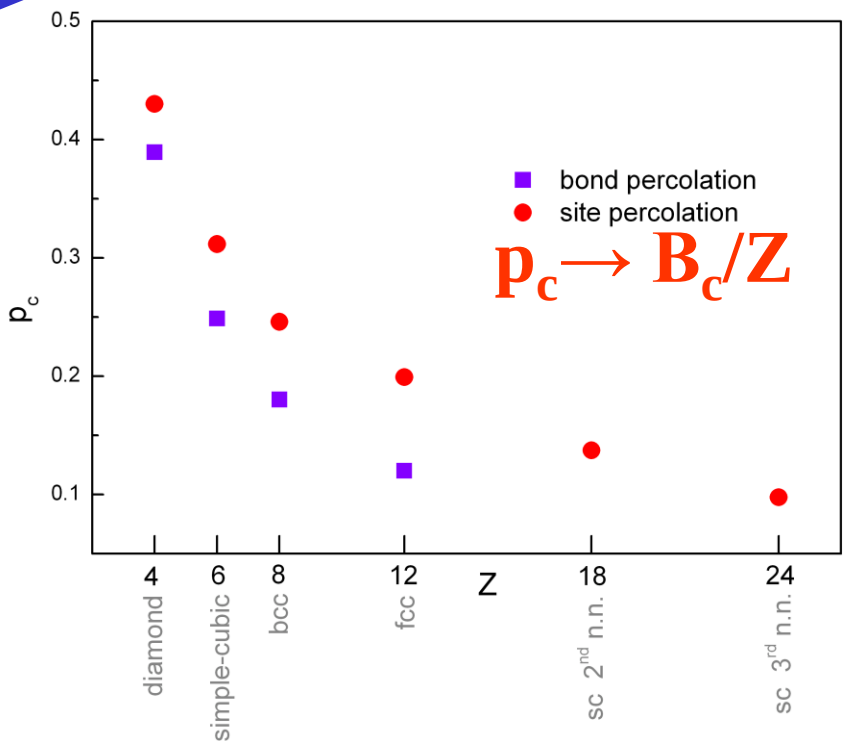

J. Phys. D: 42, 064003 (2009)

The NLB Model

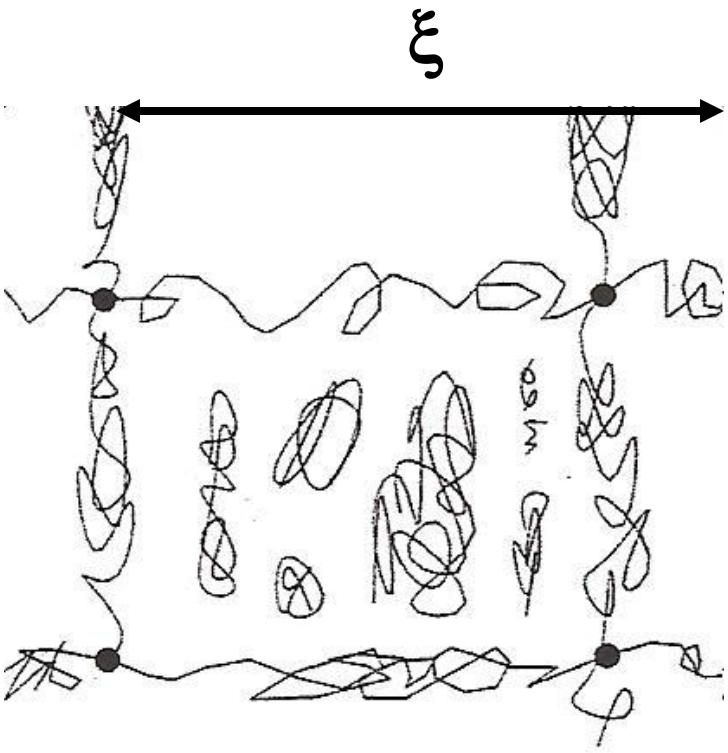

A model for the links

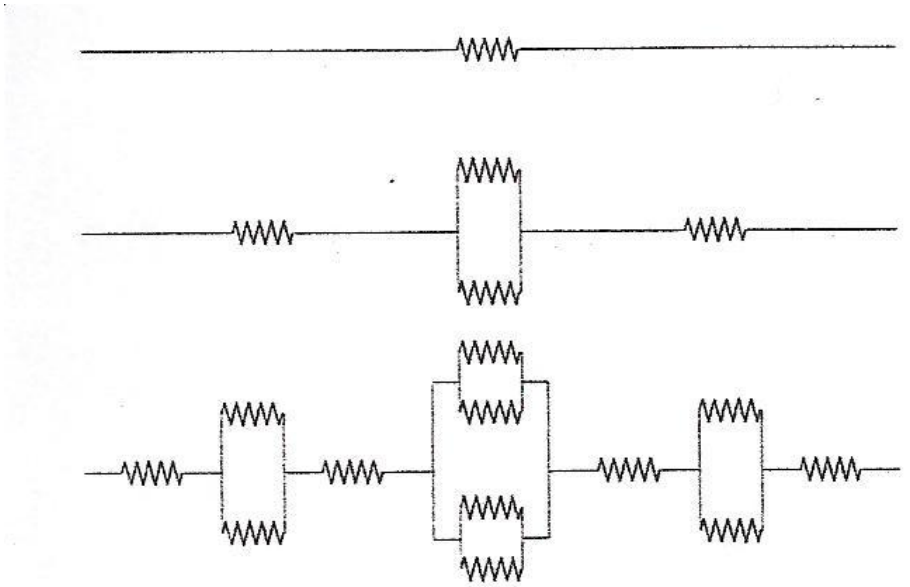

$R_\xi (\geq r_0 L_1)$ ξ

$R_L = R_\xi (L/\xi)/(L/\xi)^{D-1}$

$\propto (p-p_c)^{-[\zeta + (D-2)\nu)]} \propto (p-p_c)^{-tun}$

$(L_1 \propto (p-p_c)^{-1})$

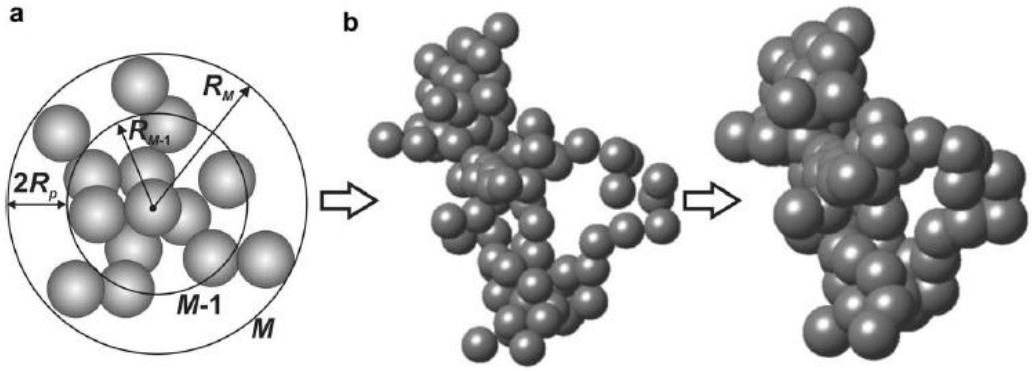

Fig. 1. Algorithm for simulation of aggregate arrangement.

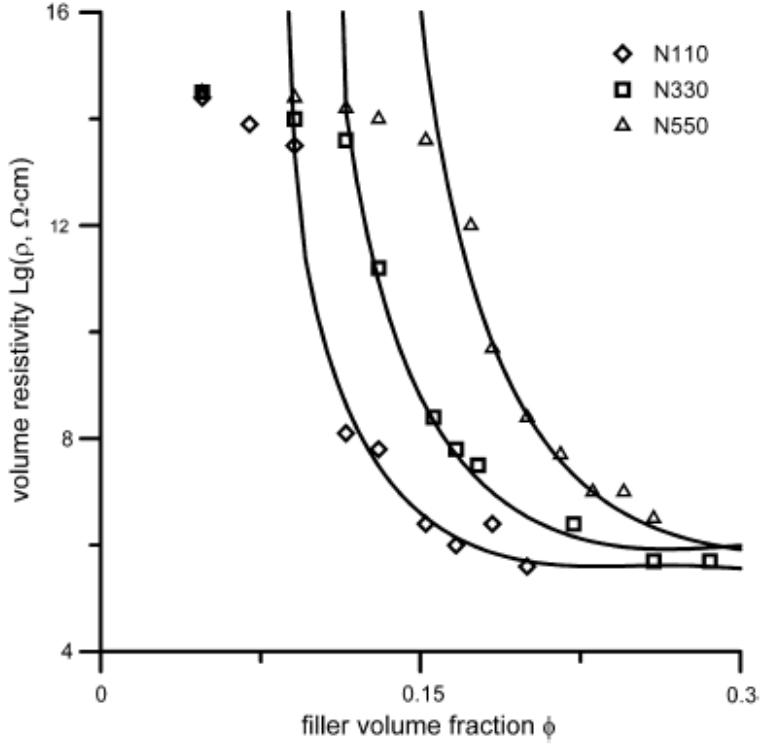

Fig. 8. Experimental relationships of Ref. [17] (single markers) and approximations (solid lines), Eq. (5) of volume resistivity versus filler volume fraction.

TABLE 2. Scaling parameters calculated for Cu-PMMA composites containing different particle size.

Composite	f_C	t	R (correlation coefficient)
Cu-PMMA (78 nm)	13.95	2.0 ± 0.097	0.997
Cu-PMMA (0.2–0.3 μm)	11.00	2.0 ± 0.100	0.996
Cu-PMMA (3.25–4.75 μm)	9.28	2.0 ± 0.100	0.997

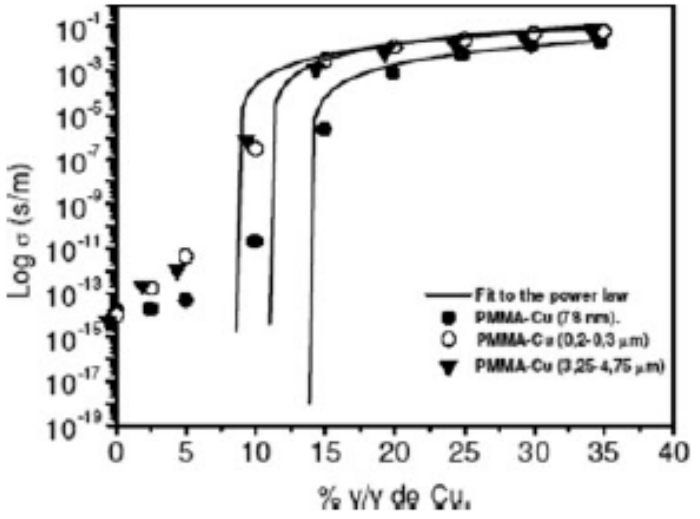

FIG. 7. Fit of electrical conductivity data to the power law. Cu-PMMA (78 nm), Cu-PMMA (0.2–0.3 μm), Cu-PMMA (3.25–4.75 μm).

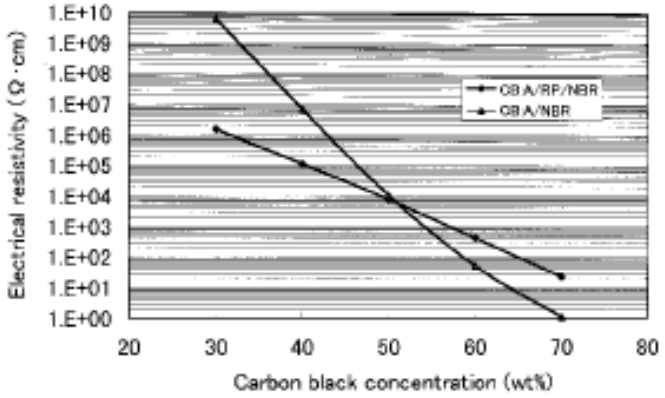

Fig. 2. Electrical resistivity of the thin NBR layers which contain carbon black A with and without polymer grafting as a function of carbon black concentration. CB, carbon black; RP, reactive polymer; NBR, acrylonitrile-butadiene rubber.

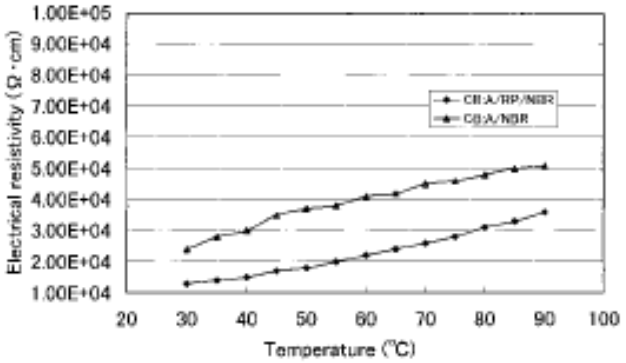

Fig. 5. Electrical resistivity of the thin NBR layers which contain carbon black A of 50 wt.% with and without polymer grafting as a function of temperature. CB, carbon black; RP, reactive polymer; NBR, acrylonitrile-butadiene rubber.

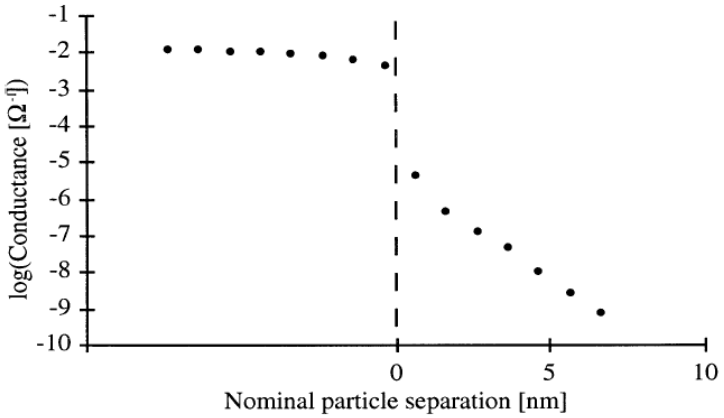

Figure 2. The conductance between two gold particles as a function of their nominal separation.

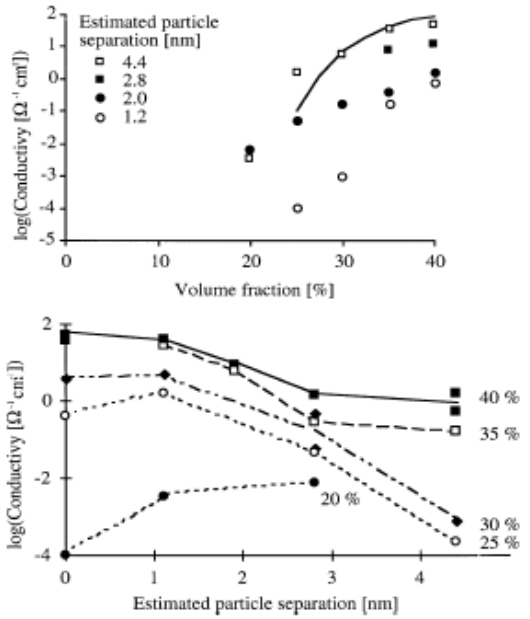

Figure 4. Effect of an alkanethiol monolayer coating the surface of particles on the mean conductivity of a polymer charged with the coated particles: (a) as a function of filler content for different layer estimated layer thicknesses, along with the model curve for uncoated particles; (b) as a function of layer thickness for the different filler volume fractions indicated.

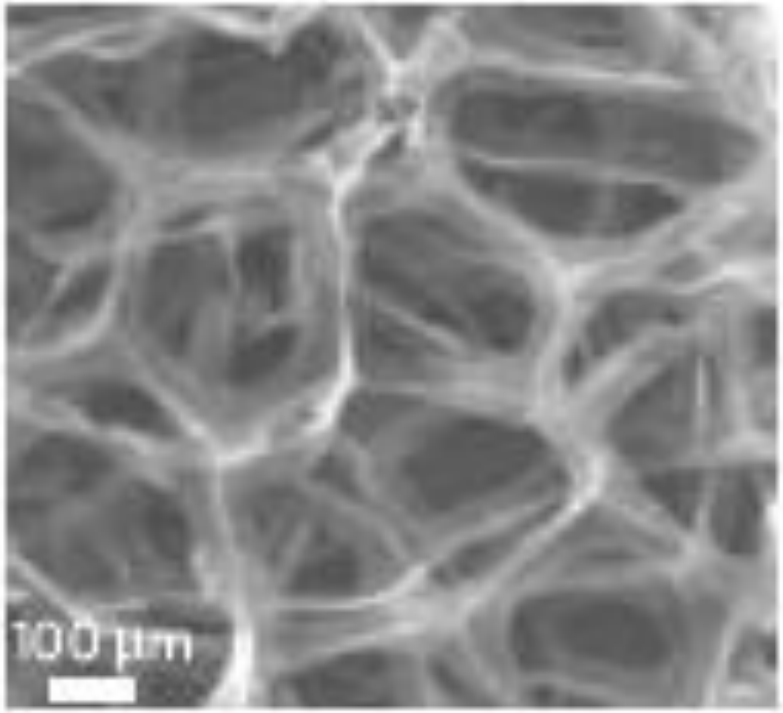
100 µm

Graphene-based composite materials

Sasha Stankovich[1]*, Dmitriy A. Dikin[1]*, Geoffrey H. B. Dommett[1], Kevin M. Kohlhaas[1], Eric J. Zimney[1], Eric A. Stach[3], Richard D. Piner[1], SonBinh T. Nguyen[2] & Rodney S. Ruoff[1]

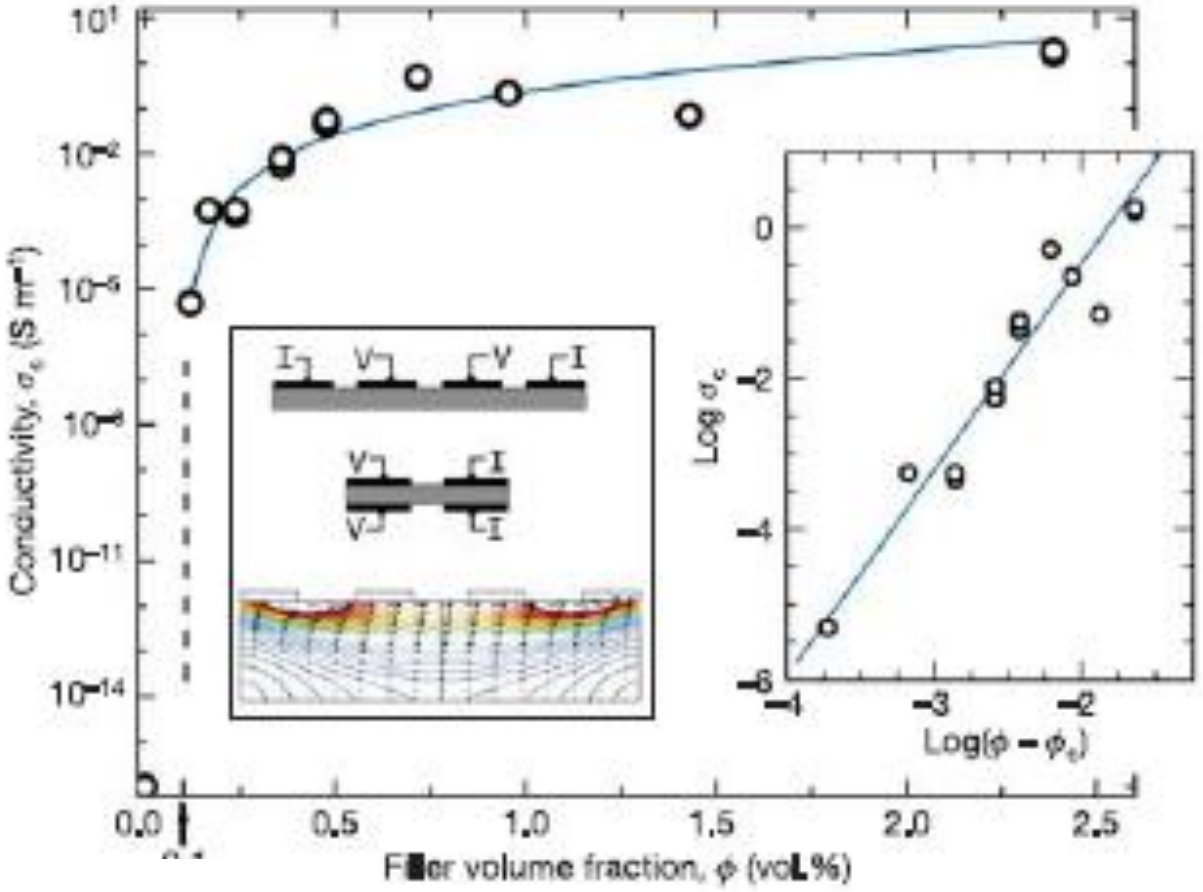

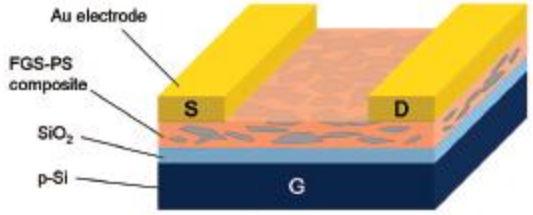

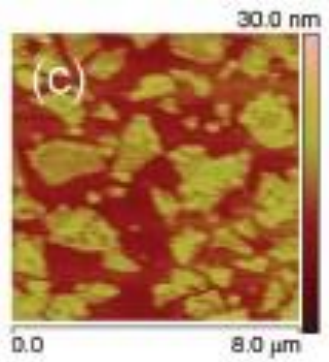

An illustration of a Graphene composite

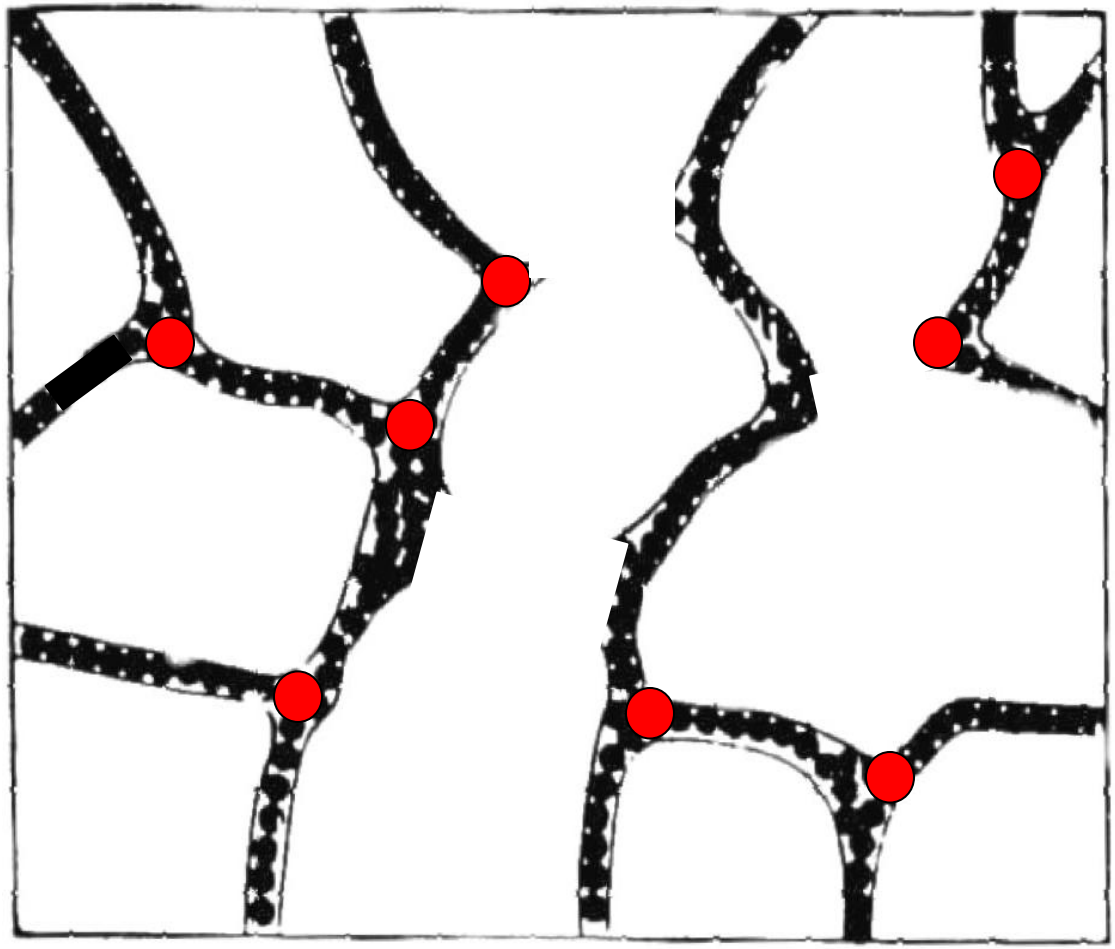

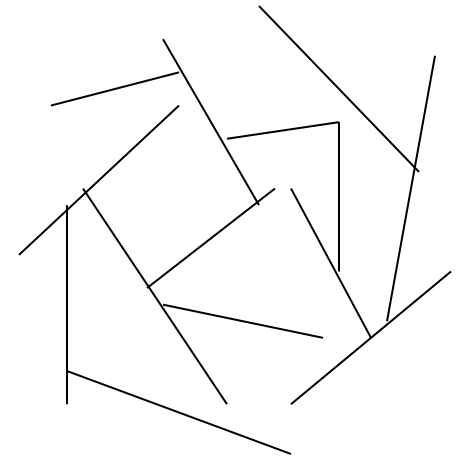

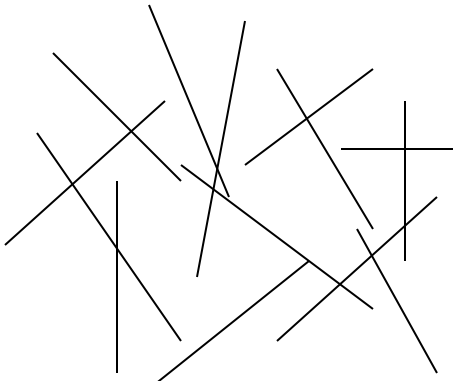

$v = \pi R^2 d$

$V_{ex} = \pi^2 R^3$

$v/Vex \propto d/R$

The Graphene-composite problem

- For example, for high density spheres
- $\delta_c = B_c D/24$,

- for cylinders $\delta_c \approx B_c R[(R/L)\langle \sin\theta \rangle]\Phi^{-1}$ and

- for discs Bc = $\pi^2(3b^2\delta+3b\delta^2+\delta^3)N$ so that
- $\delta/t \approx B_c/(3\pi\Phi)$, or $\approx \Phi \approx [t/5\delta)]$, or . $\delta \approx tB_c/(3\pi\Phi)$,